

NATIONAL LIBRARY

BIBLIOTHÈQUE NATIONALE

OTTAWA



OTTAWA

NAME OF AUTHOR.....KRISHAN M. BANSAL.....

TITLE OF THESIS...RADIOLYSIS OF DIETHYL ETHER  
...AND ETHANOL VAPORS: TEMPERATURE  
EFFECTS.  
.....

UNIVERSITY...University of Alberta, EDMONTON.....

DEGREE.....Ph-D.....YEAR GRANTED.....1968.....

Permission is hereby granted to THE NATIONAL  
LIBRARY OF CANADA to microfilm this thesis and to  
lend or sell copies of the film.

The author reserves other publication rights,  
and neither the thesis nor extensive extracts from  
it may be printed or otherwise reproduced without  
the author's written permission.

(Signed).....*Krishan M. Bansal*.....

PERMANENT ADDRESS:

KRISHAN M. BANSAL  
RADIATION LABORATORIES  
MELLON INSTITUTE  
4400 FIFTH AVENUE  
PITTSBURGH, Pennsylvania  
U.S.A 15213

DATED...*Dec. 27*...1968

THE UNIVERSITY OF ALBERTA

RADIOLYSIS OF DIETHYL ETHER AND ETHANOL VAPORS:  
TEMPERATURE EFFECTS

by



KRISHAN MURARI BANSAL

A THESIS

SUBMITTED TO THE FACULTY OF GRADUATE STUDIES  
IN PARTIAL FULFILMENT OF THE REQUIREMENTS FOR THE DEGREE  
of  
DOCTOR OF PHILOSOPHY

DEPARTMENT OF CHEMISTRY

EDMONTON, ALBERTA

June, 1968

## UNIVERSITY OF ALBERTA

## FACULTY OF GRADUATE STUDIES

The undersigned hereby certify that they have read, and recommend to the Faculty of Graduate Studies for acceptance, a thesis entitled

"RADIOLYSIS OF DIETHYL ETHER AND ETHANOL VAPORS:  
TEMPERATURE EFFECTS"

submitted by KRISHAN MURARI BANSAL, M.Sc., in partial fulfilment of the requirements for the degree of Doctor of Philosophy.

J. R. Keenan  
Supervisor

Robert H. Brown

Donald D. Betts

John W. D.

Chas. P. Stacey

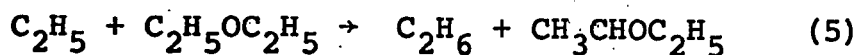
John E. Willard  
External Examiner

Date

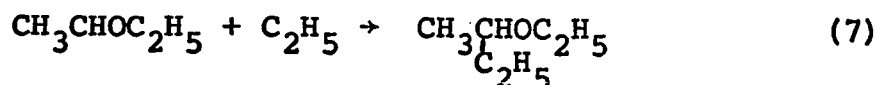
July 18/68

A B S T R A C T1. Radiolysis of diethyl ether vapor

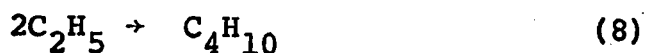
The  $\gamma$ -radiolysis of diethyl ether vapor was studied over the temperature range from 33° to 220°. At temperatures greater than 80°, the formation of acetaldehyde and ethane is explained in terms of a free radical chain mechanism in preference to an ionic chain mechanism. The activation energies of reactions 4 and 5 were found to



be  $E_4 = 19 \text{ kcal mole}^{-1}$  and  $E_5 = 9 \text{ kcal mole}^{-1}$ . The main chain termination reaction in the temperature range 100° to 140° is reaction 7, whereas at higher temperatures the



main termination reaction is 8.



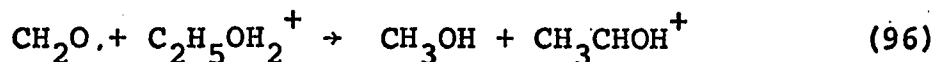
At temperatures greater than 80°, the total primary yield of radicals is  $G(\text{ether} \rightarrow \text{R} + \text{R}') = 5.8$ .

2. Vapor phase radiolysis of ethanol

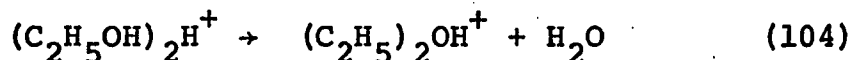
The  $\gamma$ -radiolysis of ethanol vapor was studied over the temperature range from 60° to 375°. At temperatures above 200°, the yields of hydrogen, acetaldehyde, methane, formaldehyde and ethylene are explained by free radical chain mechanisms. The formation of methanol is explained



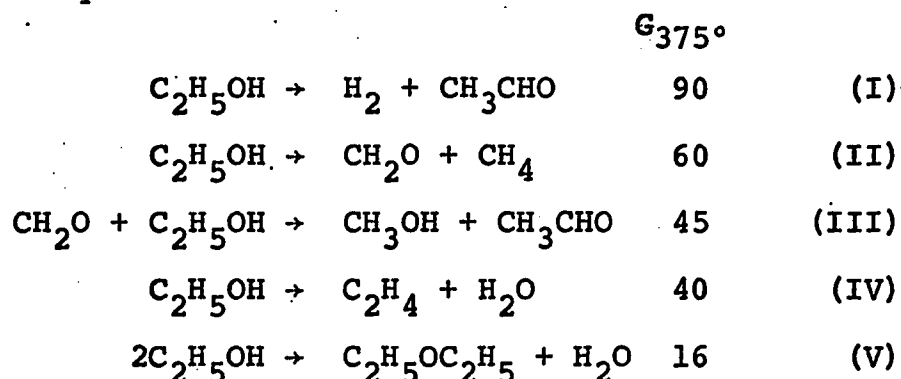
by an ionic chain mechanism involving reaction 96



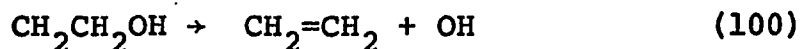
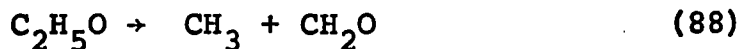
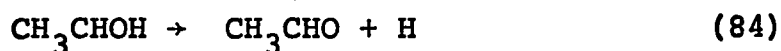
and diethyl ether is also formed by an ionic chain mechanism involving reaction 104



The overall chain reactions are represented by the stoichiometric equations I to V



The activation energies (in kcal mole<sup>-1</sup>) of reactions 84, 88 and 100 are 35 ± 5, 19 and 28 respectively.



The decomposition of CH<sub>3</sub>CHOH radicals (reaction 84) in the pressure range 65 to 1800 torr and at 350° was found to be 1.3 order at the lower pressures and 1.1 order at the higher pressures and the decomposition of C<sub>2</sub>H<sub>5</sub>O and CH<sub>2</sub>CH<sub>2</sub>OH radicals was found to be 1.8 and 1.5 order respectively in this pressure region.

The effects of the scavengers propylene, sulphur hexafluoride and ammonia on product yields in the radiolysis of

ethanol vapor at 350° was studied to provide a test for the various postulated chain mechanisms.

The effects of temperature, pressure, dose and of the additives propylene, sulphur hexafluoride and ammonia on product yields in the radiolysis of ethanol vapor at 150° (non-chain temperature region) were also studied. The decrease in the yields of hydrogen, acetaldehyde and ethylene with increase of ethanol pressure over the range from 45 to 1700 torr was interpreted in terms of reactions of excited molecules. The hydrogen and acetaldehyde yields decreased with increasing dose; this was attributed to the scavenging of electrons by acetaldehyde, with the ultimate formation of  $(\text{CH}_3\text{CHO}^-) \cdot n\text{C}_2\text{H}_5\text{OH}$ . The study of the effects of additives was carried out to obtain more information about the reaction mechanism.

A C K N O W L E D G M E N T S

The author is deeply indebted to his research director, Professor G. R. Freeman, for encouragement and invaluable assistance during the course of this work.

Many thanks are due to the National Research Council of Canada for an N.R.C. scholarship and to the Province of Alberta for a graduate fellowship.

The author also wishes to express his thanks to the members of the Radiation Chemistry Group for many helpful discussions and to Mrs. M. Waters for her preparation of the typescript.

TABLE OF CONTENTS

	<u>Page</u>
Abstract . . . . .	iii
Acknowledgments . . . . .	vi
Table of Contents . . . . .	vii
List of Tables . . . . .	xii
List of Figures . . . . .	xvi
 1. INTRODUCTION . . . . .	 1 - 30
A. General . . . . .	1
B. Reactive intermediate species and their reactions . . . . .	5
1. Reactions of positive ions . . . . .	5
2. Electrons and negative ions . . . . .	12
3. Neutral excited molecules . . . . .	13
4. Neutral free radicals . . . . .	17
C. Effect of gas density . . . . .	21
D. Effect of dose . . . . .	23
E. Chain reactions . . . . .	24
1. Free radical chains . . . . .	24
2. Ionic chains . . . . .	26
F. Previous studies in the vapor phase radiolysis of diethyl ether and ethanol . . . . .	27
1. Diethyl ether . . . . .	27
2. Ethanol . . . . .	28
G. Object of the present work . . . . .	29

	<u>Page</u>
II    EXPERIMENTAL . . . . .	31 - 71
A. Materials . . . . .	31
1. Radiolysed compounds . . . . .	31
2. Compounds used as additives . . . . .	32
3. Compounds used for identification and calibration standards . . . . .	33
B. Vacuum techniques. . . . .	35
C. Sample preparation . . . . .	38
1. Sample preparation manifold . . . . .	38
2. Irradiation bulbs . . . . .	38
3. Filling the irradiation cells . . . . .	42
D. Irradiation of the samples . . . . .	44
E. Product analysis . . . . .	46
1. Gas analysis . . . . .	46
2. Liquid product analysis . . . . .	48
F. Gas chromatography . . . . .	51
1. Gas chromatographic apparatus . . . . .	51
2. Materials used for gas chromatogra- phic analysis . . . . .	55
3. VPC columns used for analysis . . . . .	56
4. Calibration factors for chromato- graphic columns. . . . .	61
III    RESULTS . . . . .	72 - 149
<u>PART I.</u> Vapor phase radiolysis of diethyl ether . . . . .	72
A. Effect of temperature at constant ether density (1.16 g/l) . . . . .	72

	<u>Page</u>
B. Effect of ether pressure at 140° . . . . .	80
<u>PART II. Vapor phase radiolysis of ethanol . . . . .</u>	<u>86</u>
A. Effect of temperature at constant density of ethanol. . . . .	86
1. Density of ethanol 0.66 g/l . . . . .	86
2. Density of ethanol 0.16 g/l . . . . .	93
B. Detailed study at 150° . . . . .	93
1. Radiolysis of pure ethanol . . . . .	93
a. Effect of dose. Ethanol density 1.50 g/l. . . . .	93
b. Effect of ethanol pressure . . . . .	96
2. The effect of inhibitors . . . . .	103
a. Ethanol-propylene mixtures. Ethanol density 1.50 g/l . . . . .	103
b. Ethanol-propylene mixtures. Ethanol density 0.16 g/l . . . . .	104
c. Ethanol-ammonia mixtures. Ethanol density 1.50 g/l . . . . .	107
d. Ethanol-sulphur hexafluoride mixtures. Ethanol density 1.50 g/l . . . . .	112
C. Effect of ethanol pressure at 230° . . . . .	117
D. Detailed study at 350° . . . . .	117
1. The effect of inhibitors . . . . .	117
a. Ethanol-propylene mixtures. Ethanol density 0.66 g/l . . . . .	117
b. Ethanol-ammonia mixtures. Ethanol density 0.66 g/l . . . . .	125
c. Ethanol-sulphur hexafluoride mixtures. Ethanol density 0.66 g/l . . . . .	129

	<u>Page</u>
2. Effect of ethanol pressure . . . . .	136
E. Pyrolysis of ethanol. . . . .	136
1. Pure ethanol at 350° and density 0.66 g/l .	136
2. Mixtures of ethanol with sulphur hexafluoride, ammonia or propylene at 350°. Ethanol density 0.66 g/l . . . . .	143
3. Pure ethanol at 375° and density 0.66 g/l .	145
<u>PART III</u> Vapor phase radiolysis of propylene . . .	147
A. Effect of temperature at constant density (1.96 g/l). . . . .	147
B. Effect of propylene pressure at 150° . . . . .	147
<u>IV</u> DISCUSSION. . . . .	150-256
A. Vapor phase radiolysis of diethyl ether . . . .	150
1. The chain reaction . . . . .	150
2. Other reactions . . . . .	165
B. Vapor phase radiolysis of ethanol . . . . .	169
1. General. . . . .	169
2. Detailed study at 150° . . . . .	172
a. Effect of dose. Ethanol density 1.50 g/l	174
b. Ethanol-propylene mixtures. Ethanol density 1.50 g/l . . . . .	181
c. Ethanol-propylene mixtures at lower ethanol density (0.16 g/l). . . . .	189
d. Ethanol-ammonia mixtures. Ethanol density 1.50 g/l . . . . .	195

	<u>Page</u>
e. Ethanol-sulphur hexafluoride mixtures. Ethanol density 1.50 g/l . . . . .	196
f. Ethanol-sulphur hexafluoride-propylene mixture. Ethanol density 1.50 g/l. . . . .	201
g. Effect of ethanol pressure . . . . .	203
3. Effect of ethanol pressure at 230° . . . . .	209
4. The chain reactions . . . . .	210
5. Inhibition studies at 350° . . . . .	239
REFERENCES . . . . .	257-268
APPENDIX . . . . .	269-283
A. Effect of electric field strength on $\gamma$ -rad- iolysis of cyclohexane liquid . . . . .	269
1. Introduction . . . . .	269
2. Experimental . . . . .	269
a. Materials used . . . . .	271
b. VPC columns used for analysis . . . . .	272
c. High voltage source. . . . .	273
d. Electric circuit . . . . .	273
e. Cell for irradiation of cyclohexane liquid	273
f. Cell for dosimetry . . . . .	276
g. Sample preparation and product analysis. .	276
3. Results and discussion . . . . .	277
B. Calculation of stopping power ratios . . . . .	281



L I S T   O F   T A B L E S

<u>Table</u>		<u>Page</u>
II-1	Typical calibration factors for gaseous products. Detector-Thermal Conductivity.	62
II-2	Typical calibration factors for liquid products. Detector-Thermal Conductivity.	66
II-3	Typical calibration factors for liquid products. Detector-Flame Ionization.	67
III-1	Gas phase radiolytic product yields at 33° in the vapor phase radiolysis of diethyl ether.	73
III-2	Effect of temperature on the G values of chain products in the $\gamma$ -radiolysis of diethyl ether vapor.	74
III-3	Effect of temperature on the G values of non-chain products in the $\gamma$ -radiolysis of diethyl ether vapor.	75
III-4	Effect of pressure on the yields of chain products in the radiolysis of diethyl ether at 140°.	81
III-5	Effect of pressure on the yields of non-chain products in the radiolysis of diethyl ether at 140°.	82
III-6, III-7	Yields of products from ethanol radiolysis as a function of temperature. Density of ethanol = 0.66 g/l.	87,88
III-8	Yields of products from ethanol radiolysis as a function of temperature. Density of ethanol = 0.16 g/l.	94
III-9	Product yields as a function of dose in the vapor phase radiolysis of ethanol at 150°. Density of ethanol = 1.50 g/l.	97
III-10	Effect of pressure on the G values of the products in the $\gamma$ -radiolysis of ethanol. Temperature = 150°.	100
III-11	Product yields from the vapor phase radiolysis of ethanol-propylene mixtures at 150°. Ethanol density = 1.50 g/l.	105

<u>Table</u>		<u>Page</u>
III-12	Product yields from the vapor phase radiolysis of ethanol-propylene mixtures at 150°. Ethanol density = 0.16 g/l.	108
III-13	Product yields from vapor phase radiolysis of ethanol-ammonia mixtures at 150°. Ethanol density = 1.50 g/l.	110
III-14	Product yields from vapor phase radiolysis of ethanol-sulphur hexafluoride mixtures at 150°. Ethanol density = 1.50 g/l.	113
III-15	Effect of pressure on product yields in the vapor phase radiolysis of ethanol at 230°.	118
III-16	Product yields from the radiolysis of ethanol-propylene mixtures at 350°. Ethanol density = 0.66 g/l.	121
III-17	Product yields from the radiolysis of ethanol-ammonia mixtures at 350°. Ethanol density = 0.66 g/l.	126
III-18	Gaseous product yields in the radiolysis of ethanol-sulphur hexafluoride mixtures at 350°. Ethanol density = 0.66 g/l.	130
III-19	Yields of liquid products in the radiolysis of ethanol-sulphur hexafluoride mixtures at 350°. Ethanol density = 0.66 g/l.	131
III-20	Product yields as a function of pressure in the radiolysis of ethanol at 350°.	137
III-21	Product yields from the pyrolysis of pure ethanol at 350°. Ethanol density = 0.66 g/l.	141
III-22	Product yields from the pyrolysis of ethanol scavenger mixtures at 350°. Ethanol density = 0.66 g/l.	144

<u>Table</u>		<u>Page</u>
III-23	Product yields from the pyrolysis of pure ethanol at 375°. Ethanol density = 0.66 g/l.	146
III-24	The variation of hydrogen and methane yields with temperature in the radiolysis of propylene. Propylene density = 1.96 g/l.	148
III-25	Hydrogen and methane yields as a function of pressure in the radiolysis of propylene at 150°.	148
IV-1	Material balance for pure diethyl ether vapor.	151
IV-2	Ratio of the products of radical-radical reactions in the radiolysis of diethyl ether vapor.	160
IV-3a	Heats of formation of some molecules, radicals and ions in kcal/mole at 25°	162
IV-3b	Ionization potentials of some molecules in kcal/mole.	162
IV-4	Chain length and percent decomposition of ether at various temperatures. Dose = $1.6 \times 10^{20}$ eV/g.	166
IV-5	Ratio of the G values of products ( $G_{200^\circ}/G_{60^\circ}$ and $G_{375^\circ}/G_{200^\circ}$ ) in the vapor phase radiolysis of ethanol (0.66 g/l) at different temperatures.	170
IV-6	Ratio of the G values of products in the radiolysis of ethanol vapor at lower density (0.16 g/l) at different temperatures.	171
IV-7	Material balance of products in the radiolysis of ethanol vapor (1.50 g/l) at 150°.	173
IV-8	Product yields extrapolated to zero dose in the radiolysis of ethanol vapor (1.50 g/l) at 150°.	175

<u>Table</u>		<u>Page</u>
IV-9	Heats of formation of molecules, radicals and ions in kcal/mole at 25°.	177
IV-10	Data for kinetic plot from propylene additive in the radiolysis of ethanol vapor (1.50 g/l) at 150°.	184
IV-11	Data for kinetic plot from propylene additive in the radiolysis of ethanol vapor (0.16 g/l) at 150°.	190
IV-12	Summary of kinetic parameters in the radiolysis of ethanol-propylene mixtures at 150°.	193
IV-13	Data for kinetic plot in the radiolysis of ethanol vapor at 150° and at different ethanol densities (0.078-2.96 g/l).	205
IV-14	Summary of the results of the effects of scavengers on product yields in the radiolysis of ethanol at 350°.	240
IV-15	Data for kinetic plot from propylene additive in the radiolysis of ethanol vapor at 350°. Ethanol density = 0.66 g/l.	243
A-1	Effect of electric field on product yields in the radiolysis of cyclohexane liquid. Total dose = $8.5 \times 10^{19}$ eV/cc.	278
A-2	Values of $Z$ , $I$ , $(dT/dX)'$ for various compounds.	283

L I S T O F F I G U R E S

<u>Figure</u>		<u>Page</u>
1.	Main vacuum manifold	36
2.	Gas storage assembly 1	37
3.	Gas storage assembly 2	39
4.	Sample preparation manifold	40
5.	Storage bulb for ethanol	41
6.	Gas analysis system	47
7.	Liquid sample bulbs for product analysis	49
8.	Gas chromatographic system (thermal conductivity detector)	52
9.	Gas sampler	54
II-1	Representative gas chromatographic calibrations for methane and ethylene.	63
II-2	Representative gas chromatographic calibrations for carbon monoxide and propane.	64
II-3	Representative gas chromatographic calibrations for 2,3-diethoxybutane and ethyl isopropyl ether.	68
II-4	Representative gas chromatographic calibration for acetaldehyde.	69
II-5	Representative gas chromatographic calibrations for acetaldehyde and methanol.	70
II-6	Representative gas chromatographic calibrations for 2,3-butanediol and acetal.	71
III-1, III-2, III-3, III-4.	Product yields from ether radiolysis as a function of temperature. Ether density 1.16 g/l.	76,77 78,79

<u>Figure</u>		<u>Page</u>
III-5, III-6	Product yields from ether radiolysis as a function of pressure. Temperature = 140°	83, 84
III-7, III-8, III-9, III-10	Product yields from ethanol radiolysis as a function of temperature. Ethanol den- sity = 0.66 g/l.	89,90, 91,92
III-11	Product yields from ethanol radiolysis as a function of temperature. Ethanol den- sity = 0.16 g/l.	95
III-12, III-13	Product yields from ethanol radiolysis as a function of dose. Ethanol density = 1.50 g/l. Temperature = 150°	98,99
III-14, III-15	Product yields from ethanol radiolysis as a function of pressure. Temperature = 150°	101, 102
III-16	Product yields from ethanol-propylene mix- tures. Temperature = 150°. Density of ethanol = 1.50 g/l.	106
III-17	Product yields from the radiolysis of ethanol-propylene mixtures. Temperature = 150°. Ethanol density = 0.16 g/l.	109
III-18	Product yields from the radiolysis of ethanol-ammonia mixtures. Temperature = 150° Ethanol density = 1.50 g/l.	111
III-19, III-20	Product yields in the radiolysis of ethanol-sulphur hexafluoride mixtures. Temperature = 150°. Ethanol density = 1.50 g/l.	114, 115
III-21, III-22	Product yields from ethanol radiolysis as a function of pressure. Temperature = 230°	119, 120
III-23, III-24	Product yields in the radiolysis of ethanol- propylene mixtures. Temperature = 350° Ethanol density = 0.66 g/l.	122, 123
III-25, III-26	Product yields in the radiolysis of ethanol- ammonia mixtures. Temperature = 350°. Ethanol density = 0.66 g/l.	127, 128

<u>Figure</u>		<u>Page</u>
III-27, III-28, III-29, III-30	Product yields in the radiolysis of ethanol-sulphur hexafluoride mixtures. Temperature = 350°. Ethanol density = 0.66 g/l.	132, 133, 134, 135
III-31, III-32	Product yields from ethanol as a function of pressure. Temperature = 350°.	138, 139
III-33	Hydrogen and methane yield as a function of pressure in the radiolysis of propylene. Temperature = 150°.	149
IV-1	Arrhenius plot of ethane and acetaldehyde yields in the radiolysis of diethyl ether vapor.	157
IV-2	Kinetic plot of hydrogen and methane yields in the radiolysis of ethanol-propylene mixtures at 150°. Ethanol density = 1.50 g/l.	185
IV-3	Kinetic plot of hydrogen and methane yields in the radiolysis of ethanol-propylene mixtures at 150°. Ethanol density = 0.16 g/l.	191
IV-4	Kinetic plot of the effect of pressure on hydrogen and acetaldehyde yields in the radiolysis of ethanol vapor at 150°.	206
IV-5, IV-6	Product yields from ethanol radiolysis as a function of pressure. Temperature = 350°.	214, 215
IV-7	Arrhenius plot of hydrogen and methane yields in the radiolysis of ethanol vapor (0.66 g/l).	218
IV-8	Arrhenius plot of (methanol + formaldehyde), ethylene and diethyl ether in the radiolysis of ethanol vapor (0.66 g/l).	226
IV-9	Kinetic plot for the hydrogen yield in the radiolysis of ethanol-propylene mixtures at 350°. Ethanol density = 0.66 g/l.	244
A-1	Electric circuit.	274
A-2	Cell for irradiation of cyclohexane liquid.	275
A-3	Effect of electric field on product yields in the radiolysis of cyclohexane liquid.	279

## I N T R O D U C T I O N

### A. General.

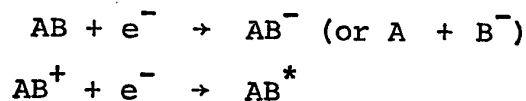
Radiation chemistry is the study of the chemical effects produced by the absorption of high energy radiation in matter. The high energy radiations commonly used are  $\alpha$ -,  $\beta$ -,  $\gamma$ -rays, x-rays, high energy charged particles (electrons, protons, deuterons, helium ions) from accelerators and fast neutrons (1).

The work described later in this thesis deals with the study of the chemical changes produced by the absorption of energy from  $^{60}\text{Co}$   $\gamma$ -rays in organic vapors. In this section, an attempt will be made to trace the various advances that have been made toward the understanding of the primary and secondary chemical phenomena in the radiolysis of gases. To understand the radiation chemical action one needs to know the nature, mode of formation, spatial distribution and various possible reactions of the intermediate species.

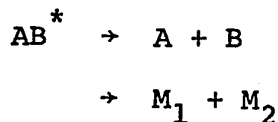
The decay of  $^{60}\text{Co}$  nuclei leads to the emission of  $\gamma$ -photons of mean energy 1.25 MeV. When these  $\gamma$ -photons pass through matter they can transfer energy to the matter. Of the several possible interactions that can contribute to the energy absorption from the  $\gamma$ -rays, the Compton process is the most important. The high energy primary electrons (mean energy 0.6 MeV) produced by the interaction of the



$\gamma$ -rays with the medium, create further ionization and excitation of the medium. The electrons set in motion by the primary electrons are called secondary electrons. These secondary electrons produce further ionizations and excitations. When the electron energy has been reduced to below the first ionization potential of the molecule, only excitation of the molecules takes place. Ultimately, the electrons, having lost most of their energy, become thermalized and may then be captured by neutral molecules to form negative ions or undergo neutralization with positive ions:



The excited molecules may dissociate to form radicals or smaller molecules:



The lower energy secondary electrons usually travel a distance of more than  $1 \mu$  before being thermalized in the  $\gamma$ -irradiation of gases at atmospheric pressure (2).

The probability that the electrons escape the field of their parent positive ions in the irradiation of gases at atmospheric pressure is close to unity. Similarly, a pair of neutral free radicals formed from the decomposition

of a given molecule in a gas at atmospheric pressure have a negligible chance of back-reacting with each other (2).

These intermediate species (electrons, positive ions, excited molecules, radicals) can undergo several possible types of reactions to form the final products.

For quantitative measurements, the radiation chemist must know the amount of energy absorbed by the medium from the  $\gamma$ -rays. The determination of this quantity constitutes radiation dosimetry. The yields of various products can then be expressed in terms of the energy absorbed by the medium. As early as 1910, Lind pointed out that in gas phase radiolysis the product yields can be expressed as the number of molecules formed per ion pair  $(\frac{M}{N})$  (3). However, the number of ion pairs formed in condensed systems could not be measured, so the term G value was introduced to express the product yields. Thus G(X) means the number of molecules of the product X formed for each 100 eV of energy absorbed by the medium. The G value is related to the ion pair yield by the following formula:

$$G = \frac{M}{N} \times \frac{100}{W}$$

where W is the average energy expended to form an ion pair.

Several gas phase chemical dosimeters have been suggested. Radiation induced polymerization of acetylene with  $G(-C_2H_2) = 71.9$  has been used (4). The measurement of the amount of

nitrogen formed in the radiolysis of nitrous oxide has also been suggested, but lack of agreement in the reported  $G(N_2)$  values in the literature (5,6,7) makes the use of this dosimeter undesirable. Back (8) has suggested the measurement of hydrogen in the radiolysis of ethylene as a suitable gas phase dosimeter. Simple manometric measurements of the pressure of carbon disulphide has also been recommended (9). The drop in pressure of carbon disulphide caused by  $\gamma$ -rays, electrons or protons was found to be independent of dose, dose rate or carbon disulphide pressure.

The measurement of the saturation ionization current is the most direct method of gas phase dosimetry (8,10). The saturation current is measured as a function of the amount of gas in the cell. From these measurements, the number of amps. per mole of the gas ( $J$ ), is calculated. The dose rate is given by the following equation:

$$\text{Dose rate (ion pairs/mole sec)} = \frac{J}{e}$$

where  $e$  is the electronic charge =  $1.602 \times 10^{-19}$  coulombs.

To convert this dose rate into terms of energy for calculation of  $G$  values,  $\frac{J}{e}$  is multiplied by the  $W$  value of the irradiated gas. Many research workers adopted this method of dosimetry because  $W$  values can be readily measured (11, 12, 13). Meisels (11) determined  $W$  values for the partial absorption of 1 MeV electrons by organic and in-

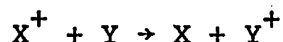
organic compounds and found these values to be the same as those reported earlier for lower energy electrons. Meisels concluded that stopping powers can be used to calculate the relative energy absorption in gases.

B. Reactive intermediate species and their reactions.

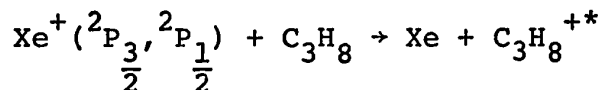
1. Reactions of positive ions.

The various reactions that the positive ions undergo will be described.

a. Charge transfer: If a positive ion  $X^+$  collides with a neutral molecule Y (ionization potential of  $Y < X$ ), charge transfer can occur.



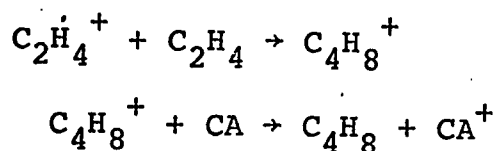
Charge transfer reactions can be used to generate and study the reactions of certain positive ions, for example, the reaction



has been used to study the reactions of excited propane ions ( $C_3H_8^{+*}$ ) (14).

Meisels (15) noted that in the radiolysis of ethylene, the butene yield was increased by the addition of compounds that have a lower ionization potential than that of butene. The addition of compounds that have higher ionization potential than that of butene did not affect the butene yield. Meisels explained this on the basis of

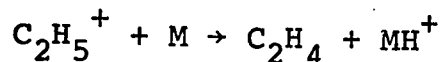
the following reaction scheme:



where CA is the charge acceptor.

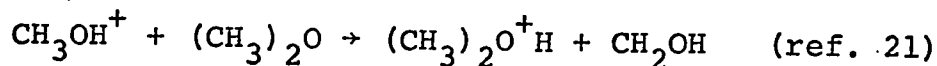
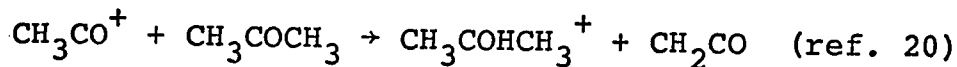
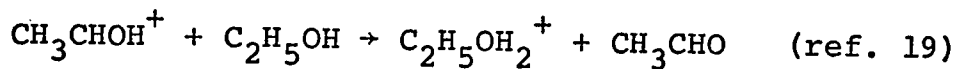
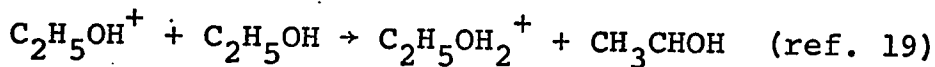
Similar observations have been reported (16,17) in the radiolysis of cyclobutane in the presence of various charge acceptors.

b. Proton transfer: A positive ion can transfer a proton to another species if its proton affinity is higher than that of the donating species. For example, it was observed that  $\text{C}_2\text{H}_5^+$  ions react with polar compounds mainly by the transfer of a proton (18):



where M =  $\text{CH}_3\text{OH}$ ,  $\text{CH}_3\text{NO}_2$ ,  $\text{CH}_3\text{OCH}_3$ ,  $(\text{CH}_3)_2\text{N}_2$ .

Proton transfer reactions such as the following have been observed in mass spectrometric investigations.

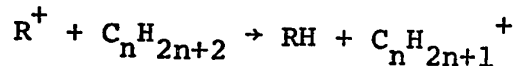


Mass spectrometric investigations by Kebarle (22) and Munson (20) have demonstrated the existence of ion clusters

in various polar gases.

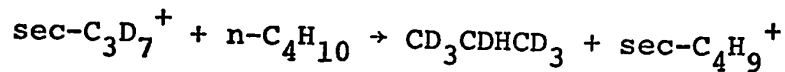
c. Hydride ion transfer: Field and Lampe (23)

showed that the reaction

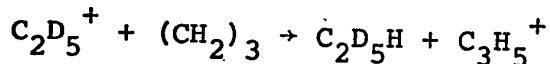


where  $R^+$  is an alkyl ion, occurs in the mass spectrometer with a high cross-section when the molecule is larger than the ion.

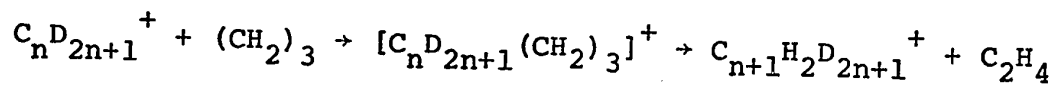
Hydride ion transfer is essentially the only mode of reaction between alkyl ions and alkane or cycloalkane (except cyclopropane) molecules (24,25).



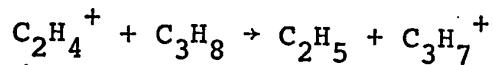
For cyclopropane, although the reaction



is exothermic by approximately 25 kcal (24), yet it has been found that in the radiolysis of deuterio propane-cyclopropane mixtures, the yield of  $\text{C}_2\text{D}_5\text{H}$  is extremely small. This indicates that an alternative reaction between the alkyl ion and cyclopropane occurs. The suggested reaction can be written as (24).



Hydride ion transfer from saturated hydrocarbons to olefinic ions is also possible (24,25).



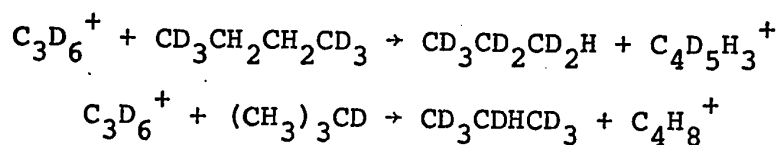
However, in these cases, transfer of  $H_2^-$  to olefinic ions competes with the  $H^-$  transfer reactions.

The occurrence of the hydride ion transfer reaction has been used for the detection of carbonium ions (26).

d.  $H_2^-$  transfer reaction: An unsaturated hydrocarbon ion or a cyclopropane ion can abstract  $H_2^-$  from larger saturated hydrocarbons (24).

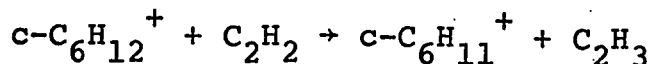
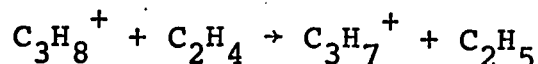


Reactions of this type were first observed in the radiolysis of propane (27) and in various mass spectrometric studies on simple alkanes (28,29). The reaction of  $C_3D_6^+$  with  $CD_3CH_2CH_2CD_3$  and  $(CH_3)_3CD$

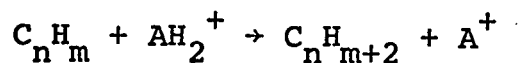


shows that the hydrogen atom on the terminal carbon atom of n-butane or isobutane is transferred to the centre carbon atom of  $C_3D_6^+$ , whereas the secondary or tertiary hydrogen atom is transferred to the terminal carbon on the  $C_3D_6^+$ .

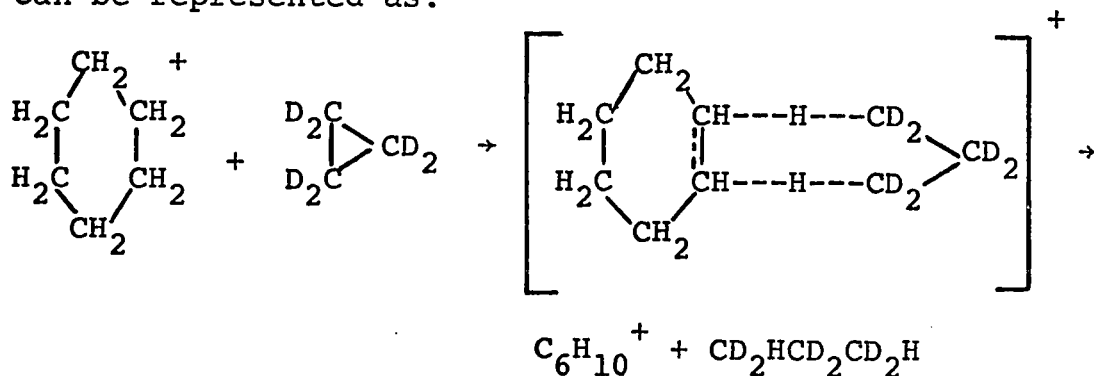
e. H<sub>2</sub> and H transfer reactions: An alkane or cycloalkane molecular ion can donate a hydrogen atom to an unsaturated molecule (30). For example



Hydrogen molecule transfer from an alkane or cycloalkane ion to an unsaturated hydrocarbon with fewer carbon atoms than the parent ion can also take place.



(CD<sub>2</sub>)<sub>3</sub> abstracts a hydrogen molecule from ions such as c-C<sub>6</sub>H<sub>12</sub><sup>+</sup>, c-C<sub>5</sub>H<sub>10</sub><sup>+</sup>, n-C<sub>5</sub>H<sub>12</sub><sup>+</sup>, i-C<sub>5</sub>H<sub>12</sub><sup>+</sup>, to form CD<sub>2</sub>HCD<sub>2</sub>CD<sub>2</sub>H (25,31). The fact that the propane product consists mainly of CD<sub>2</sub>HCD<sub>2</sub>CD<sub>2</sub>H indicates that the hydrogen molecule transfer reactions, for example, in the case of the radiolysis of cyclohexane-cyclopropane-d<sub>6</sub> mixtures, can be represented as:

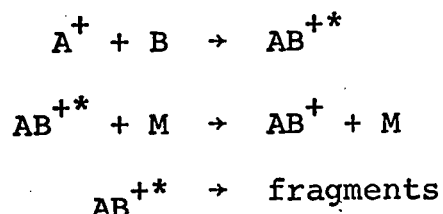


The occurrence of the hydrogen molecule transfer

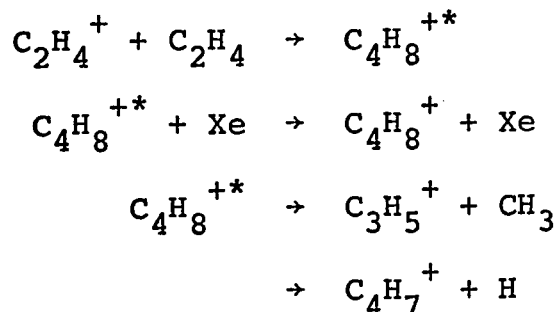


reaction in the liquid phase radiolysis of cyclopentane-cyclopropane-d<sub>6</sub> mixtures has been demonstrated (32). Schuler (33) gave evidence for the occurrence of the hydrogen molecule transfer reaction in the radiolysis of dilute solutions of <sup>14</sup>C-cyclopropane in n-hexane. He observed that the predominant radioactive product obtained was propane.

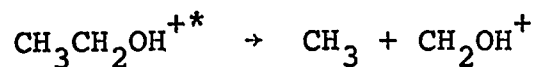
f. Condensation: Condensation reactions are those in which a strongly bound reaction complex, which may or may not be stabilized by collision, is produced (24).



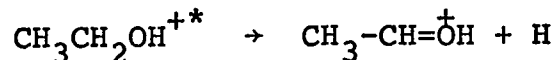
The charged species formed in the fragmentation process has a higher molecular weight than its precursor ion A<sup>+</sup>. For example (34),



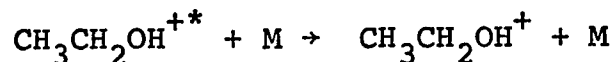
g. Decomposition: Excited polyatomic ions can decompose. For example, the reaction



accounts for half of the ionic cracking pattern in the mass spectrometer (4). The excited ion can also decompose by loss of a hydrogen atom (35a):



Labeling experiments with deuterium have shown that this characteristic M-1 ion ( $\text{CH}_3\overset{+}{\text{C}}\text{HOH}$ ) results from loss of the hydrogen atom attached to the same carbon atom as the hydroxyl group (35b). These decomposition reactions in radiolysis systems are in competition with the deactivation reaction



Decomposition is favored by large amounts of excitation energy per degree of freedom in the ion and low intermolecular collision rates in the system.

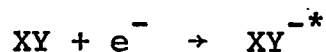
h. Neutralization: The less reactive ions in the radiolysis systems undergo neutralization. Woodward and Back (36) from their studies of the effects of dose rate and an applied electric field on the hydrogen yield produced in hydrocarbon gases, concluded that when neutralization occurs on the wall, no hydrogen is produced, while neutralization in the gas phase may result

in the formation of H atoms. The deactivating effect of the wall on the neutralization was also indicated in the radiolysis of neopentane (37).

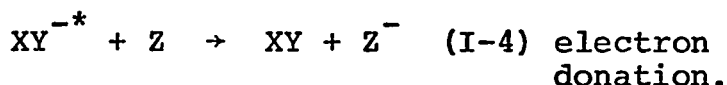
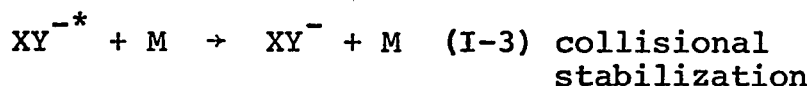
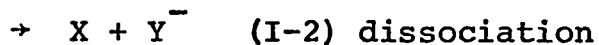
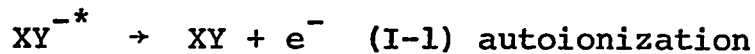
Johnson and Warman (38) observed that in the radiolysis of propane, the electron scavengers (nitrous oxide, sulphur hexafluoride, carbon tetrachloride) decrease the hydrogen yield, indicating that no hydrogen atoms are produced in a negative ion - positive ion neutralization process.

## 2. Electrons and negative ions.

a. Electrons can attach to neutral molecules which have a positive electron affinity to form an excited negative ion (2).

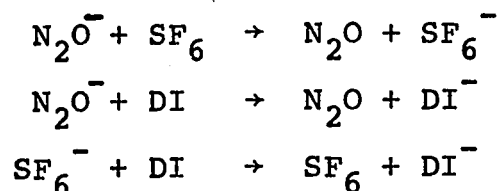


The excited negative ion may then undergo one of four possible reactions:



Reaction I-4 can only occur if the lifetime of  $XY^{-*}$  is long enough for it to encounter Z enough times for the reaction to occur. The following reactions have been

suggested to take place in the vapor phase radiolysis of methyl cyclohexane in the presence of pairs of additives  $N_2O$ , DI and  $SF_6$  (39).



b. Electron-ion neutralization and ion-ion neutralization: This has been discussed previously in the section on the reaction of positive ions.

c. Ion-molecule reactions: Negative ions can also undergo ion-molecule reactions analogous to those of the positive ions. However, at present, the information about them is very scanty.

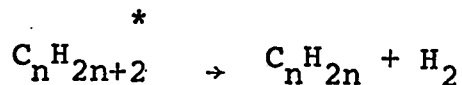
### 3. Neutral excited molecules

Most of the information concerning neutral excited molecules comes from studies of (a) photolysis, (b) gas phase radiolysis in the presence of an applied electric field.

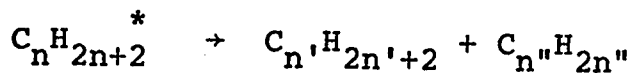
a. Photolysis: The most direct information regarding the decomposition of neutral excited molecules can be obtained from photolysis experiments carried out at photon energies below the ionization potential (2,25,40,41,42).

In the photolysis of alkanes at  $1470 \text{ \AA}$ , the elimination of a hydrogen molecule from a single carbon atom,

leading to the formation of the corresponding carbene, is an important process (42).



Molecular alkanes can also be eliminated in a primary process resulting in the formation of a carbene or olefin as the corresponding fragment:

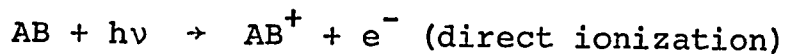


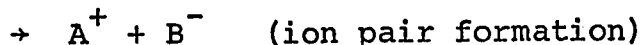
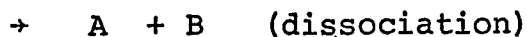
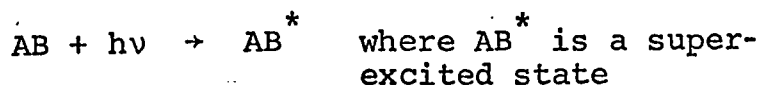
$$\text{where } (n' + n'') = n$$

It has also been found that with an increase in the photon energy, the importance of hydrogen molecule elimination decreases and that of C-C and C-H bond cleavage increases (25). It is seen that in the photolysis of cyclohexane, the yields of cyclohexene and hydrogen decrease as the photon energy is increased, demonstrating a decreased importance of the hydrogen molecule elimination process (25).

Reactions of excited olefins have also been studied (43), but relatively little work has been done.

The use of photoionization experiments has been very recently reviewed by Ausloos (44). When a molecule absorbs a photon of energy greater than its ionization potential, the following processes may take place:





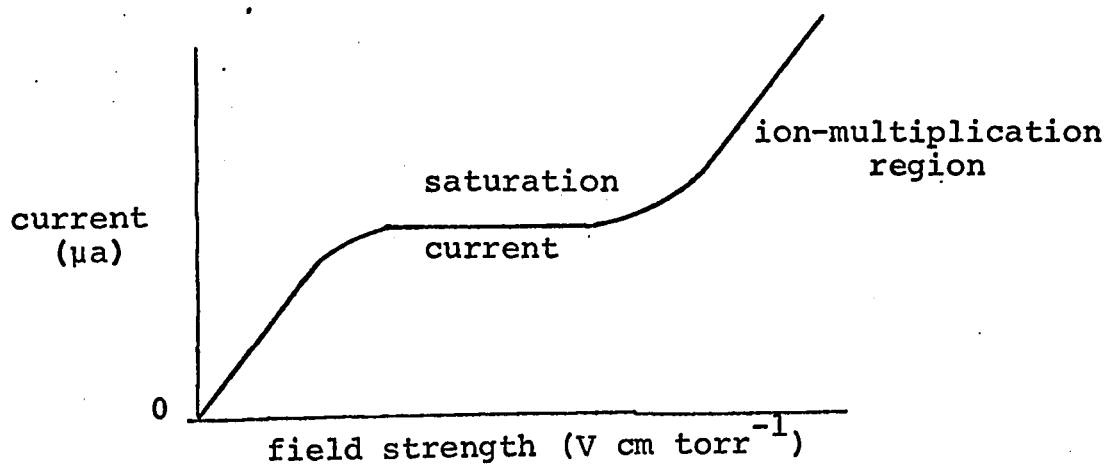
The term "superexcited state" refers to the neutral excited molecule whose energy content is larger than its first ionization potential (45).

To obtain dependable information regarding the modes of decomposition of superexcited molecules, the photon energy must be chosen in such a way that the ionization efficiency is relatively low and the ion molecule reaction mechanism is not too complex. Studies of this type have been carried out on many compounds, as for example, cyclobutane (16), and propylene (46).

b. Gas phase radiolysis in the presence of an electric

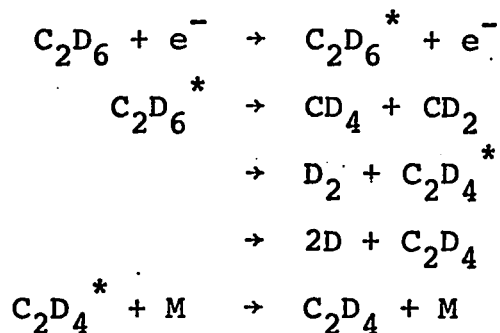
field: When an electric field is applied across a gas under irradiation, ions are collected at the electrodes. As the strength of the electric field is increased, the radiation induced current increases until it reaches a value that remains constant with further increase of field strength. This constant current is called the "saturation current". As the field strength is increased still further, the secondary electrons become sufficiently accelerated that they can cause further ionization, thereby increasing

the current by ion-multiplication.



It has been found that in the vapor phase radiolysis of hydrocarbons, with applied electric fields in the saturation current region, but below that required for electron multiplication, the yields of some of the products increase (41,47,48,49,25) and the yields of some products remain unchanged. The increase in product yields has been ascribed to the decomposition of neutral excited species formed by collisions of molecules with electrons accelerated by the applied field. The products resulting from fast ion-molecule reactions remain unaffected. The use of this technique will be illustrated by the following example: In the radiolysis of an ethane-ethane-d<sub>6</sub>-nitric oxide (1:1:0.05) mixture, the yields of methane-d<sub>4</sub> and ethylene-d<sub>4</sub> increase with an increase in the applied field strength whereas the yields of CD<sub>3</sub>H and C<sub>2</sub>D<sub>3</sub>H remain constant (41). Carmichael et al. (41) concluded from their observations that CD<sub>3</sub>H and C<sub>2</sub>D<sub>3</sub>H are formed by fast ion-molecule reactions whereas CD<sub>4</sub>

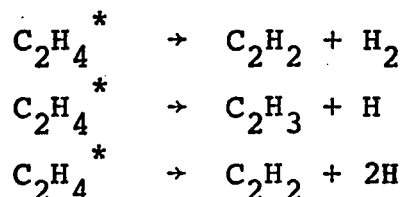
and  $C_2D_4$  are formed by the following sequence of neutral excited molecule decompositions:



The formation of  $C_2D_3H$  can be explained by the following  $H^-$  transfer reaction



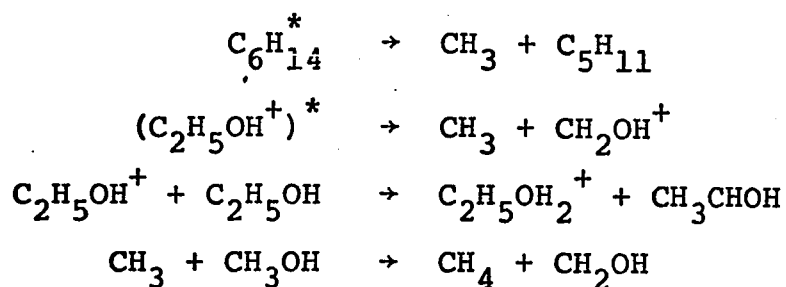
The  $CD_3H$  can be formed by several ion-molecule reactions. Reactions of excited olefins have also been studied by the electric field technique. As an example, Meisels and Sworski (43) obtained evidence for the occurrence of the following processes in the radiolysis of ethylene:



#### 4. Neutral free radicals

a. In radiolysis systems free radicals may be formed by the decomposition of excited molecules and ions, by ion-molecule reactions and by the reactions of other free radicals with molecules.



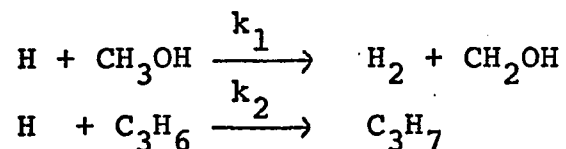


Radical scavengers are generally used to distinguish the reactions occurring by means of free radical intermediates from intramolecular processes. The radical reactions are suppressed by the scavengers and sometimes it is possible to identify the radicals by characterizing the new products formed (50). There are three distinct ways in which scavengers are used:

(i) The scavenging of a particular product is studied as a function of the scavenger concentration. The scavenger concentration is increased to the extent that there is no more change in the product yield. Scavengers generally used for this purpose are, as for example, iodine and diphenylpicrylhydrazyl. The yield of the unscavenged product can then be measured.

(ii) Competition between reactions of a given radical with the scavenger and the substrate are studied. For example, in the vapor radiolysis of methanol-propylene mixtures (51), the rapid decrease of the hydrogen yield was attributed to the

following competition reactions:



From the decrease of hydrogen yield as a function of propylene concentration, the value of  $\frac{k_2}{k_1}$  can be determined (51).

(iii) Labeled scavengers have been used to determine the yields of the different types of free radicals. Examples of such scavengers are  $^{131}\text{I}$  (52), tritium iodide, and  $^{14}\text{C}$ -containing methyl and ethyl radicals (53). These produce labeled products which can be analyzed by radio-gas-chromatography.

Electron spin resonance (esr) spectroscopy has been used to detect the free radicals. For example the presence of  $\alpha$ -hydroxyalkyl radicals have been detected during esr studies of irradiated solid primary alcohols (54,55).

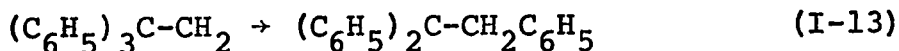
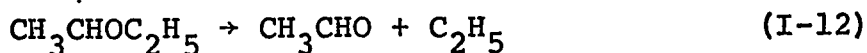
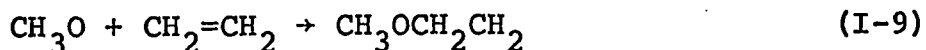
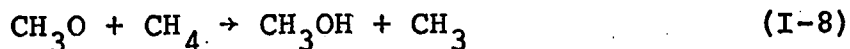
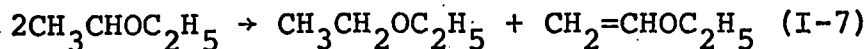
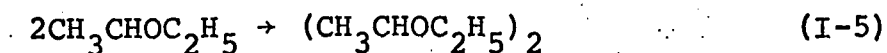
Schuler (56) used esr methods to observe alkyl radicals in liquid hydrocarbon systems during irradiation with 2.8 MeV electrons.

Using pulse radiolysis and optical absorption techniques, the rate of decay of radicals has been measured in liquids. An

ultraviolet absorption band in irradiated ethanol was attributed to  $\text{CH}_3\text{CHOH}$  radicals (57).

Smith (58) has described an indirect method of studying the vapor phase radiolysis of gases by esr techniques. A stream of vapor, irradiated with a beam of 40 KeV  $\text{Ar}^+$  ions is directed onto a surface cooled to 77°K. The solid deposit is studied by esr techniques. Any radicals observed must be formed as a consequence of ion bombardment of the vapor. In this way, the  $\text{CH}_3\text{CHOH}$  radical was detected in ethanol vapor radiolysis (58).

b. Reactions of free radicals: Several reviews of monoradical reactions have appeared (59,60,61,62). The main information that leads to the understanding of monoradical reactions comes from photolysis and pyrolysis studies. The main types of reactions that the monoradicals undergo will be illustrated by examples (i) combination (I-5), (ii) disproportionation (I-6, I-7), (iii) abstraction (I-8), (iv) addition to double bonds (I-9, I-10), (v) dissociation (I-11, I-12), (vi) isomerization I-13).



### C. Effect of gas density

It has been found in radiolysis experiments that the product yields change markedly as the density of the gas is increased over the range 0.01 - 0.4 g/cc. This change in product yields with increase of density may be due to the following causes:

- (i) Collisional deactivation of the excited molecules and ions competes with their decomposition reactions as the density of the vapor increases.
- (ii) The probability of geminate recombination of radicals increases with increase of density of the vapor.

Both these factors cause a decrease in the extent of the decomposition of the irradiated compound with the increase in the density of the vapor.

- (iii) The probability of the recapture of electrons by their parent positive ions increases. The

increased probability of geminate recombination of positive ion and electron decreases the lifetime of positive ions markedly which may, in turn, affect the secondary reactions of these ions.

Jones (63) studied the variation of product yields with density (0.0079 - 0.42 g/cc) in the vapor phase radiolysis of cyclohexane at 300°. He found that the yields of low molecular weight hydrocarbon products (methane, ethane, ethylene, propane and propylene) decrease with increasing density of cyclohexane vapor. The yields of products at high density are comparable to the yields from cyclohexane liquid at room temperature. From this, he concluded that the difference in yields is not due to a difference in phase, but is dependent on the density of cyclohexane.

The variation of product yields in the radiolysis of ethane over the density range from 0.001 to 0.30 g.cc<sup>-1</sup> (64,65) and in the radiolysis of propylene over the range 0.01 to 0.12 g.cc<sup>-1</sup> (66) have also been studied.

Toi et al. (67) studied the variation of the yields of hydrogen and nitrogen with change of density over the range  $5.5 \times 10^{-4}$  - 0.312 g.cc<sup>-1</sup> in the radiolysis of ammonia at 137°. The yields of hydrogen and nitrogen were constant up to a density of 0.05 g.cc<sup>-1</sup>. At den-

sities exceeding  $0.05 \text{ g.cc}^{-1}$ , the yields of hydrogen and nitrogen decreased markedly. Nishikawa and Shinohara (68) also observed that the yields of hydrogen and nitrogen were unaffected with change of density ( $0.0005 - 0.0067 \text{ g.cc}^{-1}$ ) in the radiolysis of ammonia at  $25^\circ$ .

Radiolysis of propane gas at  $35^\circ$  and 760 torr and also of liquid propane at  $35^\circ$  have been studied (69a). It was observed that a change from gas to liquid phase decreased  $G(-C_3H_8)$  by 14 percent and the radical yield by 4 percent (69a). Radiolysis of liquid propane in the presence of oxygen has also been studied (69b). It was observed that a change from gas to liquid phase at  $35^\circ$  decreased the ionic decomposition yield by  $\leq 69$  percent (69b).

#### D. Effect of dose.

The increase of total dose will only affect the product yields if a radiolysis product acts as a scavenger of reactive intermediates. For example, in the radiolysis of ethane, the decrease in hydrogen yield with increasing dose was attributed to the scavenging of hydrogen atoms by ethylene which is one of the radiolysis products (70). In the radiolysis of propane, the decrease in the yield of propylene with increasing dose was due to the addition of hydrogen atoms to propylene and/or the scavenging of ionic precursors of hydrogen atoms ( $C_3H_7^+$ ,  $C_3H_8^+$ ) by pro-

pylene (71).

E. Chain Reactions.

Two types of chain reactions will be considered, (i) those with free radicals as chain carriers and (ii) those which have ionic intermediates as chain carriers.

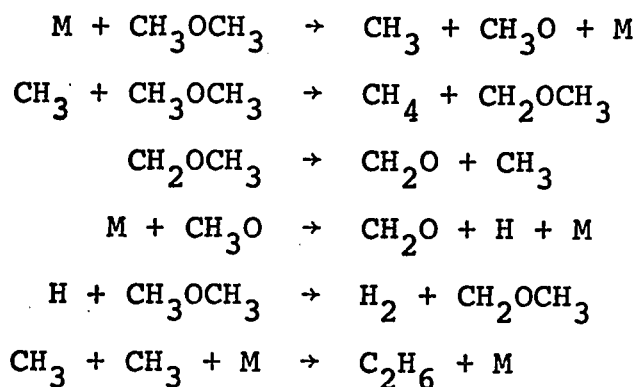
1. Free radical chains

When a chemical reaction proceeds by a chain mechanism with free radical chain carriers, the essential feature is that the chain carrier which is destroyed is replaced by a new chain carrier. The new chain carrier, which may differ chemically from the original chain carrier, takes part in another propagation reaction. Under favorable conditions this sequence of reactions may be repeated several times before the radical is destroyed, in other words, a chain reaction takes place.

The initial step in a chain reaction, the production of an atom or radical from a molecule is often a difficult one because of the high activation energy requirements. Before the molecule can decompose, it must possess a certain amount of internal energy. This energy can be supplied by several methods, as for example thermal, photolytic and radiolytic methods. Most of the information concerning the free radical chain reactions at present is available from pyrolysis studies. Excellent discussion about chain reactions is given in many books

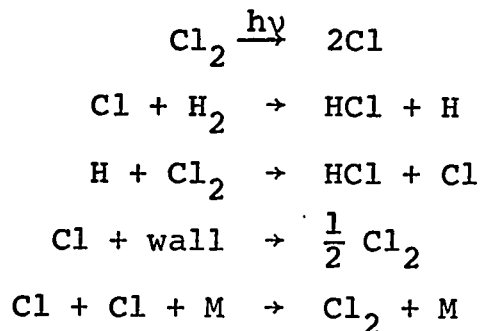
(1,72,73,74,75). In this section thermal, photolytic and radiolytic methods of chain initiation will be illustrated by examples.

The following mechanism has been suggested in order to explain the pyrolysis of dimethyl ether (72).



where M is a third body.

The reaction of hydrogen and chlorine provides a good illustration of a photochemical chain reaction (75). When a mixture of hydrogen and chlorine is irradiated with light of wavelengths less than  $4000 \text{ \AA}$  an extremely fast reaction takes place. The following mechanism has been suggested (75):

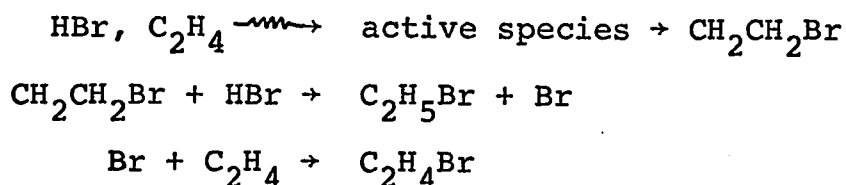


McNesby (76) studied the chain decomposition of propane induced by light of wavelength  $1470 \text{ \AA}$  over the temp-



erature range 25° to 320°.

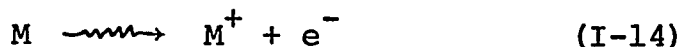
The  $\gamma$ -radiation induced addition of hydrogen bromide to ethylene with the formation of bromoethane is a well known example of a radiation induced chain reaction (1). The mechanism is:



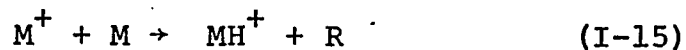
A definite termination step in the chain mechanism was not established.

## 2. Ionic chains

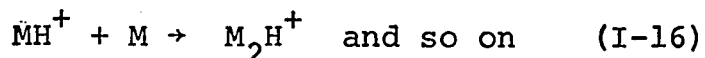
Very few examples of vapor phase ionic chain reactions are available. H. Okamoto et al. (77) have suggested that radiation induced polymerization of isobutene vapor at 25° proceeds via ionic intermediates. They found that the polymerization was markedly retarded by the presence of ammonia, indicating a cationic mechanism. They suggested the following mechanism for polymerization (77):



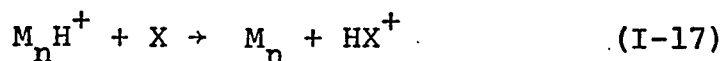
where M is isobutene



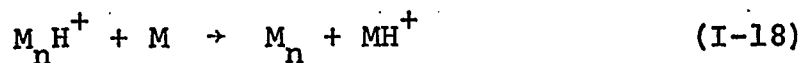
The chain carriers are carbonium ions:



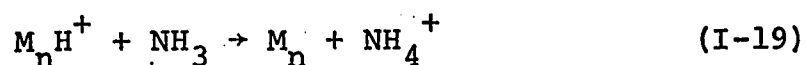
The nature of the termination reaction is less certain:



where X indicates the wall of the vessel and possibly trace impurities. Chain transfer can also take place by proton transfer from a polymer ion to a monomer molecule



The retarding effect of ammonia is attributed to proton transfer, reaction (I-19)



## F. Previous studies in the vapor phase radiolysis of diethyl ether and ethanol.

### 1. Diethyl ether

Very little work has been done on the vapor phase radiolysis of diethyl ether. Baxendale and Gilbert (78) measured the yields of hydrogen and methane in the  $\gamma$ -radiolysis of diethyl ether vapor at 116° and 140 and 470 torr pressure. They found  $G(H_2) = 6.75 \pm 0.05$  and  $G(CH_4) = 3.55 \pm 0.15$ . Ng and Freeman (79) determined the yields of various gaseous and liquid products in the  $\gamma$ -radiolysis of diethyl ether vapor (1.4 g/l) at 25°. From a comparison of the product yields from the radiolysis of  $(C_2H_5)_2O$ ,  $(CD_3CH_2)_2O$ ,  $(CH_3CD_2)_2O$  and  $(C_2D_5)_2O$ , it was noted that  $\alpha$ -C-H bond cleavage was most important in the hydrogen and methane formation, and  $\beta$ -C-H bond cleavage was most important in ethylene formation. They also studied the effect of 1,3-pentadiene on product

yields (79).

## 2. Ethanol

Although extensive work has been done on the liquid phase radiolysis of ethanol, very little information is available about the vapor phase radiolysis. The yields of various liquid and gaseous products have been measured in the  $\alpha$ -radiolysis of ethanol vapor at 108° (80). The effects of added cyclohexene and benzene on the yields of hydrogen, methane and carbon monoxide were also studied (81).

Myron and Freeman (82), studied the  $\gamma$ -radiolysis of ethanol vapor at 105° and 800 torr pressure. The yields of various gaseous and liquid products were measured and also the effect of 1,3-pentadiene on product yields was studied (82). Sieck and Johnsen (4) studied the radiolysis of ethanol vapor at 25° and 45 torr pressure, using 2.0 MeV electrons. The effect of nitric oxide, propylene and oxygen on product yields was also studied (4). H. Hotta et al. (83) studied the  $\gamma$ -radiolysis of ethanol-ethylene mixtures over the temperature range 100-200°. The major products formed were 2-alkanols, 3-methyl-3-alkanols and 2-ketones (83).

The variation of the yields of hydrogen, methane, carbon monoxide, ethane, ethylene, acetylene and acet-aldehyde as a function of hydrochloric acid concentration

has also been studied in the  $\gamma$ -radiolysis of ethanol-hydrochloric acid mixtures at 105° (84). The yields of methane, carbon monoxide, acetylene, ethylene and ethane were independent of hydrochloric acid concentration. The yield of hydrogen increases from 6.35 to 8.73 as the hydrochloric acid concentration is increased from 0.0 to 1.05 mole percent. The yield of acetaldehyde first increases from 3.54 to 4.43 with increase of acid concentration from 0.0 to 0.265 mole percent and then decreases to 1.93 as the acid concentration is further increased to 1.05 mole percent (84).

G. Object of the present work.

The pyrolysis mechanisms of diethyl ether (85,86) and ethanol (87,88) vapors are very complex partly because of the high temperature ( $>500^{\circ}\text{C}$ ) used to initiate the chain reactions. At these high temperatures, several secondary reactions take place. It was felt that by initiating the chain reaction by  $\gamma$ -radiation, we could study the chain decomposition of diethyl ether and ethanol vapors at much lower temperatures, thereby, making the systems less complex.

In the radiation induced chain decomposition of ethanol, free radical, electron and proton scavengers were used to study the contribution of free radical and ionic chain carriers in the overall mechanism of product formation.

During the course of this work, a detailed study was made of the vapor phase radiolysis of ethanol at 150°, at which temperature chain decomposition does not occur.

E X P E R I M E N T A L

A. Materials.

1. Radiolysed Compounds

a. Diethyl ether: Spectrograde diethyl ether from Eastman Organic Chemicals Co. was dried over sodium and was stored in a reservoir in the vacuum system. No impurities were detected by gas chromatographic analysis of the diethyl ether on silicone grease, di-2-ethyl hexyl sebacate and tetraethylene glycol dimethyl ether columns. It was used as supplied after drying over sodium.

b. Ethanol: Benzene free absolute ethanol from Reliance Chemical Co. was used. The specifications quoted were:

Ethanol by volume > 99.9%  
water content < 0.1%  
benzene < 0.0009%

In order to remove the trace amounts of acetaldehyde present, 2 liters of ethanol were refluxed for 2 hrs after the addition of 3 g of 2,4-dinitro phenyl hydrazine and 2 ml. of concentrated sulphuric acid. It was then distilled through a column packed with glass helices into a reservoir attached to the vacuum line. Only the middle fraction was collected. During the refluxing and distillation, the alcohol and the distillation system were protected from atmospheric oxygen and moisture by a stream of dry nitrogen. The purified ethanol was degassed and stored under vacuum

in a Pyrex reservoir.

2. Compounds used as additives

- a. Ammonia: Anhydrous ammonia from Canadian Industries Ltd. was used. It was subjected to several trap to trap distillations in the vacuum line, using liquid nitrogen as coolant. The condenser trap was pumped on during the distillations. The ammonia was finally condensed into a storage reservoir in the Gas Storage Assembly 2 (Fig. 3, page 39).
- b. Propylene: Phillips research grade propylene had a stated purity of 99.99 mole percent. It was degassed by trap to trap distillation and then condensed into a storage reservoir in the Gas Storage Assembly 2 (Fig. 3, page 39) of the vacuum system.
- c. Sulphur hexafluoride: Sulphur hexafluoride from Matheson Co. was degassed by trap to trap distillations, using liquid nitrogen coolant. After degassing, the sulphur hexafluoride was condensed into a storage reservoir in the Gas Storage Assembly 2 (Fig. 3, page 39) of the vacuum system. Only the middle fraction was retained.

3.      Compounds Used for Identification and  
         Calibration Standards

<u>No.</u>	<u>Compound</u>	<u>Supplier</u>
1.	Acetal	Eastman Organic Chemicals Co.
2.	Acetaldehyde	Eastman Organic Chemicals Co.
3.	Acetylene	Matheson of Canada Ltd.
4.	n-butane	Phillips Research Grade (Mole percent purity 99.9).
5.	2,3-butanediol	Anachemia Chemicals Ltd.
6.	sec-butyl alcohol	Eastman Organic Chemicals
7.	sec-butyl ethyl ether	Frinton Labs.
8.	Carbon monoxide	Matheson of Canada Ltd.
9.	2,3-diethoxybutane	Prepared by Moore's method (89) and was distilled before use. This was further purified by gas chromatography using a silicone grease column.
10.	Diethoxymethane	Eastman Organic Chemicals Co.
11.	Ethane	Phillips Research Grade (Mole percent purity 99.92)
12.	Ethylene	Phillips Research Grade (Mole percent purity 99.99).
13.	Ethyl isopropyl ether	Frinton Labs.
14.	Ethyl methyl acetal	This was prepared by the method described by Juvet and Chiu (90) and was distilled before use.
15.	Ethyl vinyl ether	Eastman Organic Chemicals Co.



- |     |                       |   |
|-----|-----------------------|---|
| 16. | Formaldehyde solution | Fischer Scientific Co.                                  |
| 17. | Isopropyl alcohol     | The Nichols Chemical Co.<br>Ltd.                        |
| 18. | Methane               | Phillips Research Grade (Mole<br>percent purity 99.58)  |
| 19. | Methanol              | Shawinigan Co.  |
| 20. | Paraformaldehyde      | Shawinigan Co.  |
| 21. | Propane               | Phillips Research Grade (Mole<br>percent purity 99.99). |
| 22  | 1,2-Propanediol       | Eastman Organic Chemicals Co.                           |

The compounds were used as supplied

## B. Vacuum techniques

1. Main Vacuum Manifold (Fig. 1): A vacuum system was used for sample preparation and gas analysis. It was constructed of Pyrex glass tubing, stopcocks and traps. Stopcock  $S_3$  was greased with silicone grease (Dow Corning). Stopcocks  $S_1, S_2, S_5$  to  $S_9$  (4mm bore high vacuum stopcocks) and  $S_4$  (10 mm bore high vacuum stopcock) were greased with Apiezon N grease (Associated Electrical Industries Ltd). When the system was in use, trap  $T_1$  was immersed in liquid nitrogen. The system was evacuated by the mechanical pump (Welch Duo-Seal Model No. 1405-6) and mercury diffusion pump. The pressure was measured with a Pirani Vacuum Gauge (Type GP 110, Consolidated Electrodynamics). When the system was not in use, the liquid nitrogen was removed from around the trap  $T_1$  and stopcock  $S_2$  was opened to the atmosphere.
2. Gas Storage Assembly 1 (Fig. 2): The gas needed for gc calibration purposes was transferred through stopcock  $S_9$  to the gas analysis system. Before the storage bulbs were filled with gases, each gas was freed of air by subjecting it to several trap to trap distillations. The condenser trap, cooled by liquid nitrogen, was pumped on during the distillation to remove non-condensables.

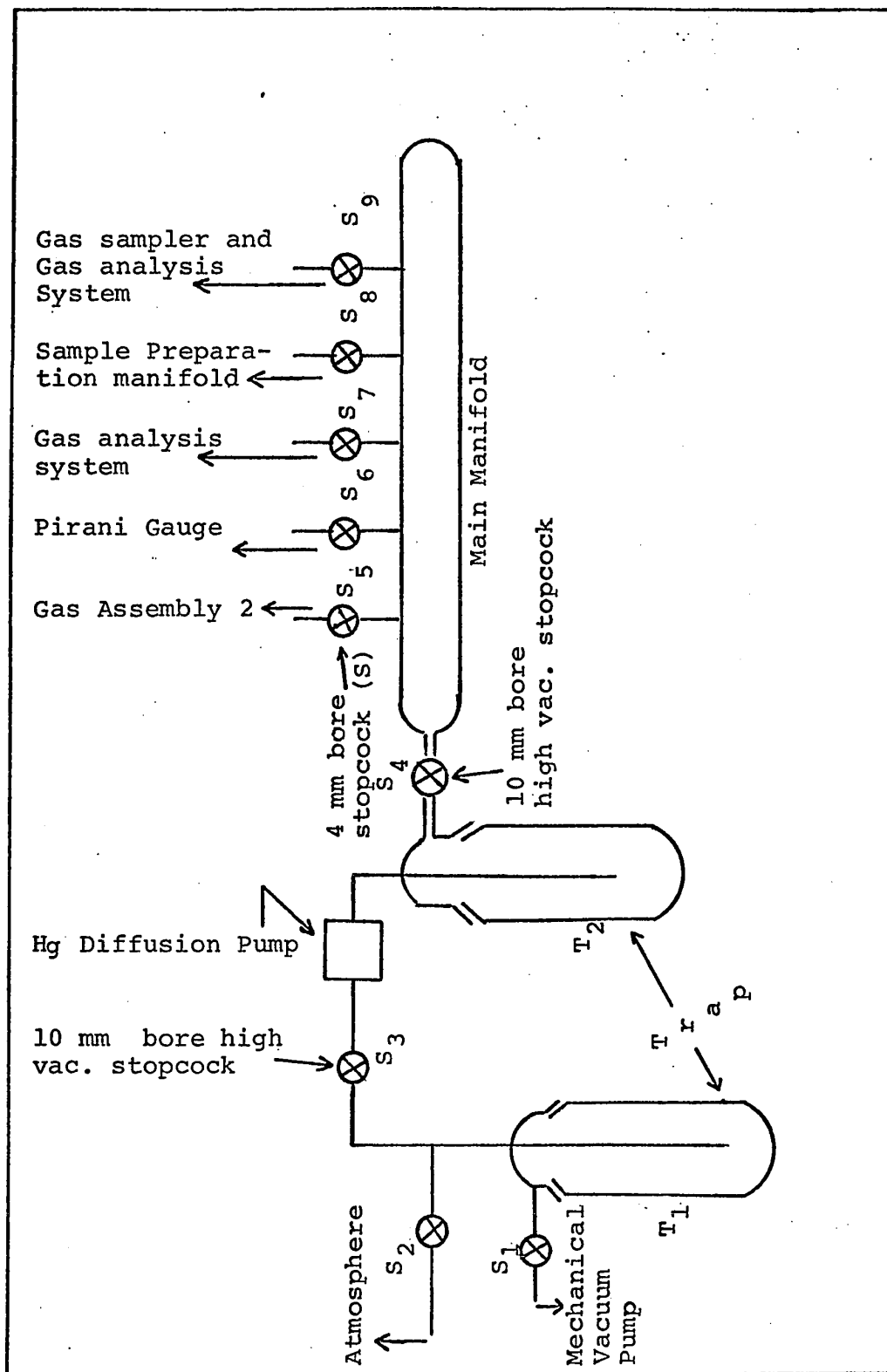


Fig. 1 Main Vacuum Manifold

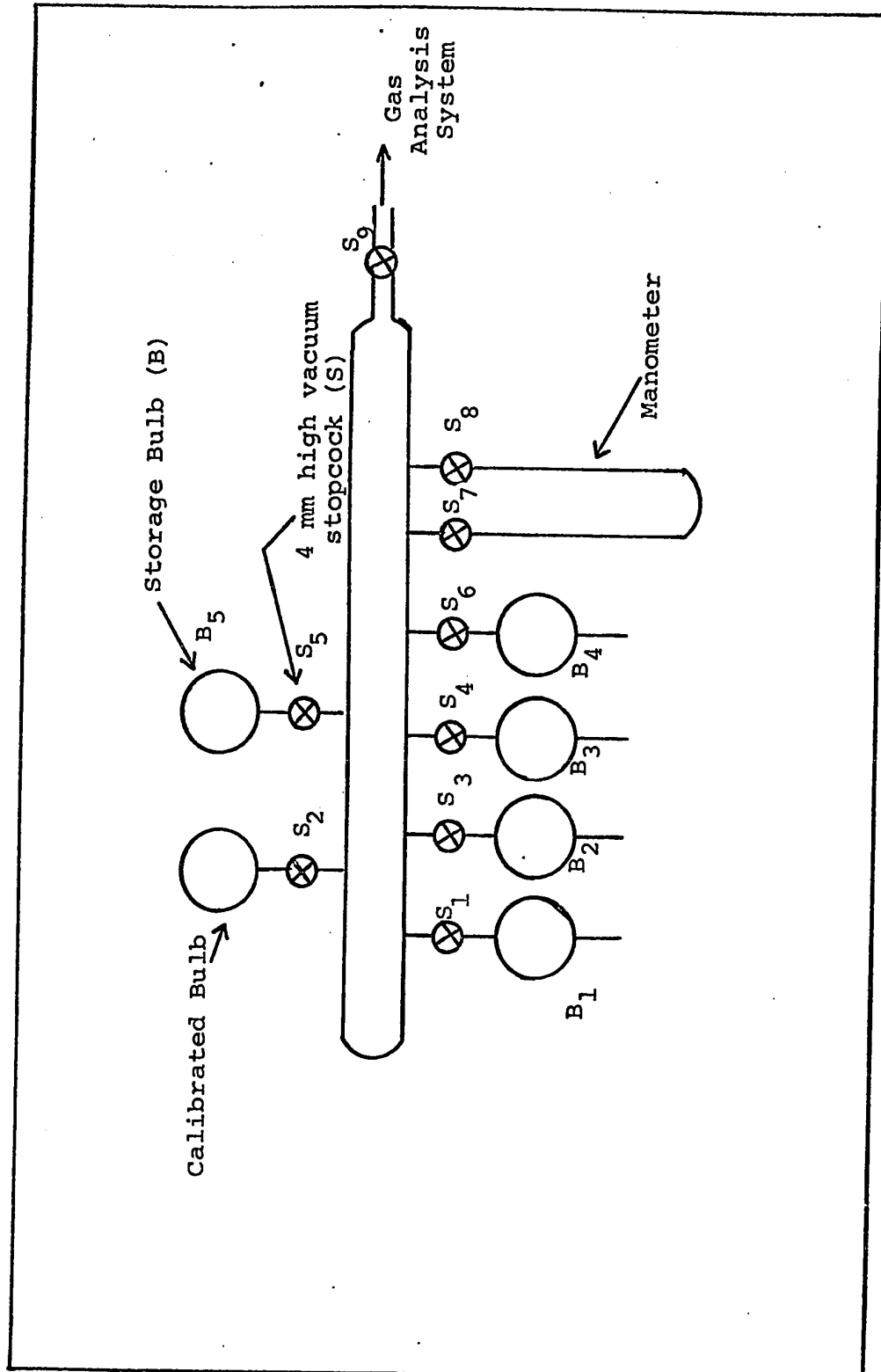


Fig. 2 Gas Storage Assembly 1

3. Gas Storage Assembly 2 (Fig. 3): The gases to be used as additives in the radiolysis study were degassed and stored in the bulbs  $SB_1$ ,  $SB_2$ ,  $SB_3$ .

C. Sample Preparation

1. Sample Preparation Manifold: This manifold is shown in Fig. 4. For diethyl ether storage, the storage bulb (S.B.) was a 1000 ml round bottom flask. For storing ethanol, the storage bulb used was of the type shown in Fig. 5.
2. Irradiation Bulbs: These were 500 ml round bottom Pyrex glass flasks with break seals and filling tubes attached. The break seal was at the end of a 14/20 Standard-Taper inner joint. The bulbs were cleaned with permanganic acid, followed by thorough washing with tap water. They were then rinsed with a dilute solution of nitric acid and hydrogen peroxide and finally several times with double-distilled water. The break seal was then made at the end of the 14/20 Standard Taper inner joint. The irradiation cell was then attached to the vacuum line as shown in Fig. 4. Stopcock  $S.C_3$  was opened to the rough vacuum manifold (not shown in Fig. 4). Water was pumped off the walls of the irradiation cell and the sample preparation line, except the stopcocks, by heating them with a flame and

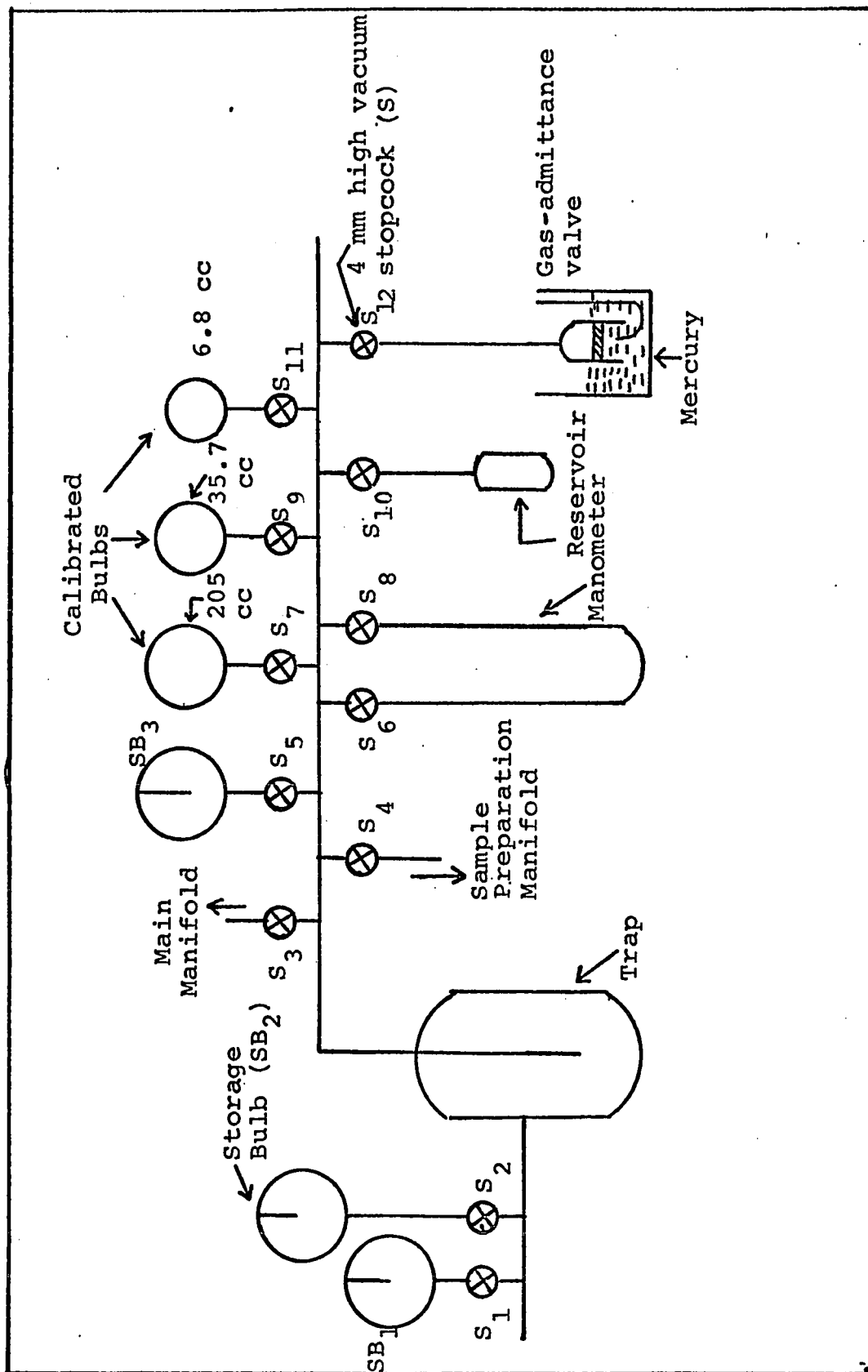


Fig. 3 Gas Storage Assembly 2

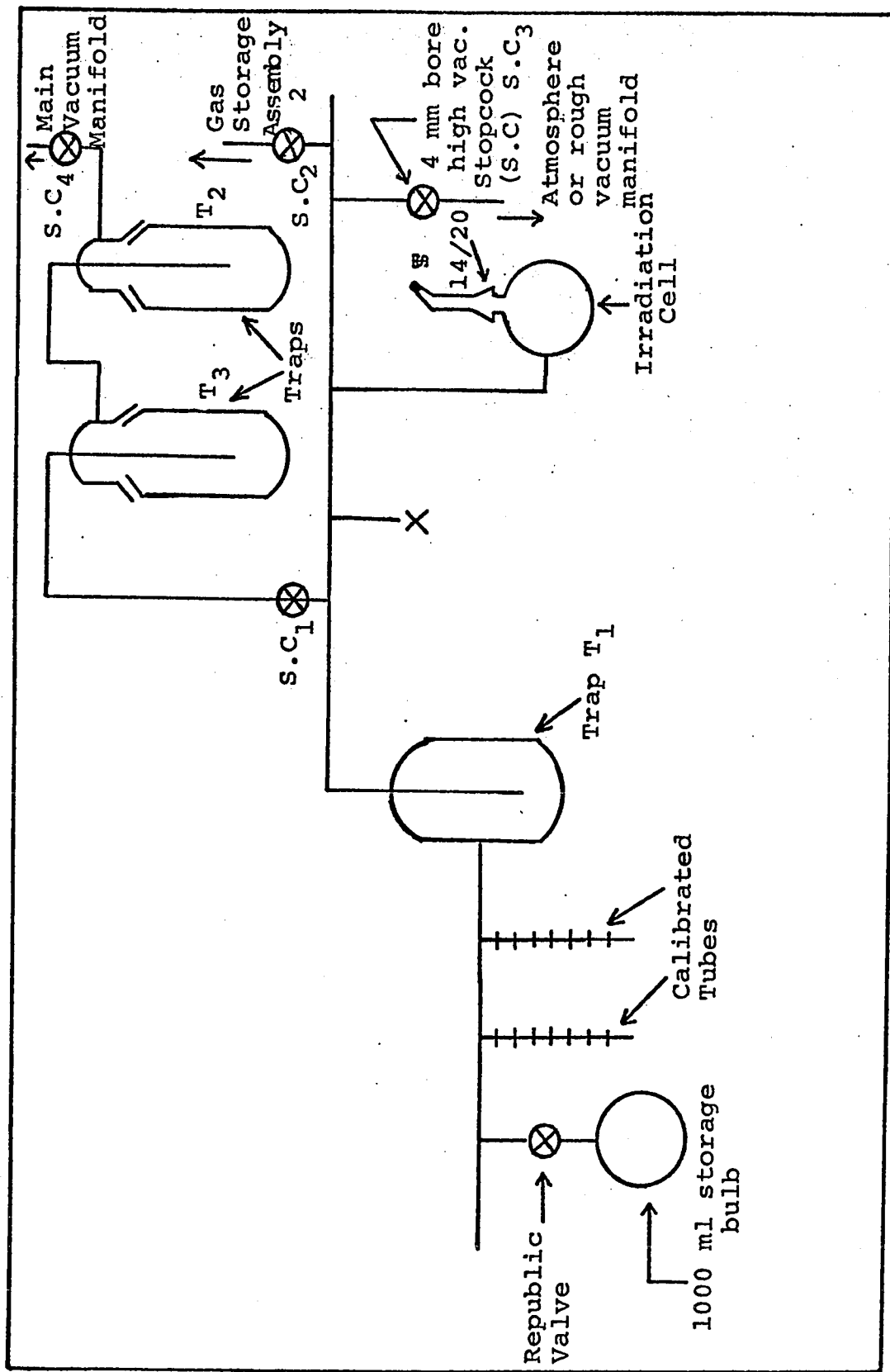


Fig. 4 Sample Preparation Manifold

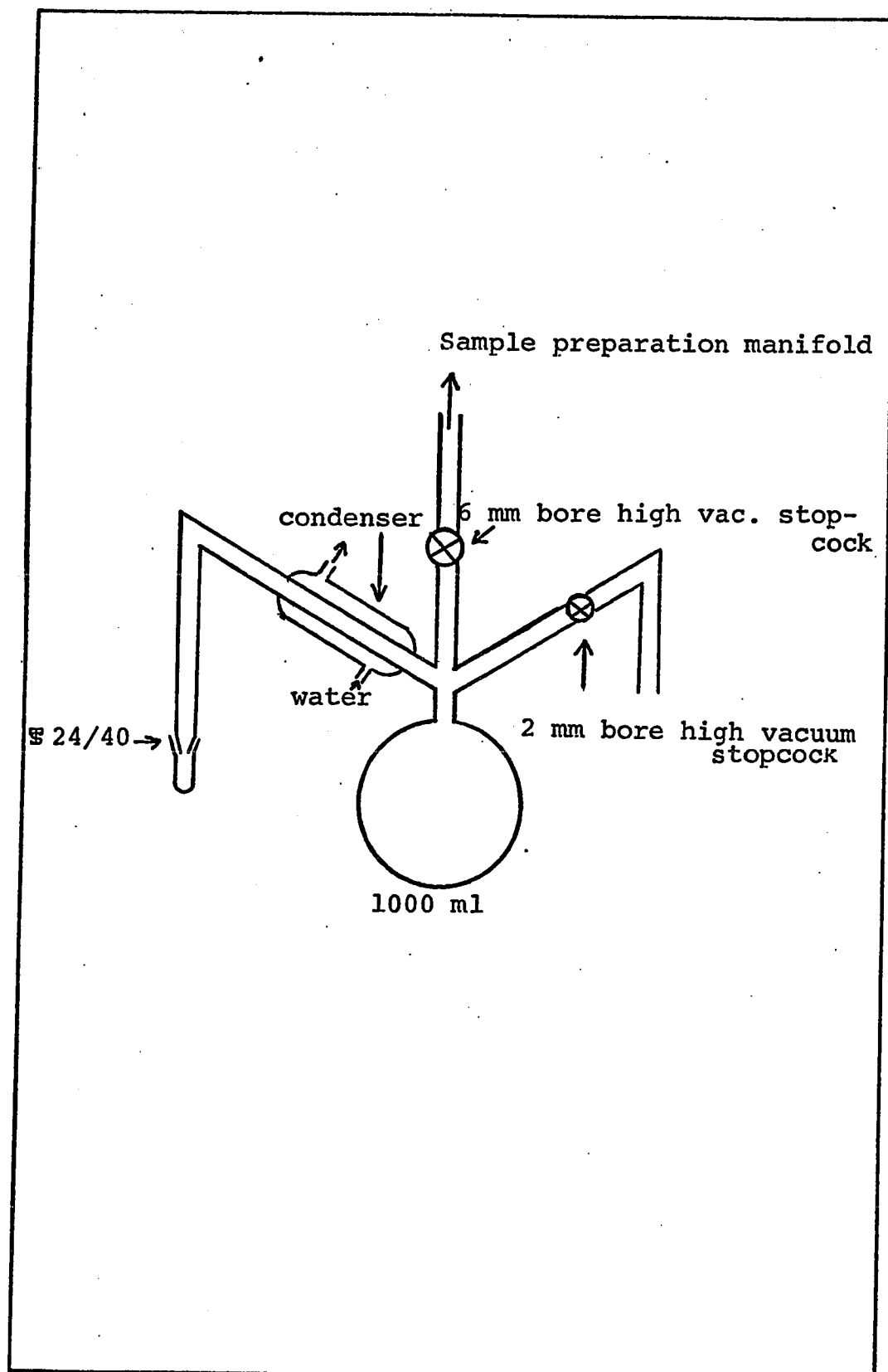


Fig. 5. Storage Bulb for Ethanol



pumping at the same time. Stopcock S.C<sub>3</sub> was then closed and stopcock S.C<sub>1</sub> was opened to the high vacuum side. The bulbs were baked at a temperature of about 450°C, while being evacuated, for 3 - 4 hours before filling.

### 3. Filling the Irradiation Cells

- a. Diethyl ether samples: Diethyl ether was vacuum distilled from the reservoir into the 1 ml calibrated tube, which was immersed in a Dry Ice-acetone slush bath, by opening the Republic valve. The valve was then closed and the desired volume of ether was measured at the temperature of the Dry Ice-acetone slush bath (-83°C). This was then distilled into the trap T<sub>1</sub> (Fig. 4), which was immersed in liquid nitrogen. Trap T<sub>1</sub> was pumped on during the distillation. Traps 2 and 3 were also immersed in liquid nitrogen during sample preparation. Stopcock S.C<sub>1</sub> was then closed and the ether was distilled back into the graduated tube. Trap T<sub>1</sub> was again immersed in liquid nitrogen. Stopcock S.C<sub>1</sub> was opened to the high vacuum side. The sample was distilled into the trap T<sub>1</sub>. This procedure was repeated three times. The sample was then distilled into the irradiation bulb which was finally sealed off from the vacuum line with a flame.

- b. Ethanol samples: Ethanol was vacuum distilled from the reservoir into the 1 ml graduated tube which was immersed in an ethylene dichloride slush bath ( $-35^{\circ}\text{C}$ ). The volume of ethanol was measured at  $-35^{\circ}\text{C}$ . The rest of the procedure adopted for transferring the ethanol into the irradiation bulbs was the same as for the diethyl ether samples.
- c. Ethanol plus gaseous additives ( $\text{C}_3\text{H}_6$ ,  $\text{NH}_3$ ,  $\text{SF}_6$ ): The gas to be used as scavenger was transferred from the storage bulb into the calibrated bulb attached to the gas storage assembly 2 (Fig. 3). The pressure and temperature of the gas was measured. This known amount was then condensed into the irradiation bulb by opening stopcock  $\text{S}_4$  (Fig. 3) to the sample preparation manifold.
- d. Ethanol plus formaldehyde: Formaldehyde was obtained by heating paraformaldehyde under vacuum. Paraformaldehyde was weighed in a break seal tube and was thoroughly degassed using liquid nitrogen as coolant. After degassing, it was sealed off from the vacuum line with a flame and was then attached at point X on the sample preparation manifold (Fig. 4). A known volume of ethanol was distilled into the irradiation cell. The break seal and the glass tubing

connecting it to the irradiation cell were heated by wrapping it with heating tape. The seal was broken. Paraformaldehyde, on heating forms formaldehyde, which then condensed directly into the irradiation cell. The ethanol plus formaldehyde in the irradiation cell were degassed once again and finally the cell sealed off from the vacuum line with a flame.

D. Irradiation of the samples.

1. The samples were irradiated at various temperatures. The irradiation cells were enclosed in a heating mantle. The cells were brought to the desired temperature and the temperature was controlled to  $\pm 1^{\circ}\text{C}$ . The temperature was measured with an iron constantan thermocouple.

The irradiation source was a 12,000 curie Gamma-cell-220 obtained from Atomic Energy of Canada Ltd. The leads for electrical and thermocouple connections were brought into the irradiation chamber through the top of the Gammacell.

2. Dosimetry: Ethylene was used for dosimetry. A 500 ml bulb was filled with a known pressure of ethylene. The amount of ethylene taken into the cell was such that the electron density of the ethylene samples was

approximately the same as that of the ether in ether samples and of the ethanol in ethanol samples. The total yield of the non-condensable gaseous products was measured by a Toepler-McLeod apparatus. The gases were analysed on a Molecular Sieve column. The gas collected at  $-210^{\circ}\text{C}$  (solid nitrogen temperature) contained hydrogen and methane. The amount of hydrogen was calculated by subtracting the methane yield from the total gases. The dose rate value in ethylene, calculated on the basis of  $G(\text{H}_2) = 1.28 (8)$ , was  $4.8 \times 10^{19}$  ev/ghr. To prevent ethylene from entering the McLeod gauge, a solid nitrogen trap was used. The dose rate was calculated as shown below:

$$\text{Dose rate } \left( \frac{\text{ev}}{\text{ghr}} \right) \text{ in ethylene} = \frac{\text{no. of moles of } \text{H}_2 \times 6.023 \times 10^{25}}{1.28 \times \text{Irradiation time} \times \text{no. of grams of ethylene in hrs}}$$

The value for  $G(\text{CH}_4) = 0.07$  was obtained in the radiolysis of  $\text{C}_2\text{H}_4$  at  $25^{\circ}\text{C}$  and at a pressure of 44.67 cms. The dose rate in ethylene was  $4.8 \times 10^{19}$  ev/ghr. This value of  $G(\text{CH}_4) \approx 0.07$  is in good agreement with the value  $G(\text{CH}_4) \approx 0.07$  reported by Dorfman (91). Dose rates  $\left( \frac{\text{ev}}{\text{ghr}} \right)$  in diethyl ether and ethanol were

calculated from the dose rate in ethylene by using Bethe's equation (see Appendix B).

E. Product analysis

1. Gas analysis: The gas analysis system is shown in Fig. 6. After the system was evacuated, the mercury float valve was closed between the diffusion pump and the traps. The irradiated bulb and traps  $T_1$  and  $T_2$  were immersed in liquid nitrogen. Solid nitrogen was prepared in the solid nitrogen trap. The break seal on the irradiated sample was broken. The mercury float valve was then opened. The liquid nitrogen was removed from around the irradiated bulb and the sample was allowed to distill into trap  $T_1$ . During the distillation, the non-condensable gases were collected in the McLeod-Toepler apparatus. Then liquid nitrogen was removed from around the trap  $T_1$  and the sample was allowed to distill into trap  $T_2$ . Pumping with the Toepler pump was continued throughout the distillation. When no more gas was being collected, as shown by a constant reading in the McLeod gauge, the mercury float valve was closed. The pressure and temperature of the gas were measured in a known volume. The total number of moles of gas was calculated. The gas was directly transferred on to the gas chromatographic column by means of the gas sampler (Fig. 9). The gas

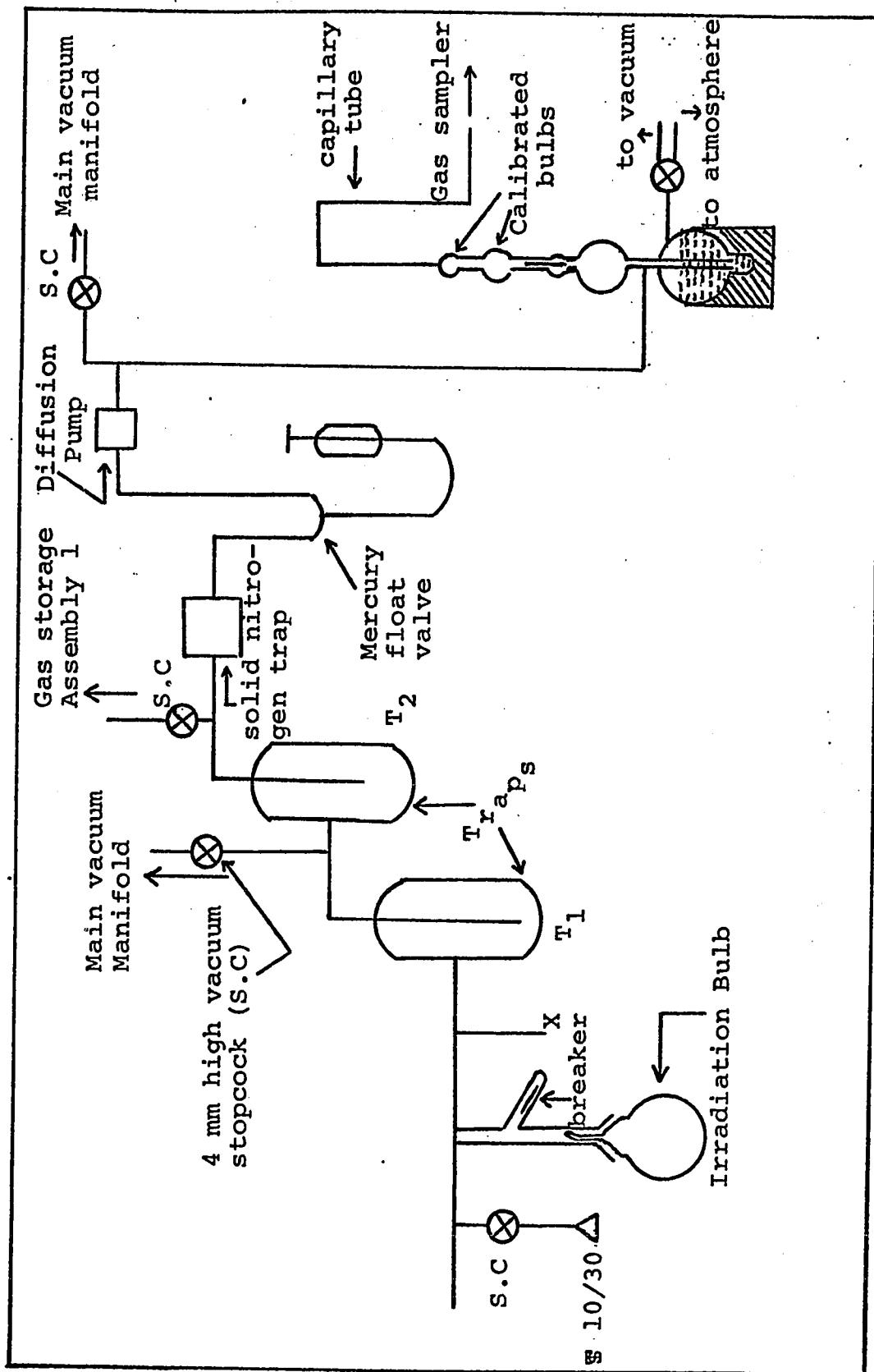


Fig. 6 Gas Analysis System

collected at  $-210^{\circ}\text{C}$  (solid nitrogen temperature) contained hydrogen, methane and carbon monoxide.

The remainder of the gaseous products was removed in a second distillation using an n-pentane slush ( $-130^{\circ}\text{C}$ ) around the traps. In some experiments ethanol slush ( $-112^{\circ}\text{C}$ ) was used in place of n-pentane slush.

The  $\text{C}_2 - \text{C}_4$  hydrocarbons were sometimes analyzed by condensing the entire irradiated sample into a small thin walled bulb and transferring the contents of the bulb directly into the gas chromatographic carrier gas stream using a bulb crushing apparatus.

## 2. Liquid product analysis:

- a. Irradiated diethyl ether samples: After removal of the gaseous products, the remainder of the sample was distilled into a small bulb of the type shown in Fig. 7a, attached to the gas analysis system at X (Fig. 6). The bulb was then sealed off the analysis line with a flame. 50  $\mu\text{l}$  of the liquid was withdrawn by means of a syringe through the Neoprene seal on the side arm of the small bulb and was then injected onto the gas chromatographic column. In most of the cases, separate irradiated samples that had not been used for gas analysis, were used for quantitative determination of the liquid products. While transferring the liquid products into the small bulb (Fig. 7a), freezing of the sample

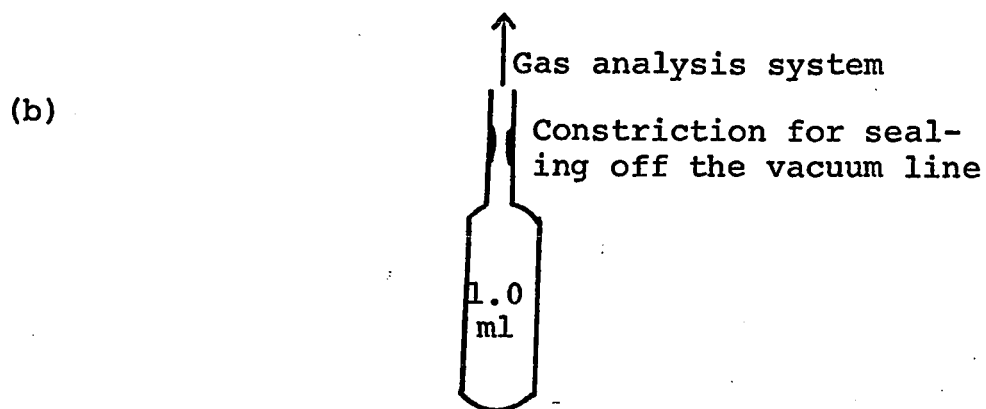
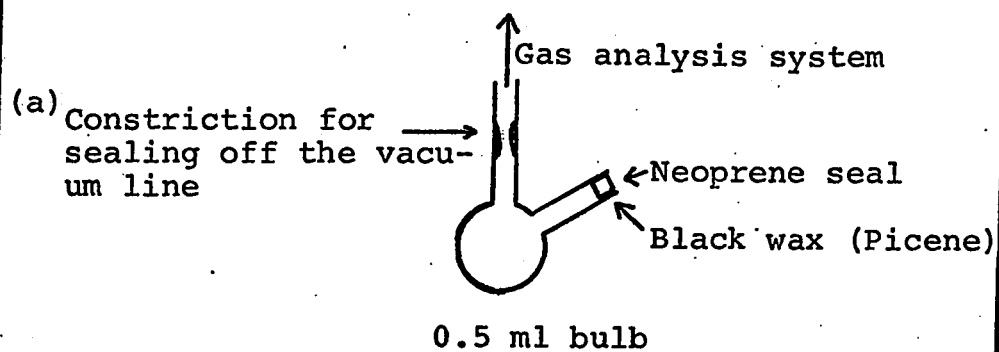


Fig. 7 Liquid Sample Bulbs, for Product Analysis



was avoided, to prevent polymerization of the product aldehydes.

- b. Irradiated ethanol samples: For irradiated ethanol samples, the small bulb used for liquid products collection was of the type shown in Fig. 7b. After the removal of the gaseous products, the remainder of the sample was distilled into the small bulb and this then was sealed off from the analysis line with a flame. In most of the cases, separate irradiated samples were used for liquid product analysis. The gaseous product yields from these samples were not measured and while transferring the liquid products into the small bulb, freezing of the sample was avoided, to prevent polymerization of the aldehyde products. The bulb that had been removed from the gas analysis line was opened and a one microliter aliquot of the liquid was injected into the gas chromatograph equipped with a suitable column for the analysis.
- c. Formaldehyde analysis: Aqueous formaldehyde solution (37 weight percent) from Fischer Scientific Corporation was used for the preparation of the calibrating solutions. The weight percent of formaldehyde in the aqueous solution was checked using the sodium sulphite method (92). Calibration solutions of formaldehyde

with concentrations in the same range as found in the irradiated samples of diethyl ether and ethanol were prepared. The chromotropic acid method was used (80). The method was modified for formaldehyde analysis in diethylether (79).

F. Gas Chromatography

1. Gas Chromatographic Apparatus: The gas chromatographic unit is illustrated in Fig. 8. The thermal conductivity detector with W-2 filaments and the power supply for W-2 filament bridges were manufactured by Gow Mac Instrument Co. A recorder from E. H. Sargent and Co. (Cat. No. S72180) was used. The columns were 2½ meter heated U tubes. When in use, the column was enclosed in a box packed with glass wool. To measure the temperature of the column, an iron-constantan thermocouple was inserted in the effluent end of the column. Helium was the carrier gas. The gas flow was controlled with fine needle valves (Edward High Vacuum Ltd). The flow rate was measured with a bubble flow meter. The drying tube was packed with Molecular Sieve 13X. The detector temperature was kept at 205°C. A detector current of 250 mA was used. Liquid samples were injected directly onto the column at point I using a Hypodermic syringe. The gas samples were transferred by means of the gas

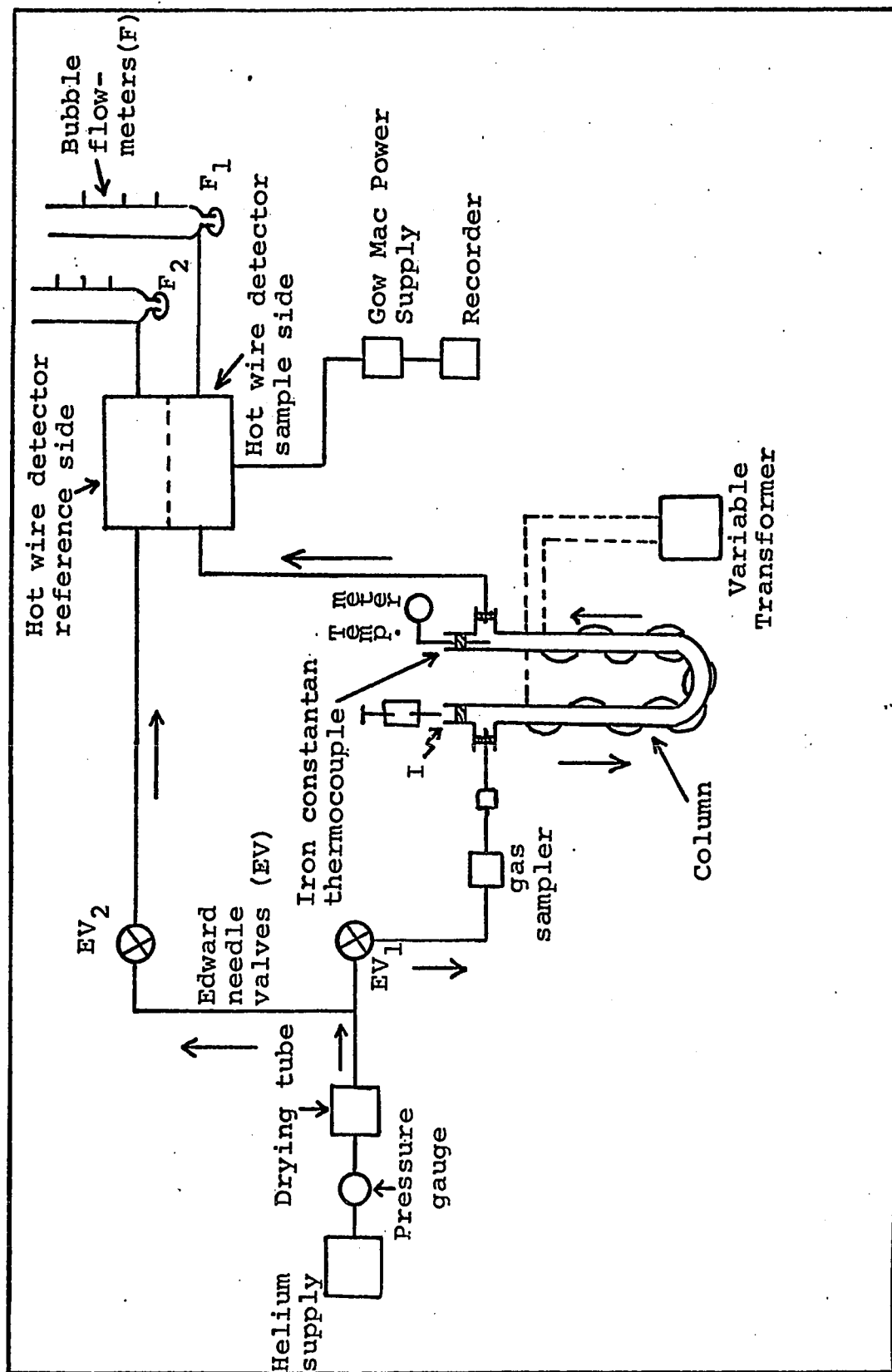


Fig.8 Gas Chromatographic System  
(Thermal conductivity detector)

sampler (Fig. 9).

Two other gas chromatographs (Perkin Elmer Model 881 and F & M Scientific Corp. Model 5750) equipped with flame ionization detectors were used with coiled columns made from Pyrex glass tubing.

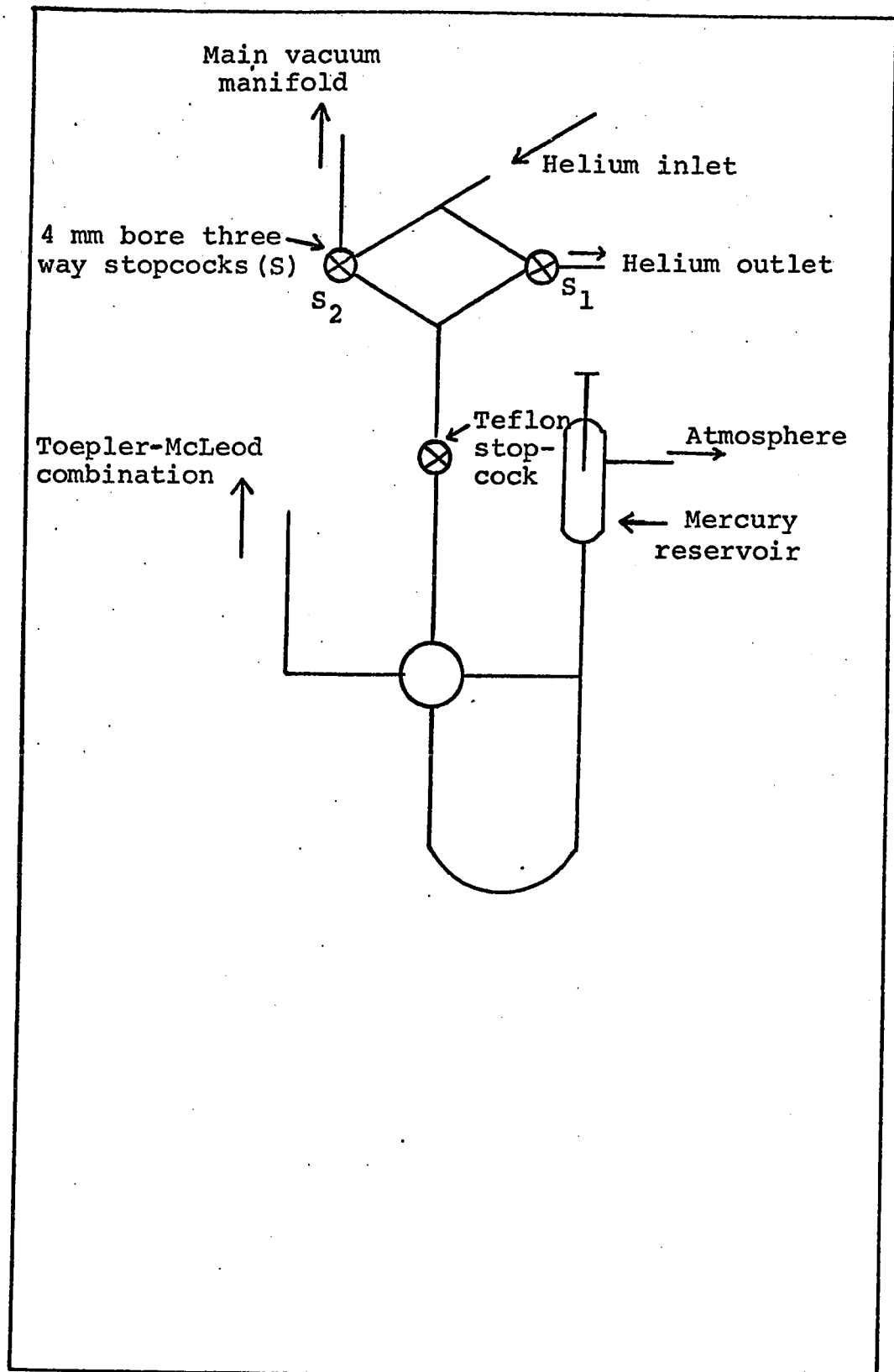


Fig. 9 Gas Sampler

2. Materials used for Gas Chromatographic

Analysis

<u>No</u>	<u>Material</u>	<u>Supplier</u>
1.	Celite-Kromat Ce	Burrell Corporation
2.	Carbowax 4000 on Chromosorb W	F & M Scientific Corp.
3.	Di-2-ethyl hexyl sebacate on Diatoport WAW 60-80 mesh	F & M Scientific Corp.
4.	Molecular Sieve 13 x, 60-80 mesh	F & M Scientific Corp.
5.	Polypak-1, 40-80 mesh	F & M Scientific Corp.
6.	Polypak-2, 40-80 mesh	F & M Scientific Corp.
7.	Porapak T, 80-100 mesh	Waters Assoc., Inc.
8.	Silica gel (Medium activity)	Burrell Corporation
9.	Silicone grease on Diatoport WAW 60-80 mesh	F & M Scientific Corp.
10.	Tetra ethylene glycol dimethyl ether on Diatoport WAW 60-80 mesh	F & M Scientific Corp.
11.	1,2,3, Tris-2-cyanoethoxy propane	F & M Scientific Corp.
12.	Ucon LB 1800 X	Carbide and Carbon Chemicals Ltd.

---

VPC Columns used for Analysis  
Detector - Thermal Conductivity  
Temperature of the Detector - 205°C

3a.

<u>Column</u> (stationary phase concentrations are given in percent by weight)	<u>Temperature</u>	<u>Helium flow rate</u> ml/min	<u>Compounds Separated</u> Relative retention times in parenthesis
1. 2½ meter, molecular sieve 13X, 60-80 mesh	35°C (col. voltage 10)	75	Retention time relative to hydrogen: Retention time for H <sub>2</sub> (0.8 min) Hydrogen (1) Methane (6.88) Carbon monoxide (7.88).
2. 2½ meter, silica gel (medium activity)	25° - 80°C (col. voltage 30 after 9 minutes)	75	Retention time relative to Ethane: Retention time of ethane 2 min. Ethane (1), Ethylene (1.75), Propane (3.35) Acetylene (5), n-butane (8.5)
3. 2½ meter, 2% Apiezon-L on silica gel (medium activity)	25° - 90°C (col. voltage 40 after 3 minutes)	75	Retention time relative to ethane: Retention time for ethane 1 min. 32 sec. Ethane (1), Ethylene (2.12), Propane (3.37) Acetylene (5.43), n-butane (6.52), Propylene (7.06)

cont'd

VPC Columns used for Analysis cont'd

4. 2½ meter, 10% silicone grease column on Diatoport WAW 60-80 mesh.	25-75° (Col. voltage 30 after 10 minutes.)	75	Retention time relative to ethyl ether. Retention time for ethyl ether 2 min. Ethyl ether (1), ethyl isopropyl ether (3.75), sec-butyl ethyl ether (7), ethyl methyl acetal (8.25) acetal (11), 2,3-diethoxybutane (14).
5. 2½, 10% Di-2-ethyl hexyl sabacate on Diatoport WAW (60-80 mesh)	25°	75	Retention time relative to ethyl ether. Retention time for diethyl ether (5 min): acetaldehyde (0.4), diethyl ether (1), ethyl isopropyl ether (1.9), ethanol (2.3).
6. 6½ meter, the first half of which was packed with 10% tetraethylene glycol dimethyl ether on Diatoport WAW and the second half with 25% Ucon LB 1800 X on celite	25°	75	Retention times relative to ethyl ether. Retention time for ethyl ether 11 min: ethyl ether (1), ethyl vinyl ether (1.39), ethyl isopropyl ether (1.64).
7. 2 meter, Porapak-T, 50-80 mesh	135° (col. voltage) 44	75	Retention times relative to ethanol. Retention time for ethanol 11 min 10 secs. water (.37), methanol and acetaldehyde (.46), ethanol (1)



3b.

VPC Columns used for analysis  
Detector-Flame Ionization

Column (stationary phase concent- rations are given in wt. percent.)	Temper- ature	Helium flow rate (ml/min)	Detector temp. (°C)	Injector Compounds separated temp. (°C)	Relative retention times in parenthesis
---	------------------	------------------------------	---------------------------	---	--

1.

2 meter, Poly-  
pak-1, 40-80  
mesh

85-160°C  
The temper-  
ature was  
kept constant  
at 85°C for 7  
minutes and  
then temper-  
ature programmed  
at 16°C/minute  
to 160°C.

Reference  
flow rate  
(60)  
Col. flow  
rate (60)

150

90

Retention times rela-  
tive to ethanol. Re-  
tention time for  
ethanol 7 min. 40 secs.  
methanol (0.48), acet-  
aldehyde (0.68), ethanol  
(1.0), isopropyl alco-  
hol and ether (1.40), n-  
propyl alcohol (1.59),  
sec. butyl alcohol (1.73)  
n-butyl alcohol and  
diethoxy methane (1.95),  
acetal (2.12), ethylene  
glycol (2.21), 1,2-  
propanediol (2.41),  
2,3-butanediol (2.75).

cont'd.....

VPC Columns used for analysis cont'd

2.	2 meter, Poly-pak-2, 40-80 mesh	185°C Isothermal	Ref. flow rate (40) Col. flow rate (40)	200	130	Retention time relative to ethanol. Retention time for ethanol 50 sec. ethanol (1), 1,2-Propanediol (5.8), 1,3-propanediol and 2,3-butanediol (8.9), 1,3-butanediol (13.50), 1,4-butanediol (20.0)
3.	4 meter, the first 2.75 meters were packed with 25% 1,2,3 Tris-2-cyanoethoxy propane on Kromat FB (30-60 mesh) and the next 1.25 meters packed with 10% carbowax 4000 on chromosorb w.	90°C Isothermal	Ref. flow rate (50) Col. flow rate (50)	155	90	Retention time relative to ethanol. Retention time for ethanol 8 min. 25 sec. ethyl ether (.22), acetaldehyde (.47), diethoxy methane (.65), acetal (1.0) ethanol (1.0)

VCP Columns used for analysis

4.

2 meter, Porapak-T, 80-100 mesh	158°C Isothermal	Ref. flow rate (50) Col. flow rate (50)	210	150	Retention time relative to ethanol. Retention time of ethanol 7 min. 40 sec. formaldehyde (.21) methanol (.53) acetal- dehyde (.58) ethanol (1) diethyl ether (1.16) isopropyl alcohol (1.94)
------------------------------------	---------------------	--	-----	-----	--

4. Calibration factors for chromatographic columns.

- a. Gaseous Products: The gas to be calibrated was measured in the Toepler-McLeod apparatus. This was then transferred directly to the gas chromatographic column through the gas sampler (Fig. 9). The number of moles of the gas was calculated using the ideal gas law equation. The area of the peak was measured using the planimeter. The number of moles of the gas was varied and the areas of the peaks were measured. A graph of the number of moles of the gas vs peak area was plotted. The calibration factor ( $\frac{\text{no. of moles}}{\text{area}}$ ) was determined from the slope of the graph. This procedure was repeated for each gas. The calibration factors were checked before each series of samples was analyzed. Typical calibration factors are presented in Table II-1 and are plotted in Figs. II-1 and II-2.
- b. Liquid Products: Calibration solutions of the product compounds, with concentrations in the range found in the irradiated solutions, were prepared. These solutions were prepared in diethyl ether for quantitative analysis of irradiated diethyl ether samples and in ethanol for quantitative analysis of irradiated ethanol samples. A known amount of

TABLE II-1

Typical Calibration Factors for Gaseous Products

Detector - Thermal Conductivity

<u>Compound Calibrated</u>	<u>G.C. Column</u>	<u>Calibration factor: No. of moles area</u>
Methane	Molecular Sieve	$11.42 \times 10^{-10}$
Carbon monoxide	Molecular Sieve	$10.12 \times 10^{-10}$
Ethylene	Silica gel	$9.23 \times 10^{-10}$
Propane	Silica gel	$7.43 \times 10^{-10}$
Ethane	Silica gel	$8.11 \times 10^{-10}$
n-Butane	Silica gel	$5.26 \times 10^{-10}$

---

---

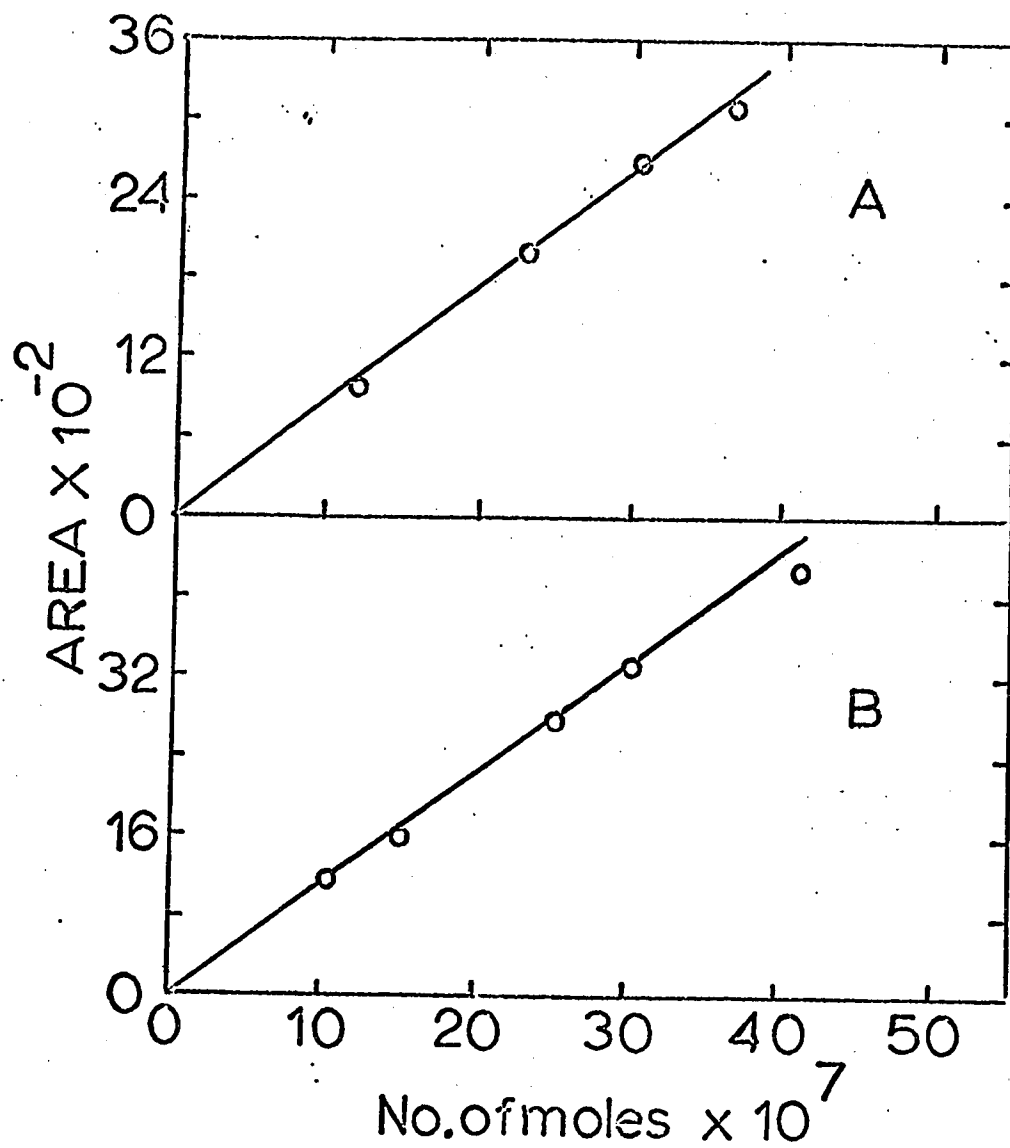


Figure II-1

Representative Gas Chromatographic Calibrations

A. Column = Molecular Sieve  
Compound = Methane

B. Column = Silica gel  
Compound = Ethylene

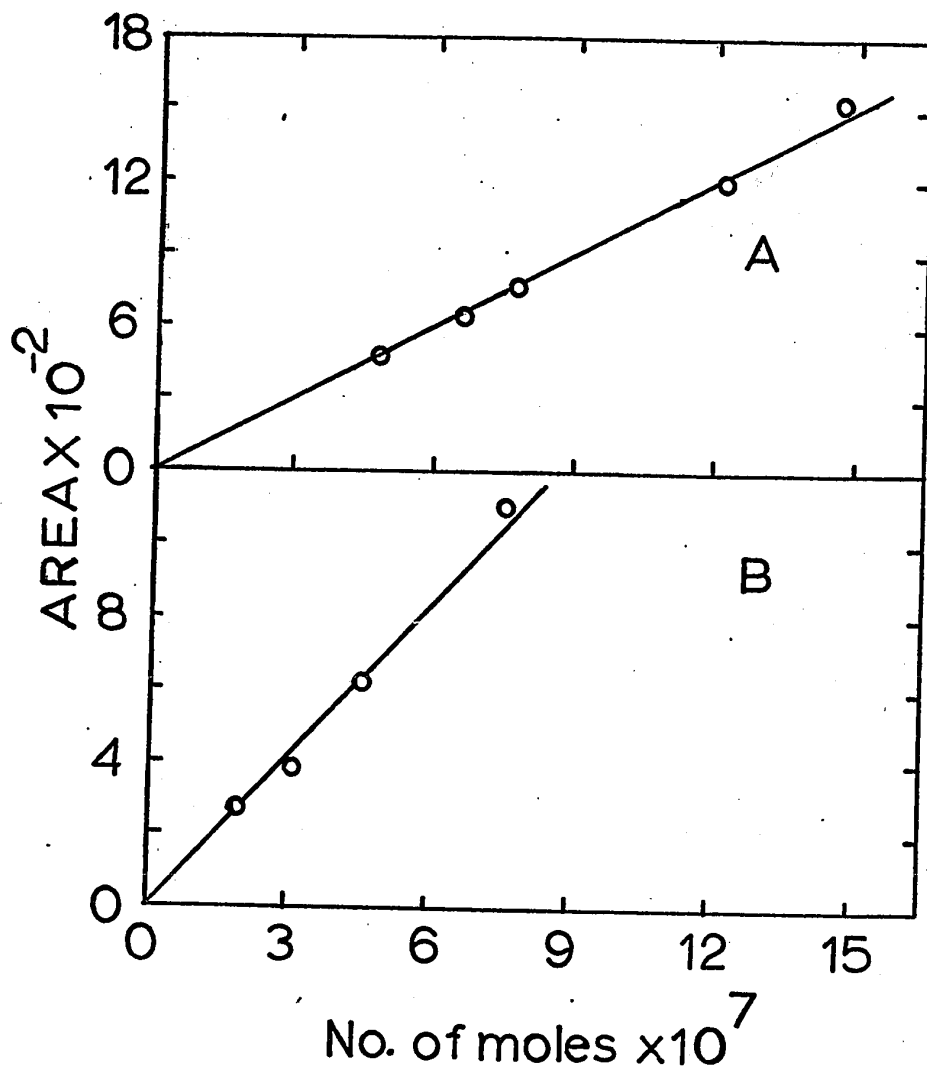


Figure II-2

Representative Gas Chromatographic Calibrations

A. Column = Molecular sieve  
Compound = Carbon monoxide

B. Column = Silica gel  
Compound = Propane

the solution was then injected on the column in the gas chromatograph. The area of each peak was measured with a planimeter. The weight percent of each compound in the calibration solution was calculated and the area percent of the peak corresponding to each compound was also determined. A graph of weight percent vs area percent for each compound was plotted. From the area percent in the irradiated sample the weight percent of the product was read off the graph. The G value was determined using the following formula.

G(Product) =

$$\frac{\text{wt.\%} \times \text{wt of sample(g)} \times 6.023 \times 10^{23} \frac{\text{molecules}}{\text{mole}} \times 100(\text{ev})}{100 \times (\text{Mol.wt})_{\text{Product}} (\text{g/mole}) \times \text{Total dose (ev)}}$$

Calibration factors were determined each time before starting a series of samples. Typical calibration factors are presented in Table II-2 and II-3 and are plotted in Figs. II-3, II-4, II-5, and II-6.



TABLE II-2

Typical Calibration Factors for Liquid Products

(a) Detector - Thermal Conductivity

<u>Compound</u> <u>Calibrated</u>	<u>G.C. Column</u>	<u>Calibration factor</u> <u>No. of moles</u> <u>Area</u>
Acetaldehyde	Di-2 ethyl hexyl sabacate	$7.69 \times 10^{-10}$

(b) <u>Compound</u> <u>Calibrated</u>	<u>G.C. Column</u>	<u>Calibration factor</u> <u>weight percent</u> <u>area percent</u>
---	--------------------	---

Ethyl isopropyl ether	Silicone grease	2.25
sec-butyl ethyl ether	Silicone grease	1.09
Diethoxy methane	Silicone grease	1.11
Acetal	Silicone grease	1.23
2,3 Diethoxy butane	Silicone grease	1.66
Ethyl isopropyl ether	Di-2 ethyl hexyl sabacate	1.50
Ethanol	Di-2 ethyl hexyl sabacate	1.10
Ethyl isopropyl ether	20' column, first 10' packed with tetra ethylene glycol dimethyl ether and last 10' packed with Ucon LB 1800 X on celite	1.64
Ethyl vinyl ether	20' column, first 10' packed with tetraethylene glycol dimethyl ether on Diatoport WAW and last 10' packed with Ucon LB 1800 X on celite	1.31

TABLE II-3

Typical Calibration Factors for Liquid Products

Detector - Flame Ionization

<u>Compound</u> <u>Calibrated</u>	<u>G. C. Column</u>	<u>Calibration Factor</u> <u>Weight %/Area %</u>
Methanol	Polypak-1	1.02
Acetaldehyde	Polypak-1	1.40
Diethyl ether plus isopropyl alcohol	Polypak-1	0.93
sec-butyl alcohol	Polypak-1	0.74
Diethoxy methane	Polypak-1	1.04
Acetal	Polypak-1	1.15
1,2-Propanediol	Polypak-2	1.48
2,3-Butanediol	Polypak-2	2.08
Diethyl ether	1,2,3 Tris-2-cyano- ethoxy propane and carbowax 4000 (Column X)	0.57
Acetaldehyde	Column X	1.21
Diethoxymethane	Column X	0.81
Acetal	Column X	0.76

---

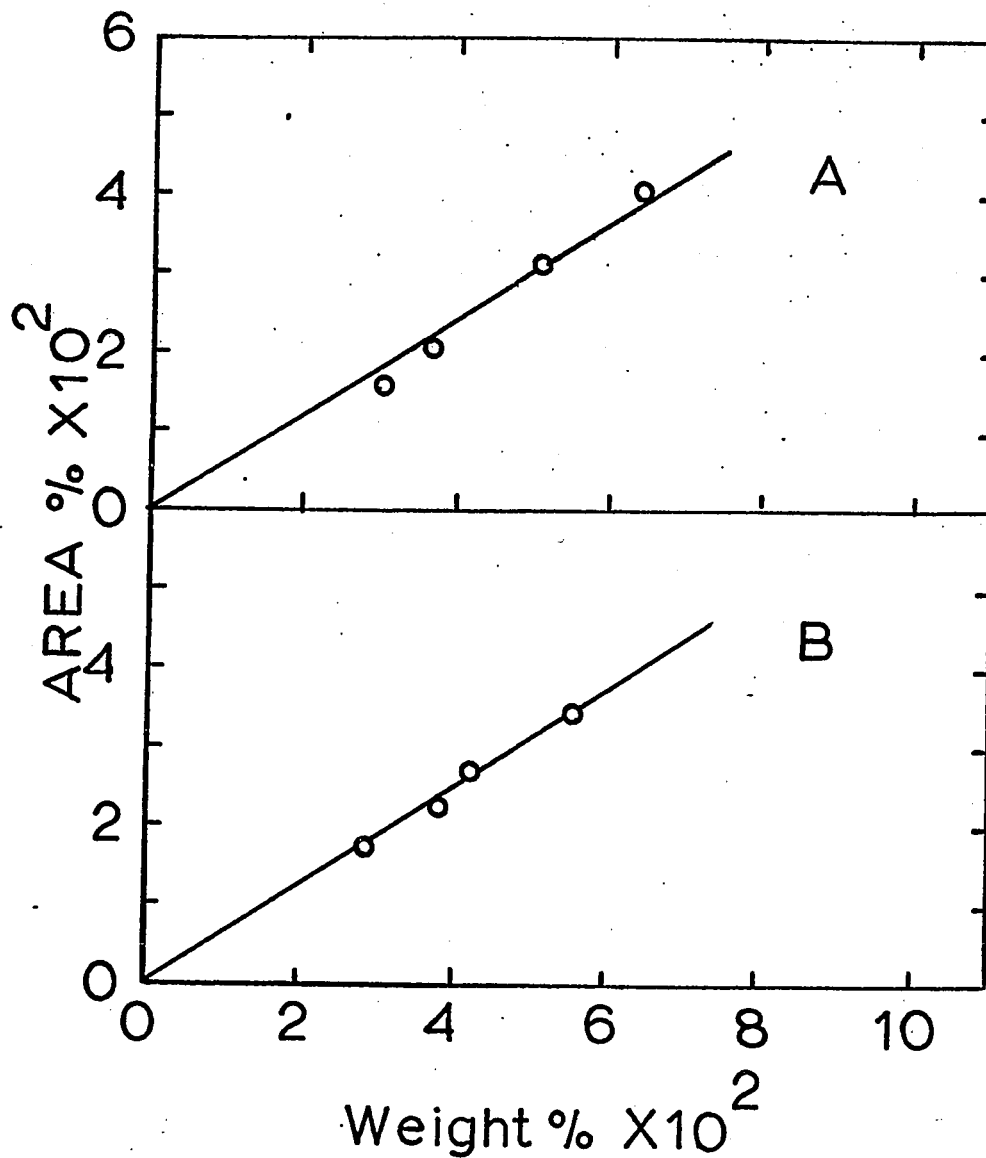


Figure III-3

Representative Gas Chromatographic Calibrations

- A. Column = Silicone grease  
Compound = 2,3-Diethoxybutane
- B. Column = Tetraethylene glycol  
dimethyl ether + Ucon LB. 1800X  
Compound = Ethyl isopropyl ether

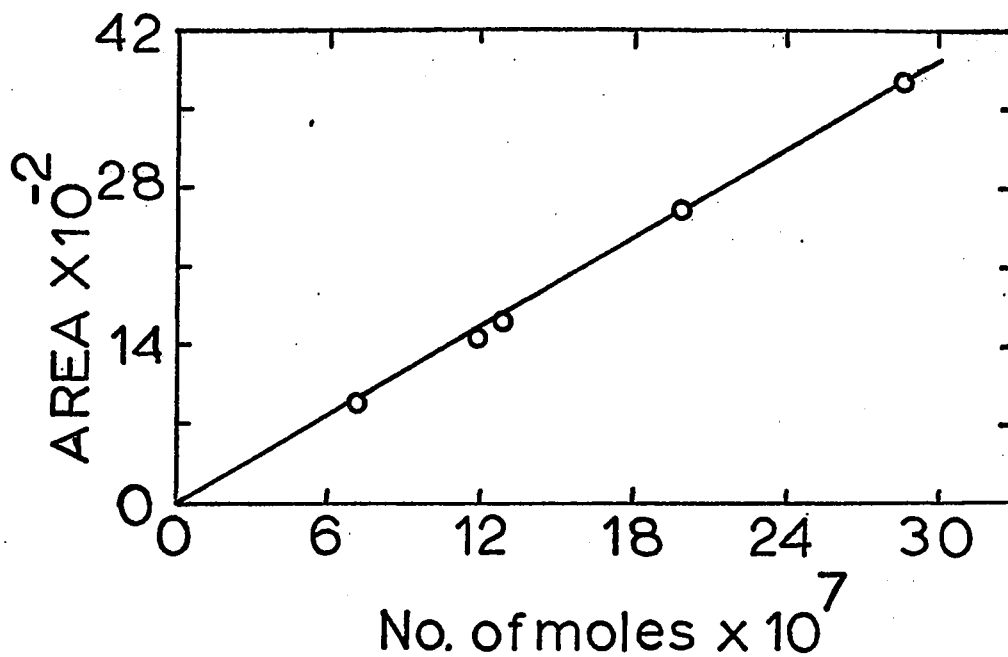


Figure II-4

Representative Gas Chromatographic Calibrations

A. Column = Di-2-ethyl hexyl sebacate

Compound = Acetaldehyde

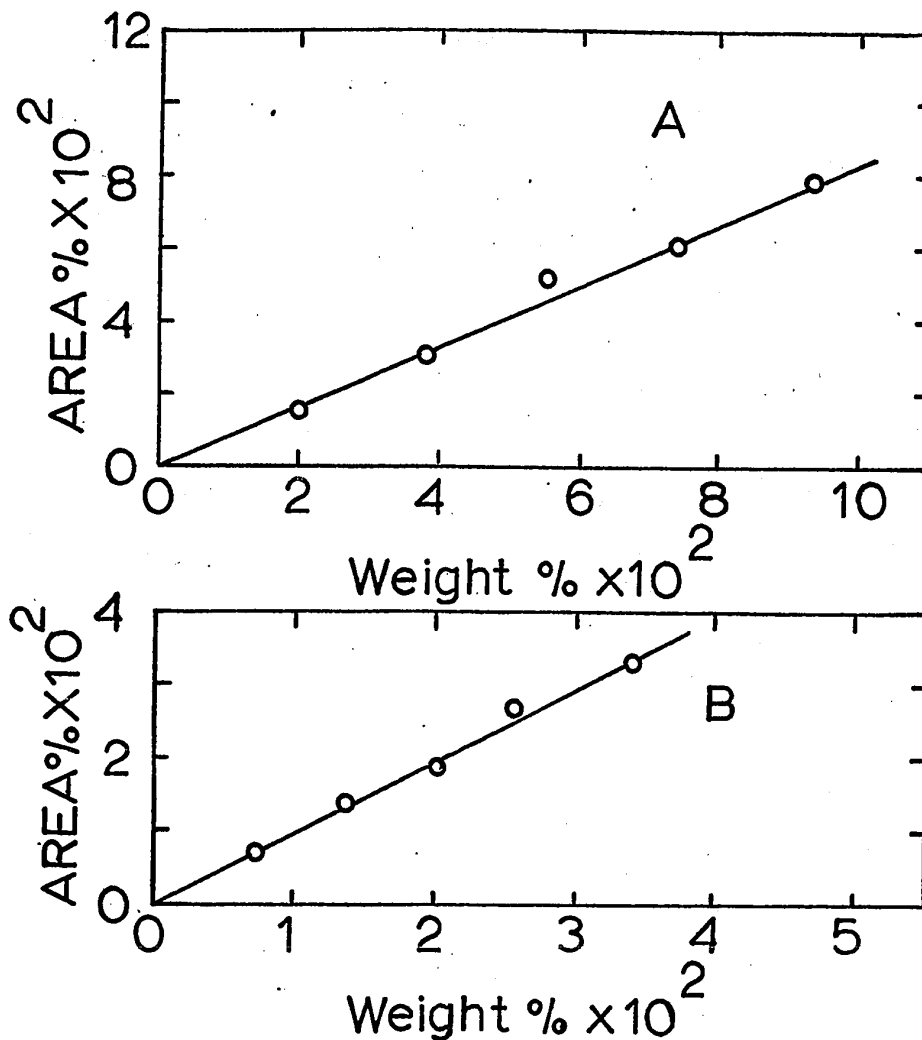


Figure II-5

Representative Gas Chromatographic Calibrations

- A. Column = 1,2,3-Tris-2-cyanoethoxy propane  
Compound = Acetaldehyde
- B. Column = Polypak-1  
Compound = Methanol

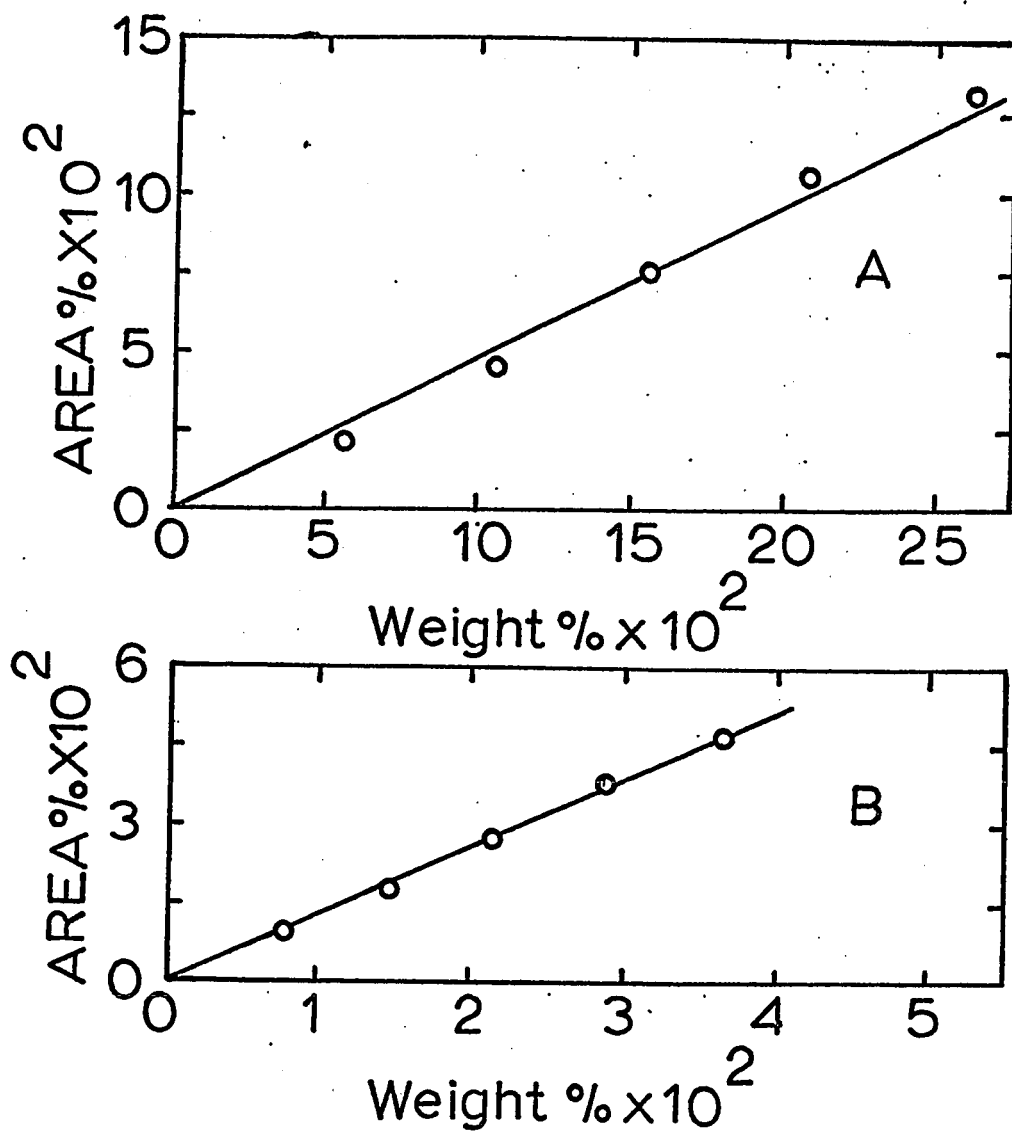


Figure II-6

Representative Gas Chromatographic Calibrations

- A. Column = Polypak-2  
Compound = 2,3-butanediol
- B. Column = 1,2,3,Tris-2-cyanoethoxy  
propane + carbowax 4000  
Compound = Acetal

## R E S U L T S

### Part 1. Vapor Phase Radiolysis of Diethyl ether

#### A. Effect of temperature at constant ether density (1.16 g/l)

Samples of liquid diethyl ether were vaporized into 500 ml bulbs. The temperature at which diethyl ether vapor was irradiated was varied over the range from 33° to 220°. The concentration of diethyl ether was kept constant in all the samples. All samples were irradiated for the same length of time, giving them a dose of  $1.6 \times 10^{20}$  eV/g. The amount of ether in the bulb corresponded to a pressure of 404 torr at 140°.

The G values of the products at 33° are presented in Table III-1 together with the results of an earlier study (79). The agreement between the two sets of results is quite good.

The variation of the G values of products with temperature are presented in Tables III-2 and III-3 and are plotted in Figures III-1, III-2, III-3 and III-4.

The yields of the products ethane, acetaldehyde, methane, carbon monoxide, n-butane, ethylene, formaldehyde and ethanol increase with increase of temperature over the range 33°-220° in the following way: ethane from 0.4 to 202, acetaldehyde from 1.4 to 137, methane from 1.6 to 29.9, carbon monoxide from 0.5 to 29.4, n-butane from 0.1 to 5.1, ethylene from 1.8 to

TABLE III-1

Gas Phase Radiolytic Product Yields at 33°C

<u>Product</u>	<u>This Study</u>	<u>Ref. (79)</u>
Hydrogen	5.85	6.40
2,3-Diethoxybutane	2.12	2.40
Ethylene	1.79	2.10
Acetaldehyde	1.40	1.40
Methane	1.55	1.30
Ethyl isopropyl ether	1.08	1.00
Formaldehyde	0.64	0.90
Ethyl sec-butyl ether	0.78	0.83
Ethanol	0.63	0.65
Ethane	0.40	0.44
Carbon monoxide	0.47	0.40
Ethyl vinyl ether	0.37	0.40
Ethyl methyl acetal	0.34	0.22
Propane	0.22	0.14
Acetal	<0.03	0.09
Acetylene	0.23	0.03
n-butane	0.06	----

---

---



TABLE III-2

Effect of Temperature on the G values of Chain Products in the  $\gamma$ -radiolysis of diethyl ether vapor

Temperature °C	33	50	80	110	125	140	160	180	220
G(ethane)	0.40	0.40	0.96	3.26	---	17.4	39.23	60.84	201.8
G(acetaldehyde)	1.40	1.33	1.74	5.88	6.72	18.19	31.52	57.97	137.1
G(methane)	1.55	1.91	2.57	2.95	3.14	3.51	4.88	7.53	29.90
G(Carbon monoxide)	0.47	0.42	0.44	0.52	0.66	0.87	2.18	4.88	29.44
G(2,3-diethoxy butane)	2.12	2.42	2.93	1.65	1.21	0.56	<0.04	<0.04	<0.04
G(sec-butyl ethyl ether)	0.78	0.98	1.55	2.36	2.69	2.52	1.52	0.84	0.23
G(n-butane)	0.06	0.06	0.21	0.83	-----	2.50	3.62	4.00	5.05

TABLE III-3

Effect of temperature on the G values of non-chain products in the  $\gamma$ -radiolysis of di-ethyl ether vapor.

Temperature °C	33	50	80	110	125	140	160	180	220
G(hydrogen)	5.85	5.77	4.79	4.37	4.31	4.25	4.52	4.62	4.46
G(ethylene)	1.79	1.88	1.77	2.08	-----	2.23	2.68	2.86	2.97
G(ethanol)	0.63	0.45	1.04	1.58	2.26	2.26	2.23	2.32	2.70
G(ethyl isopropyl ether)	1.08	0.82	0.36	0.09	0.13	<0.02	<0.02	<0.02	<0.02
G(formaldehyde)	0.64	0.69	0.53	0.58	-----	0.67	1.10	2.20	-----
G(ethyl methyl acetal)	0.34	0.61	0.73	0.71	0.78	0.72	0.69	0.56	0.38
G(propane)	0.22	0.22	0.14	0.13	-----	0.13	0.09	0.09	0.09
G(acetylene)	0.23	0.23	0.26	0.24	-----	0.24	0.24	0.21	0.17
G(isobutane)	0.03	0.03	0.09	-----	-----	-----	-----	-----	-----
G(acetal)	-----	-----	-----	-----	0.17	-----	0.11	0.09	-----
G(ethyl vinyl ether)	0.37	0.37	0.42	0.42	0.20	0.15	<0.02	<0.02	<0.02

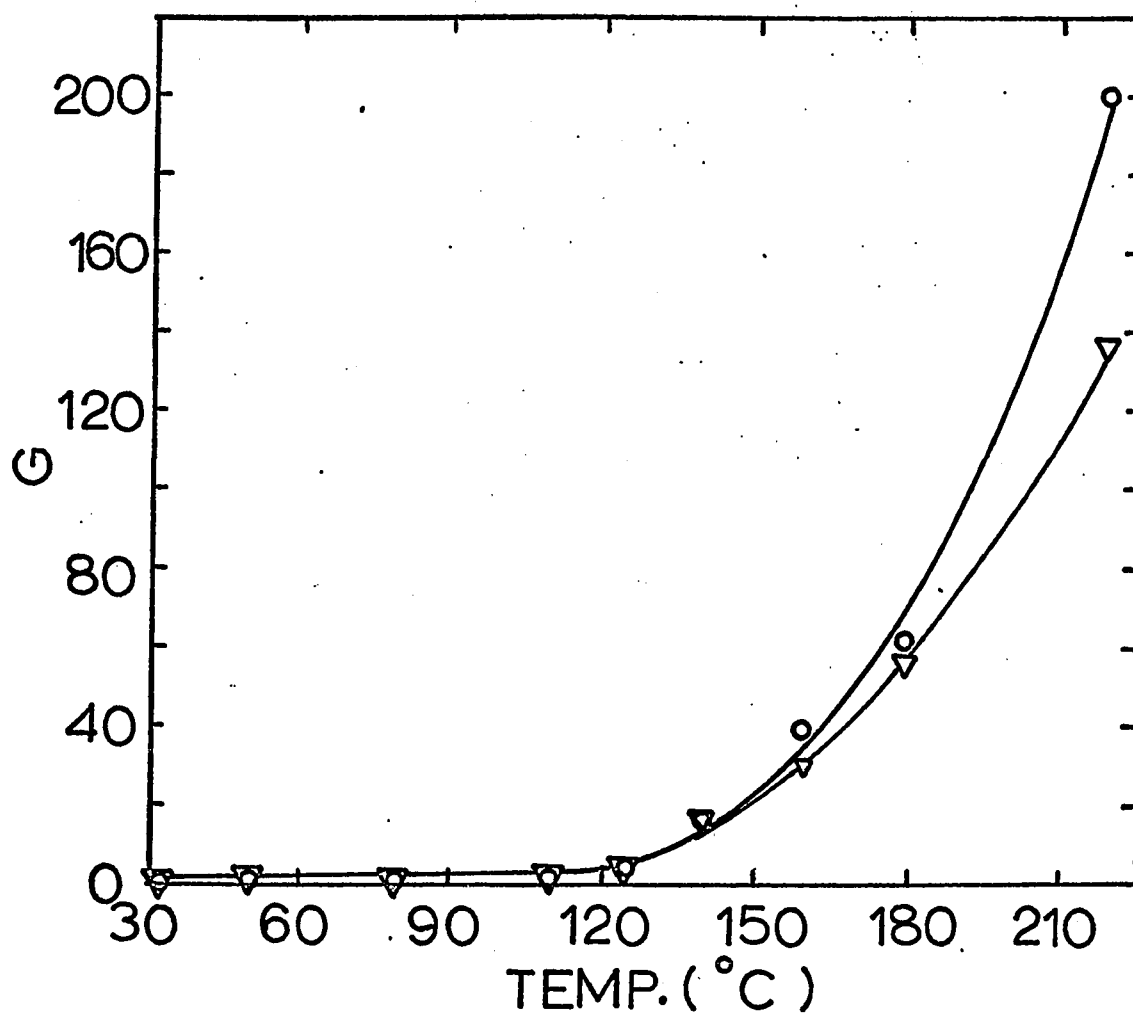


FIGURE III - 1

Products from ether radiolysis as a function of temperature. Ether density = 1.16 g/l.

O Ethane

▽ Acetaldehyde

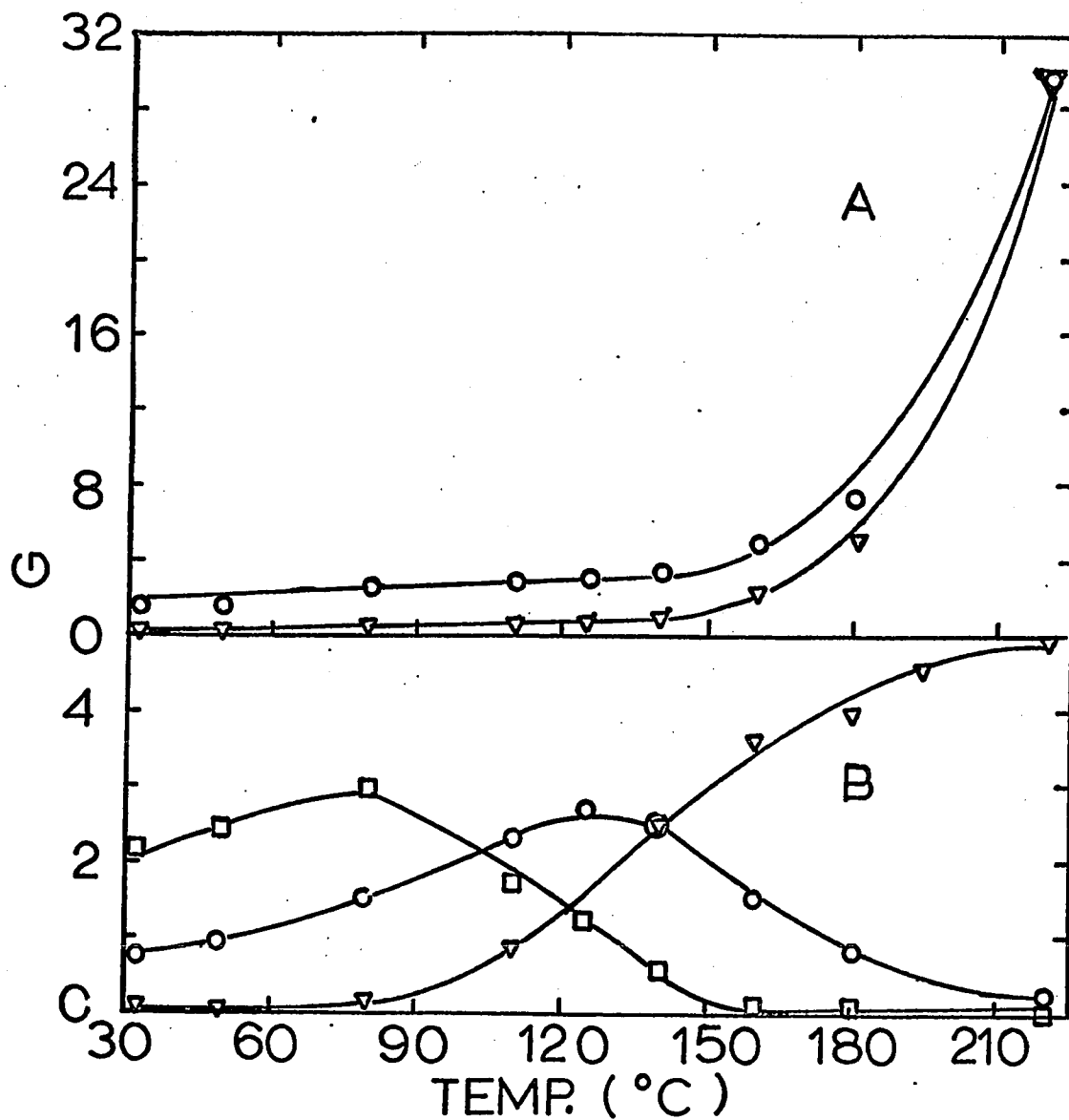


FIGURE III - 2

Products from ether radiolysis as a function of temperature. Ether density = 1.16 g/l.

- A. O Methane
- ∇ Carbon monoxide
- B. O sec-butyl ethyl ether
- 2,3-diethoxybutane
- ∇ n-butane

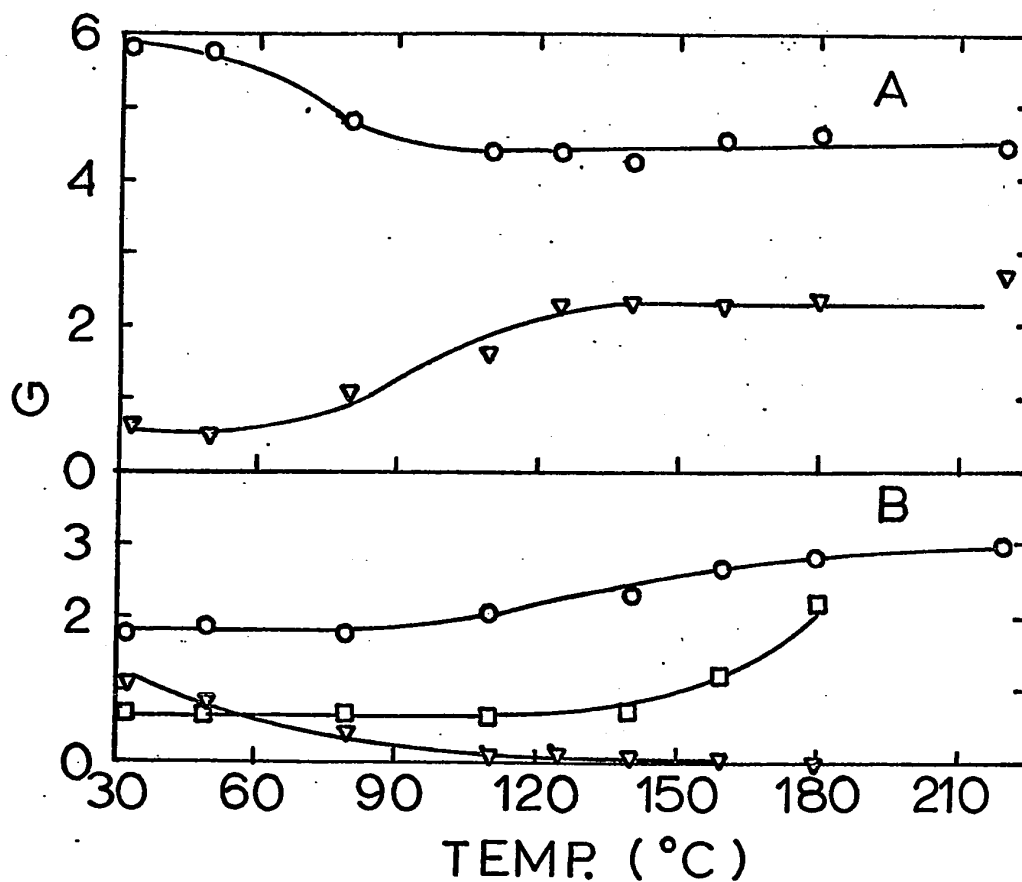


FIGURE III - 3

Products from ether radiolysis as a function of temperature. Ether density = 1.16 g/l

A. O Hydrogen

▽ Ethanol

B. O Ethylene

▽ Ethyl isopropyl ether

□ Formaldehyde

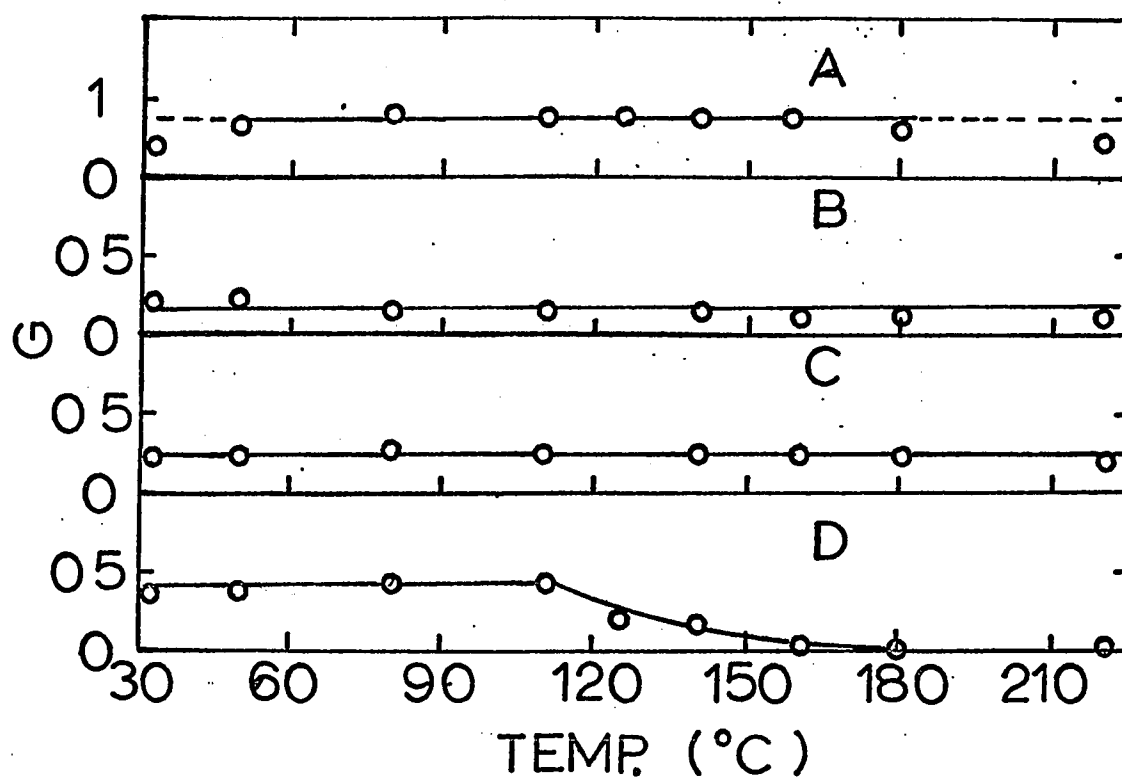


FIGURE III - 4

Products from ether radiolysis as a function of temperature. Ether density = 1.16 g/l.

- A. O Ethyl methyl acetal
- B. O Propane
- C. O Acetylene
- D. O Ethyl vinyl ether

3.0, formaldehyde from 0.6 to 2.2 and ethanol from 0.6 to 2.7. The yields of ethyl methyl acetal, propane and acetylene were unaffected. The yield of 2,3-diethoxy butane increases, at first, from 2.1 at 33° to 2.9 at 80° and then decreases to <0.04 as the temperature is increased from 80° to 220°. The yield of sec-butyl ethyl ether also increases, at first, from 0.8 at 33° to 2.7 at 125° and then decreases to 0.2 as the temperature is increased from 125° to 220°. The yield of hydrogen decreases from 5.9 to 4.5 with increase of temperature.

B. Effect of ether pressure at 140°.

The effect of pressure on the G values of the radiolysis products from diethyl ether vapor was determined over the range 172 to 622 torr (0.50 - 1.78 g/l). The pressure of ether was varied by varying the volume of liquid ether that was vaporized into the irradiation bulb. The pressure was calculated by using the ideal gas law equation. The samples were irradiated to a dose of  $1.6 \times 10^{20}$  eV/g.

The G values of products as a function of pressure are presented in Tables III-4 and III-5 and are plotted in Figures III-5 and III-6. The yields of ethane, acetaldehyde, methane, carbon monoxide, ethyl methyl acetal,

TABLE III-4

Effect of pressure on the chain products in the  $\gamma$ -  
radiolysis of diethyl ether at 140°C

Pressure (torr)	172	288	404	520	622
G(ethane)	n.d.	15.17	17.4	16.14	15.36
G(acetaldehyde)	14.66	17.16	18.19	15.1	17.05
G(methane)	3.36	3.13	3.51	3.29	3.47
G(carbon monoxide)	0.74	0.77	0.87	0.82	0.83
G(2,3 diethoxy- butane)	n.d.	0.18	0.56	0.67	0.78
G(sec-butyl ethyl ether)	1.40	1.94	2.52	2.60	n.d.
G(n-butane)	n.d.	3.06	2.50	2.16	1.80



TABLE III-5

Effect of pressure on non-chain products in the  $\gamma$ -radiolysis  
of diethyl ether vapor at 140°C

Pressure (torr)	172	288	404	520	622
G(hydrogen)	4.61	4.86	4.25	4.27	4.38
G(ethylene)	n.d.	2.10	2.23	2.08	1.78
G(ethanol)	1.98	1.81	2.26	2.94	1.81
G(ethyl isopropyl ether)	<0.02	<0.02	<0.02	<0.02	<0.02
G(formaldehyde)	n.d.	n.d.	.67	n.d.	n.d.
G(ethyl methyl acetal)	0.61	0.72	0.72	0.74	0.67
G(propane)	n.d.	0.16	0.13	0.11	0.10
G(acetylene)	n.d.	0.26	0.24	0.22	0.29
G(acetal)	n.d.	n.d.	n.d.	0.17	0.17
G(ethyl vinyl ether)	n.d.	0.15	0.15	0.10	0.35

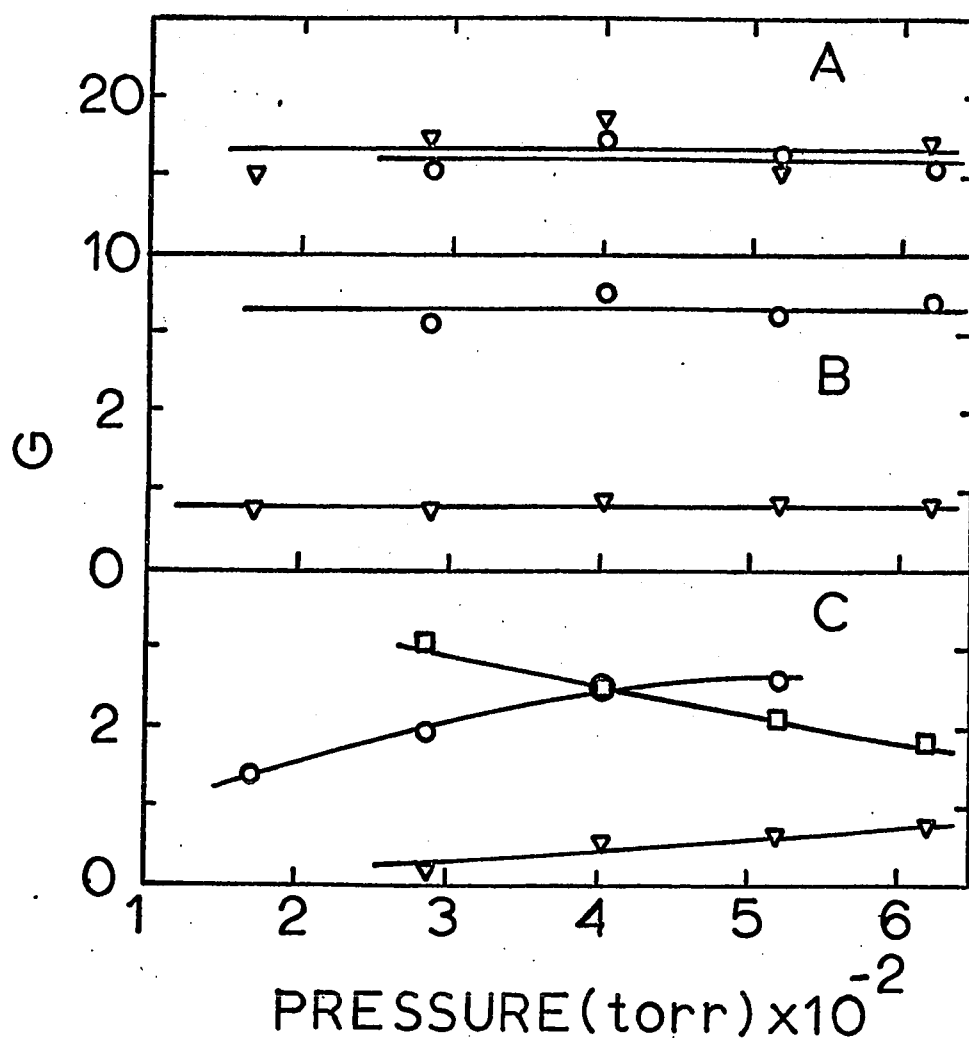


FIGURE III-5

Products from ether radiolysis as a function of pressure. Temperature = 140°C.

- A. O Ethane
- ∇ Acetaldehyde
- B. O Methane
- ∇ Carbon monoxide
- C. □ n-butane
- O Sec-butyl ethyl ether
- ∇ 2,3-diethoxybutane

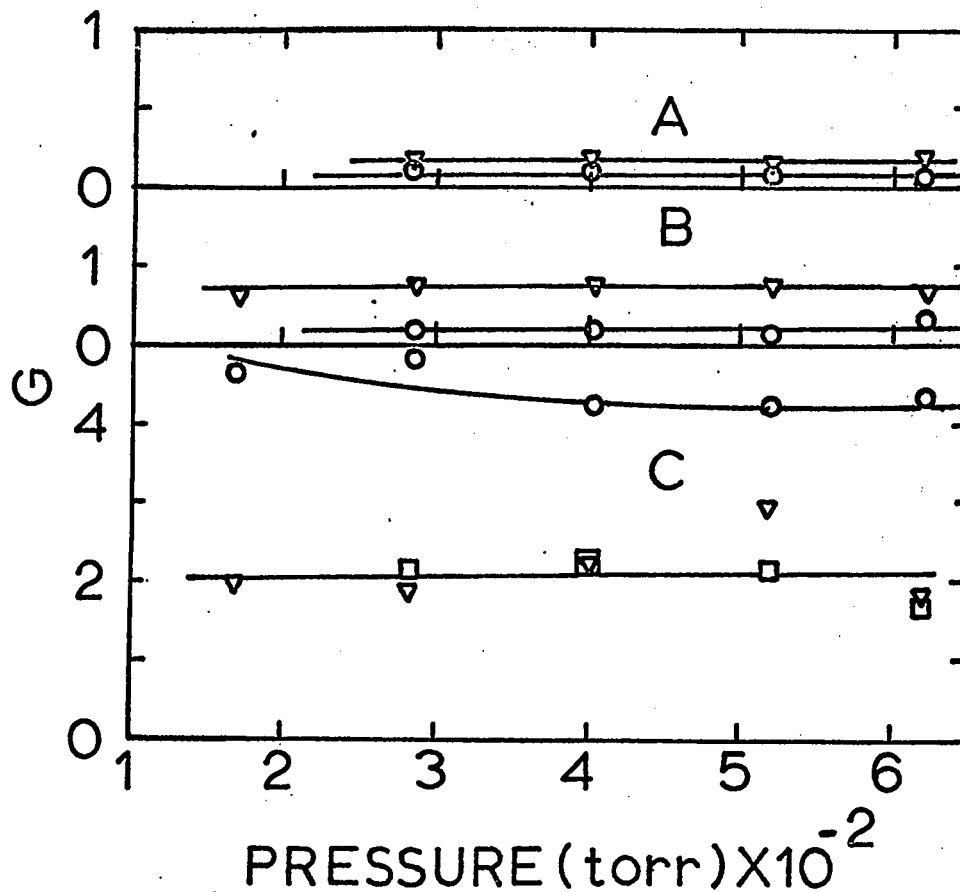


FIGURE III - 6

Products from ether radiolysis as a function of pressure. Temperature = 140°C

- A. O Propane
- ▽ Acetylene
- B. O Ethyl vinyl ether
- ▽ Ethyl methyl acetal
- C. O Hydrogen
- ▽ Ethanol
- Ethylene

propane, acetylene, ethanol and ethylene are unaffected by pressure. The yields of hydrogen and n-butane decrease from 4.70 and 3.1 to 4.2 and 1.80 respectively with pressure. The yields of sec-butyl ethyl ether and 2,3-diethoxybutane increase from 1.40 and 0.2 to 2.60 and 0.8 respectively.

Part II Vapor Phase Radiolysis of Ethanol.

A. Effect of temperature at constant density of ethanol.

1. Density of ethanol 0.66 g/l

Samples of liquid ethanol were vaporized into 500 ml irradiation cells and irradiated to a dose of  $1.3 \times 10^{20}$  eV/g. The temperature was varied over the range 60° to 375°. The amount of ethanol in the irradiation cell corresponded to a pressure of 385 torr at 150°.

The variation of the G values of the products with temperature is presented in Tables III-6 and III-7 and Figures III-7, III-8, III-9 and III-10. The G value of water was only measured at two temperatures, 350° and 375°, and is also presented in Table III-6.

Below 260°, temperature had only a small effect on the yields of hydrogen, acetaldehyde, methane, carbon monoxide, ethylene, formaldehyde, water and methanol. The yields increased rapidly as the temperature was increased above 260°. Over the range 260° to 375°, the yields increased in the following way: hydrogen from 8.9 to 90.4, acetaldehyde from 7.1 to 119.3, methane from 6.3 to 81.6, carbon monoxide from 1.1 to 29.6, and ethylene from 1.9 to 40.9. Below 260°, no detectable peak for methanol was observed. The G values of methanol and diethyl ether increase from 3.3 and 1.0 to 45.0 and 15.9 respectively as the temperature is increased

TABLE III-6

Yield of Products from ethanol radiolysis as a function of temperature  
 Density of ethanol = 0.66 g/l

Temp. (°C)	60	80	110	140	150	170	200	230	260	290	320	350	375
Product	G												
H <sub>2</sub>	7.74	8.21	8.45	8.64	8.49	9.00	8.78	8.81	n.d.	11.16	16.39	45.86	90.4
CH <sub>3</sub> CHO	2.43	2.95	3.79	n.d.	3.76	3.63	3.86	4.64	7.14	9.2	21.88	41.75	119.3
CH <sub>4</sub>	1.37	1.82	2.69	n.d.	3.00	2.92	3.83	4.94	n.d.	10.22	16.93	38.92	81.58
CO	0.46	0.57	0.65	0.67	0.75	0.61	0.71	0.87	n.d.	1.37	2.56	9.77	29.62
CH <sub>3</sub> OH	---	---	---	---	---	---	---	---	2.67	3.27	4.89	17.0	45.0
HCHO	n.d.	n.d.	n.d.	n.d.	n.d.	n.d.	n.d.	3.03	n.d.	3.03	10.42	12.86	14.32
C <sub>2</sub> H <sub>4</sub>	1.21	1.22	.91	1.30	1.05	1.62	1.4	1.86	n.d.	3.77	6.81	19.78	40.88
H <sub>2</sub> O	n.d.	n.d.	n.d.	n.d.	n.d.	n.d.	n.d.	n.d.	n.d.	n.d.	n.d.	65.0	75.6
C <sub>2</sub> H <sub>6</sub>	0.24	0.24	0.14	0.33	0.28	0.48	0.68	0.96	---	1.25	1.53	3.45	7.52
C <sub>2</sub> H <sub>5</sub> OC <sub>2</sub> H <sub>5</sub>	---	---	---	---	0.17	---	---	---	1.21	0.95	1.10	5.60	15.85

n.d. - not determined

TABLE III-7

Yield of products from ethanol radiolysis as a function of temperature

Density of ethanol = 0.66 g/l

Temp. (°C)	60	80	110	140	150	170	200	230	260	290	320	350	375
Product	G												
C <sub>3</sub> H <sub>8</sub>	0.04	0.02	n.d.	n.d.	n.d.	n.d.	n.d.	n.d.	n.d.	0.02	0.02	0.12	0.27
C <sub>2</sub> H <sub>2</sub>	0.21	0.21	0.10	n.d.	n.d.	0.10	0.1	0.1	n.d.	n.d.	n.d.	n.d.	n.d.
n-C <sub>4</sub> H <sub>10</sub>	0.01	0.01	0.02	n.d.	0.01	0.01	0.01	0.02	n.d.	0.09	0.08	0.03	0.23
Diethoxy methane	---	---	---	---	---	---	---	---	0.10	0.12	0.21	0.66	0.43
Acetal	---	---	---	---	---	---	---	---	0.27	0.12	0.21	0.48	0.40
1,2-Propane-diol	0.40	0.37	0.40	---	0.34	0.30	0.36	0.40	1.38	1.48	1.66	2.42	1.82
2,3-butane-diol	2.44	2.60	2.64	---	2.70	3.04	3.37	3.40	2.33	2.49	1.91	0.61	---
1,3-butane-diol	---	---	---	---	---	---	---	---	1.80	1.64	---	---	---
Isopropyl alcohol	---	---	---	---	---	---	---	---	---	---	---	<0.4	<0.4
sec-butyl alcohol	---	---	---	---	---	---	---	---	0.51	0.55	1.18	2.84	1.59
n-butyl alcohol	---	---	---	---	---	---	---	---	0.1	0.1	0.1	0.1	0.1

n.d. - not determined

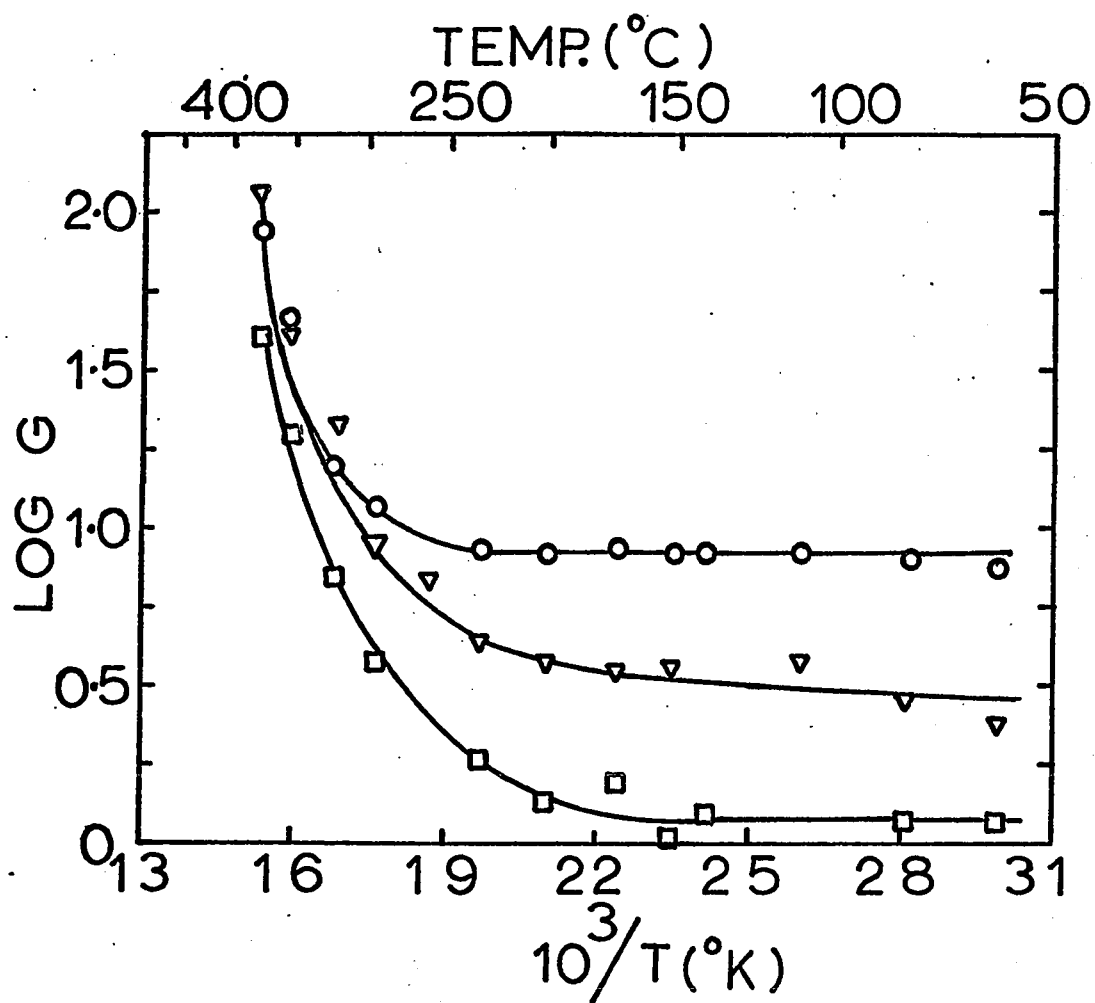


FIGURE III - 7

Products from ethanol radiolysis as a function of temperature. Ethanol density = 0.66 g/l.

- O Hydrogen
- ▽ Acetaldehyde
- Ethylene



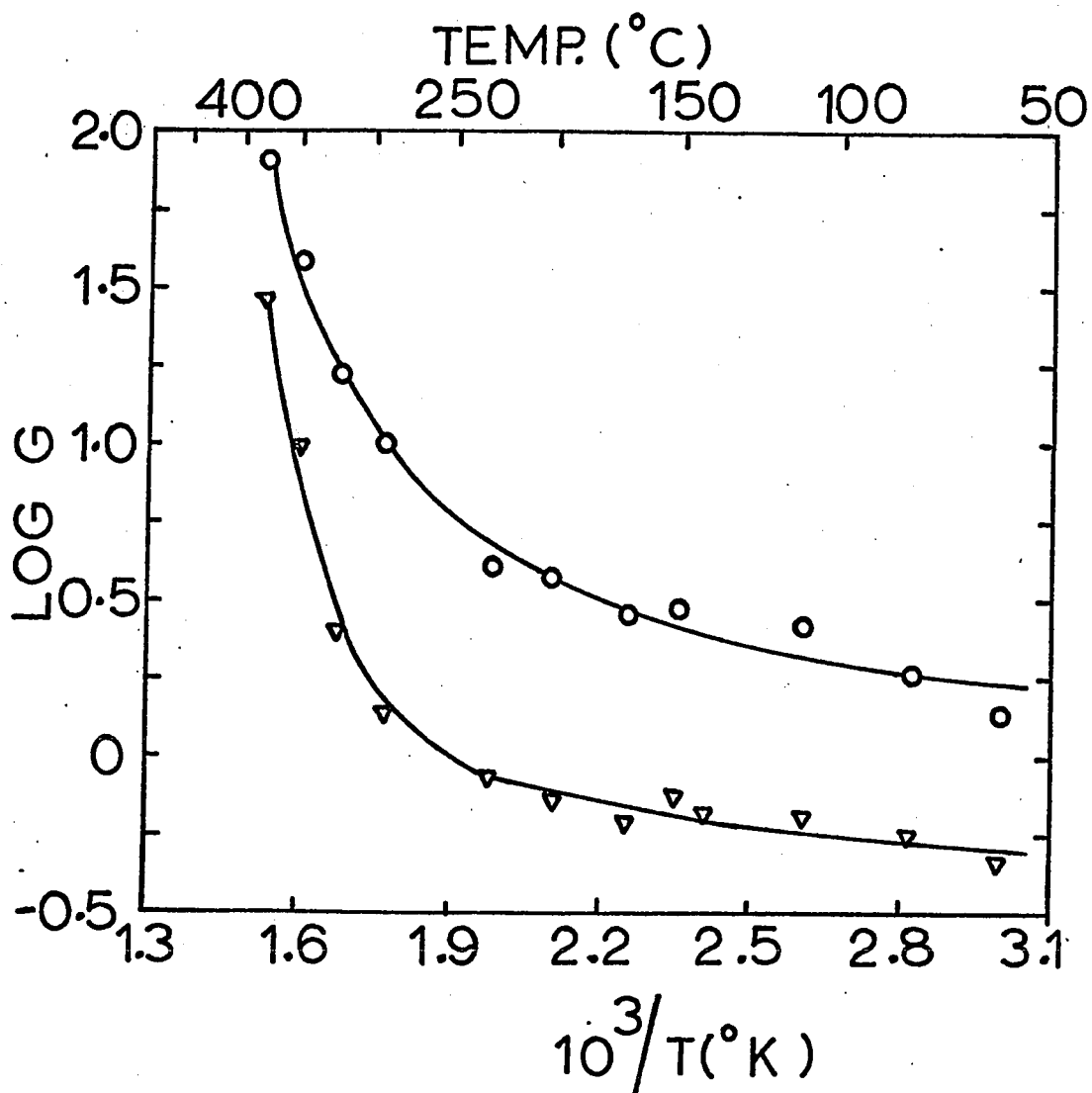


FIGURE III - 8

Products from ethanol radiolysis as a function of temperature. Ethanol density = 0.66 g/l.

O Methane

▽ Carbon monoxide

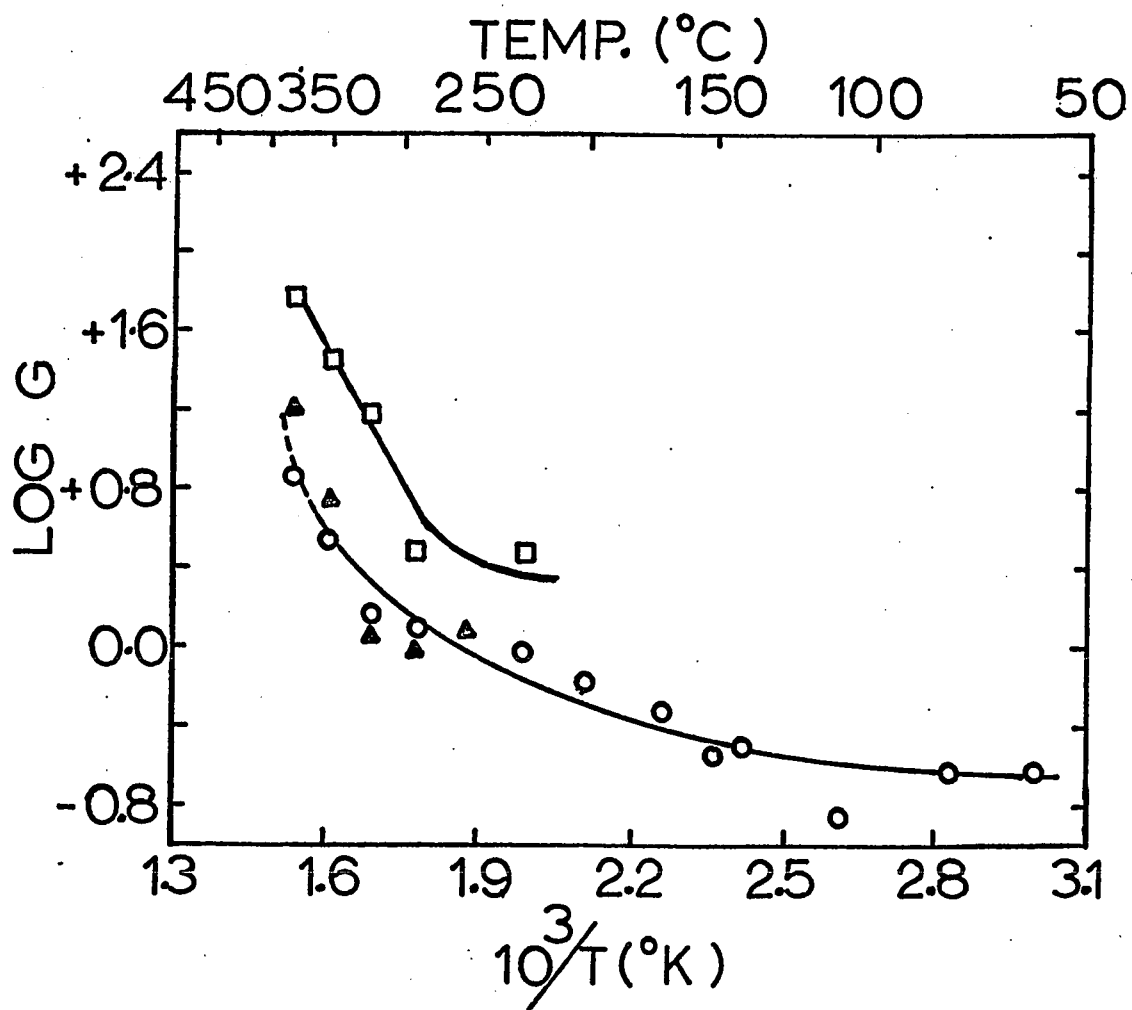


FIGURE III - 9

Products from ethanol radiolysis as a function of temperature.

Ethanol density = 0.66 g/l

○ Ethane

Δ Diethyl ether

□ Formaldehyde + Methanol

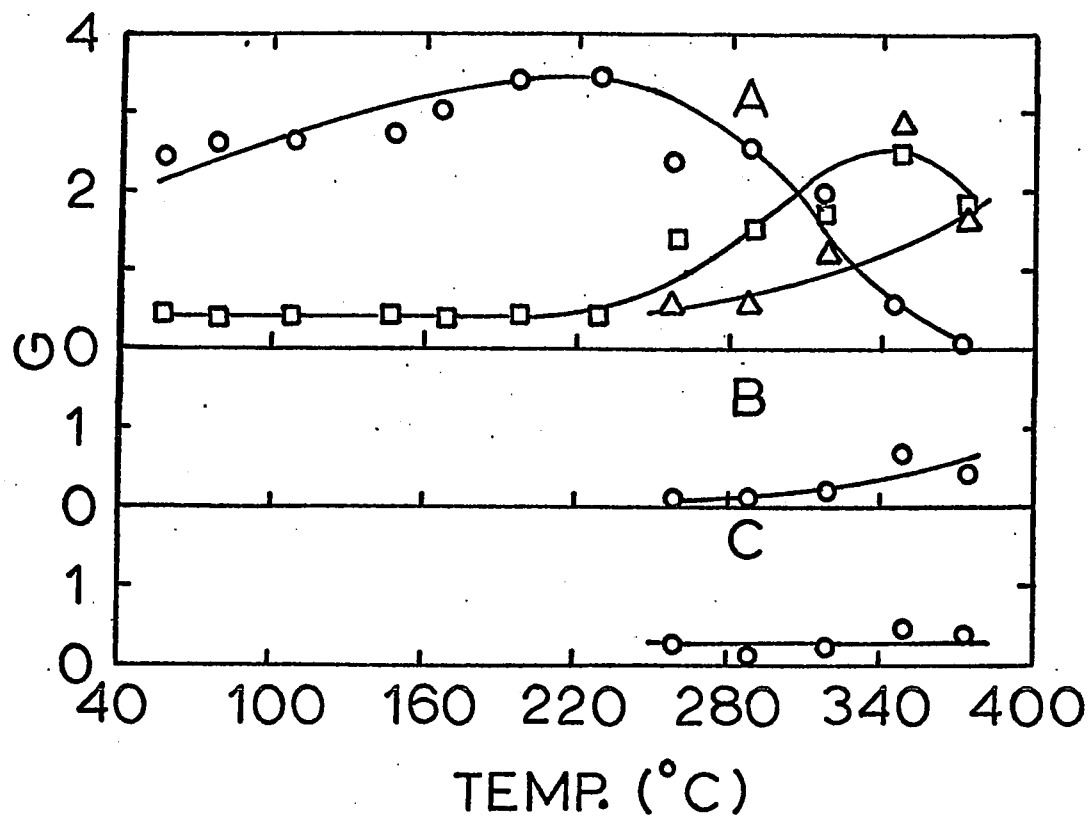


FIGURE III - 10

Products from ethanol radiolysis as a function of temperature. Ethanol density = 0.66 g/l.

- A    O    2,3-butanediol
- 1,2-propanediol
- Δ    sec. butyl alcohol
  
- B    O    diethoxy methane
  
- C    O    acetal

over the range 290° to 375°. Temperature has a small effect on the yields of other products.

2. Density of ethanol 0.16 g/l: Samples of liquid ethanol were vaporized into 500 ml irradiation cells and irradiated to a dose of  $1.3 \times 10^{20}$  eV/g. The temperature was varied over the range 60° to 230°. The amount of ethanol in the irradiation cell corresponded to a pressure of 93 torr at 150°.

Only the G values of the gaseous products were measured. The product yields as a function of temperature are presented in Table III-8 and Figure III-11. The G value of hydrogen is unaffected by change of temperature. Other gaseous product yields increase with temperature slightly, as follows: methane from 1.2 to 4.5, carbon monoxide from 0.2 to 0.6, ethane from 0.2 to 1.0 and ethylene from 1.3 to 2.0.

B. Detailed study at 150°

1. Radiolysis of pure ethanol

a. Effect of dose. Ethanol density 1.50 g/l.

Samples of ethanol were irradiated at a temperature of 150°. The pressure of ethanol in the irradiation cell was 865 torr. The dose was varied over the range  $1.0 \times 10^{19}$  eV/g to  $5.5 \times 10^{20}$  eV/g.

The variation of the product yields with dose are

TABLE III-8

Yields of products from ethanol radiolysis as a function  
of temperature

Density of ethanol = 0.16 g/l

Temp. (°C)	60	80	110	150	170	200	230
<u>Product</u>	<u>G</u>						
H <sub>2</sub>	9.60	10.00	10.00	9.16	9.35	9.77	10.10
CH <sub>4</sub>	1.15	1.64	2.25	2.86	3.48	3.70	4.49
CO	0.23	0.27	0.30	----	0.37	0.32	0.57
C <sub>2</sub> H <sub>6</sub>	0.23	0.23	0.23	0.35	0.57	0.67	1.00
C <sub>2</sub> H <sub>4</sub>	1.25	1.39	1.54	1.67	1.55	1.76	2.20
n-C <sub>4</sub> H <sub>10</sub>	----	----	----	0.01	----	----	0.01

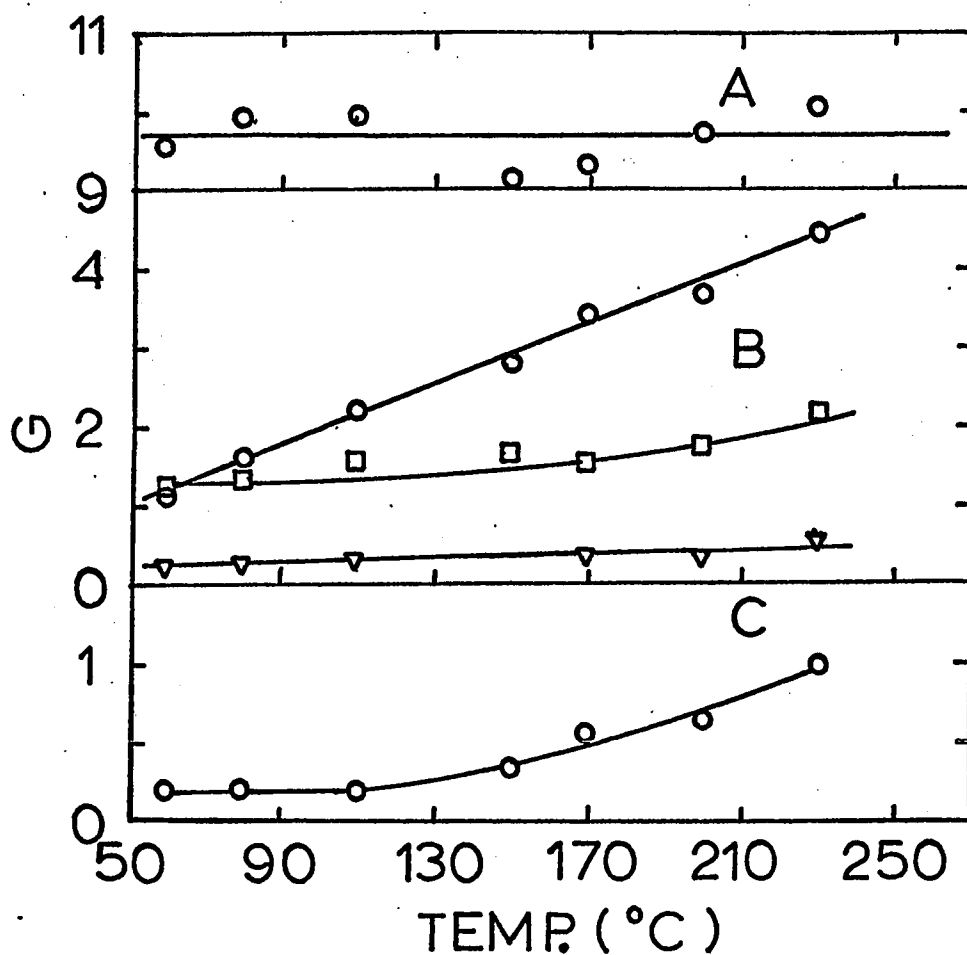


Figure III - 11

Products from ethanol radiolysis as a function of temperature. Ethanol density = 0.16 g/l.

A    O    Hydrogen

B    O    Methane

□    Ethylene

▽    Carbon monoxide

C    O    Ethane

presented in Table III-9 and Figures III-12 and III-13. The G values of butane and propane in Table III-9 may be low by a factor of 2 or 3, because these compounds could not be completely separated from the liquid during the  $-112^{\circ}$  distillation. The yields are negligible ( $<0.1$ ) in any case. The G values of ethane, ethylene, diethyl ether, 1,2-propanediol, 2,3-butanediol, propane, acetylene and n-butane were unaffected by change of dose. The large amount of scatter in the glycol results is due to the difficulties in the analysis. The G values of methane and carbon monoxide increase from 3.3 and 0.7 to 3.6 and 1.1 respectively. The yields of hydrogen and acetaldehyde decrease in the following way: hydrogen from 9.7 to 7.2, and acetaldehyde from 3.5 to 2.5.

b. Effect of ethanol pressure.

The dependence of product yields on pressure was studied by varying the pressure of ethanol in the irradiation cells over the range 45 to 1700 torr (0.078 - 2.96 g/l). The pressure was varied by varying the amount of ethanol that was vaporized in the irradiation cells. The samples were irradiated to a dose of  $8 \times 10^{19}$  eV/g.

The variation of the G values of the products with pressure are presented in Table III-10 and Figures III-14 and III-15. The G values of methane, ethane, carbon monoxide, n-butane, 1,2-propanediol and 2,3-butanediol

TABLE III-9

Product yields as a function of dose in the vapor phase radiolysis of ethanol at 150°C.

Dose (ev/g)	Density of ethanol = 1.50 g/l									
	$1.1 \times 10^{19}$	$3.17 \times 10^{19}$	$6.34 \times 10^{19}$	$8.18 \times 10^{19}$	$1.31 \times 10^{20}$	$2.54 \times 10^{20}$	$3.81 \times 10^{20}$	$5.50 \times 10^{20}$		
Product	G									
CH <sub>4</sub>	3.27	3.11	3.22	3.00	2.63	3.31	3.56	3.57		
CO	0.66	0.64	0.65	0.67	0.72	0.82	1.00	1.05		
H <sub>2</sub>	9.67	9.11	8.46	8.16	7.78	7.27	7.44	7.26		
C <sub>2</sub> H <sub>6</sub>	0.39	0.40	0.38	0.28	0.28	0.32	0.43	0.40		
C <sub>2</sub> H <sub>4</sub>	1.21	1.11	1.10	1.05	1.03	1.03	0.95	0.88		
C <sub>3</sub> H <sub>8</sub>	---	---	---	---	---	>0.02	>0.05	>0.03		
C <sub>2</sub> H <sub>2</sub>	n.d.	n.d.	0.29	0.25	n.d.	0.25	0.24	0.24		
n-C <sub>4</sub> H <sub>10</sub>	n.d.	>0.01	>0.01	n.d.	>0.02	>0.01	>0.01	>0.01		
C <sub>2</sub> H <sub>5</sub> OC <sub>2</sub> H <sub>5</sub>	n.d.	0.17	0.22	0.17	n.d.	0.16	0.13	0.12		
CH <sub>3</sub> CHO	3.50	3.23	4.21	3.04	3.10	3.11	2.55	2.54		
1,2-propane- diol	n.d.	n.d.	n.d.	0.25	0.45	0.78	0.42	0.53		
2,3-butane- diol	n.d.	0.58	1.41	2.7	3.70	3.30	1.20	2.3		



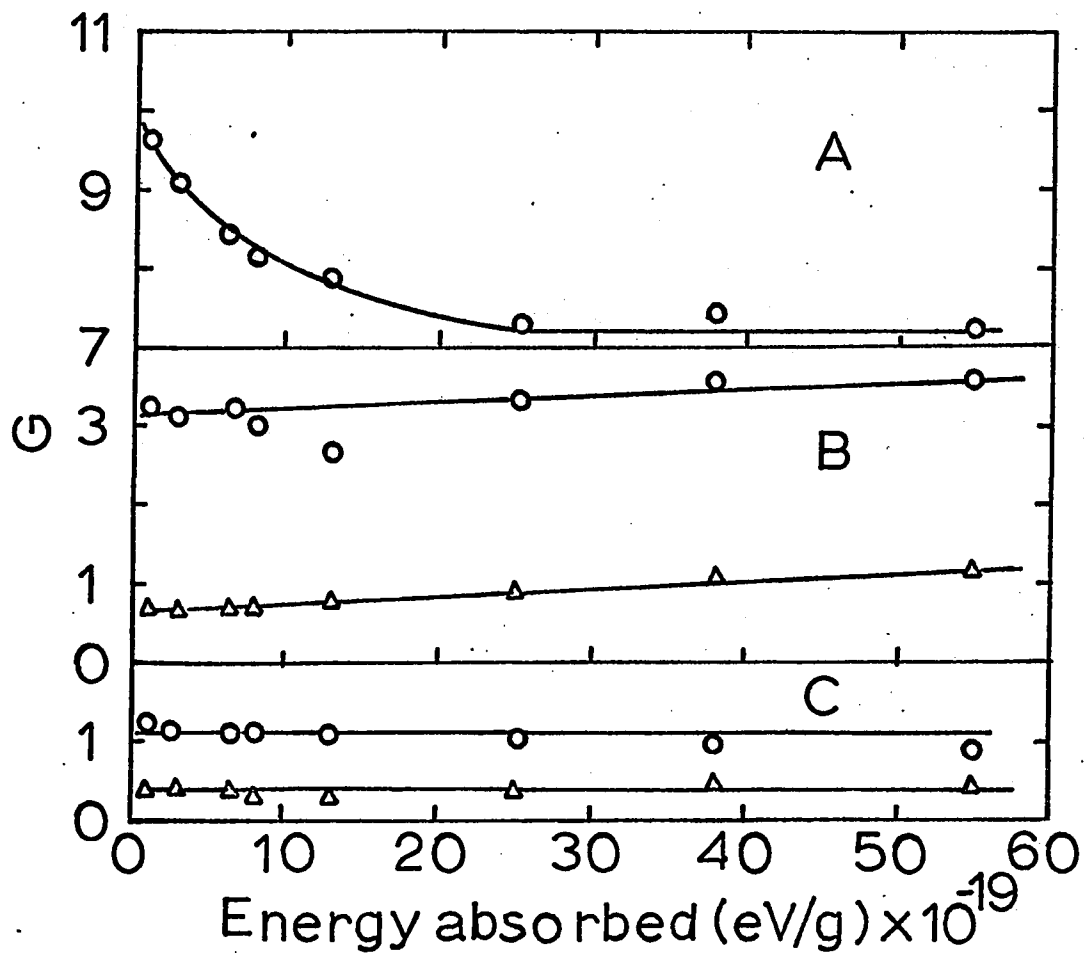


Figure III - 12

Products from ethanol radiolysis as a function of dose. Ethanol density = 1.50 g/l  
Temperature = 150°C.

- |   |   |                 |
|---|---|-----------------|
| A | O | Hydrogen        |
| B | O | Methane         |
|   | Δ | Carbon monoxide |
| C | O | Ethylene        |
|   | Δ | Ethane          |

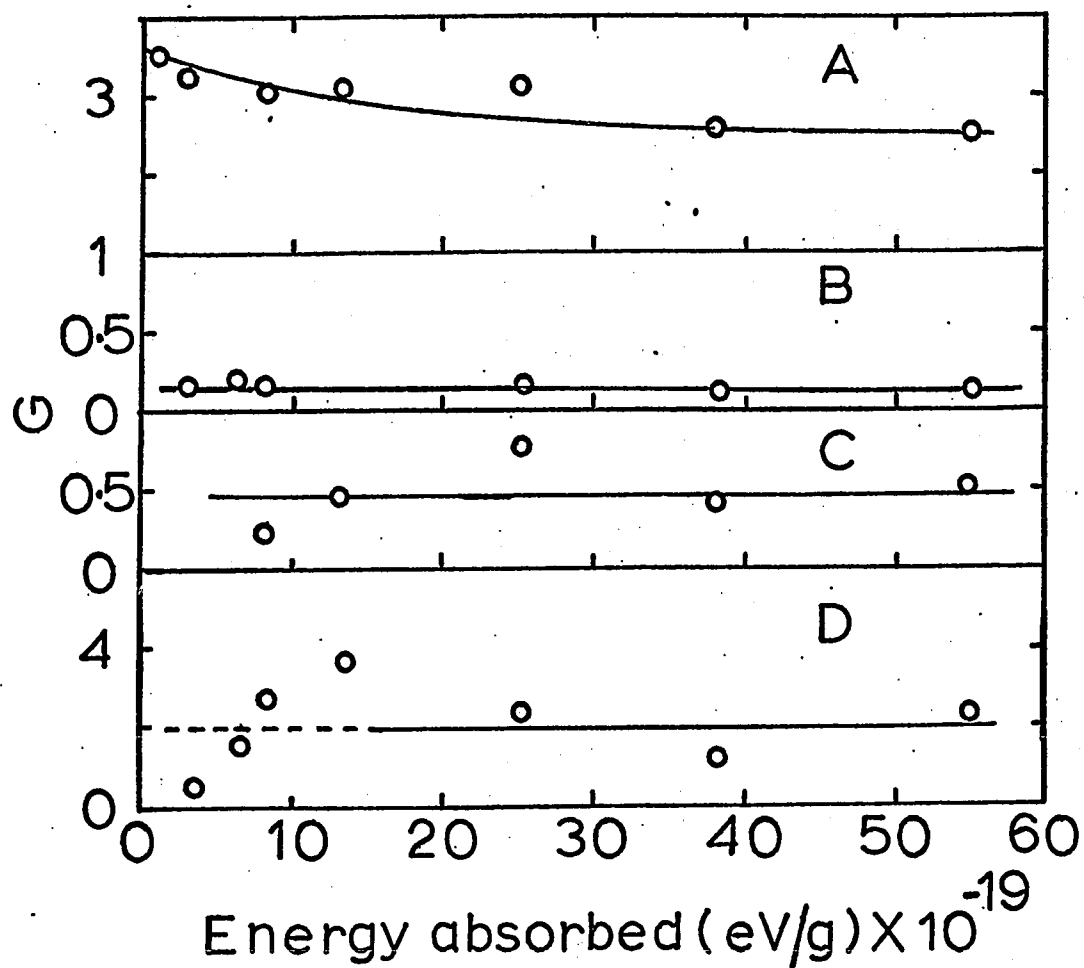


FIGURE III-13

Products from ethanol radiolysis as a function of dose. Ethanol density = 1.50 g/l. Temperature = 150°C.

- A Acetaldehyde
- B Diethyl ether
- C 1,2-Propanediol
- D 2,3-Butanediol.

TABLE III-10

Effect of pressure on the G values of the products in the  $\gamma$ -radiolysis of ethanol

Temperature = 150°C

<u>Pressure</u> <u>(torr)</u>	<u>45.7</u>	<u>93.2</u>	<u>286.7</u>	<u>385.5</u>	<u>625.2</u>	<u>865.6</u>	<u>913.5</u>	<u>1303</u>	<u>1598</u>	<u>1693</u>
<u>Product</u>	<u>G</u>									
H <sub>2</sub>	10.18	9.16	8.95	8.66	7.81	8.16	n.d.	7.23	n.d.	7.01
CH <sub>4</sub>	2.97	2.86	2.64	2.99	2.80	3.00	n.d.	2.88	n.d.	2.86
CO	0.45	0.60	0.81	0.68	1.00	0.67	n.d.	0.64	n.d.	0.64
C <sub>2</sub> H <sub>6</sub>	0.47	0.35	0.32	0.28	0.33	0.28	n.d.	0.22	n.d.	0.25
C <sub>2</sub> H <sub>4</sub>	1.95	1.67	1.35	1.05	1.20	1.05	n.d.	0.96	n.d.	0.93
C <sub>3</sub> H <sub>8</sub>	n.d.	n.d.	n.d.	n.d.	n.d.	n.d.	n.d.	n.d.	n.d.	n.d.
C <sub>2</sub> H <sub>2</sub>	0.04	0.05	0.04	n.d.	n.d.	0.25	n.d.	n.d.	n.d.	n.d.
n-C <sub>4</sub> H <sub>10</sub>	n.d.	>0.01	>0.01	>0.01	>0.01	>0.01	n.d.	>0.02	n.d.	>0.01
CH <sub>3</sub> CHO	5.86	4.70	3.44	3.76	3.45	3.04	3.19	n.d.	2.62	n.d.
1,2-propane- diol	0.30	0.37	0.34	0.34	0.38	0.25	0.52	n.d.	0.67	n.d.
2,3-butane- diol	0.77	0.96	3.66	3.53	3.16	2.7	3.62	n.d.	3.64	n.d.

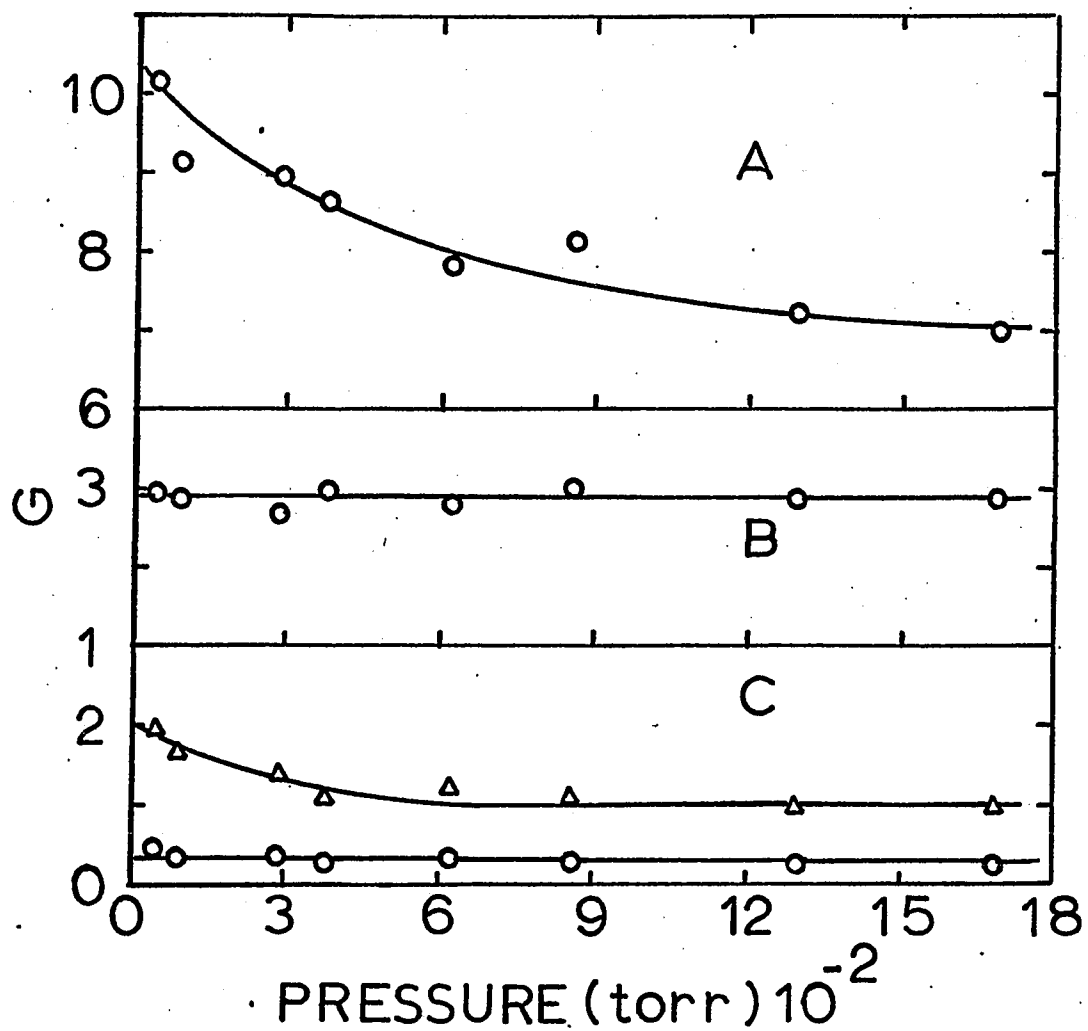


FIGURE III - 14

Products from ethanol radiolysis as a function of pressure. Temperature = 150°C.

A	O	Hydrogen
B	O	Methane
C	O	Ethane
	Δ	Ethylene

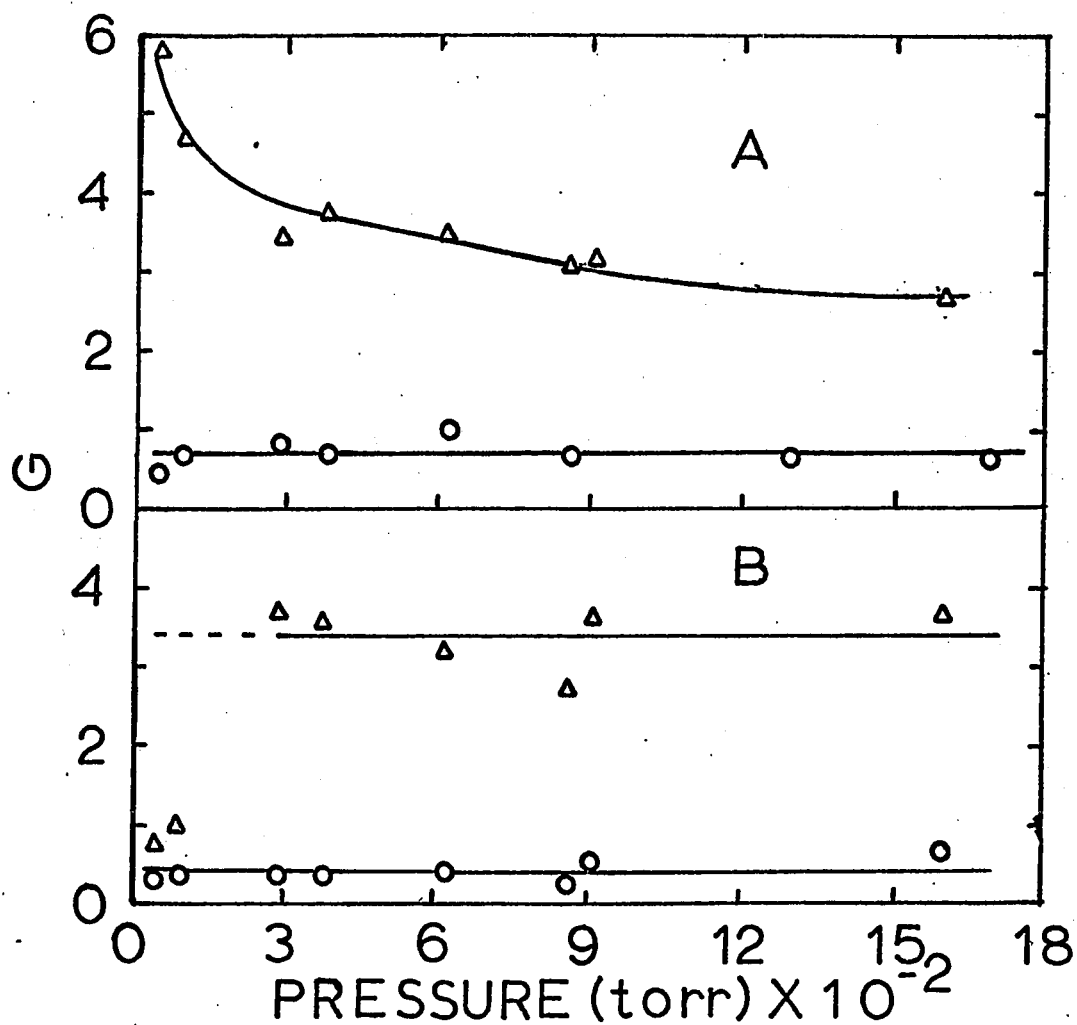


FIGURE III - 15

Products from ethanol radiolysis as a function of pressure. Temperature = 150°C.

- |   |   |                 |
|---|---|-----------------|
| A | O | Carbon monoxide |
|   | Δ | Acetaldehyde    |
| B | Δ | 2,3-Butanediol  |
|   | O | 1,2-Propanediol |

were unaffected by change of pressure. The yields of hydrogen, ethylene, and acetaldehyde decrease with pressure in the following manner: hydrogen from 10.2 to 7.0, ethylene from 2.0 to 1.0 and acetaldehyde from 5.9 to 2.7.

2. The effect of inhibitors.

The product yields from radiolysis of ethanol-inhibitor mixtures are reported as g values. The g value is defined as

$$g(\text{Product}) = \frac{G(\text{Product})_{\text{observed}} - G(\text{Product})_{\text{scavenger}} \times \epsilon_{\text{scavenger}}}{\epsilon_{\text{C}_2\text{H}_5\text{OH}}}$$

where  $\epsilon_{\text{scavenger}}$  and  $\epsilon_{\text{C}_2\text{H}_5\text{OH}}$  are the electron fractions of the scavenger and ethanol respectively.

a. Ethanol-propylene mixtures. Ethanol density 1.50 g/l

Samples containing 1.50 g/l of ethanol plus 0 to 41 mole percent of propylene were irradiated to a dose of  $8 \times 10^{19}$  ev/g. The pressure of ethanol in the irradiation cell was 865 torr.

The gaseous products measured at all propylene concentrations were hydrogen, methane and carbon monoxide. Ethane and ethylene could not be measured when greater than 1.3 mole percent propylene was present in the samples because of the interference of the latter compound.

At higher propylene concentrations (greater than

5 mole percent), a very complex mixture of liquid products was obtained. No attempt was made to identify these products. At greater than 15 mole percent propylene in ethanol samples, such a complex mixture of liquid products was obtained that even acetaldehyde could not be separated from other products. Furthermore, on the Polypak-2 column,  $C_5$  alcohols and 1,2-propanediol have the same retention time, so g(1,2-propanediol) is not reported in Table III-11.

The g values of various gaseous and liquid products as a function of propylene concentration are presented in Table III-11 and Figure III-16. The g values of hydrogen and methane were corrected for hydrogen and methane produced from the propylene, using  $G(H_2)_{C_3H_6} = 1.27$  and  $G(CH_4)_{C_3H_6} = 0.23$ , which were obtained under the following conditions: temperature  $150^\circ$ , pressure 1227 torr.

Propylene decreases the product yields as follows: hydrogen from 8.2 to 1.5, methane from 3.0 to 1.2, 2,3-butanediol from 2.7 to 0.0, and (acetaldehyde + acetal) from 3.0 to 1.8. The yield of carbon monoxide remains unchanged. The yields of ethane, ethylene and ether were unaffected within 0.1 units or less, by the presence of 1.3 mole percent of propylene.

- b. Ethanol-propylene mixtures. Ethanol density 0.16 g/l  
Samples of ethanol with varying amounts of propylene,

TABLE III-11

Product yields from the vapor phase radiolysis of  $C_2H_5OH-C_3H_6$  mixtures at 150°C

Ethanol density = 1.50 g/l

Mole % $C_3H_6$	g									
	$H_2$	$CH_4$	$CO$	$C_2H_6$	$C_2H_4$	$C_3H_8$	ether	$CH_3CHO$	Acetal	$CH_3CHO$ + acetal diol
0	8.16	3.00	0.67	0.28	1.05	n.d.	0.17	3.04	----	3.04 2.70
0.48	6.38	2.80	0.67	0.28	1.09	0.06	0.18	1.10	1.76	2.86 1.00
1.30	5.03	2.62	0.63	0.25	0.99	0.15	0.15	2.10	0.37	2.47 0.32
5.13	2.95	2.17	0.59	n.d.	n.d.	n.d.	n.d.	1.03	0.79	1.82 ----
10.43	2.90	1.98	0.63	n.d.	n.d.	n.d.	n.d.	1.30	0.44	1.74 ----
15.46	2.40	1.75	0.61	n.d.	n.d.	n.d.	n.d.	1.68	0.34	2.02 ----
25.55	1.93	1.26	0.58	n.d.	n.d.	n.d.	n.d.	n.d.	n.d.	n.d. ----
40.95	1.83	1.12	0.62	n.d.	n.d.	n.d.	n.d.	n.d.	n.d.	n.d. ----



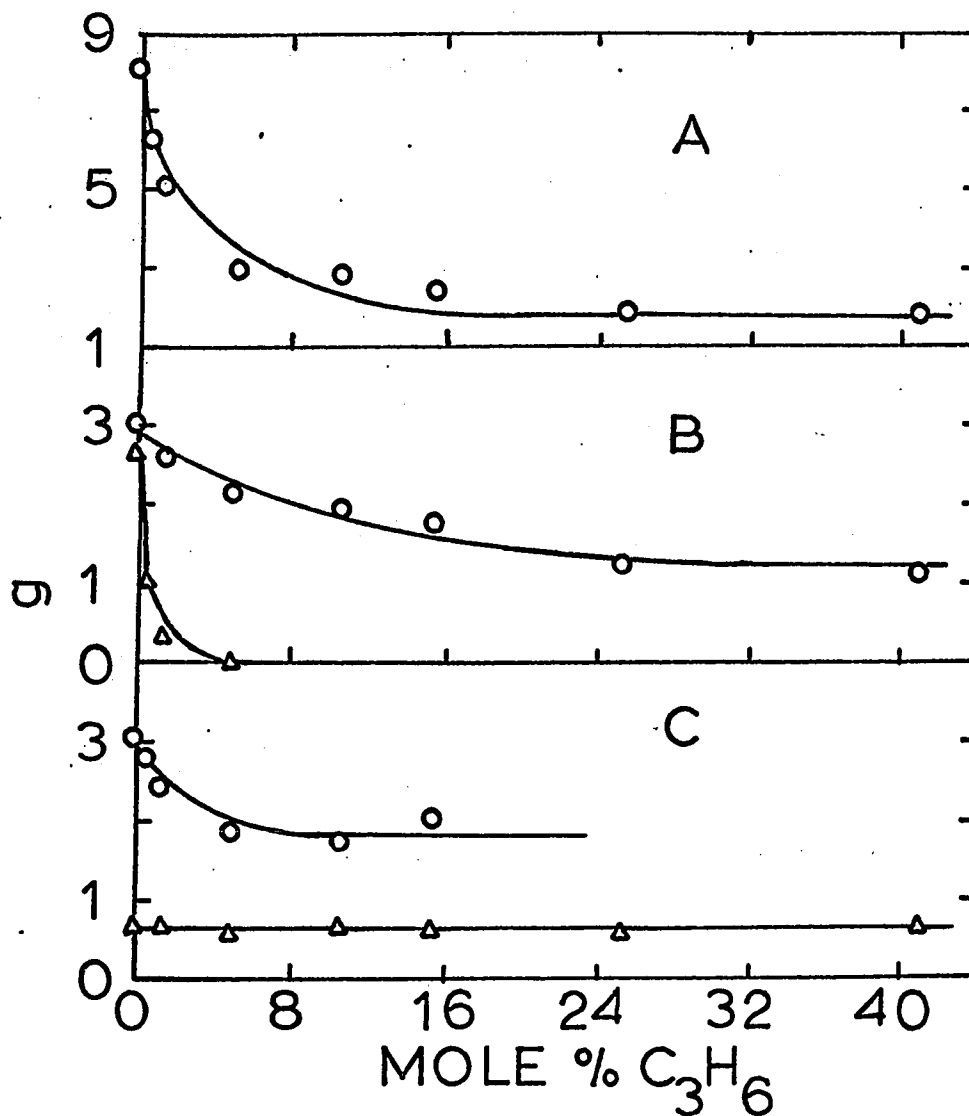


FIGURE III - 16

Product yields from ethanol-propylene mixtures  
Temperature = 150°C. Density of ethanol = 1.50 g/l

A O Hydrogen

B O Methane

Δ 2,3-butanediol

C O Acetaldehyde + Acetal

Δ Carbon monoxide.

over the range 0 to 39 mole percent, were irradiated to a dose of  $8 \times 10^{19}$  eV/g. The concentration of ethanol was 0.16 g/l in all the samples, which corresponded to a pressure of 93 torr at 150°.

The g values of hydrogen, methane, carbon monoxide and acetaldehyde are presented in Table III-12 and Figure III-17. The values of  $g(H_2)$  and  $g(CH_4)$  were corrected for hydrogen and methane produced from the propylene, using  $G(H_2)_{C_3H_6} = 1.72$ ,  $G(CH_4)_{C_3H_6} = 0.27$ , which were obtained under the following conditions: temperature 150°, pressure 130 torr.

Propylene decreases the product yields as follows: hydrogen from 9.7 to 2.4, methane from 3.0 to 1.5, and acetaldehyde from 4.7 to 2.5. The yield of carbon monoxide remains unchanged.

c. Ethanol-ammonia mixtures. Ethanol density 1.50 g/l

Binary mixtures of ethanol and ammonia were irradiated to a dose of  $8 \times 10^{19}$  eV/g. The pressure of ethanol in each sample was 865 torr. The concentration of ammonia was varied over the range 0 to 7 mole percent.

The g values of various products as a function of ammonia concentration are presented in Table III-13 and Figure III-18. Acetaldehyde reacts with ammonia (93), so the yield of this product could not be determined. The value of  $g(H_2)$  was corrected for hydrogen produced

TABLE III-12

Product yields from vapor phase radiolysis of  $C_2H_5OH-C_3H_6$   
mixtures at 150°C. Ethanol density = 0.16 g/l

<u>Mole % <math>C_3H_6</math></u>	<u>g</u>			
	<u><math>H_2</math></u>	<u><math>CH_4</math></u>	<u>CO</u>	<u><math>CH_3CHO</math></u>
0.0	9.7	3.0	0.67	4.70
1.29	5.80	2.69	0.71	3.68
3.54	4.20	2.53	0.71	3.34
7.32	3.49	2.48	0.73	2.63
16.44	2.75	1.83	0.74	2.19
24.51	2.73	1.50	0.73	2.69
38.59	2.39	1.30	0.71	2.69

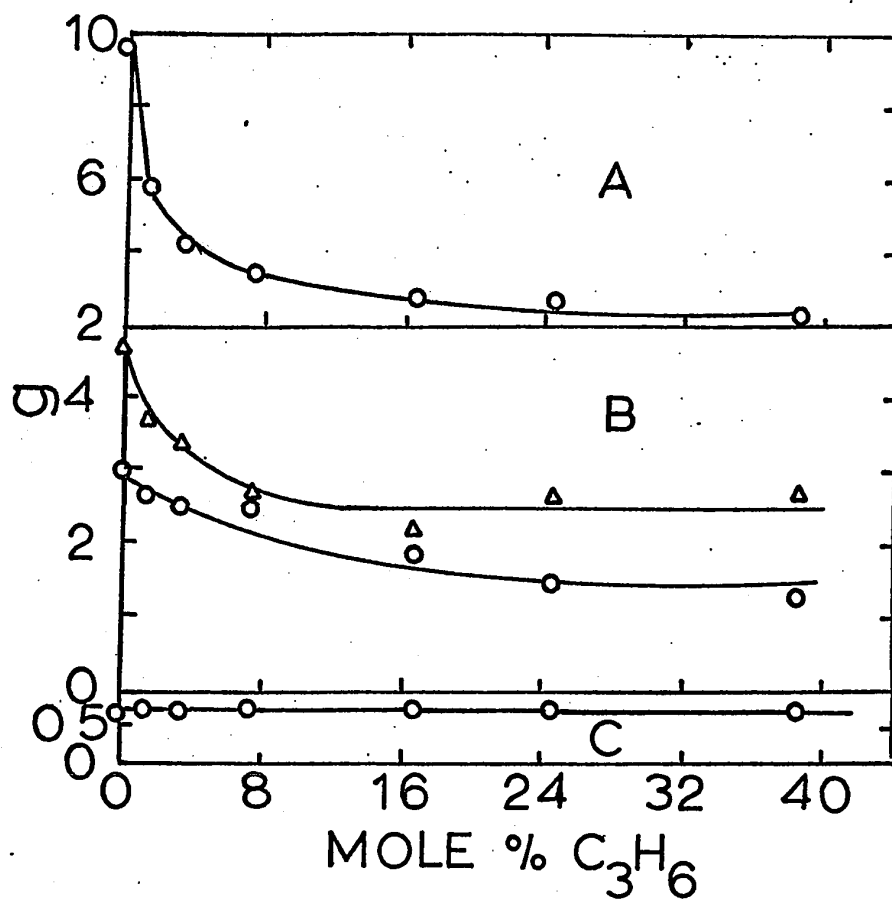


FIGURE III-17

Product yields from the radiolysis of ethanol-propylene mixtures. Temperature = 150°C.  
Ethanol density = 0.16 g/l

A	O	Hydrogen
B	Δ	Acetaldehyde
	O	Methane
C	O	Carbon monoxide

TABLE III-13

Product yields from vapor phase radiolysis of  $C_2H_5OH-NH_3$

mixtures at 150°C

Ethanol density = 1.50 g/l

<u>Mole % <math>NH_3</math></u>	<u>0</u>	<u>0.10</u>	<u>1.36</u>	<u>2.06</u>	<u>7.10</u>
Product	g				
Hydrogen	8.16	8.03	8.12	8.28	8.31
Methane	3.00	2.90	2.72	2.69	2.85
Carbon monoxide	0.67	0.63	0.68	0.64	0.62
Ethane	0.28	0.11	0.12	0.12	0.12
Ethylene	1.05	0.83	1.00	1.01	0.97
Diethyl ether	0.17	0.17	0.18	0.19	0.18
2,3-butane- diol	2.70	1.70	1.79	2.13	1.97

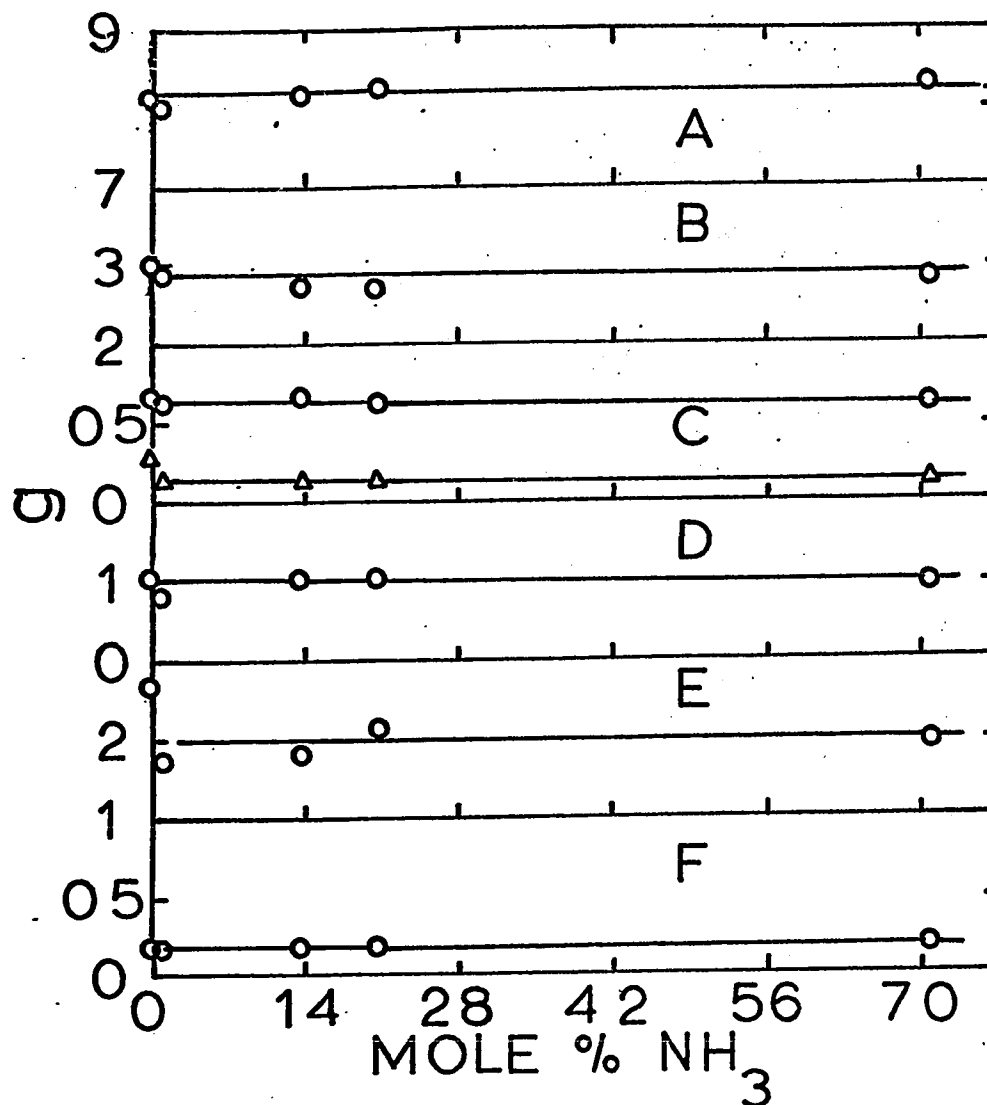


FIGURE III-18

Product yields from the radiolysis of ethanol-ammonia mixtures. Temperature = 150°C.

Ethanol density = 1.50 g/l

A	O	Hydrogen
B	O	Methane
C	O	Carbon monoxide
	Δ	Ethane
D	O	Ethylene
E	O	2,3-butanediol
F	O	Diethyl ether

from the ammonia, using  $G(\text{H}_2)_{\text{NH}_3} = 10.0$  (94), which was obtained under the following conditions: temperature 150°, 570 torr, dose rate =  $8.4 \times 10^{21}$  eV/ghr.

The g values of hydrogen, methane, carbon monoxide, ethane, ethylene, 2,3-butanediol and ether were unaffected by the presence of ammonia.

d. Ethanol-sulphur hexafluoride mixtures. Ethanol density 1.50 g/l.

Binary mixtures of ethanol and sulphur hexafluoride were irradiated to a dose of  $8 \times 10^{19}$  eV/g. The ethanol pressure was 865 torr in all the samples. The concentration of sulphur hexafluoride was varied over the range 0 to 6 mole percent.

The g values of various products as a function of sulphur hexafluoride concentration are presented in Table III-14a and Figures III-19 and III-20. The yield of ethane is not reported in Table III-14a, as it could not be separated from sulphur hexafluoride on 2% Apiezon-L on silica gel column.

At an ethanol density of 1.50 g/l, sulphur hexafluoride changes the product yields as follows: the yield of hydrogen decreases from 8.2 to 5.2, and that of 2,3-butanediol from 2.7 to 1.2. Sulphur hexafluoride does not affect the yields of methane, carbon monoxide,

TABLE III-14a

Product yields from vapor phase radiolysis of  $C_2H_5OH-SF_6$   
mixtures at 150°C.

Ethanol density = 1.50 g/l

Mole % $SF_6$	0	0.065	.15	.36	.63	1.02	3.13	5.91
Product	g							
$H_2$	8.16	n.d.	5.22	5.32	4.87	5.12	5.53	5.54
$CH_4$	3.00	n.d.	3.05	3.03	3.14	3.13	3.16	3.43
CO	0.67	n.d.	0.68	0.73	0.70	0.71	0.70	0.82
$C_2H_4$	1.05	n.d.	1.27	1.34	1.02	1.32	1.41	1.65
$C_2H_2$	0.25	n.d.	0.24	0.24	n.d.	0.34	0.41	0.24
n- $C_4H_{10}$	0.01	n.d.	0.02	0.01	n.d.	0.01	0.01	0.01
$CH_3CHO$	3.04	---	n.d.	----	----	----	----	----
Acetal	----	5.51	n.d.	5.10	5.37	5.55	5.94	6.34
$CH_3CHO$ + acetal	3.04	5.51	n.d.	5.10	5.37	5.55	5.94	6.34
$C_2H_5OC_2H_5$	0.17	1.66	n.d.	1.38	1.64	1.96	2.48	2.30
Diethoxy methane	0.24	0.35	n.d.	0.39	0.65	0.67	1.08	0.58
1,2-propane- diol	0.25	0.67	n.d.	0.76	1.29	1.31	1.99	1.47
2,3-butane- diol	2.70	n.d.	n.d.	1.16	n.d.	1.23	1.53	n.d.

TABLE III-14b

Mole % $SF_6$	Mole % $C_3H_6$	g( $H_2$ )	g( $CH_4$ )	g(CO)
3.19	5.16	2.55	2.46	0.65



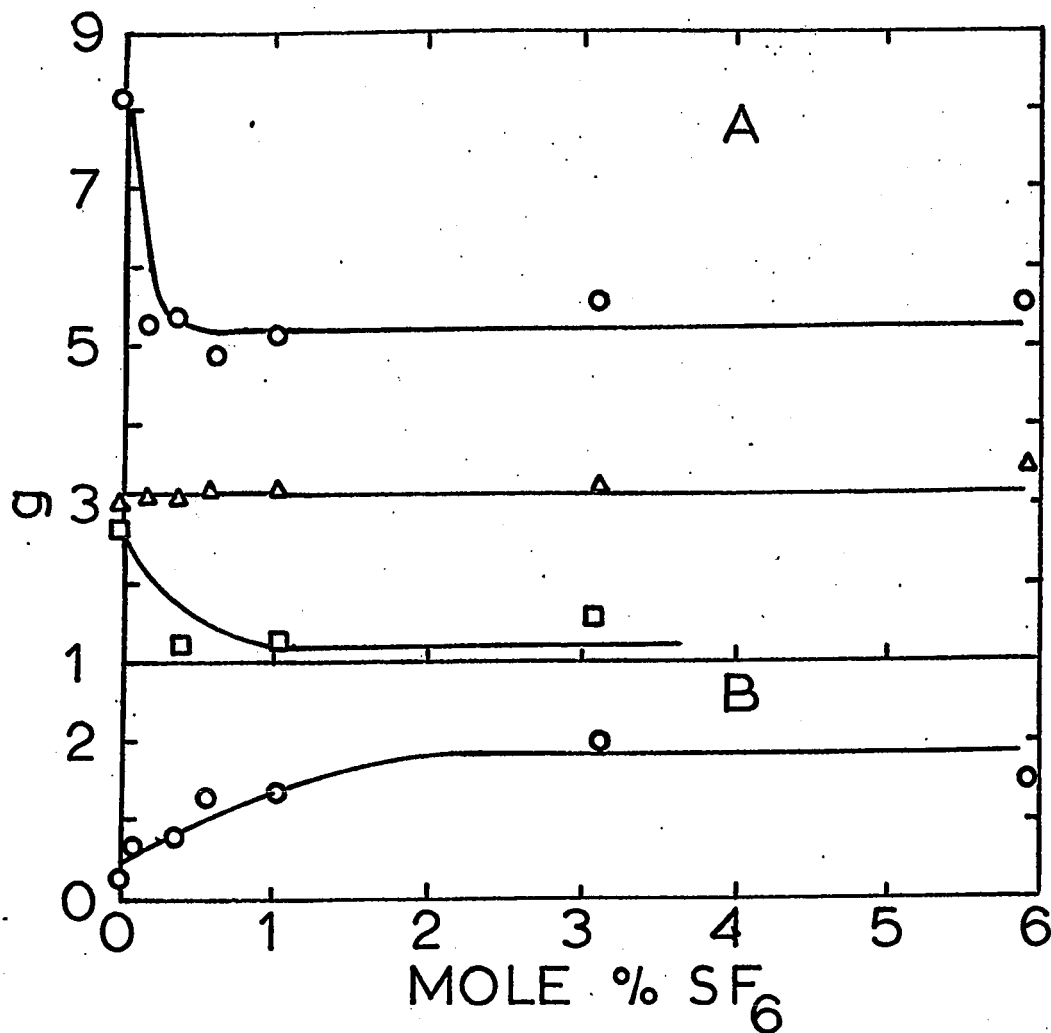


FIGURE III-19

Product yields in the radiolysis of ethanol - sulphur hexafluoride mixtures. Temperature=150°C.

Ethanol density = 1.50 g/l

- |   |   |                 |
|---|---|-----------------|
| A | O | Hydrogen        |
|   | Δ | Methane         |
|   | □ | 2,3-butanediol  |
| B | O | 1,2-Propanediol |

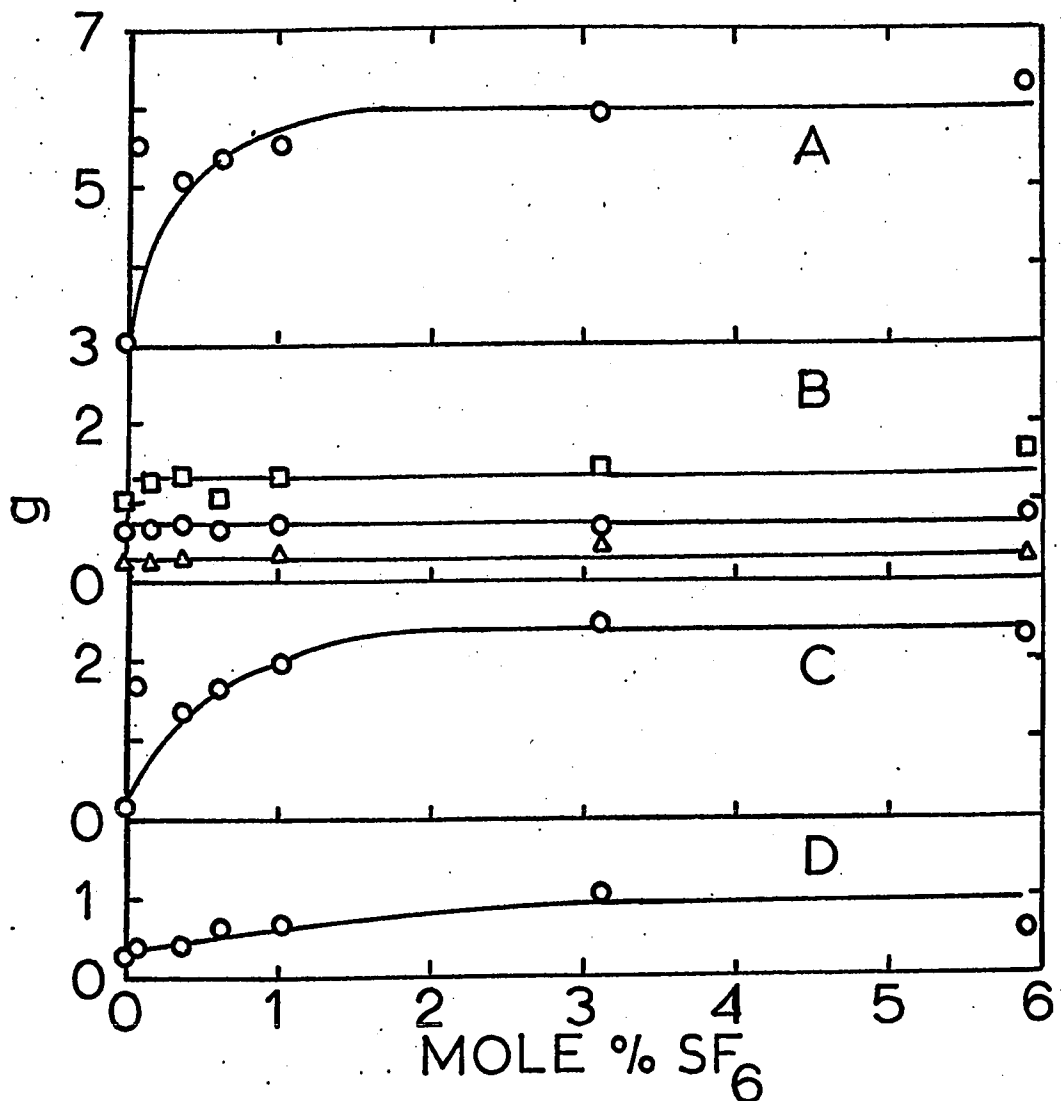


FIGURE III - 20

Product yields from the radiolysis of ethanol-sulphur hexafluoride mixtures Temperature 150°C

Ethanol density = 1.50 g/l

A	O	Acetaldehyde + Acetal
B	O	Carbon monoxide
	Δ	Acetylene
	□	Ethylene
C	O	Diethyl ether
D	O	Diethoxy methane

acetylene, ethylene and n-butane. The yield of 1,2-propanediol increases from 0.3 to 1.8, that of (acetaldehyde + acetal) from 3.0 to 6.0, that of diethyl ether from 0.2 to 2.4, and that of diethoxy methane from 0.2 to 1.0.

Two blank samples of ethanol containing 0.37 and 5.91 mole percent  $\text{SF}_6$  were prepared in exactly the same way as the samples for irradiation studies. They were heated for 2 hours at  $150^\circ\text{C}$  (time for which the samples were irradiated in the irradiation study). They were then analyzed for gaseous and liquid products. A procedure similar to one for irradiated samples was adopted. No detectable peak for any of the liquid and gaseous product was obtained.

One sample of ethanol (1.50 g/l) containing 5.16 mole percent  $\text{C}_3\text{H}_6$  and 3.19 mole percent  $\text{SF}_6$  was also irradiated at a temperature of  $150^\circ\text{C}$  and to a dose of  $8 \times 10^{19}$  eV/g. This sample was analyzed for only hydrogen, methane and carbon monoxide. The g values are reported in Table III-14b. The product yields decrease as follows: hydrogen from 8.2 to 2.6 and methane from 3.0 to 2.5. The yield of carbon monoxide was unaffected.

C. Effect of ethanol pressure at 230°.

The variation of product yields with pressure was studied by varying the pressure of ethanol in the irradiation cells over the range 54 to 1900 torr (0.078 - 2.78 g/l). The samples were irradiated to a dose of  $8 \times 10^{19}$  eV/g.

Only the G values of the gaseous products were determined. The product yields as a function of pressure are reported in Table III-15 and Figures III-21 and III-22. The variation of pressure has no effect on the yields of ethane and acetylene. The yields of hydrogen and ethylene decrease from 12.8 and 2.7 to 7.2 and 1.3 respectively. The yields of methane and carbon monoxide increase from 4.4 and 0.5 to 5.3 and 1.1 respectively.

D. Detailed study at 350°

1. The effect of inhibitors

a. Ethanol-propylene mixtures. Ethanol density 0.66 g/l

Binary mixtures of ethanol and propylene were irradiated to a dose of  $7.5 \times 10^{19}$  eV/g. The pressure of ethanol was 568 torr in all the samples.

The g values of various gaseous and liquid products as a function of propylene concentration are presented in Table III-16 and Figures III-23 and III-24. The hydrogen and methane yields were corrected for the direct

TABLE III-15

Effect of pressure on product yields in the vapor phase

radiolysis of C<sub>2</sub>H<sub>5</sub>OH at 230°C

Pressure (torr)	G							
	CH <sub>4</sub>	CO	H <sub>2</sub>	C <sub>2</sub> H <sub>6</sub>	C <sub>2</sub> H <sub>4</sub>	C <sub>3</sub> H <sub>8</sub>	C <sub>2</sub> H <sub>2</sub>	n-C <sub>4</sub> H <sub>6</sub>
54.37	4.39	0.47	12.76	1.12	2.65	n.d.	n.d.	n.d.
110.9	4.49	0.57	10.10	1.00	2.20	n.d.	n.d.	>0.02
341	5.27	1.14	11.71	1.06	1.81	>0.003	0.47	>0.03
458.5	4.94	0.87	8.81	0.96	1.86	n.d.	0.20	>0.01
743.5	4.52	1.18	8.41	0.65	1.14	>0.001	0.22	>0.01
1086	5.33	1.02	7.51	0.79	1.36	n.d.	0.13	>0.01
1901	5.82	1.18	7.20	0.80	1.21	>0.004	0.19	>0.02

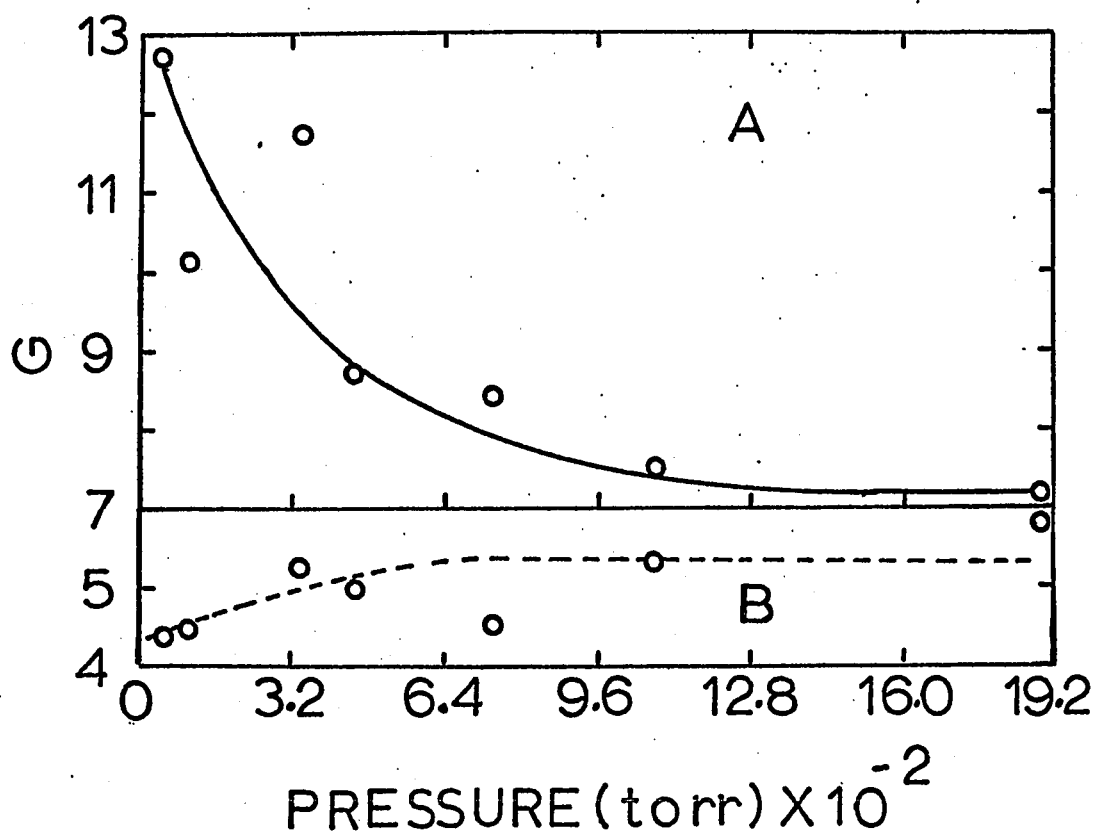


FIGURE III-21

Product yields from ethanol radiolysis as a function of pressure. Temperature =  $230^{\circ}\text{C}$

A	O	Hydrogen
B	O	Methane

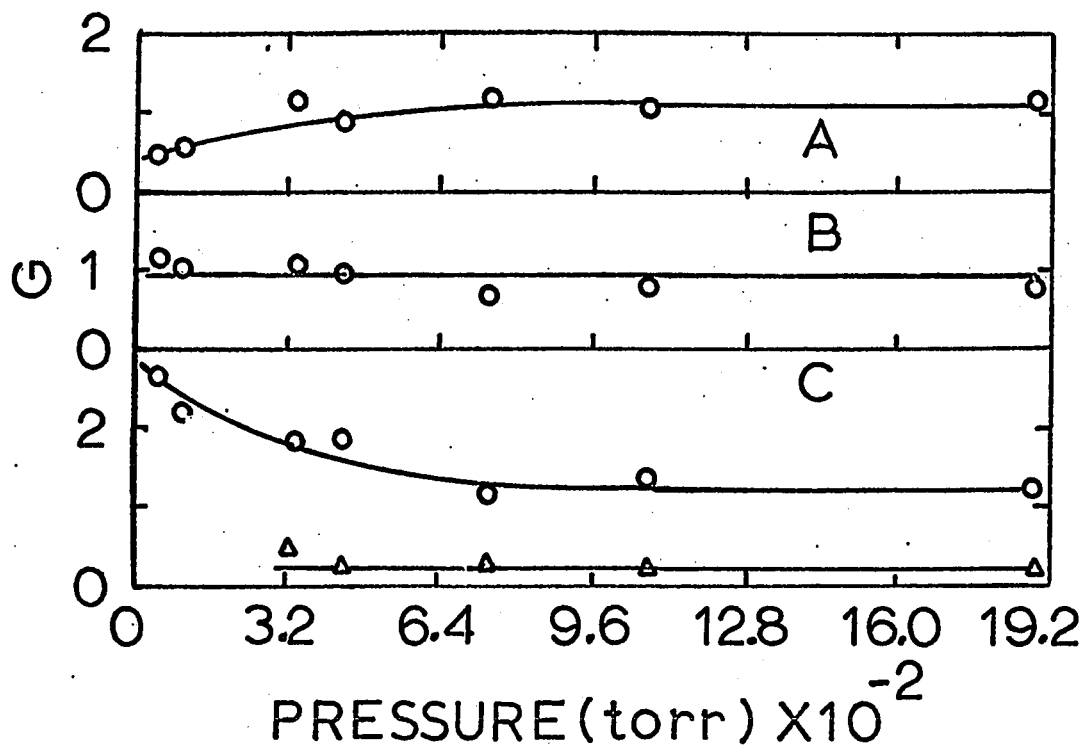


FIGURE III - 22

Product yields from ethanol radiolysis as a function of pressure. Temperature = 230°C.

- |   |   |                 |
|---|---|-----------------|
| A | O | Carbon monoxide |
| B | O | Ethane          |
| C | O | Ethylene        |
|   | Δ | Acetylene       |

TABLE III-16

G values of products in the radiolysis of  $C_2H_5OH-C_3H_6$  mixtures at 350°C

Mole % $C_3H_6$ Product	Ethanol density 0.66 g/l									
	0	.43	1.44	1.82	8.68	16.41	24.69	40.7		
$H_2$	45.9	39.1	n.d.	23.4	14.0	9.7	14.9	11.8		
$CH_4$	38.9	31.9	27.3	19.6	17.5	22.1	19.3	17.2		
CO	9.8	5.9	4.1	2.7	2.4	3.0	3.3	3.0		
$C_2H_6$	3.5	2.0	2.6	n.d.	n.d.	n.d.	n.d.	n.d.		
$C_2H_4$	19.8	13.9	15.3	n.d.	n.d.	n.d.	n.d.	n.d.		
$C_3H_8$	0.1	n.d.	9.1	n.d.	n.d.	n.d.	n.d.	n.d.		
$C_2H_5OC_2H_5$	5.6	2.9	11.1	1.9	5.9	10.6	n.d.	n.d.		
$CH_3CHO$	41.8	37.9	41.8	1.0	34.7	9.7	n.d.	n.d.		
Acetal	0.5	----	1.0	27.1	0.3	34.3	n.d.	n.d.		
$CH_3CHO$ + acetal	42.3	37.9	42.8	28.1	35.0	44.0	n.d.	n.d.		
$CH_3OH$	17.0	11.1	22.6	6.3	6.1	8.0	n.d.	n.d.		
Isopropyl alcohol	--	----	----	----	----	----	n.d.	n.d.		
sec-butyl alcohol	2.8	0.9	2.0	0.6	3.5	n.d.	n.d.	n.d.		
Diethoxy methane	0.6	0.6	0.6	0.8	n.d.	n.d.	n.d.	n.d.		



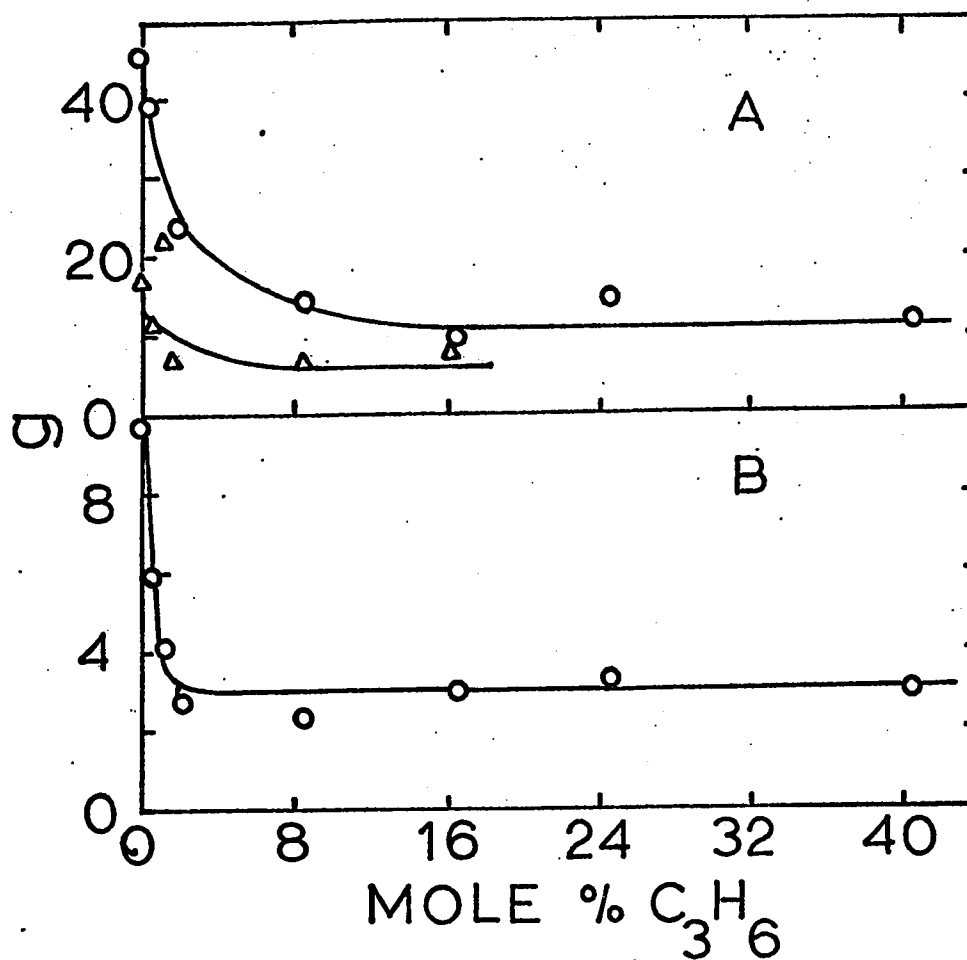


FIGURE III - 23

Product yields in the radiolysis of ethanol-propylene mixtures. Temperature = 350°C.

Ethanol density = 0.66 g/l.

- |   |   |                 |
|---|---|-----------------|
| A | O | Hydrogen        |
|   | Δ | Methanol        |
| B | O | Carbon monoxide |

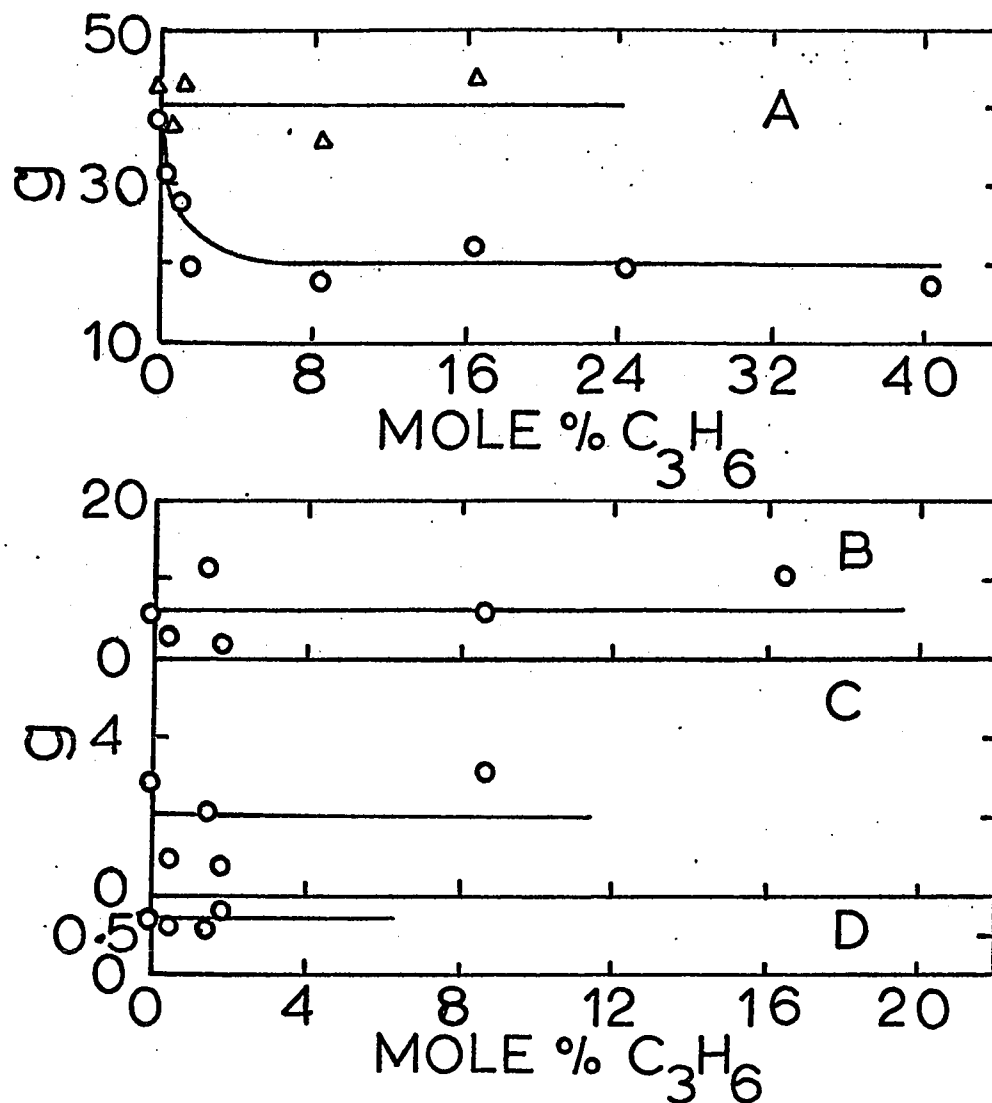


FIGURE III - 24

Product yields in the radiolysis of ethanol-propylene mixtures. Temperature = 350°C.

Ethanol density = 0.66 g/l.

- A O Methane
- Δ Acetaldehyde
- B O Diethyl ether
- C O sec-butyl alcohol
- D O Diethoxy methane

radiolysis of propylene, using  $G(H_2)_{C_3H_6} = 1.36$  and  $G(CH_4)_{C_3H_6} = 2.64$ , which were obtained when propylene was irradiated at 350° and 805 torr.

The gaseous products measured at all propylene concentrations were hydrogen, methane and carbon monoxide. Ethane and ethylene could not be measured when greater than 1.5 mole percent propylene was present in the samples because of the interference of the latter compound during -112° distillation. The g values of  $C_2H_6$ ,  $C_2H_4$  and  $C_3H_8$  for the sample containing 1.44 mole percent  $C_3H_6$  were determined using methanol slush bath (-98°C) during distillation in place of ethanol slush bath (-112°) and these values are also reported in Table III-16. Using methanol slush bath during the distillation, it was observed that  $C_2H_6$ ,  $C_2H_4$ ,  $C_3H_8$  and  $C_3H_6$  could be completely separated during the distillation.

At concentrations greater than 5 mole percent of propylene, a complex mixture of liquid products was obtained. These liquid products were not identified. At greater than 20 mole percent propylene in ethanol samples, such a complex mixture of liquid products was obtained that even acetaldehyde could not be separated from other products. Furthermore, on the Polypak-2 column  $C_5$  alcohols and 1,2-propanediol could not be separated, so  $g(1,2\text{-propanediol})$  is not reported in

Table III-16.

At an ethanol density of 0.66 g/l, propylene decreases the various product yields as follows: hydrogen from 45.9 to 11.0, methane from 38.9 to 20.0, carbon monoxide from 9.8 to 3.0, and methanol from 17.0 to 6.0. The yields of ethane, ethylene and propane change from 3.5, 19.8 and 0.1 to 2.6, 15.3 and 9.1 respectively by the presence of 1.44 mole percent propylene. The yields of acetaldehyde, diethyl ether, sec-butyl alcohol and diethoxy methane were unaffected.

b. Ethanol-ammonia mixtures. Ethanol density 0.66 g/l

Ethanol samples containing 0 to 16 mole percent ammonia were irradiated at 350° to a dose of  $7.5 \times 10^{19}$  eV/g. The ethanol pressure of 568 torr was kept constant in all the samples. The variation of product yields with ammonia concentration is presented in Table III-17 and Figures III-25 and III-26. Acetaldehyde reacts with ammonia (93) so the yield of this product could not be determined. The hydrogen yield was corrected for the direct radiolysis of ammonia, using  $G(H_2)_{NH_3} = 15.0$  (94), which was obtained when ammonia was irradiated at 250° and 835 torr.

At an ethanol density of 0.66 g/l, ammonia decreases the product yields as follows: carbon monoxide

TABLE III-17

G values of products in the radiolysis of  $C_2H_5OH-NH_3$

mixtures at 350°C.

Ethanol density = 0.66 g/l

Mole % <u><math>NH_3</math></u>	0	0.29	4.85	9.24	10.65	15.26
<u>Product</u>	g					
Hydrogen	45.8	48.8	35.5	42.3	n.d.	32.5
Methane	38.2	37.1	34.7	37.0	n.d.	35.6
Carbon monoxide	9.7	7.9	4.7	5.1	n.d.	4.7
Ethane	3.4	1.4	1.6	1.7	n.d.	1.1
Ethylene	19.7	18.0	16.1	17.8	n.d.	15.4
Diethyl ether	5.6	0.7	2.4	1.5	n.d.	0.4
Methanol	17.3	12.9	6.8	6.2	9.0	7.6

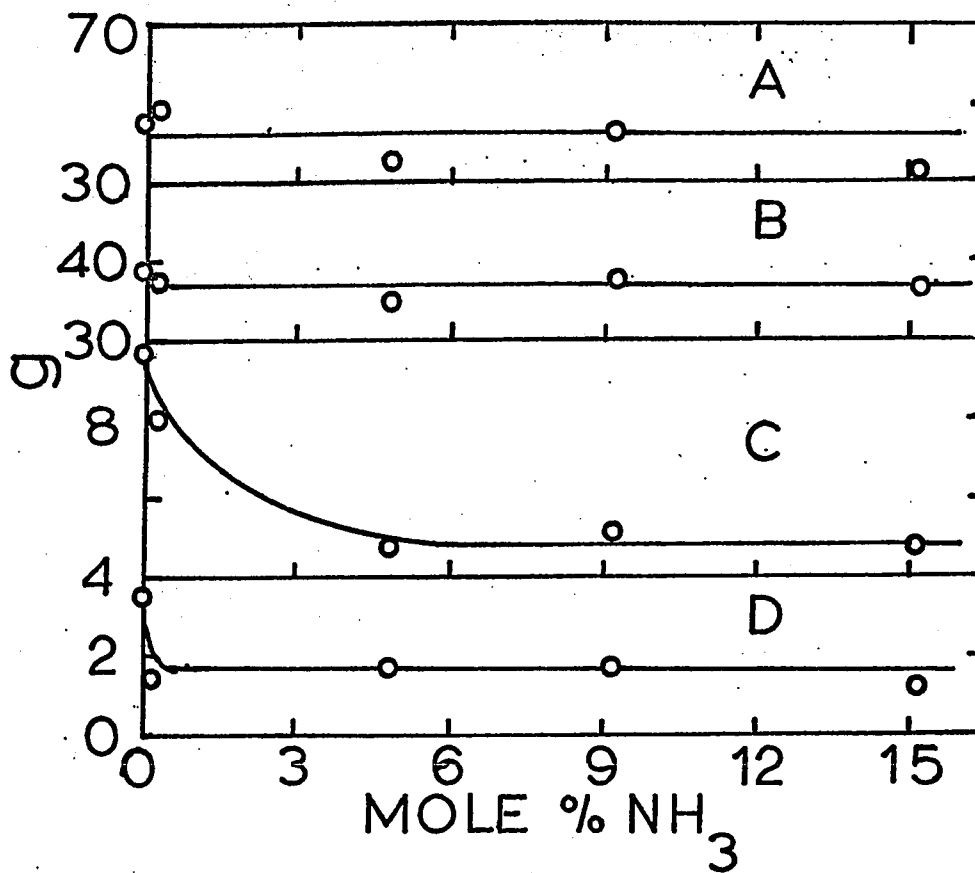


FIGURE III - 25

Product yields in the radiolysis of ethanol-ammonia mixtures. Temperature = 350°C.

Ethanol density = 0.66 g/l.

- |   |   |                 |
|---|---|-----------------|
| A | O | Hydrogen        |
| B | O | Methane         |
| C | O | Carbon monoxide |
| D | O | Ethane          |

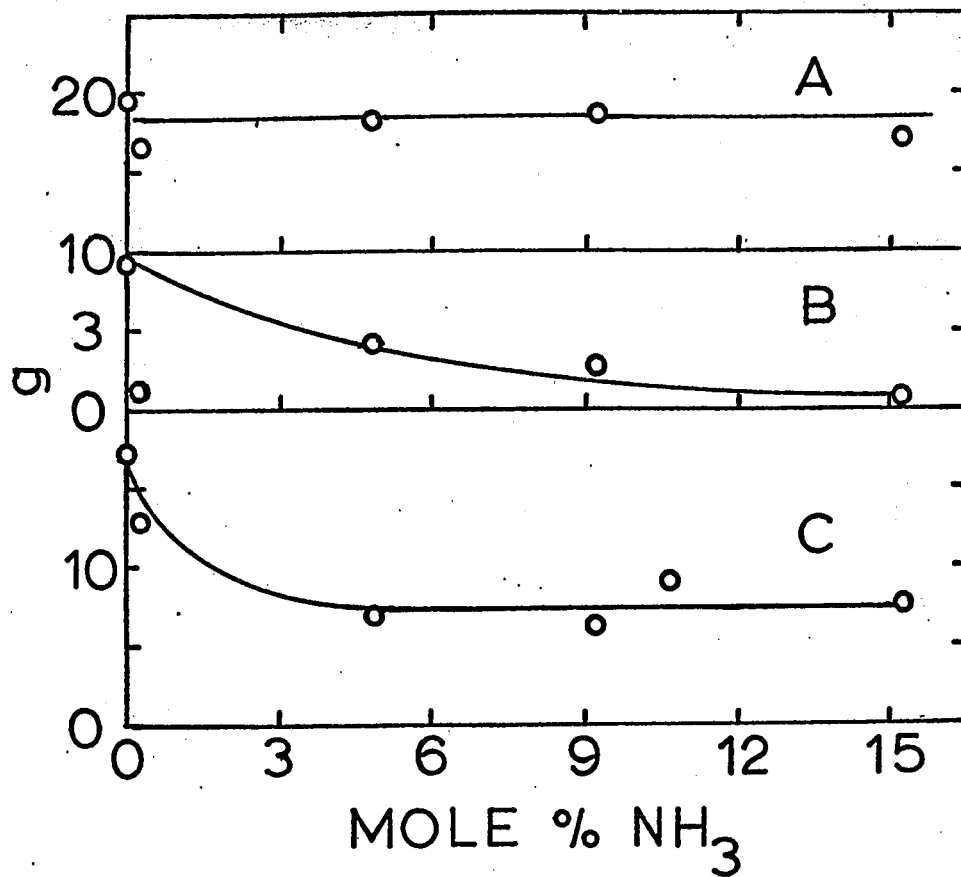


FIGURE III - 26

Product yields from the radiolysis of ethanol-ammonia mixtures. Temperature = 350°C.

Ethanol density = 0.66 g/l

A	O	Ethylene
B	O	Diethyl ether
C	O	Methanol

from 9.8 to 4.8, ethane from 3.5 to 1.6, diethyl ether from 5.6 to 0.3, and methanol from 17.4 to 7.5. The yields of hydrogen, methane and ethylene were unaffected.

c. Ethanol-sulphur hexafluoride mixtures. Ethanol  
density  $0.66 \text{ gl}^{-1}$

Samples of ethanol plus 0 to 20 mole percent sulphur hexafluoride were irradiated to a dose of  $7.5 \times 10^{19} \text{ ev g}^{-1}$ . The ethanol pressure of 568 torr was kept constant in all the samples.

The g values of various gaseous and liquid products as a function of sulphur hexafluoride concentration are presented in Tables III-18 and III-19 and Figures III-27, III-28, III-29 and III-30. The g values of ethane are not reported in Table III-18 because it could not be separated from sulphur hexafluoride on 2% Apiezon-L on silica gel column.

At an ethanol density of  $0.66 \text{ gl}^{-1}$ , sulphur hexafluoride decreases the product yields as follows: hydrogen from 45.9 to 16.8, methane from 38.9 to 9.0, carbon monoxide from 9.8 to 1.0, ethylene from 19.8 to 8.2, sec-butyl alcohol from 2.8 to 0.1, and methanol from 17.0 to 6.3. The yield of (acetaldehyde + acetal) appears to remain constant by the presence of up to 1 mole percent of sulphur hexafluoride. The increase of sulphur hexafluoride concentration over the range 1 to 20 mole percent



TABLE III-18

g values of gaseous products in the radiolysis of  $C_2H_5OH + SF_6$  mixtures at  $350^\circ$

Mole % $SF_6$	Ethanol density = 0.66 g/l							
	$H_2$	$CH_4$	CO	$C_2H_6$	$C_2H_4$	$C_3H_8$	$C_2H_2$	n- $C_4H_{10}$
	g							
0.0	45.9	38.9	9.8	3.5	19.8	0.1	n.d.	0.1
0.0021	32.9	27.5	6.0	n.d.	12.6	0.2	0.06	0.03
0.0051	32.3	19.0	4.2	n.d.	9.4	0.03	0.04	0.2
0.024	33.4	9.2	1.3	n.d.	8.7	n.d.	0.06	0.3
0.025	n.d.	7.8	1.2	n.d.	7.2	n.d.	0.05	0.3
0.08	21.8	10.0	1.3	n.d.	10.6	n.d.	0.05	0.07
0.20	20.2	8.2	1.0	n.d.	7.3	n.d.	0.03	0.2
0.32	22.1	8.5	1.0	n.d.	9.4	n.d.	n.d.	0.3
0.62	20.6	7.3	0.8	n.d.	n.d.	n.d.	n.d.	n.d.
0.99	21.3	9.0	1.0	n.d.	8.2	n.d.	0.03	0.04
14.6	16.8	9.0	1.0	n.d.	n.d.	n.d.	n.d.	n.d.

TABLE III-19

G values of liquid products in the radiolysis of  $C_2H_5OH-SF_6$  mixtures at 350°C

Ethanol density = 0.66 g/l

Mole % $SF_6$	g						
	ether acetalde- hyde	acetal	acetalde- hyde + acetal	1,2-propane- diol	methanol	sec butyl alcohol	diethoxy methane
0.0	5.6	41.8	----	2.4	17.0	2.8	0.7
0.0022	5.5	2.4	36.9	1.2	11.9	1.0	0.8
0.0051	5.8	31.5	14.9	1.3	24.4	1.7	0.5
0.024	12.9	0.5	44.9	0.7	8.5	n.d	0.7
0.086	12.5	0.4	34.8	1.5	0.9	0.07	1.3
0.091	7.5	n.d	n.d	1.6	3.3	0.09	1.2
0.20	14.2	0.7	51.4	1.3	7.3	0.04	1.5
0.41	7.1	0.3	27.6	1.4	5.8	0.08	1.1
0.62	4.9	0.4	31.0	n.d	n.d	n.d	n.d
1.13	7.7	0.2	22.2	1.4	2.8	0.08	1.2
2.98	8.7	0.4	48.0	0.7	7.6	n.d	0.9
5.5	7.9	1.	65.0	n.d	n.d	n.d	n.d
9.2	15.4	0.7	66.8	2.0	6.3	0.05	2.3
14.6	10.2	1.9	30.6	n.d	n.d	n.d	n.d
19.8	9.6	0.7	84.0	2.0	8.5	n.d	3.0

1 131 1

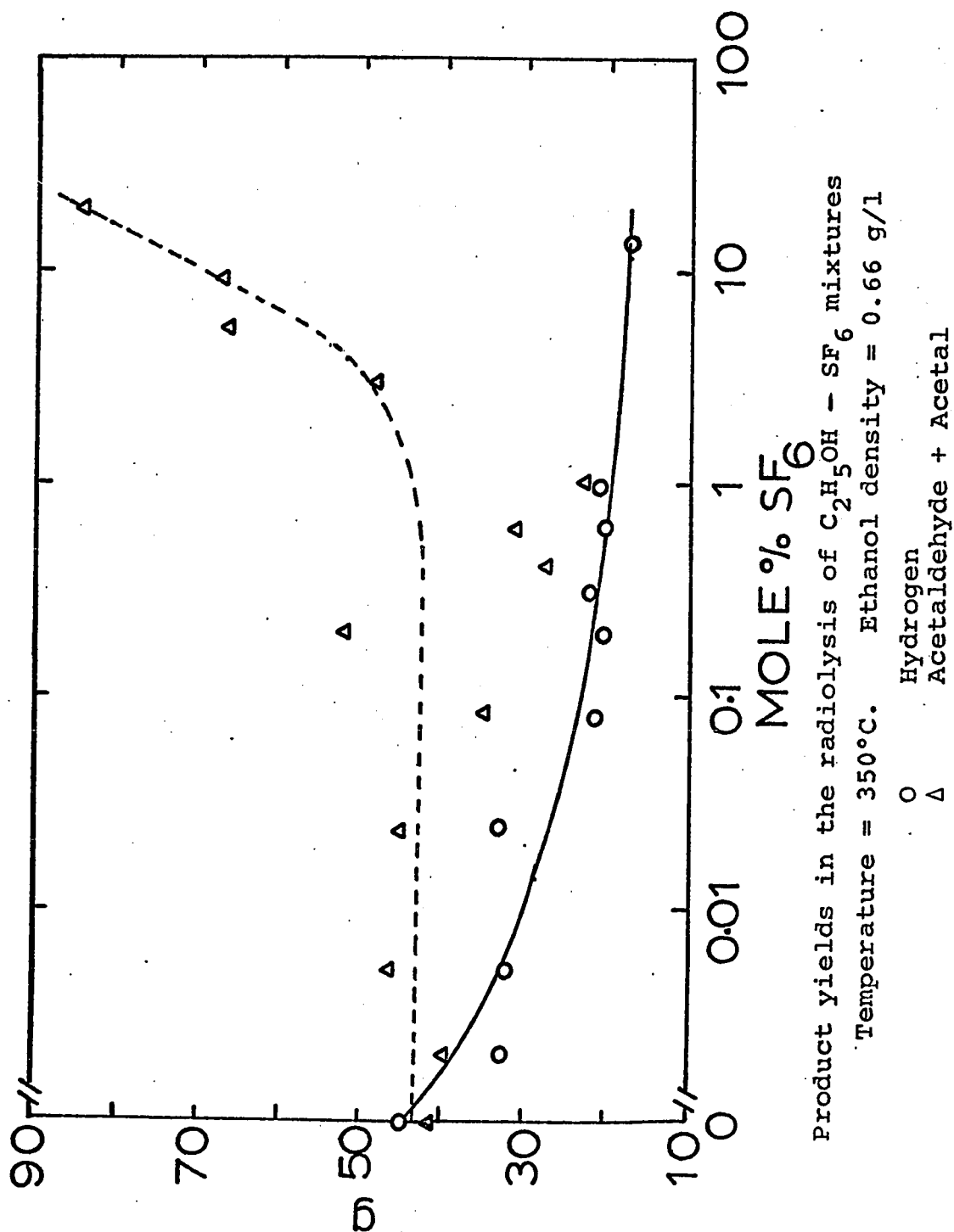


FIGURE III-27

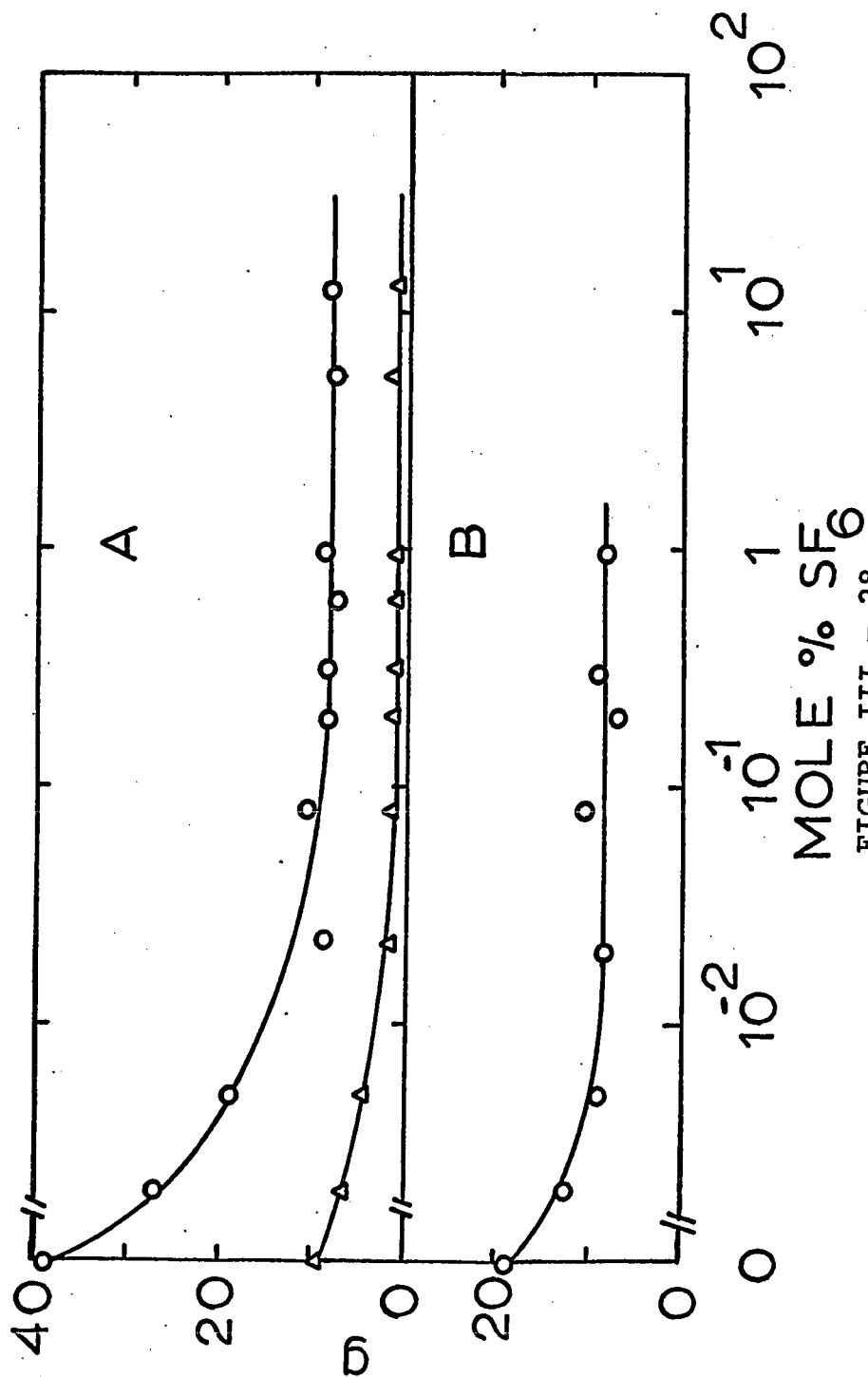


FIGURE III - 28  
Product yields in the radiolysis of ethanol-sulphur hexafluoride mixtures. Temperature =  $350^\circ\text{C}$ . Ethanol density =  $0.66 \text{ g/l}$ .

A	O	Methane
	$\Delta$	Carbon monoxide
B	O	Ethylene

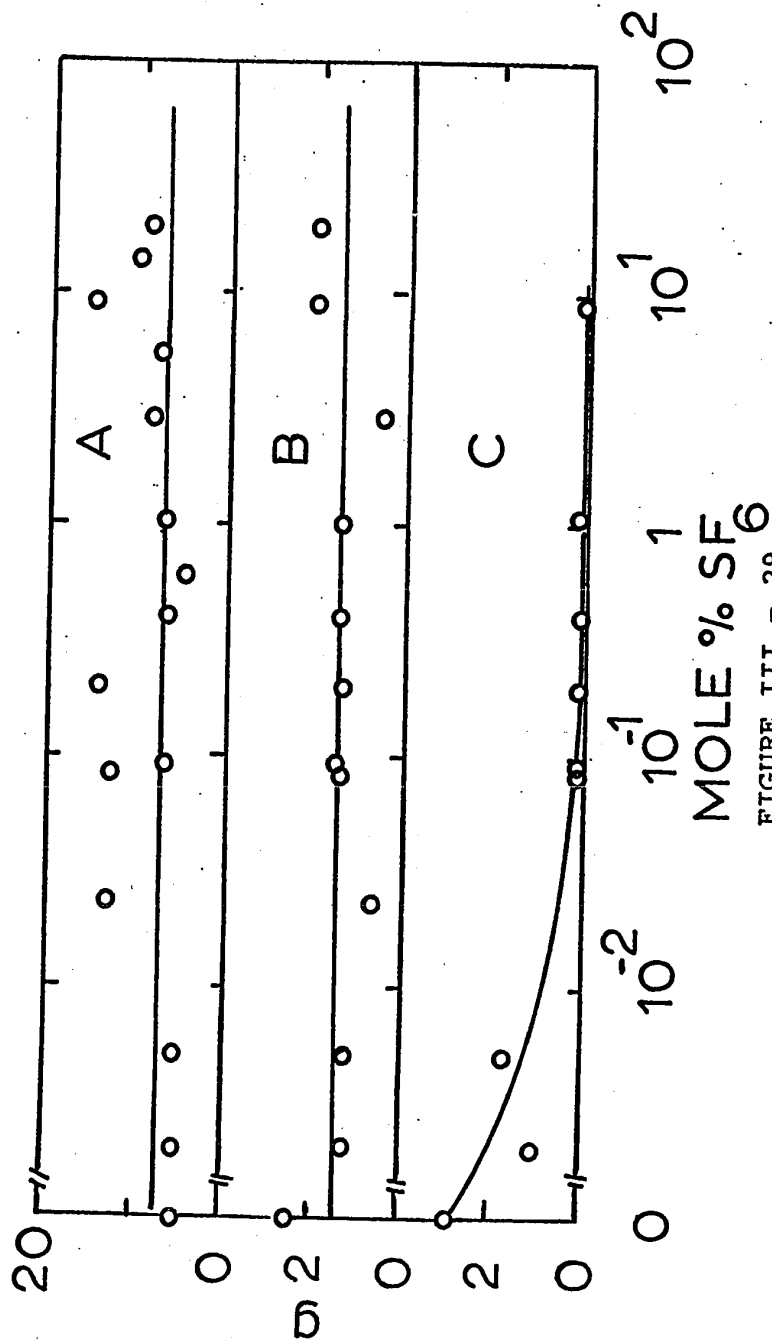


FIGURE III - 29  
Product yields in the radiolysis of ethanol-sulphur hexafluoride mixtures. Temperature =  $350^\circ\text{C}$ . Ethanol density =  $0.66 \text{ g/l}$ .

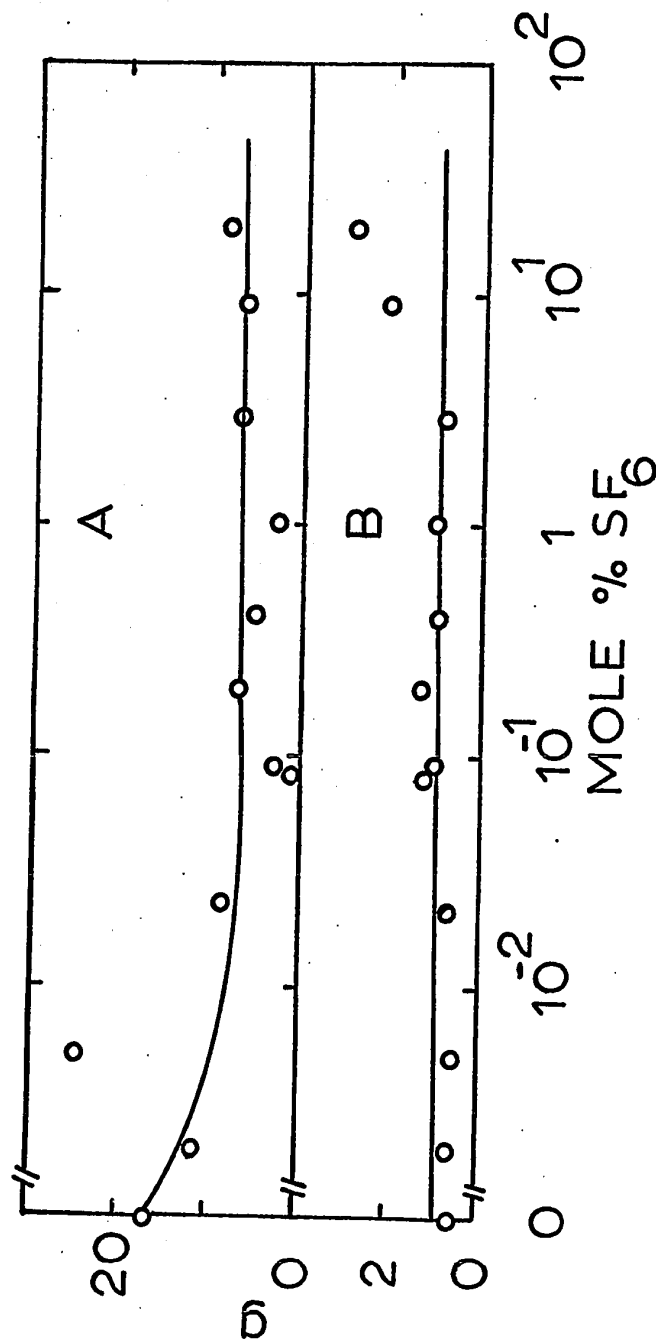


FIGURE III - 30

Product yields in the radiolysis of ethanol-sulphur hexafluoride mixtures. Temperature = 350°C. Ethanol density = 0.66 g/l.

A	O	CH <sub>3</sub> OH
B	O	Diethoxy methane.

increases the yield of (acetaldehyde + acetal) from about 43 to 84 g units (Fig. III-27. The yields of propane, acetylene, n-butane, diethoxy methane, diethyl ether and 1,2-propanediol were unaffected.

2. Effect of ethanol pressure.

The dependence of product yields on pressure was studied by varying the pressure of ethanol in the irradiation cells over the range 65 to 1800 torr ( $0.076 - 2.14 \text{ g l}^{-1}$ ). The samples were irradiated to a dose of  $7.5 \times 10^{19} \text{ eV g}^{-1}$ .

The yields of various products as a function of pressure are presented in Table III-20 and Figures III-31 and III-32. The yields of ethane and ethylene were unaffected by change of pressure. The yields of methane, methanol, sec-butyl alcohol and carbon monoxide increase in the following manner: methane from 18.2 to 52.8, methanol from 4.5 to 25.8, sec-butyl alcohol from 1.5 to 3.2, and carbon monoxide from 3.3 to 10.5. The yields of diethyl ether, hydrogen and acetaldehyde decrease in the following way: diethyl ether from 10.2 to 0.90, hydrogen from 75.8 to 28.9, and acetaldehyde from 73.0 to 59.9.

E. Pyrolysis of ethanol

1. Pure ethanol at  $350^\circ$  and density  $0.66 \text{ g l}^{-1}$ .

Two samples of pure ethanol were prepared in exactly the same manner as the samples for irradiation study. The

TABLE III-20

Product yields as a function of pressure in the radiolysis  
of ethanol at 350°C

<u>Pressure (torr)</u>	<u>67.4</u>	<u>279</u>	<u>568</u>	<u>1789</u>
<u>Product</u>	G			
Hydrogen	75.8	58.4	45.9	28.9
Methane	18.2	31.9	38.9	52.8
Carbon monoxide	3.3	5.9	9.8	10.5
Ethane	2.5	2.4	3.5	2.2
Ethylene	18.3	18.5	19.8	16.8
Diethyl ether	10.2	7.3	5.6	0.9
Acetaldehyde	72.9	79.5	41.5	59.9
Methanol	4.5	10.3	17.0	25.8
sec-butyl alcohol	1.5	1.6	2.8	3.2



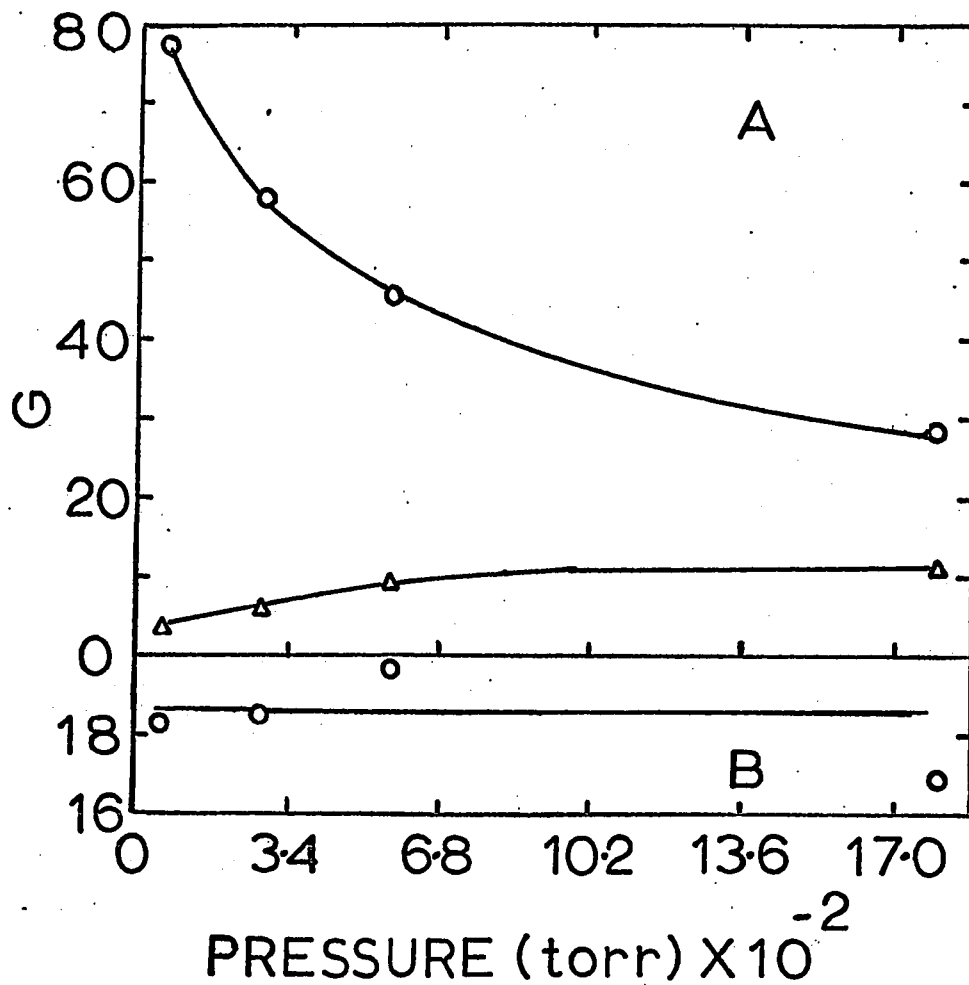


FIGURE III-31

Product yields from ethanol as a function of pressure. Temperature = 350°C

A	O	Hydrogen
	$\Delta$	Carbon monoxide
B	O	Ethylene

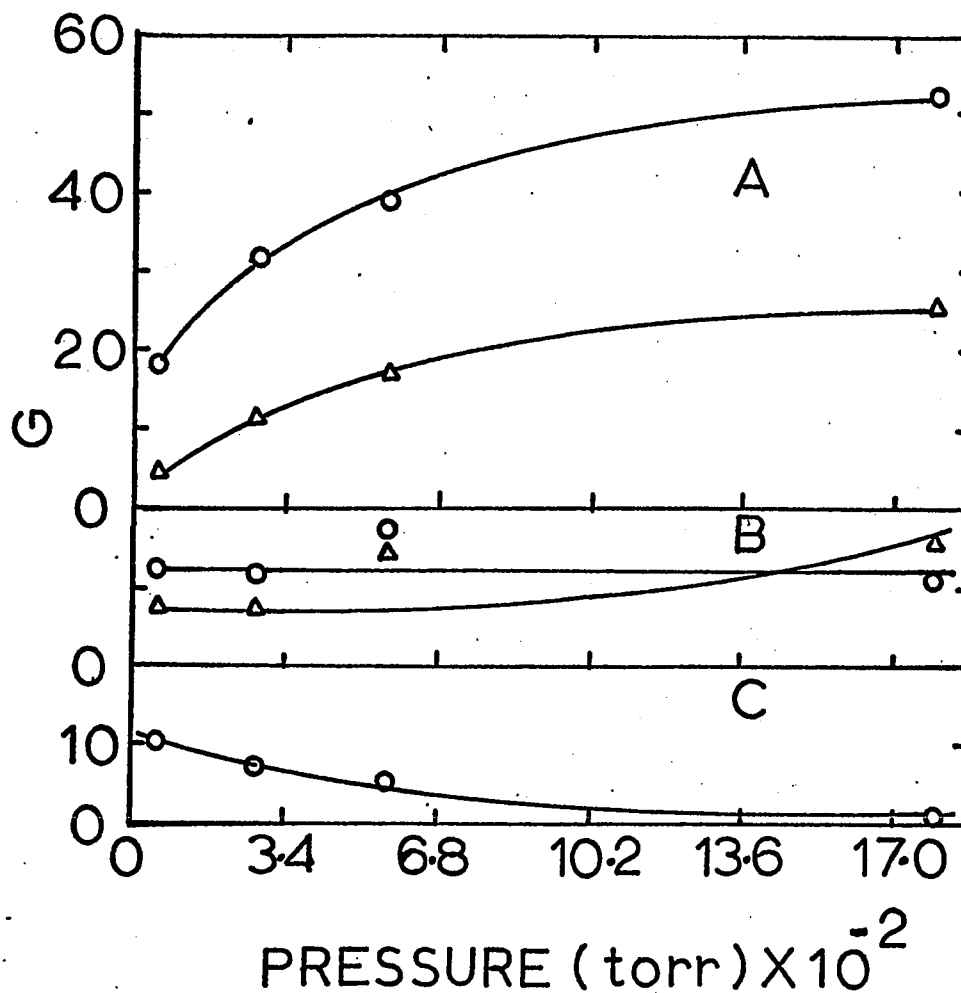


FIGURE III - 32

Products from ethanol radiolysis as a function of pressure. Temperature = 350°C.

A	O	Methane
	Δ	Methanol
B	O	Ethane
	Δ	sec-butyl alcohol
C	O	Diethyl ether

density of ethanol in these samples was the same as for ethanol in irradiation samples. One sample was heated for 2 hr (irradiation time for ethanol samples) at 350° and the second sample was heated for 20 hours at 350°. These samples were analyzed for liquid and gaseous products in a way identical to that for irradiation samples. The number of moles of each of the gaseous and liquid product was calculated. The results are presented in Table III-21. The number of moles of the various products obtained from irradiation of ethanol at 350° for 2 hrs are also presented in Table III-21 together with the ratio  $X_1$ .

$$X_1 = \frac{\text{no. of moles of a product from pyrolysis sample}}{\text{no. of moles of the same product from irradiation sample}}$$

For the pyrolysis sample that was heated for 20 hr at 350°, the number of moles of each product was divided by 10 to get the number of moles of the product for 2 hr pyrolysis time. This was then divided by the number of moles of the same product from irradiation of pure ethanol at 350° for 2 hrs to get the ratio  $X_1$ . The value of this ratio was largest for hydrogen and acetaldehyde (0.32 and 0.29 respectively) and the smallest for methane (0.0040). For ethane, ethylene and diethyl ether, the value of the ratio  $X_1$  is 0.012, 0.026, and 0.068 respectively. The differences in the values of  $X_1$  between the 2 hour and 20 hour pyrolyses (Table III-21) cannot be understood without the thorough study of the pyrolysis reaction.

TABLE III-21

Products from pyrolysis of pure ethanol at 350°. Ethanol density = 0.66 g<sup>-1</sup>

Pyrolysis time (hours)	Product	No. of moles of the product x 10 <sup>6</sup>		X <sub>1</sub>
		Pyrolysis sample	Irradiated sample*	
2	Hydrogen	6.49	20.6	0.32
	Methane	0.064	17.4	0.0040
	Carbon monoxide	----	4.4	----
	Ethane	0.019	1.6	0.012
	Ethylene	0.23	8.9	0.026
	Diethyl ether	0.17	2.5	0.068
20	Acetaldehyde	5.50	18.7	0.29
	Hydrogen	15.13		0.073 +
	Methane	0.60		0.0034 +
	Carbon monoxide	0.055		----
	Ethane	0.022		0.0013 +
	Ethylene	5.98		0.068 +

cont'd .....

TABLE III-21 (continued)

\*The sample was irradiated for 2 hours at 350°

†The number of moles of each of the product from the pyrolysis sample was divided by 10, to get the number of moles of the product for 2 hours pyrolysis time. This was then divided by the number of moles of the same product from the irradiated sample, to obtain the ratio  $X_1$ .

2. Mixtures of ethanol with sulphur hexafluoride, ammonia or propylene at 350°. Ethanol density 0.66 gl<sup>-1</sup>

Binary mixtures of ethanol and the scavenger were prepared in a manner similar to that used for the irradiation samples. The samples were heated for 2 hrs at 350° (time for which the samples were irradiated). After heating, the samples were analyzed for the liquid and gaseous products. The method used was the same as that for irradiation samples. The number of moles of the various products obtained in the pyrolysis study is presented in Table III-22. The number of moles of the various products obtained in the radiolysis of (ethanol + scavenger) at 350° and the ratio  $X_2$ .

$$X_2 = \frac{\text{No. of moles of a product from pyrolysis samples of ethanol + Z mole \% scavenger}}{\text{No. of moles of the same product from the radiolysis of ethanol + Z mole \% scavenger}}$$

are also presented in Table III-22.

The value of the ratio  $X_2$  for hydrogen, when sulphur hexafluoride was used as the scavenger, was largest ( $X_2 = 0.88$ ). The ratio  $X_2$  for (acetaldehyde + acetal), ethylene, diethyl ether and methane was 0.30, 0.08, 0.04, and 0.02 respectively (Table III-22). Similar conclusions were obtained when propylene or ammonia were used as the scavengers.

TABLE III-22

Products from pyrolysis of ethanol-scavenger mixtures at 350°. Ethanol density=0.66 gl<sup>-1</sup>

Scavenger	Mole % Scavenger	Product	No. of moles of the product x 10	Pyrolysis* study	Irradiated† sample	X <sub>2</sub>
SF <sub>6</sub>	5.6	Hydrogen	6.6	7.56	0.88	
		Methane	0.069	3.36	0.020	
		Carbon monoxide	---	0.42	---	
		Ethylene	0.28	3.36	0.08	
SF <sub>6</sub>	1.2	Acetaldehyde + Acetal	5.50	18.06	0.30	
		Diethyl ether	0.13	2.94	0.04	
C <sub>3</sub> H <sub>6</sub>	16.2	Hydrogen	5.9	4.62	1.27	
		Methane	0.13	8.40	0.015	
		Carbon monoxide	0.01	1.26	0.008	
		Acetaldehyde	5.7	16.80	0.34	
NH <sub>3</sub>	13.9	Hydrogen	6.7	17.64	0.38	
		Methane	0.13	15.54	0.008	
		Carbon monoxide	---	2.02	---	

\*Pyrolysis time 2 hr  
†Irradiation time 2 hr

- 144 -

3. Pure ethanol at 375° and density=0.66 g/l

A procedure similar to the one for pyrolysis of ethanol studies at 350° was used. The number of moles of hydrogen, methane, carbon monoxide, ethane and ethylene obtained in the pyrolysis study and from irradiation study at 375° are presented in Table III-23. The ratio

$$X_3 = \frac{\text{No. of moles of a product from pyrolysis sample at 375°}}{\text{No. of moles of the same product from irradiated sample at 375°}}$$

is also reported in Table III-23. The value of the ratios  $X_1$  and  $X_3$  (Tables III-21 and III-23) for methane is nearly the same. The values of the ratio  $X_3$  for hydrogen, ethane and ethylene are lower than the corresponding  $X_1$  values (Tables III-21 and III-23).



TABLE III-23

Products from pyrolysis of pure ethanol at 375°. Ethanol density = 0.66 g/l

Pyrolysis time (hours)	Product	No. of moles of the product x 10 <sup>+6</sup>		x <sub>3</sub>
		Pyrolysis sample	Irradiated* sample	
3	Hydrogen	11.3	63.0	0.18.
	Methane	0.2	56.9	0.0035
	Carbon monoxide	0.02	20.7	0.0010
	Ethane	0.03	5.2	0.0057
	Ethylene	0.3	28.5	0.011

- 146 -

\* The sample was irradiated for 3 hours at 375°.

Part III      Vapor Phase Radiolysis of Propylene

A. Effect of temperature at constant density ( $1.96 \text{ g l}^{-1}$ )

Samples of propylene were irradiated in 500 ml irradiation cells at various temperatures ( $25^\circ$ ,  $150^\circ$  and  $350^\circ$ ) to a dose of  $7.8 \times 10^{19} \text{ eV g}^{-1}$ . The pressure of propylene was 865 torr at  $25^\circ$ . Only  $G(\text{H}_2)$  and  $G(\text{CH}_4)$  were determined. The G values are presented in Table III-24.  $G(\text{H}_2)$  changes from 1.12 to 1.36 and  $G(\text{CH}_4)$  increases from 0.30 to 2.64 as the temperature increases from  $25^\circ$  to  $350^\circ$ .

B. Effect of propylene pressure at  $150^\circ$

The dependence of  $G(\text{H}_2)$  and  $G(\text{CH}_4)$  on pressure in the radiolysis of propylene was studied by varying the pressure of propylene over the range 30 to 870 torr ( $0.048 - 1.39 \text{ g l}^{-1}$ ). Each sample was irradiated to a dose of  $7.8 \times 10^{19} \text{ eV g}^{-1}$ . The variation of  $G(\text{H}_2)$  and  $G(\text{CH}_4)$  is presented in Table III-25 and Figure III-33.  $G(\text{CH}_4)$  is unaffected by pressure.  $G(\text{H}_2)$  decreases from 1.80 to 1.27 with increase of pressure.

TABLE III - 24

The variation of  $G(H_2)$  and  $G(CH_4)$  with temperature in the radiolysis of propylene. Propylene density = 1.96 g/l

<u>Irradiation temperature (°C)</u>	<u><math>G(H_2)</math></u>	<u><math>G(CH_4)</math></u>
25	1.12	0.30
150	1.27	0.23
350	1.36	2.64

TABLE III - 25

$G(H_2)$  and  $G(CH_4)$  as a function of pressure in the radiolysis of propylene at 150°

<u>Pressure (torr)</u>	<u>density g/l</u>	<u><math>G(H_2)</math></u>	<u><math>G(CH_4)</math></u>
43.6	0.07	1.80	0.25
129.9	0.21	1.72	0.27
439.2	0.70	1.29	0.22
1228	1.96	1.27	0.23

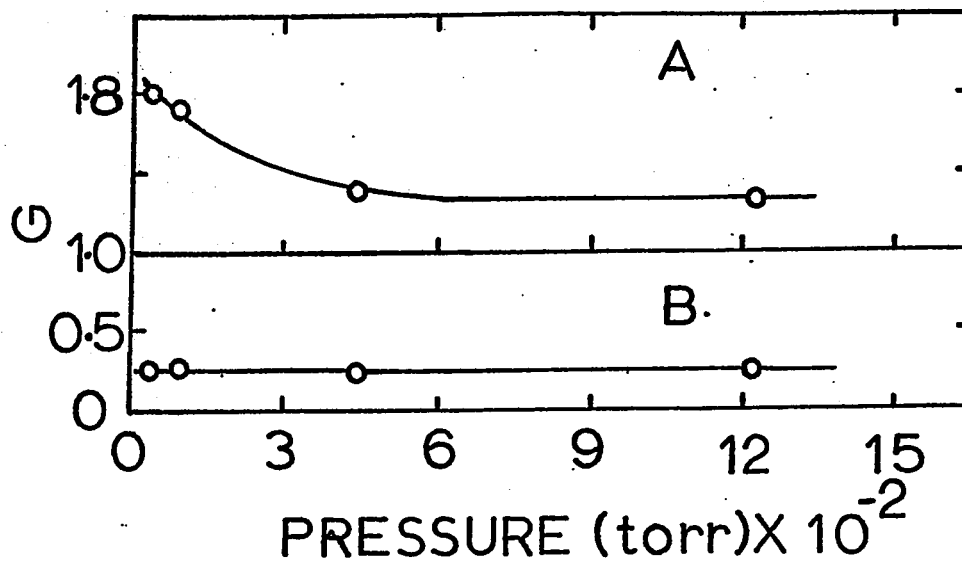


FIGURE III - 33

$G(H_2)$  and  $G(CH_4)$  as a function of pressure in the radiolysis of propylene. Temperature = 150°C.

A	O	Hydrogen
B	O	Methane

## D I S C U S S I O N

### A. Vapor phase radiolysis of diethyl ether

The material balance for the products obtained from radiolysis of diethyl ether vapor (1.16 g/l) at 33° and at a dose of  $1.6 \times 10^{20}$  eV/g is presented in Table IV-1.  $G(-\text{ether})$  is found to be 10.7. The radiolysis products add up to an empirical formula of  $\text{C}_4\text{H}_{10.3}\text{O}_{0.97}$  which corresponds to an excess of  $G(\text{H}_2) = 1.6$  and a deficiency of  $G(\text{O}_2) = 0.16$ . These values obtained in the present study agree well with the values obtained in an earlier study (95). This poor material balance might be due to the formation of polymeric products containing more than eight carbon atoms which were not measured in the present study. The total extent of decomposition of diethyl ether at 33° and at a dose of  $1.6 \times 10^{20}$  eV/g was 0.2 percent.

#### 1. The chain reaction

At high temperatures, the products ethane and acetaldehyde are produced mainly by a chain reaction (Figure III-1). Methane and carbon monoxide are also produced by the chain decomposition of acetaldehyde at these temperatures (Figure III-2A), but for the sake of simplicity in this discussion, the decomposition of acetaldehyde will be ignored and the total acetaldehyde yield will be taken as the sum of the acetaldehyde and

TABLE IV-1

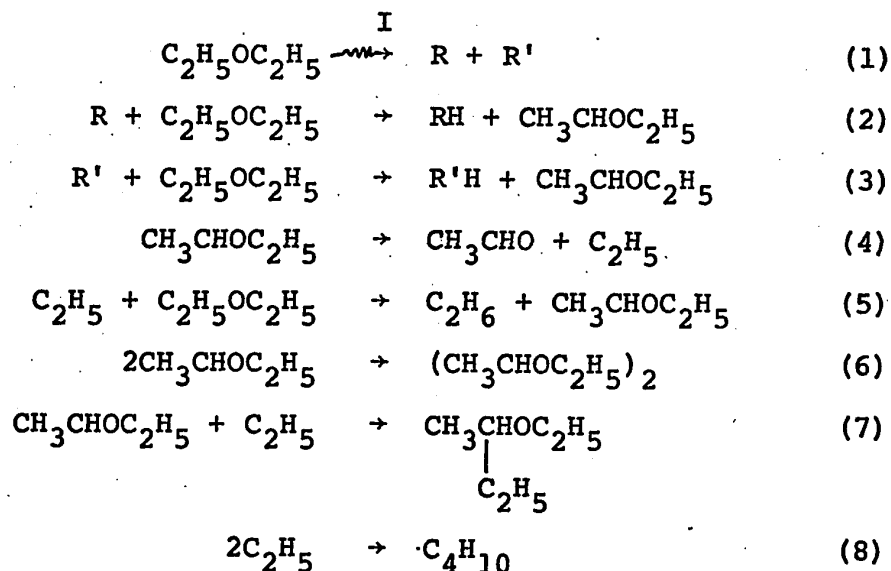
Material balance for pure diethyl ether vapor

<u>Product</u>	<u>C</u>	<u>H</u>	<u>O</u>
H <sub>2</sub>	-	11.7	-
CH <sub>4</sub>	1.55	6.20	-
CO	0.47	--	0.47
C <sub>2</sub> H <sub>6</sub>	0.80	2.40	-
C <sub>2</sub> H <sub>4</sub>	3.58	7.16	-
C <sub>3</sub> H <sub>8</sub>	0.66	1.76	-
C <sub>4</sub> H <sub>10</sub>	0.36	0.90	-
C <sub>2</sub> H <sub>2</sub>	0.46	0.46	-
CH <sub>2</sub> O	0.64	1.28	0.64
(CH <sub>3</sub> ) <sub>2</sub> CHOC <sub>2</sub> H <sub>5</sub>	5.40	12.96	1.08
CH <sub>3</sub> CH $\begin{cases} \text{OCH}_3 \\ \text{OC}_2\text{H}_5 \end{cases}$	1.70	4.08	0.68
CH <sub>3</sub> CHO	2.80	5.60	1.40
CH <sub>3</sub> CH(OC <sub>2</sub> H <sub>5</sub> ) <sub>2</sub>	-	-	-
C <sub>2</sub> H <sub>5</sub> OH	1.26	3.78	0.63
CH <sub>2</sub> =CHOC <sub>2</sub> H <sub>5</sub>	1.48	2.96	0.37
(CH <sub>3</sub> CHOC <sub>2</sub> H <sub>5</sub> ) <sub>2</sub>	16.96	38.16	4.24
CH <sub>3</sub> CH(C <sub>2</sub> H <sub>5</sub> )OC <sub>2</sub> H <sub>5</sub>	<u>4.68</u>	<u>10.92</u>	<u>0.78</u>
TOTAL	42.80	110.32	10.29

$$10.7(\text{C}_4\text{H}_{10.30}\text{O}_{0.97})$$

carbon monoxide yields.

The formation of the products ethane, acetaldehyde, n-butane, sec-butyl ethyl ether and 2,3-diethoxybutane, are explained by the following mechanism.

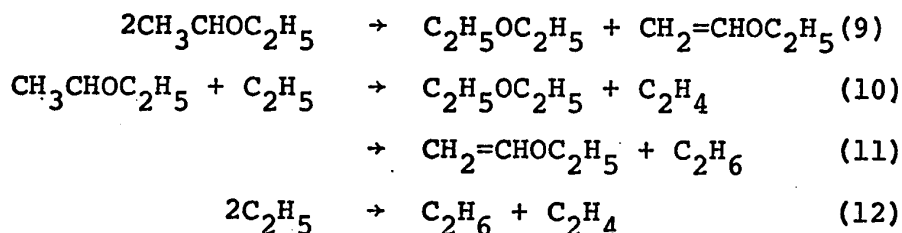


where R and R' are radicals and

$$\text{I} = 10^{-2} \text{ D G(R)} \quad (\text{i})$$

where D is the dose rate (eV/cc sec) and G(R) is the 100-ev yield of R.

The disproportionation counterparts of reactions 6, 7, and 8 occur to a smaller extent



It is known that  $\frac{k_{12}}{k_8} = 0.14$  (96). An upper limit of

$\frac{k_9}{k_6} \leq 0.14$  is obtained from the ratio of the yields of ethyl vinyl ether and 2,3-diethoxybutane at 80°. An upper limit of  $\frac{k_{11}}{k_7} \leq 0.07$  is obtained from the ratio of the yields of ethyl vinyl ether and sec-butyl ethyl ether at 125°, and it is reasonable to assume that  $(k_{10} + k_{11})/k_7 \leq 0.14$ .

Since reactions 9-12 occur to a much smaller extent than do the reactions 6-8, the discussion of the chain mechanism will be further simplified by neglecting the disproportionation reactions. This will not alter the conclusions or the values of the activation energies obtained.

The sum of the G values of the products of the chain-terminating reactions 6-8 is constant at  $5.1 \pm 0.3$  at temperatures greater than 80°, so steady state kinetics can be applied to the simplified chain mechanism in this temperature region. The value of G(R) is approximately  $5.1 \times 1.14 = 5.8$ .

The yields of the chain-termination products 2,3-diethoxybutane, sec-butyl ethyl ether and n-butane (Fig. III-2B) indicate that, in the temperature region from about 100° to 140°, the average kinetic effects of reaction 6-8 are approximately the same as those that would be observed if chain termination occurred only by reaction 7.

The steady state treatment for the radicals R, R',



$C_2H_5$ ,  $CH_3CHOC_2H_5$  gives:

$$\frac{d[R]}{dt} = 0 = I - k_2[R][C_2H_5OC_2H_5] \quad (13)$$

$$\frac{d[R']}{dt} = 0 = I - k_3[R'][C_2H_5OC_2H_5] \quad (14)$$

$$\begin{aligned} \frac{d[C_2H_5]}{dt} = 0 = & k_4[CH_3CHOC_2H_5] - k_5[C_2H_5][C_2H_5OC_2H_5] \\ & - k_7[CH_3CHOC_2H_5][C_2H_5] \end{aligned} \quad (15)$$

$$\begin{aligned} \frac{d[CH_3CHOC_2H_5]}{dt} = 0 = & k_2[R][C_2H_5OC_2H_5] + k_3[R'][C_2H_5OC_2H_5] \\ & - k_4[CH_3CHOC_2H_5] + k_5[C_2H_5][C_2H_5OC_2H_5] \\ & - k_7[CH_3CHOC_2H_5][C_2H_5] \end{aligned} \quad (16)$$

On solving 13, 14, 15 and 16 we get

$$[CH_3CHOC_2H_5] = \frac{I}{k_7[C_2H_5]} \quad (17)$$

$$[C_2H_5] = \frac{-k_7I + \{k_7^2I^2 + 4k_4k_5k_7I[C_2H_5OC_2H_5]\}^{\frac{1}{2}}}{2k_5k_7[C_2H_5OC_2H_5]} \quad (18)$$

$$\frac{d[C_2H_6]}{dt} = k_5[C_2H_5][C_2H_5OC_2H_5] \quad (19)$$

Substituting for  $[C_2H_5]$  from 18 into 19 and solving, we get

$$\frac{d[C_2H_6]}{dt} = \frac{-I}{2} + \left\{ \left( \frac{I}{2} \right)^2 + \frac{k_4k_5}{k_7} I [C_2H_5OC_2H_5] \right\}^{\frac{1}{2}} \quad (ii)$$

Furthermore, chain initiation is first order in ether concentration, i.e.

$$I = A' [C_2H_5OC_2H_5] \quad (iii)$$

where  $A'$  is a proportionality constant that depends on the  $\gamma$ -beam intensity, the ether molecular absorption coefficient, and the efficiency of reaction 1. Therefore

$$\frac{d[C_2H_6]}{dt} = \left\{ -A + \left( A^2 + \frac{2k_4k_5}{k_7} A \right)^{\frac{1}{2}} \right\} [C_2H_5OC_2H_5] \quad (iv)$$

where  $A = \frac{A'}{2}$ . The value of  $G(C_2H_6)$  is given by

$$G(C_2H_6) = \frac{10^2}{D} \frac{d[C_2H_6]}{dt} \quad (v)$$

From equations i, iii, iv and v we obtain

$$G(C_2H_6) = \frac{G(R)}{2} \left\{ -1 + \left( 1 + \frac{2k_4k_5}{k_7A} \right)^{\frac{1}{2}} \right\} \quad (vi)$$

Since  $G(R)$  is expected to be independent of ether concentration,  $G(C_2H_6)$  should also be independent of ether concentration in this temperature region.

It can readily be shown that  $G(CH_3CHO)$  should also be independent of ether concentration in this temperature region. Values of  $G(C_2H_6)$  and  $G(CH_3CHO)$  at  $140^\circ$  were found to be independent of ether pressure over the range 172 to 622 torr (Fig. III-5A) as expected. At temperatures greater than  $80^\circ$ ,  $\frac{G(R)}{2} = 2.9$ . Thus equation vi can be rearranged to

$$\left[ \frac{G(C_2H_6)}{2.9} + 1 \right]^2 - 1 = \frac{2k_4k_5}{k_7A} \quad (vii)$$

The logarithm of the left-hand side of equation vii was plotted against  $1/T$ , where  $T$  is the absolute temperature (Figure IV-1). A small amount of ethane is formed by another mechanism ( $G = 0.40$  at  $33$  and  $50^\circ$ ), so this was subtracted from the higher temperature yields in the present treatment. The net  $G$  value is designated as  $G_{cor}$ . The acetaldehyde yields were similarly treated and are also plotted in Figure IV-1. From the slope of the curve in the region that corresponds to temperatures  $110^\circ$  to  $140^\circ$ , the value  $(E_4 + E_5 - E_7) = 28$  kcal/mole was calculated, where  $E_4$  is the activation energy of reaction 4, and so on. However,  $E_7 \approx 0$ , so  $(E_4 + E_5) = 28$  kcal/mole.

At temperatures greater than  $200^\circ$ , the main chain termination product is n-butane (Fig. III-2B), so termination occurs mainly by reaction 8. Under these conditions, the value of  $G(C_2H_6)$  can be shown to be

$$G(C_2H_6) = \frac{k_5}{k_8} \left\{ \frac{[C_2H_5OC_2H_5]}{A'} \right\}^{\frac{1}{2}} G(R) \quad (viii)$$

The concentration of ether was constant in these experiments, so one could obtain the value of  $(E_5 - \frac{1}{2}E_8)$  by plotting  $\log G(C_2H_6)$  vs.  $\frac{1}{T}$ . The yields of ethane are so large at

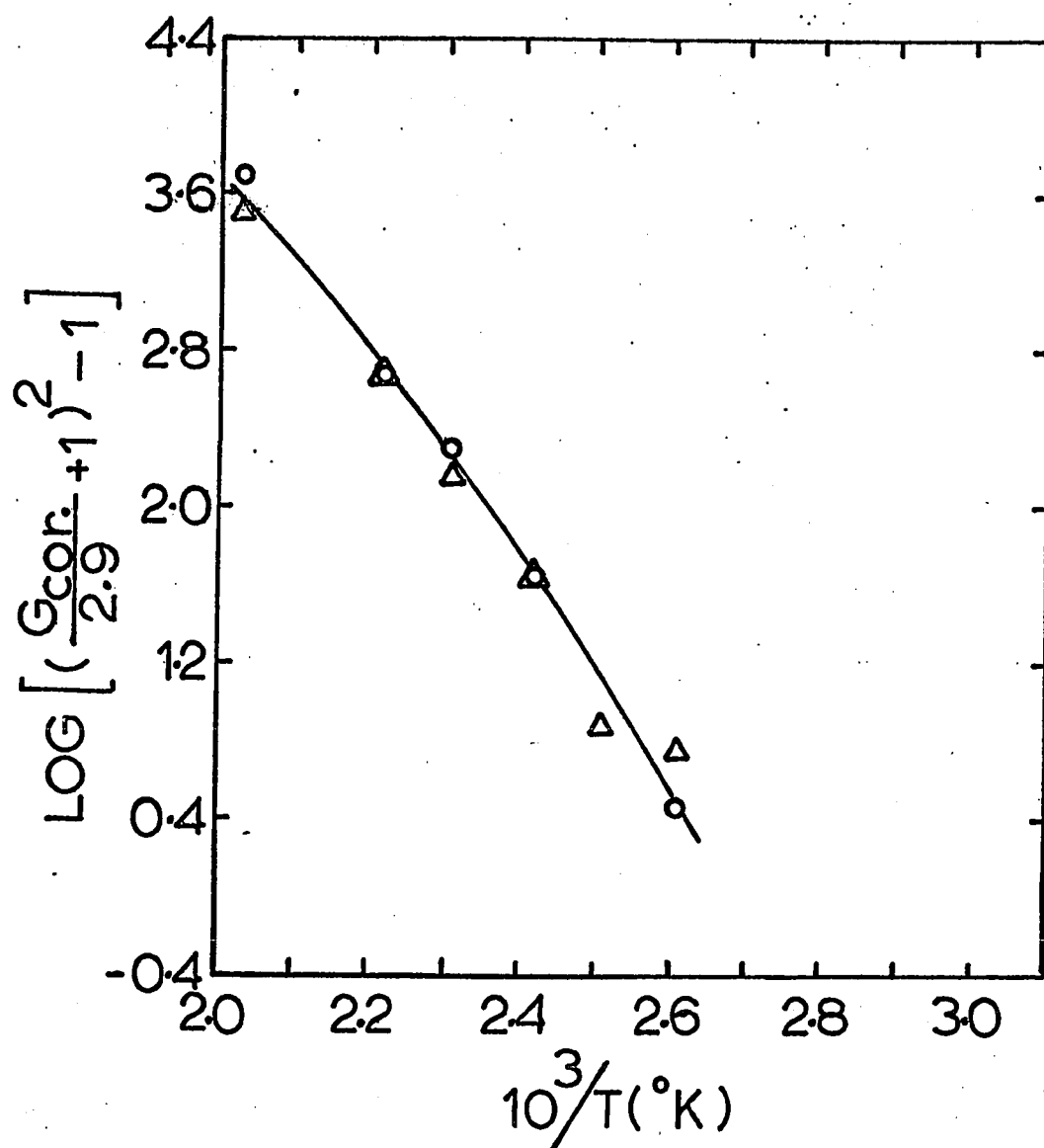
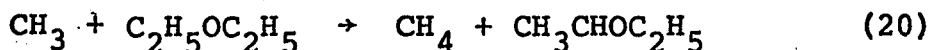


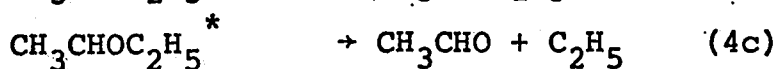
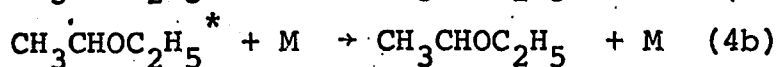
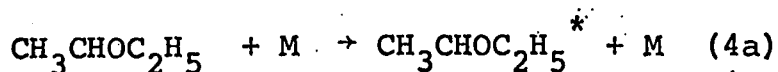
FIGURE IV-1

Arrhenius plot of ethane (O) and acetaldehyde (Δ) yields:  $G(\text{C}_2\text{H}_6)_{\text{cor.}} = G(\text{C}_2\text{H}_6) - 0.40$ ;  
 $G(\text{CH}_3\text{CHO} + \text{CO})_{\text{cor.}} = G(\text{CH}_3\text{CHO} + \text{CO}) - 1.8$

temperatures greater than 160° that the left-hand side of equation vii is essentially equal to  $[G(C_2H_6)/2.9]^2$ . Thus the value of  $(2E_5 - E_8)$  can be calculated from the slope of the upper portion of the curve in Figure IV-1. The value of  $E_8$  is zero, so  $E_5 = 9$  kcal/mole. Therefore,  $E_4 = 19$  kcal/mole. By comparison, Long and Skirrow (97) have reported  $E_4 = 23.5 \pm 2$  kcal/mole and  $E_{20} = 9.75 \pm 0.5$  kcal/mole



The order of reaction 4 is expected to be about 1.5 in the pressure range investigated (172 - 622 torr). This was estimated from the following information. The decomposition of methoxymethyl radicals at 248° and at pressures in the vicinity of 300 torr has been found to be 1.4 order (98). In the thermal decomposition of ethyl radicals over the pressure range 4 to 650 torr and the temperature range 400° to 500°, the order of reaction varies from 1.6 for the lowest pressure to 1.4 at the highest pressure (99). The decomposition of sec-butoxyl radicals to ethyl radicals and acetaldehyde, over the temperature range 150° - 190° and the pressure range 12 - 200 torr, was found to be in the transition zone between first and second order (100). Therefore, reaction 4 should be represented as 4a-c.



where M stands for diethyl ether. An overall order of 1.5 for the decomposition reaction means that it is 0.5 order in M and 1.0 order in  $\text{CH}_3\text{CHOC}_2\text{H}_5$  radicals. On the other hand reaction 5 is proportional to first power of ether concentration. So, as the pressure of diethyl ether increases, the lifetime of ethyl radicals in the system decreases more rapidly than does that of the  $\text{CH}_3\text{CHOC}_2\text{H}_5$  radicals. Therefore, as the ether pressure increases, reaction 7 contributes progressively more and reaction 8 progressively less to the termination of the chains. This causes the yield of n-butane to decrease and that of 2,3-diethoxybutane to increase with increasing ether pressure (Figure III-5C).

$$\text{The value of the ratio } \frac{G(\text{C}_4\text{H}_9\text{OC}_2\text{H}_5)}{[G(\text{n-C}_4\text{H}_{10}) \times G((\text{CH}_3\text{CHOC}_2\text{H}_5)_2)]^{\frac{1}{2}}}$$

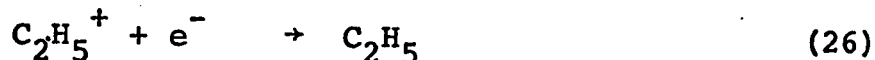
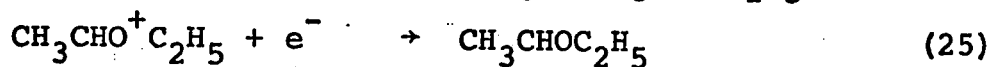
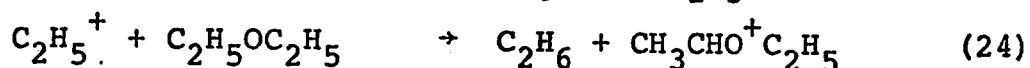
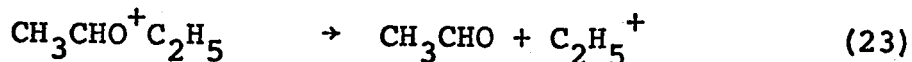
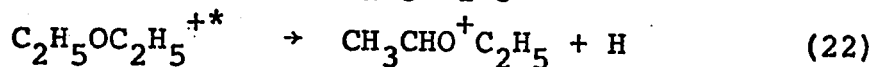
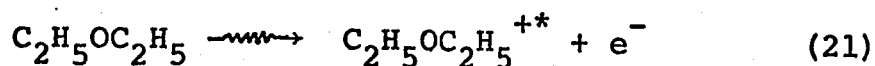
is  $2.2 \pm 0.2$  at all temperatures at which it could be determined (Table IV-2). This value is consistent with the suggestion that these products are formed exclusively by reactions 6-8.

In addition to the above mentioned free radical chain mechanism, the following chain mechanism with ionic chain carriers was also considered.

TABLE IV-2

Ratio of Products of Radical-Radical  
Reactions

Temperature °C	$\frac{G(C_4H_9OC_2H_5)}{[G(n-C_4H_{10}) \times G(CH_3CHOC_2H_5)_2]^{\frac{1}{2}}}$
33	2.18
50	2.58
80	1.98
110	2.01
140	2.13
Average	$2.2 \pm 0.2$



$\Delta H$  (23) and  $\Delta H$ (24) were calculated to be  $64.2 \text{ kcal mole}^{-1}$  and  $-63.9 \text{ kcal mole}^{-1}$  respectively. The values of heats of formation of ions and molecules and the ionization potentials of molecules needed for calculation of  $\Delta H$  (23) and  $\Delta H$  (24) are presented in Tables IV-3a and IV-3b. The comparison of the endothermicity values of reactions 23 ( $\Delta H=64.2$ ) and 4 ( $\Delta H=5$ ) shows that reaction 23 will be very slow and, therefore, negligible as compared to reaction 4. Therefore, the free radical chain mechanism is favored much more than the ionic chain mechanism considered above. Furthermore, the following two causes also support rejection of the above mentioned ionic chain mechanism.

(i) The proton affinity of diethyl ether is about  $204 \text{ kcal mole}^{-1}$ . This was estimated from the following proton affinity values in  $\text{kcal mole}^{-1}$ :  $\text{CH}_3\text{OH}$ ,  $180 \pm 3$  (2);  $\text{C}_2\text{H}_5\text{OH}$ ,  $193 \pm 8$  (2);  $\text{CH}_3\text{OCH}_3$ ,  $191 \pm 10$  (2). Therefore, reaction 27 should also be considered in addition to reaction 24.

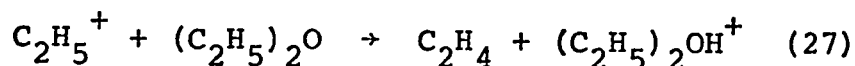




TABLE IV-3a

Heats of formation ( $\Delta H_f^\circ$ ) of some molecules, radicals  
and ions in kcal mole<sup>-1</sup> at 25°

<u>Species</u>	<u><math>\Delta H_f^\circ</math></u>	<u>Species</u>	<u><math>\Delta H_f^\circ</math></u>
C <sub>2</sub> H <sub>6</sub>	- 20.2 (101)	CH <sub>3</sub> CHO	- 39.8 (105)
CH <sub>3</sub> OCH <sub>3</sub>	- 44.0 (101)	C <sub>2</sub> H <sub>5</sub> OCH <sub>3</sub>	- 51.7 (106)
C <sub>2</sub> H <sub>5</sub> OC <sub>2</sub> H <sub>5</sub>	- 60.3 (102)	H	52.1 (101)
C <sub>2</sub> H <sub>5</sub>	26.7 (101)	CH <sub>3</sub> CHOC <sub>2</sub> H <sub>5</sub>	- 18.4 *
C <sub>2</sub> H <sub>5</sub> <sup>+</sup>	224 (103)	CH <sub>3</sub> CHO <sup>+</sup> C <sub>2</sub> H <sub>5</sub>	120 †
CH <sub>3</sub> CHO <sup>+</sup> CH <sub>3</sub>	135 (104)		

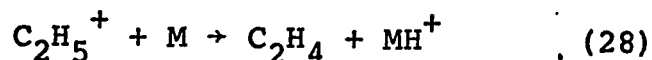
TABLE IV-3b

Ionization potentials (IP) of some molecules in kcal mole<sup>-1</sup>

<u>Molecule</u>	<u>IP</u>
CH <sub>3</sub> OCH <sub>3</sub>	230.5 (107)
C <sub>2</sub> H <sub>5</sub> OCH <sub>3</sub>	226.1 (107)
C <sub>2</sub> H <sub>5</sub> OC <sub>2</sub> H <sub>5</sub>	219.7 (107)

$$\begin{aligned}
 * \Delta H_f(\text{CH}_3\text{CHOC}_2\text{H}_5) &= D(\text{C}_2\text{H}_5\text{OCH}(\text{CH}_3)\text{-H}) - \Delta H_f(\text{H}) + \Delta H_f(\text{C}_2\text{H}_5\text{OC}_2\text{H}_5) \\
 D(\text{C}_2\text{H}_5\text{OCH}(\text{CH}_3)\text{-H}) &= 94 \quad (108), \text{ where } D \text{ is the bond dissociation energy} \\
 \dagger \Delta H_f(\text{CH}_3\text{CHO}^+\text{C}_2\text{H}_5) &= \Delta H_f(\text{CH}_3\text{CHO}^+\text{CH}_3) + \Delta H_f(\text{C}_2\text{H}_5\text{OC}_2\text{H}_5) \\
 &\quad - \Delta H_f(\text{C}_2\text{H}_5\text{OCH}_3) + \text{IP}(\text{C}_2\text{H}_5\text{OC}_2\text{H}_5) \\
 &\quad - \text{IP}(\text{C}_2\text{H}_5\text{OCH}_3)
 \end{aligned}$$

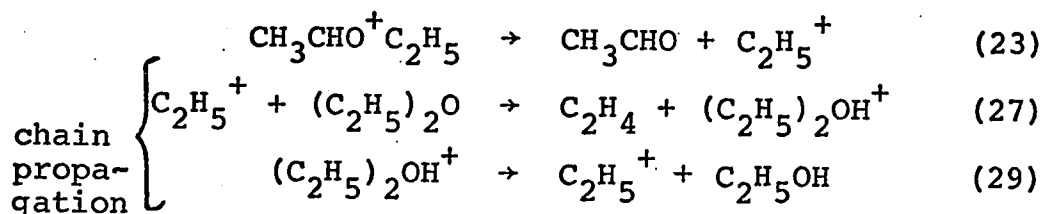
From the study of the radiolysis of propane-d<sub>8</sub> in the presence of various polar compounds M (where M is CH<sub>3</sub>OH, CH<sub>3</sub>NO<sub>2</sub>, CH<sub>3</sub>OCH<sub>3</sub> or (CH<sub>3</sub>)<sub>2</sub>N<sub>2</sub>), it was observed that the rate of proton transfer, reaction 28, is 10 to 100 times that of the com-

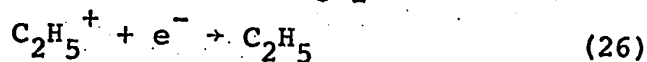
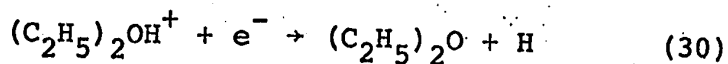


peting hydride ion transfer reaction (18). This fact shows that reaction 27 is much more important than reaction 24.

(ii) In the reactions of esters with CH<sub>5</sub><sup>+</sup> and C<sub>2</sub>H<sub>5</sub><sup>+</sup>, it was found that there were notably more (MW + 1)<sup>+</sup> than (MW-1)<sup>+</sup> ions produced (109,110), where MW is molecular weight. It was also found in the reactions of ethers with CH<sub>5</sub><sup>+</sup> and C<sub>2</sub>H<sub>5</sub><sup>+</sup> that there were notably more (MW + 1)<sup>+</sup> than (MW-1)<sup>+</sup> ions produced (111). This also shows that reaction 27 is more important than reaction 24.

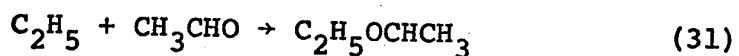
If reaction 24 is replaced by reaction 27, the chain propagation steps in the ionic chain mechanism can be written as:



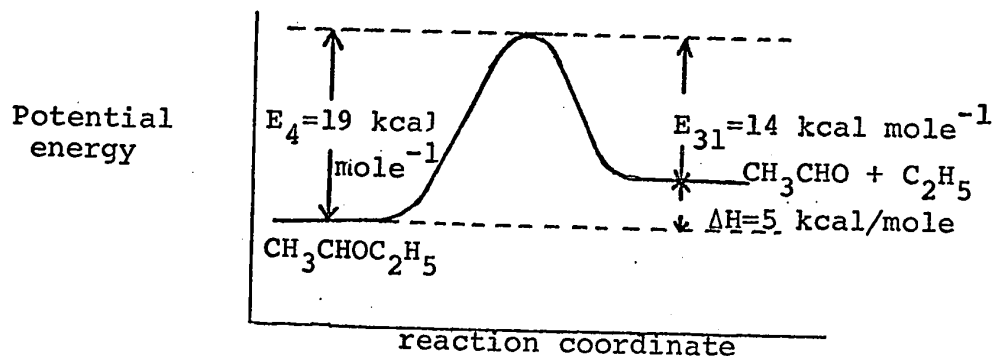
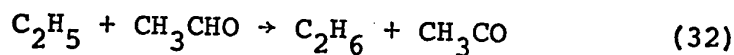


If reactions 27 and 29 were the chain propagation steps, then ethylene and ethanol would be chain products, which is not observed. This mechanism is also discarded.

a. Energetics of reaction 4. Reaction 4 is 5 kcal mole<sup>-1</sup> endothermic. The thermochemical data needed to calculate  $\Delta H$  of reaction 4 is presented in Table IV-3a. The fact that  $E_4 = 19$  kcal mole<sup>-1</sup> indicates that the activation energy of the reverse reaction



is  $E_{31} = 14$  kcal/mole. This accounts for the fact that reaction 31 has never been observed to occur. The more favorable metathetical reaction 32 occurs instead (112). The abstraction reaction 32 has an activation energy of only 7-8 kcal/mole. (112).



Similar energetics have been observed in the decomposition of methoxymethyl radical ( $\text{CH}_3\text{OCH}_2$ ) and other oxygen containing radicals.

	$\Delta H$ kcal/mole	E kcal/mole
$\text{CH}_3\text{OCH}_2 \rightarrow \text{CH}_3\text{O} + \text{CH}_2$	9.3 (98)	25.5 (98)
$\text{C}_2\text{H}_5\text{O} \rightarrow \text{CH}_3 + \text{CH}_2\text{O}$	10 (62)	21 (62)
$(\text{CH}_3)_3\text{CO} \rightarrow \text{CH}_3 + (\text{CH}_3)_2\text{CO}$	4.7 (62)	12 (113)

b. Chain length. The average chain length is defined as the number of molecules of the desired product produced per initial chain carrier. In the present study, the total primary yield of radicals is  $G(\text{ether} \rightarrow \text{R} + \text{R}') = 5.8$  at temperatures greater than  $80^\circ$ . Therefore, the primary yield of ethyl radicals  $G(\text{C}_2\text{H}_5)$  and also the primary yield of  $\text{CH}_3\text{CHOC}_2\text{H}_5$  radicals ( $G(\text{CH}_3\text{CHOC}_2\text{H}_5)$ ) is 5.8. The chain length at temperatures greater than  $80^\circ$  will be  $\frac{G(\text{C}_2\text{H}_6)}{5.8}$  for ethane formation. In Table IV-4, chain lengths for ethane formation at temperatures greater than  $80^\circ$  and also percent decomposition of diethyl ether are presented.

## 2. Other Reactions.

The hydrogen yield decreased ( $\Delta G(\text{H}_2) = 1.5$ ) by approximately the same amount as the ethanol yield increased ( $\Delta G(\text{C}_2\text{H}_5\text{OH}) = 1.6$ ) as the temperature was increased from  $33^\circ$  to  $125^\circ$  (Figure III-3A). The yields of these products

TABLE IV-4

Chain length and percent decomposition ether at various  
temperatures. Dose =  $1.6 \times 10^{20}$  eV/g

<u>Temperature</u> <u>(°C)</u>	<u>G(C<sub>2</sub>H<sub>6</sub>)<sub>cor.</sub></u>	<u>% decomposition</u> <u>diethyl ether</u>	<u>chain</u> <u>length</u>
110	2.8	0.30	0.5
140	17.0	0.54	2.9
160	38.8	0.85	6.7
180	60.4	1.30	10.4
220	201	3.48	34.7

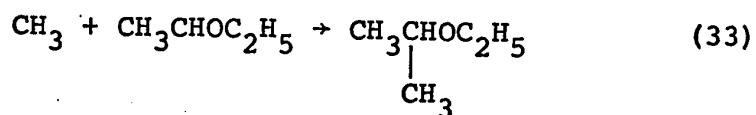
---

are independent of temperature in the range 125° to 220° and at these temperatures are nearly the same as the yields in the liquid phase radiolysis at 33°. In the high temperature vapor,  $G(H_2) = 4.4$  and  $G(C_2H_5OH) = 2.3$  whereas the liquid phase yields at 33° are  $G(H_2) = 3.7$  and  $G(C_2H_5OH) = 2.1$  (114). The reason for this similarity is not obvious.

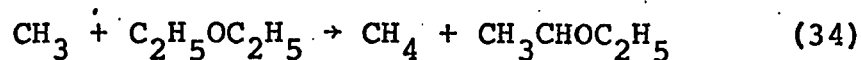
The inverse parallelism in the changes of the hydrogen and ethanol yields with increasing temperature in the gas phase indicates that one of the low temperature precursors of hydrogen becomes a precursor of ethanol at higher temperatures.

Most of the increase in ethylene yield (Figure III-3b) with increasing temperature results from the disproportionation of ethyl radicals. The non-radical yield of ethylene is constant at  $G = 1.8$  up to 140°, then increases gradually to 2.2 at 220°.

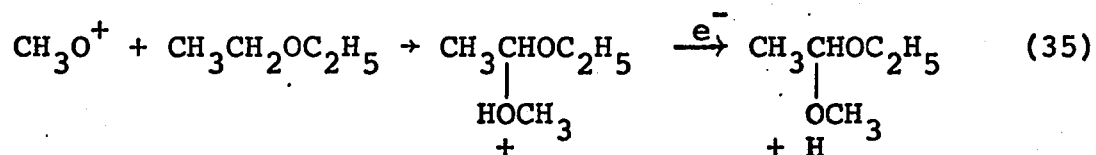
Ethyl isopropyl ether is presumably formed by the reaction



The yield of this product decreases with increasing temperature (Figure III-3b) because the ether radicals decompose (reaction 4) and the methyl radicals react metathetically.



The yield of ethyl methyl acetal is independent of temperature over the range 50° to 180° (Figure III-4a). This product may have been formed by the reactions



The product tentatively identified as diethoxymethane in the earlier work (79) was probably ethyl methyl acetal, because the latter compound was not formed in the present experiment.

There is not sufficient information to make speculation about the modes of formation of the other products worthwhile.

B. Vapor Phase Radiolysis of Ethanol

1. General

The variation of the product yields in the radiolysis of ethanol vapor (0.66 g/l) was studied over the temperature range 60° - 375°. The results are presented in Tables III-6, III-7 and Figures III-7, III-8, III-9 and III-10. In Table IV-5, the ratios of the product yields at two sets of temperatures, namely  $\frac{G_{200^\circ}}{G_{60^\circ}}$  and  $\frac{G_{375^\circ}}{G_{200^\circ}}$  are presented. From Table IV-5 it is evident that below 200° temperature has a relatively small effect on the product yields, whereas over the temperature range 200° - 375° the yields of hydrogen, acetaldehyde, methane, carbon monoxide, methanol, ethylene, ethane and diethyl ether increase markedly.

The variation of the gaseous product yields in the radiolysis of ethanol vapor at a lower density (0.16 g/l) was also studied over the temperature range 60° - 230°. The results are presented in Table III-8 and Figure III-11. In Table IV-6, the ratio  $\frac{G_{200^\circ}}{G_{60^\circ}}$  is presented for each measured product. Comparison of Tables IV-5 and IV-6 shows that the ratio  $\frac{G_{200^\circ}}{G_{60^\circ}}$  is virtually independent of ethanol density over the range 0.16 to 0.66 g/l.

Those products whose yields increase rapidly in the temperature range 200° - 375° (Table IV-5) must be formed by chain reactions. For the sake of simplicity the overall



TABLE IV-5

Ratio of the G values of products  $\left( \frac{G_{200^\circ}}{G_{60^\circ}} \text{ and } \frac{G_{375^\circ}}{G_{200^\circ}} \right)$   
in the vapor phase radiolysis of ethanol (0.66 g/l) at  
different temperatures

<u>Product</u>	$\frac{G_{200^\circ}}{G_{60^\circ}}$	$\frac{G_{375^\circ}}{G_{200^\circ}}$
Hydrogen	1.1	10
Acetaldehyde	1.6	31
Methane	2.8	21
Carbon monoxide	1.5	42
Methanol	---	30
Formaldehyde	---	4.7
Ethylene	1.2	29
Ethane	2.8	11
Diethyl ether	---	$\sim 16$
1,2-Propanediol	1.0	4.6
2,3-Butanediol	1.4	0.0
Isopropyl alcohol	---	0.0

TABLE IV-6

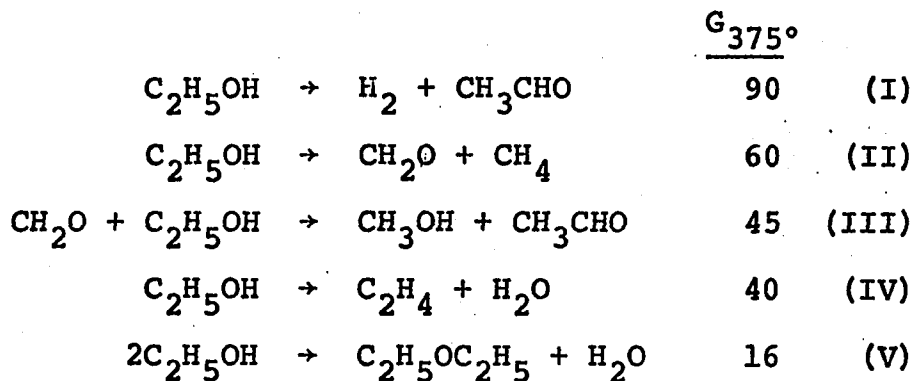
Ratio of G values of products  $\frac{G_{200^\circ}}{G_{60^\circ}}$  in the radiolysis  
of ethanol vapor at lower density (0.16 g/l) at dif-  
ferent temperatures.

---

<u>Product</u>	$\frac{G_{200^\circ}}{G_{60^\circ}}$
Hydrogen	1.0
Methane	3.2
Carbon monoxide	1.4
Ethylene	1.4
Ethane	2.9

---

chain reactions can be represented by the following stoichiometric equations.



Because of the experimental difficulties in the quantitative determination of the yield of water, this was only measured at 350° and 375°, so could not be included in Table IV-5.

Detailed studies of the vapor phase radiolysis of ethanol were made at 150° (a convenient temperature in the non-chain temperature region), and at 350° (in the region where radiation sensitized chain decomposition of ethanol occurs).

## 2. Detailed Study at 150°

The material balance for the products obtained from radiolysis of ethanol vapor (1.50 g/l) at 150° and at a dose of  $8 \times 10^{19}$  eV/g is presented in Table IV-7.

$G(-C_2H_5OH)$  is found to be 14.7. The radiolysis products add up to an empirical formula of  $C_2H_{6.10}O_{1.00}$  which corresponds to an excess of  $G(H_2) = 0.74$ . This good

TABLE IV-7

Material balance of products in the radiolysis of ethanol  
vapor (1.50 g/l) at 150°

<u>Product</u>	<u>G(Product)</u>	<u>C</u>	<u>H</u>	<u>O</u>
Hydrogen	8.16	----	16.32	----
Methane	3.00	3.00	12.00	----
Carbon monoxide	0.67	0.67	----	0.67
Ethane	0.28	0.56	1.68	----
Ethylene	1.05	2.10	4.20	----
Acetylene	0.25	0.50	0.50	----
n-Butane	0.01	0.04	0.10	----
Diethyl ether	0.17	0.68	1.70	0.17
Acetaldehyde	3.04	6.08	12.16	3.04
1,2-Propanediol	0.25	0.75	2.00	0.50
2,3-Butanediol	2.7 ± 0.5	10.80	27.00	5.40
Formaldehyde	3.0	3.00	6.00	3.00
Diethoxy methane	0.24	1.20	2.88	0.48
Water	1.50*	----	3.0	1.5
		<hr/>	<hr/>	<hr/>
TOTAL		29.38	89.54	14.76

14.69 (C<sub>2</sub>H<sub>6.10</sub>O<sub>1.00</sub>)

\*The yield of water was not measured. Its value was taken to be the same as that for (ethylene + ethane + diethyl ether).

material balance shows that most of the products have been accounted for. The total extent of decomposition of ethanol at 150° and at a dose of  $8 \times 10^{19}$  ev/g was 0.09 percent.

a. Effect of dose. Ethanol density 1.50 g/l

The yields of various products obtained in the radiolysis of ethanol vapor at 150° are presented as a function of dose in Table III-9 and Figures III-12 and III-13. In Table IV-8 the yields of various products extrapolated to zero dose are presented.

Hydrogen: The yield of hydrogen decreases by 2.7 G units with increasing dose. This decrease can be explained in the following manner.

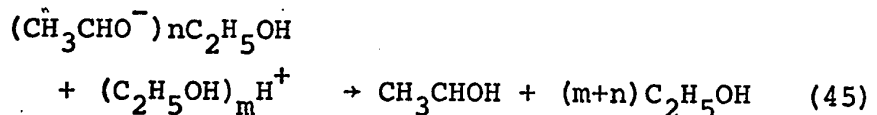
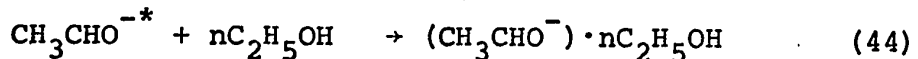
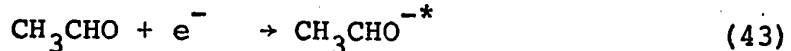
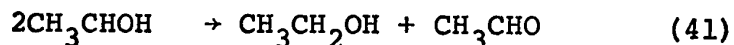
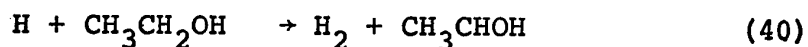
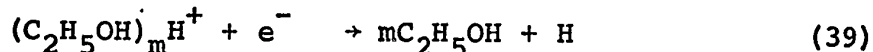
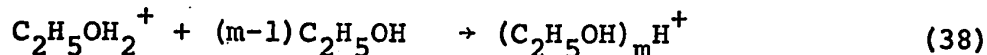
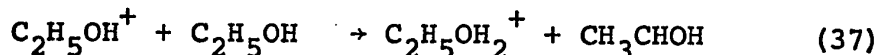
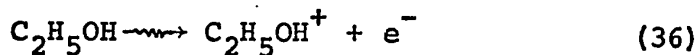


TABLE IV-8

Product yields extrapolated to zero dose in the radiolysis  
of ethanol vapor (1.50 g/l) at 150°

---

<u>Product</u>	<u>G(Product)</u>
Hydrogen	9.90
Methane	3.15
Carbon monoxide	0.60
Ethane	0.40
Ethylene	1.10
Diethyl ether	0.17
Acetaldehyde	3.70
1,2-Propanediol	0.45 $\pm$ 0.25
2,3-Butanediol	2.7 $\pm$ 0.5

---

In the study of the "solvation" of hydrogen ions by water molecules in the gas phase, Kebarle et.al (115) observed that the average extent of solvation of hydrogen ions depends on the temperature and pressure. From a consideration of their results on solvation of the hydrogen ion by water (115) and also the solvation of the hydrogen ion by mixtures of water and methanol molecules (116) it is estimated that under the conditions of the present study (150°, 865 torr), the value  $m$  is about 6, that is, the hydrogen ion will be solvated by six ethanol molecules. Reaction 39 is about 17 kcal mole<sup>-1</sup> exothermic. The thermochemical data needed to calculate  $\Delta H(39)$  is presented in Table IV-9.

At high doses reaction 43 competes with reaction 39. The decrease of 2.7 G units in hydrogen yield is similar to the decrease of 3.0 G units observed with sulphur hexafluoride in the radiolysis of ethanol-sulphur hexafluoride mixtures at 150° in the present study. At a dose of  $6.5 \times 10^{19}$  ev/g, the decrease in hydrogen yield is half of the maximum decrease in hydrogen yield with increasing dose (Fig. III-12A). The concentration of acetaldehyde calculated at this dose is  $5 \times 10^{-6}$  moles l<sup>-1</sup> ( $G(\text{CH}_3\text{CHO}) = 3.2$ , Fig. III-13A). Assuming a value  $10^{14}$  l mole<sup>-1</sup> sec<sup>-1</sup> (2) for the rate constant for the electron-ion neutralization, that is,  $k_{39} = 10^{14}$  l mole<sup>-1</sup> sec<sup>-1</sup>, the steady state

TABLE IV-9

Heats of formation ( $\Delta H_f^\circ$ ) of molecules, radicals and ions  
in kcal mole<sup>-1</sup> at 25°

Species	$\Delta H_f^\circ$	Species	$\Delta H_f^\circ$
H <sub>2</sub> O	-57.8 (101)	H <sup>+</sup>	365 (103)
CH <sub>2</sub> O	-27.7 (101)	C <sub>2</sub> H <sub>5</sub> OH <sub>2</sub> <sup>+</sup>	115.8 †
CH <sub>3</sub> OH	-48 (101)	(C <sub>2</sub> H <sub>5</sub> OH) <sub>2</sub> H <sup>+</sup>	24 ††
C <sub>2</sub> H <sub>5</sub> OH	-56.2 (101)	(C <sub>2</sub> H <sub>5</sub> OH) <sub>6</sub> H <sup>+</sup>	-268 ††
C <sub>2</sub> H <sub>5</sub> OC <sub>2</sub> H <sub>5</sub>	-60.3 (101)	C <sub>3</sub> H <sub>6</sub> <sup>+</sup>	231 (103)
H	52.1 (101)	C <sub>3</sub> H <sub>7</sub> <sup>+</sup>	190 (103)
CH <sub>3</sub> CHOH	-18.3*	CH <sub>3</sub> CHOH <sup>+</sup>	145 (104)
i-C <sub>3</sub> H <sub>7</sub>	17.6 ± 1 (101)	NH <sub>2</sub> <sup>+</sup>	300 (103)
C <sub>3</sub> H <sub>5</sub>	38 (117)	NH <sub>4</sub> <sup>+</sup>	210 (103)

$$^* \Delta H_f^\circ (\text{CH}_3\text{CHOH}) = D(\text{H}-\text{CH}(\text{CH}_3)\text{OH}) - \Delta H_f^\circ (\text{H}) + \Delta H_f^\circ (\text{CH}_3\text{CH}_2\text{OH})$$

$$D(\text{H}-\text{CH}(\text{CH}_3)\text{OH}) = 90 \text{ kcal mole}^{-1} \quad (117)$$

$$^{\dagger} \Delta H_f^\circ (\text{CH}_3\text{CH}_2\text{OH}_2^+) = \Delta H_f^\circ (\text{C}_2\text{H}_5\text{OH}) + \Delta H_f^\circ (\text{H}^+) - \text{PA}(\text{C}_2\text{H}_5\text{OH})$$

$$\text{Proton affinity (PA) of C}_2\text{H}_5\text{OH} = 193 \pm 8 \text{ kcal mole}^{-1} \quad (118)$$

$^{\dagger\dagger} \Delta H_f^\circ (\text{C}_2\text{H}_5\text{OH})_n \text{H}^+$  was estimated in the following manner.

The  $\Delta H$  values for reactions (a) to (e) are not known.

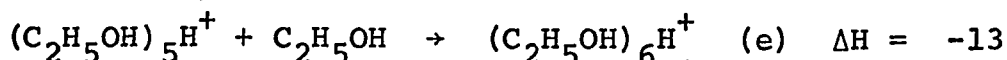
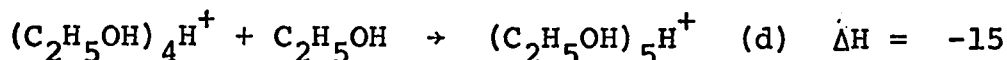
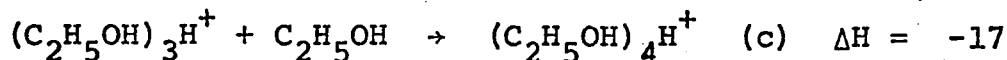
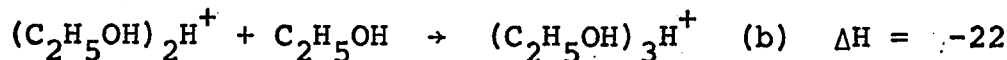
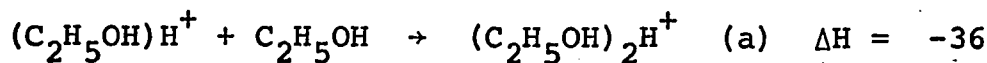




TABLE IV-9 (continued)

Therefore, these values are taken to be the same as those for the analogous reactions in water vapor. It must, however, be pointed out that the  $\Delta H$  values for reactions (a) and (b) are expected to be more negative than the values for the analogous reactions in water vapor because the proton affinity of ethanol is greater than that of water. The  $\Delta H$  values for reactions c to e are expected to be less negative than the analogous reactions in water vapor. The decrease in preference for the clustering of hydrogen ions by more than two ethanol molecules as compared to the clustering of hydrogen ions by more than two water molecules is probably due to the larger volume of the ethanol molecule.

Therefore, the overall effect for reactions (a) to (e) may not be very much different than the overall effect for analogous reactions in water vapor. The above mentioned estimates were derived from the studies of the competitive clustering of hydrogen ions by water and methanol molecules in the gas phase (116).

concentration of ions at a dose rate of  $4 \times 10^{19}$  ev/ghr is calculated to be about  $5 \times 10^{-12}$  moles  $l^{-1}$ . At a dose of  $6.5 \times 10^{19}$  ev/g, the rate of reaction 43 is roughly equal to the rate of reaction 39.

Therefore,

$$k_{39}[(C_2H_5OH)_6H^+][e^-] = k_{43}[CH_3CHO][e^-] \quad (ix)$$

so

$$k_{43} = \frac{k_{39}[(C_2H_5OH)_6H^+]}{[CH_3CHO]} \sim \frac{1 \times 10^{14} \times 5 \times 10^{-12}}{5 \times 10^{-6}} \sim 10^8 \text{ l mole}^{-1} \text{ sec}^{-1}$$

The value of  $k_{43}$  has not been previously estimated. The value may be similar to that of electron attachment to acetone. The electron attachment frequency  $\nu$  has been reported to be  $400 \text{ torr}^{-1} \text{ sec}^{-1}$  in pure acetone vapor (119). This corresponds to a rate constant of  $7.8 \times 10^6 \text{ l mole}^{-1} \text{ sec}^{-1}$ . This was calculated by using the following formula (2):

$$k_{43}(\text{l mole}^{-1} \text{ sec}^{-1}) = \left[ \frac{\nu(\text{torr}^{-1} \text{ sec}^{-1})}{5.3 \times 10^{-5} (\text{mole l}^{-1} \text{ sec}^{-1})} \right] (x)$$

Values for electron attachment frequencies are similar for similar aldehydes and ketones (119).

The relatively large value of the rate constant for electron attachment to acetaldehyde estimated in the present work is perhaps due to the stabilization of  $CH_3CHO^{-*}$  by ethanol, with the formation of  $CH_3CHO^{-} \cdot nC_2H_5OH$ .

The electron attachment frequencies  $\nu$  of several compounds mixed with different diluent gases (ethylene, carbondioxide, methanol) at total pressures of a few tens of torr have been measured (119). It was observed that the value of  $\nu$  depends on the nature of the diluent gas, as for example,  $\nu$  for 2,4-pentanedione increased by nearly two orders of magnitude, from  $1 \times 10^3 P$  to  $56 \times 10^3 P$  (where  $P$  is the gas pressure in torr), when the diluent gas was changed from ethylene to methanol (119). This indicates that the present value of  $k_{43}$  estimated for acetaldehyde in the presence of ethanol is not unreasonable.

Acetaldehyde, methane and carbon monoxide

The yield of acetaldehyde decreases by 1.1 G units with increase of dose (Fig. III-13A). A portion of the decrease in acetaldehyde yield can be explained by the mechanism written above to explain the decrease in hydrogen yield with increasing dose. Furthermore, the acetaldehyde yield will decrease because of its secondary decomposition, which in turn explains the slight increase in the yields of methane and carbon monoxide.

Ethane, ethylene, diethyl ether, 1,2-propanediol and 2,3-butanediol.

The yields of these products are unaffected by change of dose.

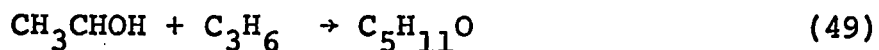
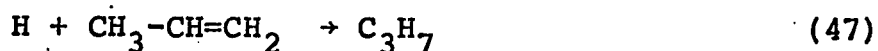
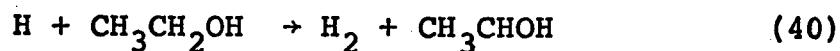
b. Ethanol-propylene mixtures. Ethanol density 1.50 g/l.

The yields of various gaseous and liquid products as a function of propylene concentration are presented in Table III-11 and Figure III-16.

Hydrogen, methane, acetaldehyde and 2,3-butanediol

The yields of these products decrease in the following manner: hydrogen from 8.2 to 1.5, methane from 3.0 to 1.2, 2,3-butanediol from 2.7 to 0.0 and acetaldehyde from 3.0 to 1.8

The decrease in the product yields can be explained by the following mechanism.



The radicals  $\text{C}_3\text{H}_7$ ,  $\text{C}_4\text{H}_9$  and  $\text{C}_5\text{H}_{11}\text{O}$  can undergo other reactions, as for example hydrogen atom abstraction, combination and disproportionation reactions. These have not been included in the above mechanism because their consideration will not change the conclusions reached about the decrease in the yields of hydrogen, methane, acetaldehyde and 2,3-butanediol. By applying

the steady state treatment to the hydrogen atom concentration, we get

$$\frac{d[H]}{dt} = 0 = 10^{-2} D g(H)_t - k_{40}[H][CH_3CH_2OH] - k_{47}[H][C_3H_6] \quad (xi)$$

where  $g(H)_t$  is the total yield of hydrogen atoms and  $D$  is the dose rate in eV/ml sec. Rearranging (xi) gives

$$[H] = \frac{10^{-2} D g(H)_t}{k_{40}[C_2H_5OH] + k_{47}[C_3H_6]} \quad (xii)$$

Now,

$$\frac{d[H_2]}{dt} = 10^{-2} D g(H_2) = k_{40}[H][C_2H_5OH] \quad (xiii)$$

Substituting for  $[H]$  from xii, into xiii, and solving, we get

$$g(H_2) = \frac{k_{40}[C_2H_5OH] g(H)_t}{k_{40}[C_2H_5OH] + k_{47}[C_3H_6]} \quad (xiv)$$

therefore,

$$\frac{1}{\Delta g(H_2)} = \frac{1}{g(H)_t} \left[ 1 + \frac{k_{40}[C_2H_5OH]}{k_{47}[C_3H_6]} \right] \quad (xv)$$

where  $\Delta g(H_2)$  is the reduction in hydrogen yield caused by the addition of propylene.

Similarly, by applying the steady state treatment to the methyl radical concentration, we get equation (xvi)

$$\frac{1}{\Delta g(\text{CH}_4)} = \frac{1}{g(\text{CH}_3)_t} \left[ 1 + \frac{k_{46}[\text{C}_2\text{H}_5\text{OH}]}{k_{48}[\text{C}_3\text{H}_6]} \right] \quad (\text{xvi})$$

The values of  $\frac{1}{\Delta g(\text{H}_2)}$ ,  $\frac{1}{\Delta g(\text{CH}_4)}$  and  $\frac{[\text{C}_2\text{H}_5\text{OH}]}{[\text{C}_3\text{H}_6]}$  are presented in Table IV-10 and plotted in Fig. IV-2.

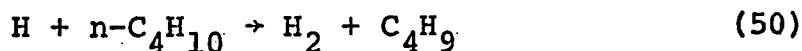
From the intercept and slope of the line in the plot of  $\frac{1}{\Delta g(\text{H}_2)}$  against  $\frac{[\text{C}_2\text{H}_5\text{OH}]}{[\text{C}_3\text{H}_6]}$  (Fig. IV-2A), we get  $g(\text{H})_t = 6.5$  and  $\frac{k_{40}}{k_{47}} = 0.0135$ . This gives

$$G(\text{H}_2)_{\text{scavengeable}} = 6.5 \text{ and } G(\text{H}_2)_{\text{unscavengeable}} = 1.7.$$

Similarly, from the intercept and the slope of the line in the plot of  $\frac{1}{\Delta g(\text{CH}_4)}$  against  $\frac{[\text{C}_2\text{H}_5\text{OH}]}{[\text{C}_3\text{H}_6]}$  (Fig. IV-2B) we get  $\frac{k_{48}}{k_{46}} = 34$  and  $g(\text{CH}_3)_t = 1.4$ . This gives

$$G(\text{CH}_4)_{\text{unscavengeable}} = 1.6.$$

The value of the rate constant  $k_{47}$  is  $1 \times 10^9$  l mole<sup>-1</sup> sec<sup>-1</sup> at 150° (120). Thus the present value of  $\frac{k_{40}}{k_{47}} = 0.0135$  corresponds to  $k_{40} = 1.4 \times 10^7$  l mole<sup>-1</sup> sec<sup>-1</sup> at 150°. The rate constant  $k_{40}$  has not been previously reported but this value is consistent with  $k_{50} = 1.1 \times 10^7$  l mole<sup>-1</sup> sec<sup>-1</sup> at 150° (120).



The value of  $k_{48} = 5.3 \times 10^4$  l mole<sup>-1</sup> sec<sup>-1</sup> at 150° and at about 3000 torr has been reported (121). The value of  $k_{48}$  at a pressure of 865 torr (pressure in the present study) has not been reported. Using the higher pressure

TABLE IV-10

Data for kinetic plot from propylene additive in the radiolysis of ethanol vapor

(1.50 g/l) at 150°

Mole % Propylene	$g(H_2)$	$g(CH_4)$	$\Delta g(H_2)$	$\Delta g(CH_4)$	$\frac{1}{\Delta g(H_2)}$	$\frac{1}{\Delta g(CH_4)}$	no. of moles of $C_3H_6$	$\frac{[C_2H_5OH]}{[C_3H_6]}$
0	8.16	3.00	-----	-----	-----	-----	-----	-----
0.48	6.38	2.80	1.78	0.20	0.56	5.0	$7.87 \times 10^{-5}$	208
1.30	5.03	2.62	3.13	0.38	0.32	2.63	$21.32 \times 10^{-5}$	76.9
5.13	2.95	2.17	5.21	0.83	0.19	1.20	$84.13 \times 10^{-5}$	19.5
10.43	2.90	1.98	5.26	1.02	0.19	0.98	$171.0 \times 10^{-5}$	9.59
15.46	2.40	1.75	5.76	1.25	0.17	0.80	$253.5 \times 10^{-5}$	6.47
25.55	1.93	1.26	6.23	1.74	0.16	0.57	$419.0 \times 10^{-5}$	3.91
40.95	1.83	1.12	6.33	1.88	0.16	0.53	$671.6 \times 10^{-5}$	2.44

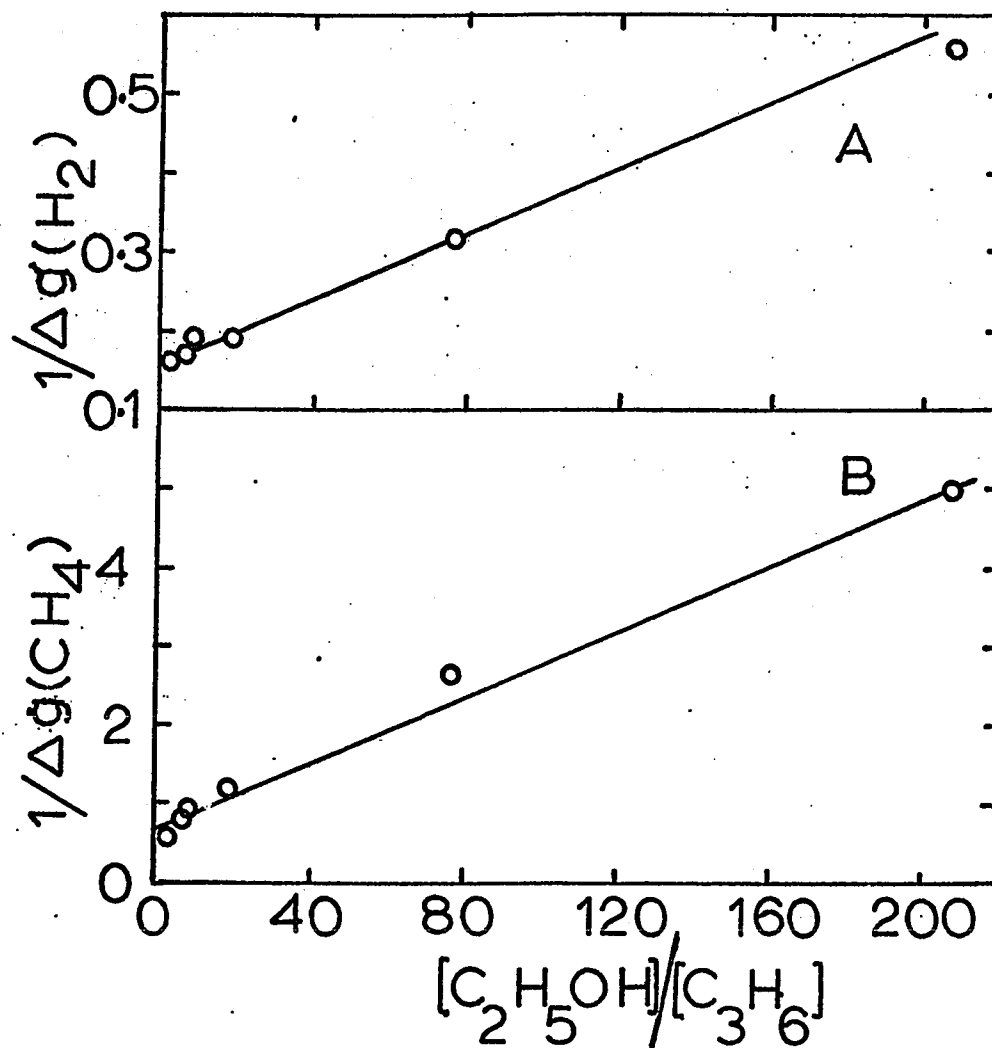


FIGURE IV-2

Kinetic plot for (A) hydrogen yield (B) methane yield in the radiolysis of ethanol-propylene mixtures at 150°. Ethanol density = 1.50 g/l.



value for  $k_{48}$  and the present value of the ratio  $k_{48}/k_{46}$ , the value of  $k_{46}$  is estimated to be  $1.6 \times 10^3 \text{ l mole}^{-1} \text{ sec}^{-1}$ . By way of comparison, a value of  $k_{46}/k_{51}^{\frac{1}{2}} = 9.3 \times 10^{-2} (\text{l mole}^{-1} \text{ sec}^{-1})^{\frac{1}{2}}$



at  $182^\circ$  has been reported (122). Using a value of  $k_{51} = 2.2 \times 10^{10} \text{ l mole}^{-1} \text{ sec}^{-1}$  (72) and an activation energy  $8.7 \text{ kcal mole}^{-1}$  for reaction 46 (122), the value of  $k_{46}$  at  $150^\circ$  is found to be  $6.8 \times 10^3 \text{ l mole}^{-1} \text{ sec}^{-1}$ . The reason for the discrepancy between the two estimates of  $k_{46}$  is not known.

The various kinetic parameters obtained from the present study are summarized in Table IV-12 (p. 193).

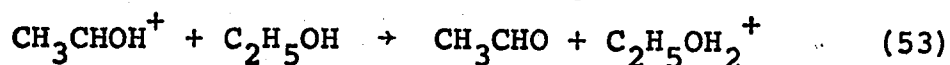
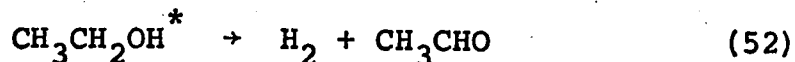
The decrease in the yields of acetaldehyde and 2,3-butanediol can be explained as follows.

(i) Due to the scavenging of hydrogen atoms and methyl radicals by propylene, the number of  $\text{CH}_3\text{CHOH}$  radicals produced by reactions 40 and 46 decrease which, in turn, decrease the yields of acetaldehyde and 2,3-butanediol.

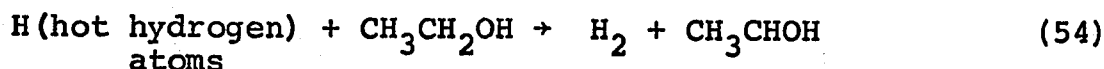
(ii) The  $\text{CH}_3\text{CHOH}$  radicals are also scavenged by propylene (reaction 49).

The fact that 2,3-butanediol is completely scavenged by propylene shows that this is formed com-

pletely from free radical intermediates. The following reactions may explain the non-scavengeable yields of hydrogen and acetaldehyde.

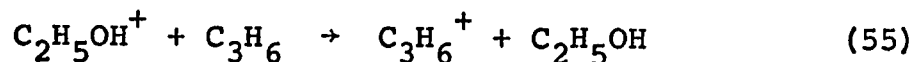


In the present work, reaction 52 would not be distinguished from reactions involving hot hydrogen atoms.



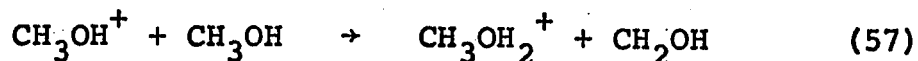
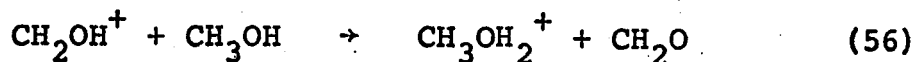
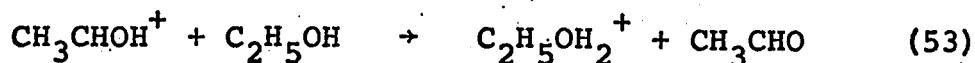
The yield of carbon monoxide ( $G(\text{CO}) = 0.7$ , Table III-11) remains unaffected by propylene. This indicates that carbon monoxide is formed from ionic or excited molecular precursors.

The above conclusions rest on the assumption that propylene does not interfere with the ionic steps in the mechanism. The simple alkenes, having negative electron affinities, cannot capture electrons and will not interfere with electron reactions. The ionization potentials of ethanol and propylene are 10.48 and 9.73 ev respectively (107). Therefore, reaction 55 might compete with reaction 37.

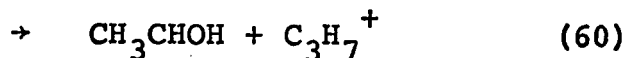
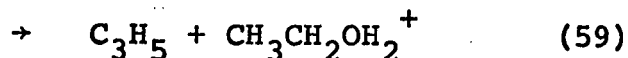
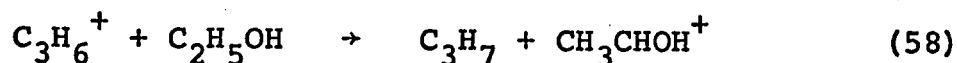


The rate constant  $k_{37}$  has a value of about  $8 \times 10^{11} \text{ l mole}^{-1} \text{ sec}^{-1}$ . This was estimated from the known rate

constant values for the following reactions



The rate constants  $k_{53}$ ,  $k_{56}$ ,  $k_{57}$  are  $7.2 \pm 3.6 \times 10^{11}$   $\text{l mole}^{-1} \text{sec}^{-1}$  (19),  $4.1 \times 10^{11}$   $\text{l mole}^{-1} \text{sec}^{-1}$  (123) and  $8.1 \times 10^{11}$   $\text{l mole}^{-1} \text{sec}^{-1}$  (123) respectively. As  $k_{53}$  is not very much different from  $k_{56}$ , therefore,  $k_{37}$  can be expected to be similar to  $k_{57}$ . Such a high value of  $k_{37}$  indicates that this reaction occurs with almost 100% collision efficiency. Therefore, it is only at very high concentrations of propylene that reaction 55 might compete with reaction 37. One must consider the fate of  $\text{C}_3\text{H}_6^+$  ions that might be formed by reaction 55. The various possible reactions that it can undergo are written below.



The  $\Delta H$  values in  $\text{kcal mole}^{-1}$  for reactions 58, 59 and 60 are -12.2, -21.0 and -3.1 respectively. This indicates that reaction 59 is most favorable, i.e. the final fate of  $\text{C}_3\text{H}_6^+$  would probably be to produce  $\text{C}_2\text{H}_5\text{OH}_2^+$ . Therefore, occurrence of a small amount of reaction 55 would not affect the product yields.

c. Ethanol-propylene mixtures at lower ethanol  
density (0.16 g/l)

The variations in the yields of hydrogen, methane, carbon monoxide and acetaldehyde as a function of propylene concentration are presented in Table III-12 and Figure III-17. Propylene decreases the product yields as follows: hydrogen from 9.7 to 2.4, methane from 3.0 to 1.5 and acetaldehyde from 4.7 to 2.5. The yield of carbon monoxide is unaffected by propylene, indicating that it is formed from ionic or excited molecular precursors. The decrease in product yields caused by propylene can be explained by reactions 40 to 42 and 46 to 49. The kinetic equations (xv) and (xvi) also apply. The values of  $\frac{1}{\Delta g(H_2)}$ ,  $\frac{1}{\Delta g(CH_4)}$  and  $\frac{[C_2H_5OH]}{[C_2H_6]}$  are presented in Table IV-11 and plotted in Fig. IV-3.

From the intercept and the slope of the line in the plot of  $\frac{1}{\Delta g(H_2)}$  against  $\frac{[C_2H_5OH]}{[C_3H_6]}$  (Fig. IV-3A), we get  $g(H)_t = 7.6$  and  $\frac{k_{40}}{k_{47}} = 0.0123$ . This gives  $G(H_2)_{\text{unscavengeable}} = 2.1$ . Using the value of  $k_{47} = 1 \times 10^9 \text{ l mole}^{-1} \text{ sec}^{-1}$  at  $150^\circ$  (120), one obtains  $k_{40} = 1.3 \times 10^7 \text{ l mole}^{-1} \text{ sec}^{-1}$ .

Similarly, from the intercept and the slope of the line in the plot of  $\frac{1}{\Delta g(CH_4)}$  against  $\frac{[C_2H_5OH]}{[C_3H_6]}$  (Fig. IV-3B), we get  $g(CH_3)_t = 1.7$  and  $\frac{k_{46}}{k_{48}} = 0.072$ . This gives  $G(CH_4)_{\text{unscavengeable}} = 1.3$ . Using the high pressure rate

TABLE IV-11

Data for kinetic plot from propylene additive in the radiolysis of ethanol vapor

(0.16 g/l) at 150°

Mole % Propylene	$g(H_2)$	$g(CH_4)$	$\Delta g(H_2)$	$\Delta g(CH_4)$	$\frac{1}{\Delta g(H_2)}$	$\frac{1}{\Delta g(CH_4)}$	no. of moles of $C_3H_6$	$\frac{[C_2H_5OH]}{[C_3H_6]}$
0.0	9.70	3.00	-----	-----	-----	-----	-----	-----
1.29	5.80	2.69	3.90	0.31	0.26	3.23	$2.27 \times 10^{-5}$	77.6
3.54	4.20	2.53	5.50	0.47	0.18	2.13	$6.25 \times 10^{-5}$	28.19
7.32	3.49	2.48	6.21	0.52	0.16	1.92	$12.9 \times 10^{-5}$	13.66
16.44	2.75	1.83	6.95	1.17	0.14	0.85	$29.0 \times 10^{-5}$	6.08
24.51	2.73	1.50	6.97	1.50	0.14	0.67	$43.2 \times 10^{-5}$	4.08
38.59	2.39	1.30	7.31	1.70	0.14	0.59	$68.0 \times 10^{-5}$	2.59

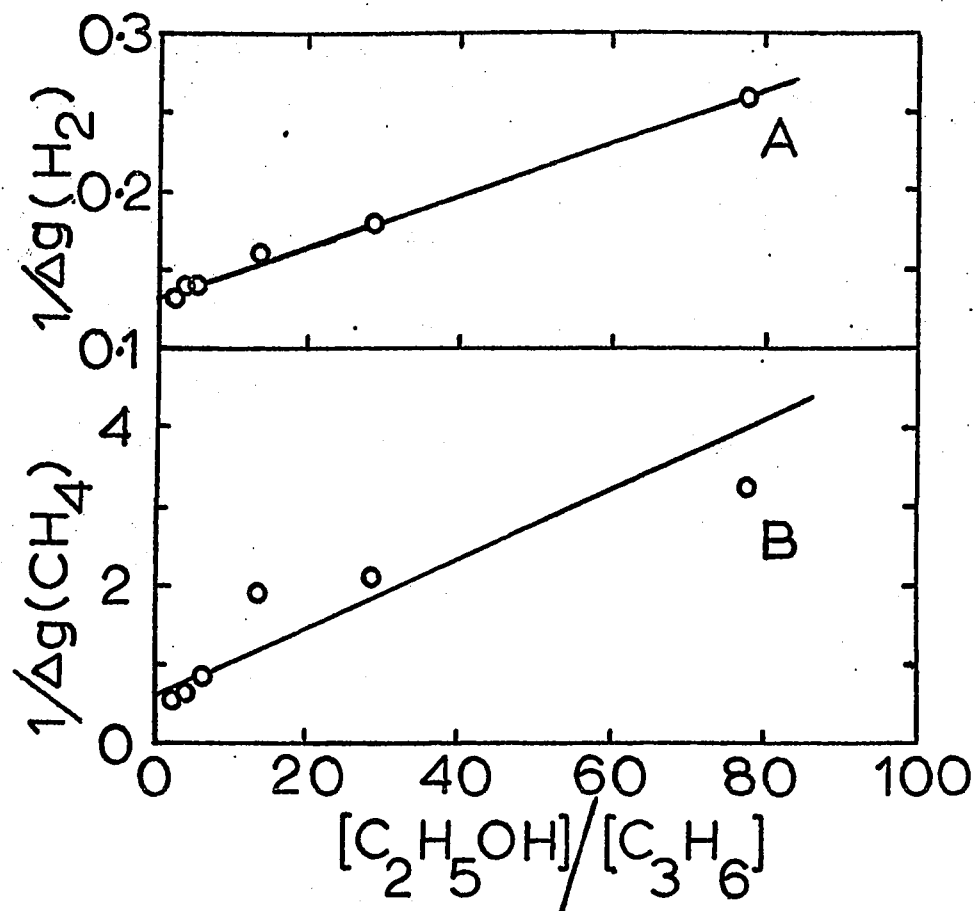


FIGURE IV-3

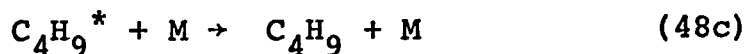
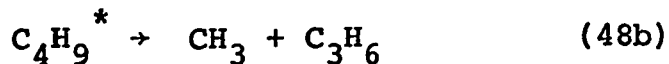
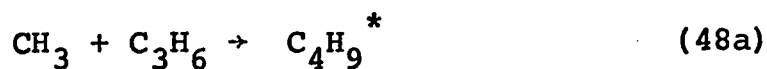
Kinetic plot for (A) hydrogen yield (B) methane yield, in the radiolysis of ethanol-propylene mixtures at 150°. Ethanol density = 0.16 g/l.

constant value  $k_{48} = 5.3 \times 10^4 \text{ l mole}^{-1} \text{ sec}^{-1}$  at  $150^\circ$  and 3000 torr (121), one obtains  $k_{46} = 3.8 \times 10^3 \text{ l mole}^{-1} \text{ sec}^{-1}$ . The values of the various kinetic parameters obtained are summarized in Table IV-12.

Effect of pressure on rate constants  $k_{40}$ ,  $k_{46}$ ,  $k_{47}$ , and  $k_{48}$ .

The values of the ratio  $\frac{k_{40}}{k_{47}}$  at ethanol pressures of 865 torr and 93 torr are very nearly the same (Table IV-12). The value of  $k_{40}$  for the metathetical reaction 40 is expected to be independent of pressure, therefore, the value of  $k_{47}$  is also independent of pressure.

The value of  $k_{46}/k_{48}$  at an ethanol pressure of 93 torr is higher than the value obtained at an ethanol pressure of 865 torr (Table IV-12). The rate constant  $k_{46}$  for the metathetical reaction 46 is expected to be independent of pressure. Therefore, the difference in the ratio  $k_{46}/k_{48}$  at two different ethanol pressures must be due to the pressure dependence of reaction 48. To explain this pressure dependence, the following reactions should be considered.



where M is a third body.

This shows that the reaction 48 written earlier is, in fact, a combination of reactions 48a-c.

TABLE IV-12

Summary of kinetic parameters in the radiolysis

of ethanol-propylene mixtures at 150°

Ethanol pressure (torr) at 150°	865	93
G(H <sub>2</sub> )	8.2	9.7
G(CH <sub>4</sub> )	3.0	3.0
G(CH <sub>3</sub> CHO)	3.0	4.7
G(H <sub>2</sub> ) <sub>unscavengeable</sub>	1.7	2.1
G(CH <sub>4</sub> ) <sub>unscavengeable</sub>	1.6	1.3
G(CH <sub>3</sub> CHO) <sub>unscavengeable</sub>	1.8	2.5
$\frac{k_{40}}{k_{47}}$	0.0135	0.0123
10 <sup>-7</sup> k <sub>40</sub> (1 mole <sup>-1</sup> sec <sup>-1</sup> )	1.4	1.3
$\frac{k_{46}}{k_{48}}$	0.029	0.072
10 <sup>-3</sup> k <sub>46</sub> (1 mole <sup>-1</sup> sec <sup>-1</sup> )	1.5	3.8*

\* probably too high because it is based upon a high pressure value of k<sub>48</sub>.



By writing

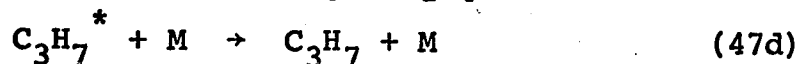
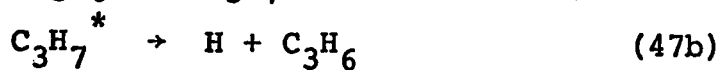
$$k_{48}[\text{CH}_3][\text{C}_3\text{H}_6] = k_{48a}[\text{CH}_3][\text{C}_3\text{H}_6] - k_{48b}[\text{C}_4\text{H}_9^*]$$

and applying the steady state treatment to the  $\text{C}_4\text{H}_9^*$  concentration, it can be shown that

$$k_{48} = k_{48a} \left( \frac{k_{48c}[\text{M}]}{k_{48b} + k_{48c}[\text{M}]} \right) \quad (\text{xvii})$$

Equation (xvii) explains the pressure dependence of the rate constant  $k_{48}$ .

Similarly the previous reaction 47 should also be represented in the following manner.



where M is a third body.

By writing

$$k_{47}[\text{H}][\text{C}_3\text{H}_6] = k_{47a}[\text{H}][\text{C}_3\text{H}_6] - k_{47b}[\text{C}_3\text{H}_7^*]$$

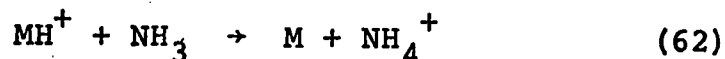
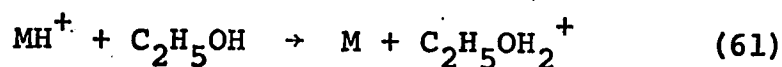
and applying the steady state treatment to the  $\text{C}_3\text{H}_7^*$  radical concentration, it can be shown that

$$k_{47} = k_{47a} \left( \frac{k_{47c} + k_{47d}^{\text{M}}}{k_{47b} + k_{47c} + k_{47d}^{\text{M}}} \right) \quad (\text{xviii})$$

In the present study,  $k_{47}$  was found to be independent of pressure. Therefore, reactions (47c + 47d) occur to the virtual exclusion of reaction 47b under the present conditions.

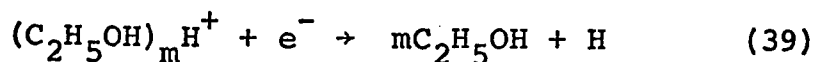
d. Ethanol-ammonia mixtures. Ethanol density 1.50 g/l

The yields of various products as a function of ammonia concentration are presented in Table III-13 and Figure III-18 (pp.111). None of the yields were affected by the presence of ammonia. The proton affinities (in kcal mole<sup>-1</sup>) of ammonia and ethanol are 202 and 193 ± 8 respectively (2). Because the proton affinity of ammonia is greater than that of ethanol, reaction 62 may compete with reaction 61.

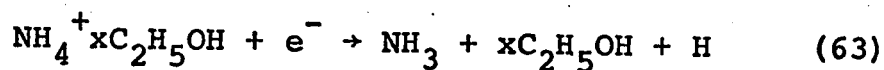


where  $MH^+$  is either the parent ethanol ion or some other ion. The positive ions  $C_2H_5OH_2^+$  and  $NH_4^+$  should, in fact, be represented as  $(C_2H_5OH)_m H^+$  and  $NH_4^+ \cdot x C_2H_5OH$ . The  $NH_4^+$  ions are represented as preferentially solvated by ethanol molecules because, in the present study, the concentration of ethanol molecules is very much higher than that of ammonia molecules. The highest concentration of ammonia used in the present study was only 7 mole percent.

In the absence of ammonia, only  $(C_2H_5OH)_m H^+$  ions will be present in the system. They eventually undergo neutralization with electrons.



In the presence of ammonia, when reaction 62 competes with reaction 61,  $\text{NH}_4^+ \cdot \text{x C}_2\text{H}_5\text{OH}$  ions will also be formed. These ions will then undergo neutralization reactions with electrons.



As the final fate of both the  $(\text{C}_2\text{H}_5\text{OH})_m\text{H}^+$  and  $\text{NH}_4^+ \cdot \text{x C}_2\text{H}_5\text{OH}$  ions upon neutralization with electrons is to produce hydrogen atoms, the occurrence of reaction 62 will not affect the product yields. This was observed (Fig. III-18).

Reaction 64 might also be possible.



Reaction 64 has an activation energy of 10-15 kcal mole<sup>-1</sup> (124). The rate constant  $k_{64}$  has a value of  $1 \times 10^4$  l mole<sup>-1</sup> sec<sup>-1</sup> at 150° (124). The value of the rate constant  $k_{40} = 1.4 \times 10^7$  l mole<sup>-1</sup> sec<sup>-1</sup> was obtained in the present study. As the value of  $k_{40}$  is much greater than that of  $k_{64}$  and also the concentration of ethanol is much greater than that of ammonia, reaction 64 would occur to a negligible extent.

e. Ethanol-sulphur hexafluoride mixtures. Ethanol  
density 1.50 g/l

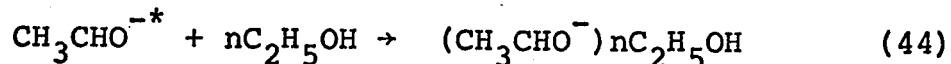
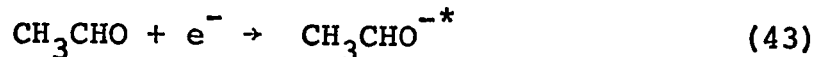
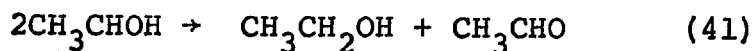
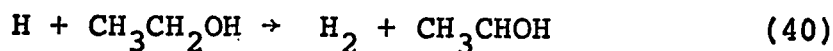
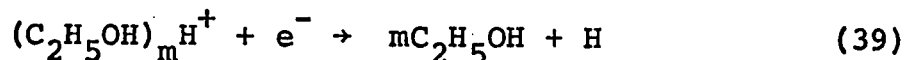
---

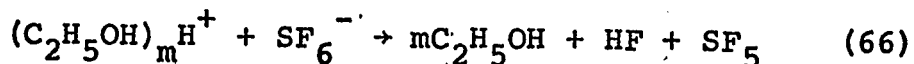
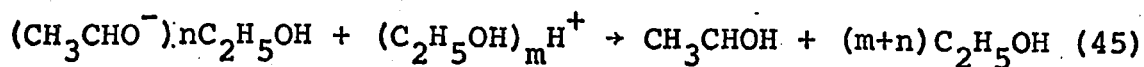
The yields of various products as a function of sulphur hexafluoride concentration are presented in

Table III-14a and Figures III-19 and III-20. Sulphur hexafluoride has a very large capture cross-section for thermal electrons (125). Therefore, it is expected to affect the product yields by interfering with the electron neutralization. The yields of methane, carbon monoxide, acetylene, ethylene and n-butane were not affected by sulphur hexafluoride indicating that these products are not formed by reactions involving positive ion-electron neutralization reactions. The yields of other measured products, however, changed in the presence of sulphur hexafluoride.

#### Hydrogen, acetaldehyde and 2,3-butanediol

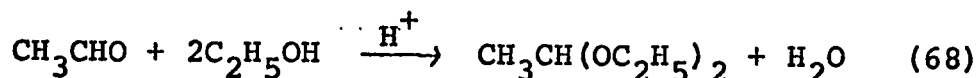
Sulphur hexafluoride changes the product yields as follows at a dose of  $8 \times 10^{19}$  ev/g: hydrogen decreases from 8.2 to 5.2, acetaldehyde (including acetal) increases from 3.0 to 6.0 and 2,3-butanediol decreases from 2.7 to 1.2 (Figures III-19A, III-20A). This change in product yields can be explained by the following mechanism:





The value of  $W_{\text{C}_2\text{H}_5\text{OH}} = 25.1$  (126), so  $G(\text{e}^-) = 4.0$ . The decrease in the yield of hydrogen is 3.0. This indicates that approximately 75% of the neutralization reactions contribute to the hydrogen yield.

The product acetaldehyde was not measurable as such from the radiolysis of ethanol-sulphur hexafluoride mixtures. It was changed into acetal, probably by reaction 68. It is known that addition of alcohols to



aldehydes occurs rapidly in the presence of acid (127), and acid is formed by reactions 66 and 67.

The decrease in the yield of hydrogen is caused by the competition between reactions 39 and 65. This competition between the two reactions might be expected, in turn, to decrease the yields of (acetaldehyde + acetal) and 2,3-butanediol. Although the yield of 2,3-butanediol decreased, that of (acetaldehyde + acetal) increased. There are two probable reasons for this.

(i) At the dose used, reaction 43 destroys acetaldehyde and reaction 65 inhibits this destruction. The value of the rate constant  $k_{65}$  is  $1.8 \times 10^9 \text{ l mole}^{-1} \text{ sec}^{-1}$  (2) and the value of the rate constant  $k_{43} = 1 \times 10^8 \text{ l mole}^{-1} \text{ sec}^{-1}$  is estimated in the present study. The concentration of acetaldehyde at a dose of  $8 \times 10^{19} \text{ eV/g}$  is about  $5 \times 10^{-6} \text{ mole l}^{-1}$ . The lowest concentration (0.065 mole percent) of sulphur hexafluoride used in the present study corresponds to  $2 \times 10^{-5} \text{ moles l}^{-1}$ . Because  $k_{65}$  is greater than  $k_{43}$  and also the concentration of sulphur hexafluoride is greater than that of acetaldehyde, reaction 65 will occur to a much greater extent than reaction 43. This explains a portion of the increase in acetaldehyde yield.

(ii) The occurrence of reaction 67 will increase the acetaldehyde yield and decrease the yield of 2,3-butanediol.

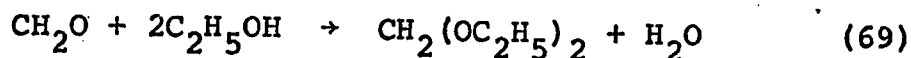
1,2-Propanediol, diethoxy methane and diethyl ether.

Sulphur hexafluoride increases the yields of these products as follows: 1,2-propanediol from 0.3 to 1.8, diethoxy methane from 0.2 to 1.0 and diethyl ether from 0.2 to 2.4.

The reason for the increase in the yield of 1,2-propanediol is not known.

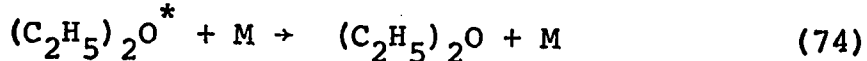
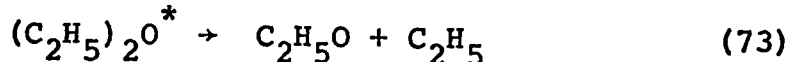
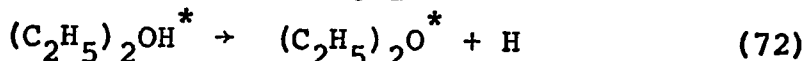
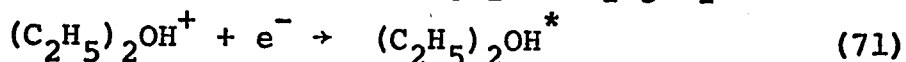
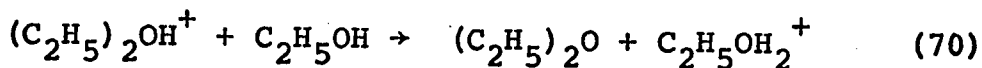
The conversion of formaldehyde to diethoxy methane,

catalysed by HF, doubtless explains the increased yield of diethoxy methane.



The yield of formaldehyde at 150° and in the absence of sulphur hexafluoride was not measured but  $G(\text{CH}_2\text{O}) \sim 1$  is expected from the extrapolation of the curve in the plot of  $G(\text{CH}_2\text{O} + \text{CH}_3\text{OH})$  against temperature (Fig. III-9 and Table III-6).

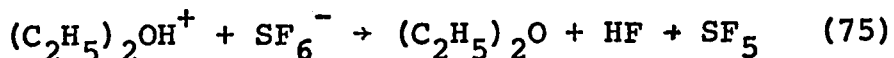
Henis (21) during a mass spectrometric study of ion-molecule reactions in methanol, found that the ion  $(\text{CH}_3)_2\text{OH}^+$  was formed. By analogy, the existence of  $(\text{C}_2\text{H}_5)_2\text{OH}^+$  ions can be expected in ethanol as a result of ion-molecule reactions. The formation of ether can be explained as follows:



Reaction 70 is 11 kcal mole<sup>-1</sup> endothermic.

$$\Delta H(70) = \Delta H_f(\text{C}_2\text{H}_5\text{OH}_2^+) + \text{PA}(\text{C}_2\text{H}_5)_2\text{O} - \Delta H_f(\text{H}^+) - \Delta H_f(\text{C}_2\text{H}_5\text{OH}) \quad (\text{xix})$$

The thermochemical data are presented in Table IV-9 (p.177). The proton affinity (PA) of diethyl ether was estimated to be  $204 \text{ kcal mole}^{-1}$ . This was estimated from the following proton affinity values in  $\text{kcal mole}^{-1}$ :  $\text{CH}_3\text{OH}$ ,  $180 \pm 3$  (2);  $\text{C}_2\text{H}_5\text{OH}$ ,  $193 \pm 8$  (2);  $\text{CH}_3\text{OCH}_3$ ,  $191 \pm 10$  (2). Therefore, the formation of diethyl ether by reaction 70 may not be an efficient process at this temperature. The  $\Delta H$  value for reaction 72, if both the diethyl ether and hydrogen atoms are formed in their ground states, is  $-109 \text{ kcal mole}^{-1}$ . This is much greater than the bond dissociation energy of  $79 \text{ kcal mole}^{-1}$  for  $\text{C}_2\text{H}_5\text{O} - \text{C}_2\text{H}_5$  (128). Therefore, the ether molecules formed can break up into the radicals  $\text{C}_2\text{H}_5\text{O}$  and  $\text{C}_2\text{H}_5$  (reaction 73). A portion of the increase in the yield of diethyl ether may be explained by the occurrence of reaction 75



which would displace reaction 71. Furthermore, some of the ether may also be formed as a result of the reaction of alcohol with sulphur tetrafluoride (129). In the present study sulphur tetrafluoride is probably formed by reaction 67.

f. Ethanol-sulphur hexafluoride-propylene mixture.

Ethanol density 1.50 g/l



The yield of hydrogen is 2.6 in the radiolysis of ethanol in the presence of 3.2 mole percent sulphur hexafluoride and 5.2 mole percent propylene (Table III-14B). This corresponds to  $\Delta g(H_2) = 5.6$  and can be explained in the following manner.

Propylene scavenges hydrogen atoms only. The maximum decrease in the hydrogen yield caused by propylene is 6.5 units (Fig. III-16A). Therefore,  $g(H)_t = 6.5$ .

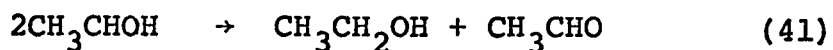
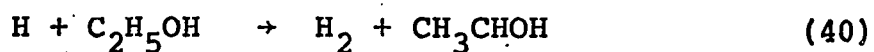
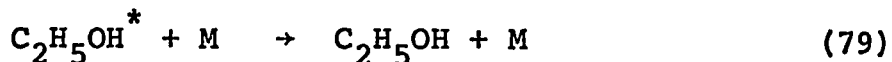
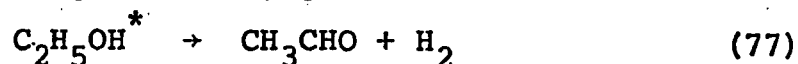
Three mole percent of sulphur hexafluoride is in the plateau region of the hydrogen inhibition curve (Fig. III-19A) and in the absence of propylene, causes  $\Delta g(H_2) = 3.0$ . The addition of 5 mole percent of propylene caused  $g(H_2)$  to decrease by another 2.6 units, which indicates that many of the hydrogen atoms are formed by processes other than ion-electron neutralization. Conversely, 5.2 mole percent of propylene, in the absence of sulphur hexafluoride would cause  $\Delta g(H_2)$  to be about 4.8 (Fig. III-16A), whereas  $\Delta g(H_2)_{\max} = 6.5$  for propylene. The addition of 3 mole percent of sulphur hexafluoride caused  $g(H_2)$  to decrease by another 0.8 units, which is the amount expected  $\left[ \frac{3.0}{6.5} \times (6.5 - 4.7) \right]$  if ion-electron neutralization produces hydrogen atoms rather than molecular hydrogen directly. Thus it may be concluded that the direct formation of molecular hydrogen from ion-electron neutralization in ethanol vapor at  $150^\circ$  is negligible. Hence,

$G(H)_{\text{ionic}} = 3.0$  and  $G(H)_{\text{non-ionic}} = 3.5$ .

g. Effect of ethanol pressure

The variation of the G values of the products with pressure is presented in Table III-10 and Figures III-14 and III-15. The yields of methane, ethane, carbon monoxide, n-butane, 1,2-propanediol and 2,3-butanediol were unaffected by change of pressure. The yields of hydrogen, acetaldehyde and ethylene decreased from 10.4, 6.3 and 2.1 to 7.0, 2.7 and 1.0 respectively as the pressure is increased from 0 to 1693 torr (Figures III-14A, III-15A, III-14C).

The decrease in hydrogen and acetaldehyde yields can be explained by the following mechanism.



where M is ethanol.

By applying the steady state treatment to the  $C_2H_5OH^*$  molecules and hydrogen atom concentrations it can be shown

that

$$\frac{I}{\frac{d[H_2]}{dt}} = 1 + \frac{k_{79}[M]}{k_{77} + k_{78}} \quad (xx)$$

therefore,

$$\frac{\Delta G(H_2)_{\max}}{\Delta G(H_2)_{\max} - \Delta G(H_2)} = 1 + \frac{k_{79}[M]}{k_{77} + k_{78}} \quad (xxi)$$

The values of  $\Delta G(H_2)_{\max}$ ,  $\Delta G(H_2)$  and the ratio

$\frac{\Delta G(H_2)_{\max}}{\Delta G(H_2)_{\max} - \Delta G(H_2)}$  are presented in Table IV-13.  $\Delta G(H_2)_{\max}$  is

the maximum decrease in hydrogen yield with pressure and

$\Delta G(H_2) = G(H_2)_0 - G(H_2)$ , where  $G(H_2)_0$  is the yield at zero

pressure. A plot of  $\frac{\Delta G(H_2)_{\max}}{\Delta G(H_2)_{\max} - \Delta G(H_2)}$  against  $[C_2H_5OH]$

is presented in Fig. IV-4A. A straight line drawn through

the points has a slope  $\frac{k_{79}}{k_{77} + k_{78}} \approx 3 \times 10^{-3}$  and an intercept

of 1.0 (Fig. IV-4A).

Similarly, the decrease in the yield of acetaldehyde can also be explained by the above mentioned mechanism. By applying the steady treatment to the concentration of  $C_2H_5OH^*$  molecules, hydrogen atoms and  $CH_3CHOH$  radicals, it can be shown that

$$\frac{I}{\frac{d[CH_3CHO]}{dt}} = \frac{k_{77} + k_{78}}{k_{77} + \frac{k_{41}k_{78}}{k_{41} + k_{42}}} + \frac{k_{79}}{k_{77} + \frac{k_{41}k_{78}}{k_{41} + k_{42}}} [M]$$

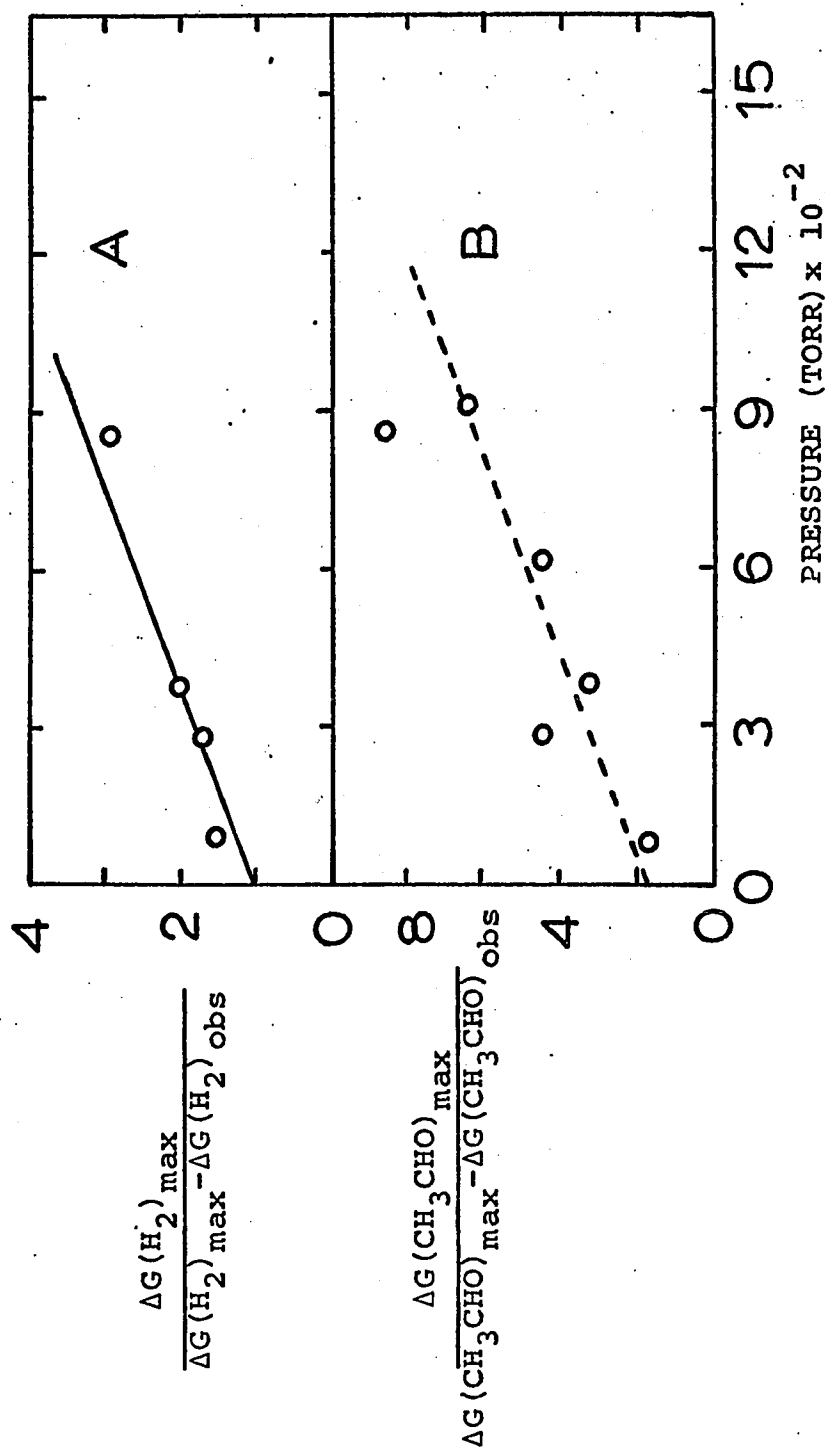
TABLE IV-13

Data for kinetic plot in the radiolysis of ethanol vapor at 150° and at  
different ethanol densities (0.078-2.96 g/l)

Pressure	$G(H_2)$	$G(CH_3CHO)$	$\Delta G(H_2)$	$\Delta G(CH_3CHO)$	$\frac{\Delta G(H_2)_{\max}}{\Delta G(H_2)_{\max} - \Delta G(H_2)}$		$\frac{\Delta G(CH_3CHO)_{\max}}{\Delta G(CH_3CHO)_{\max} - \Delta G(CH_3CHO)}$	
0	10.4*	6.3†	-----	-----	-----	-----	-----	-----
45.7	10.18	5.86	-----	-----	-----	-----	-----	-----
93.2	9.16	4.70	1.24	1.60	1.58	1.77	1.77	1.77
286.7	8.95	3.44	1.45	2.86	1.75	4.49	4.49	4.49
385.5	8.66	3.76	1.74	2.54	2.05	3.23	3.23	3.23
625.2	7.81	3.45	2.59	2.85	4.24	4.43	4.43	4.43
865.6	8.16	3.04	2.24	3.26	2.95	8.76	8.76	8.76
913.5	-----	3.19	-----	3.11	-----	6.46	6.46	6.46
1303	7.23	---	3.17	---	15.41	-----	-----	-----
1598	-----	2.62	-----	3.68	-----	-----	-----	-----

\* Extrapolated value in the plot of  $G(H_2)$  against pressure (Fig. III-14A)

† Extrapolated value in the plot of  $G(CH_3CHO)$  against pressure (Fig. III-15A)



Kinetic plot of the effect of pressure on  
(A) hydrogen and (B) acetaldehyde yield.

FIGURE IV-4

Therefore,

$$\frac{\Delta G(\text{CH}_3\text{CHO})_{\text{max}}}{\Delta G(\text{CH}_3\text{CHO})_{\text{max}} - \Delta G(\text{CH}_3\text{CHO})} = \frac{k_{77} + k_{78}}{k_{77} + \frac{k_{41}k_{78}}{k_{41} + k_{42}}} + \frac{k_{79}}{k_{77} + \frac{k_{41}k_{78}}{k_{41} + k_{42}}} \quad [\text{M}] \quad (\text{xxii})$$

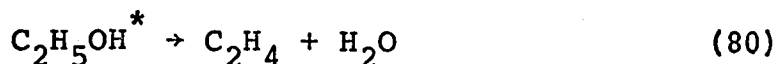
where  $\Delta G(\text{CH}_3\text{CHO})_{\text{max}}$  is the maximum decrease in the acetaldehyde yield with pressure and  $\Delta G(\text{CH}_3\text{CHO}) = G(\text{CH}_3\text{CHO})_0 - G(\text{CH}_3\text{CHO})$  where  $G(\text{CH}_3\text{CHO})_0$  is the yield at zero pressure. A plot of  $\frac{\Delta G(\text{CH}_3\text{CHO})_{\text{max}}}{\Delta G(\text{CH}_3\text{CHO})_{\text{max}} - \Delta G(\text{CH}_3\text{CHO})}$  against  $[\text{C}_2\text{H}_5\text{OH}]$  is pre-

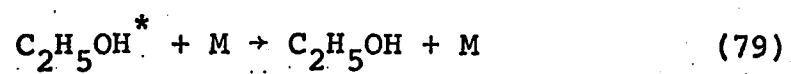
sented in Fig. IV-4B. A straight line drawn through the points has a slope  $\frac{k_{79}}{k_{77} + \frac{k_{41}k_{78}}{k_{41} + k_{42}}} \approx 5 \times 10^{-3}$  and an

$$\text{intercept} \quad \frac{k_{77} + k_{78}}{k_{77} + \frac{k_{41}k_{78}}{k_{41} + k_{42}}} = 1.7 \quad (\text{Fig. IV-4B}).$$

The dotted line in Fig. IV-4B has been drawn in such a manner that the ratio of the slopes and the intercepts of the two lines (Figs. IV-4A and IV-4B) is the same, as required by the equations (xxi) and (xxii).

The decrease in the yield of ethylene with increase of pressure can be explained by the following reactions.





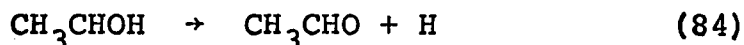
The competition between reactions 79 and 80 explains the dependence of ethylene yield on pressure.

3. Effect of ethanol pressure at 230°.

The yields of various gaseous products as a function of pressure are presented in Table III-15 and Figures III-21 and III-22. The yields of ethane and acetylene were independent of pressure. The yields of methane and carbon monoxide increase from 4.4 and 0.5 to 5.3 and 1.1 respectively as the pressure is increased from 54 to 1900 torr. The yields of hydrogen and ethylene decrease from 12.8 and 2.7 to 7.2 and 1.3 respectively with increase of pressure (Figs. III-21A and III-22C).

The reason for the increase in the yields of methane and carbon monoxide is not known.

The decrease in the yield of hydrogen can be explained by reactions 40 and 76 to 79. The high pressure value for the yield of hydrogen was about 7.0 in the study of the effect of ethanol pressure in the radiolysis at 150° (Fig. III-14A). This value compares well with the high pressure value of  $G(H_2) = 7.2$  obtained in the present study at 230°. The value of  $G(H_2)_{60}$  at 150° is 10.0 and at 230° is 12.7, where  $G(H_2)_{60}$  is the yield of hydrogen at 60 torr. This difference in the yields is probably due to the increased importance of reaction 84 at 230°



in comparison to that at 150°.

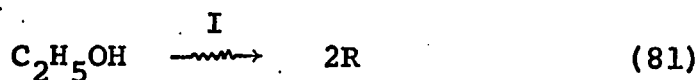
The pressure dependence of ethylene can also be explained by competition between reactions 79 and 80.



#### 4. The Chain Reactions

In the temperature range 200° to 375°, the yields of hydrogen, acetaldehyde, methane, carbon monoxide, methanol, ethylene, ethane and diethyl ether increase markedly. These products are formed by chain reactions. The overall chain reactions can be represented by the stoichiometric equations I to V (page 172). The formation of these products as represented by each of the stoichiometric equations will be discussed separately.

##### a. Radical concentrations.



where R is any radical and I is the rate of reaction 81. In the present system, several free radical chain mechanisms occur simultaneously. The initiation and termination steps of the various chains are intermingled. Any radical can initiate any chain and any radical can participate in the termination of any given chain. To terminate a given chain, only one of the chain carriers of that chain need take part in the termination step. Therefore, the total concentration of radicals R must be considered in each chain mechanism. The total concentration of radicals can be calculated as follows:

$$\frac{d[\text{R}]}{dt} = 0 = 2\text{I} - 2 k_{82} [\text{R}]^2$$

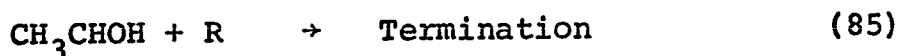
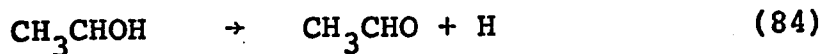
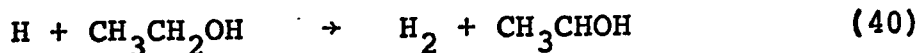
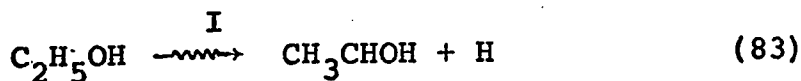
$$\text{Therefore, } [R] = \sqrt{\frac{I}{k_{82}}} \quad (\text{xxiii})$$

$$\text{where } I = \frac{1}{2} \times 10^{-2} D G(R) \quad (\text{i})$$

D is the dose rate in ev/ml sec and G(R) is the 100 ev yield of R. The factor  $\frac{1}{2}$  is included in equation (i) because two radicals are formed in reaction 81.

#### b. Hydrogen + acetaldehyde

The formation of hydrogen and acetaldehyde can be explained by the following reactions.



To simplify the presentation of an individual chain mechanism, the initiation step is written in terms of the chain carriers of that chain. The termination step is written in terms of one of the chain carriers and one general radical R. This oversimplification does not alter the forms of the derived rate equations because the initiation reaction is always first order and the termination is always second order under the present conditions. It will be assumed that the rate constants of all the free radical chain termination reactions are equal to  $k_{82}$ . Hence, in the present mechanism

$$[R] = \left( \frac{I}{k_{85}} \right)^{\frac{1}{2}} \quad (\text{xxiv})$$

Methane and carbon monoxide are also produced by the chain decomposition of acetaldehyde at these temperatures, but for the sake of simplicity in the discussion, the decomposition of acetaldehyde will be ignored and the total acetaldehyde yield will be taken as the sum of the acetaldehyde and carbon monoxide yields.

By applying the steady state treatment to the concentration of radicals  $\text{CH}_3\text{CHOH}$  and  $\text{H}$  we get:

$$\frac{d[\text{CH}_3\text{CHOH}]}{dt} = 0 = I + k_{40}[\text{H}][\text{C}_2\text{H}_5\text{OH}] - k_{84}[\text{CH}_3\text{CHOH}] - k_{85}[\text{CH}_3\text{CHOH}][R] \quad (\text{xxv})$$

$$\frac{d[\text{H}]}{dt} = 0 = I - k_{40}[\text{H}][\text{C}_2\text{H}_5\text{OH}] + k_{84}[\text{CH}_3\text{CHOH}] \quad (\text{xxvi})$$

On solving equations xxv and xxvi and substituting for  $[R]$  from xxiv, it can be shown that:

$$[\text{CH}_3\text{CHOH}] = 2 \left( \frac{I}{k_{85}} \right)^{\frac{1}{2}} \quad (\text{xxvii})$$

The factor 2 in equation xxvii arises from the "irregular" introduction of the general radical  $R$  into the mechanism and should be dropped.

$$\text{Hence, } [\text{CH}_3\text{CHOH}] = \left( \frac{I}{k_{85}} \right)^{\frac{1}{2}} \quad (\text{xxvii})$$

Rearrangement of equation xxvi and substitution of  $[\text{CH}_3\text{CHOH}]$

according to equation xxvii gives:

$$[H] = \frac{1}{k_{40}[C_2H_5OH]} \left[ I + k_{84} \left( \frac{I}{k_{85}} \right)^{\frac{1}{2}} \right] \quad (xxviii)$$

Now,

$$\frac{d[CH_3CHO]}{dt} = k_{84}[CH_3CHOH]$$

Substituting for  $[CH_3CHOH]$  from xxvii, we get:

$$\frac{d[CH_3CHO]}{dt} = k_{84} \left( \frac{I}{k_{85}} \right)^{\frac{1}{2}} \quad (xxix)$$

Similarly,

$$\frac{d[H_2]}{dt} = I + k_{84} \left( \frac{I}{k_{85}} \right)^{\frac{1}{2}}$$

and for long chains, we get:

$$\frac{d[H_2]}{dt} \approx k_{84} \left( \frac{I}{k_{85}} \right)^{\frac{1}{2}} \quad (xxx)$$

$$\text{Now } I = A[C_2H_5OH] \quad (xxxi)$$

where A is a proportionality constant that depends on the  $\gamma$ -beam intensity, the ethanol molecular absorption coefficient and the efficiency of reaction 83.

$$\text{Therefore, } \frac{d[H_2]}{dt} \approx k_{84} \left( \frac{A}{k_{85}} \right)^{\frac{1}{2}} [C_2H_5OH]^{\frac{1}{2}} \quad (xxxii)$$

This mechanism predicts that the formation of hydrogen and acetaldehyde should be 0.5 order. But the slope of the plot of  $\log G(H_2)$  vs  $\log P$  varies from about -0.2 at the lower pressures to about -0.4 at the higher pressures (Fig. IV-5B). The G value of a product may be expressed as

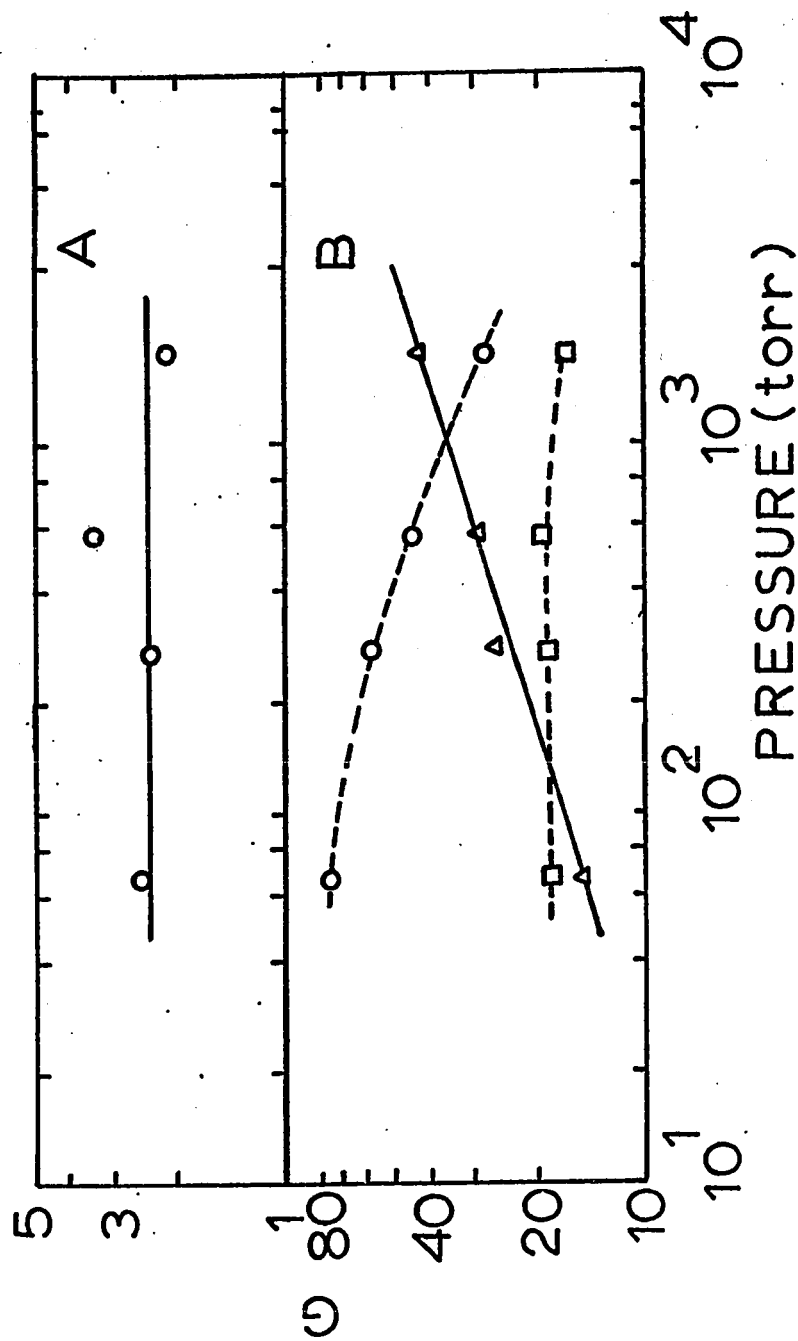


FIGURE IV-5

Product Yields from ethanol radiolysis as a function of pressure.

Temperature = 350°

A. O Ethane B. O Hydrogen  
 Δ Methane-carbon monoxide  
 □ Ethylene

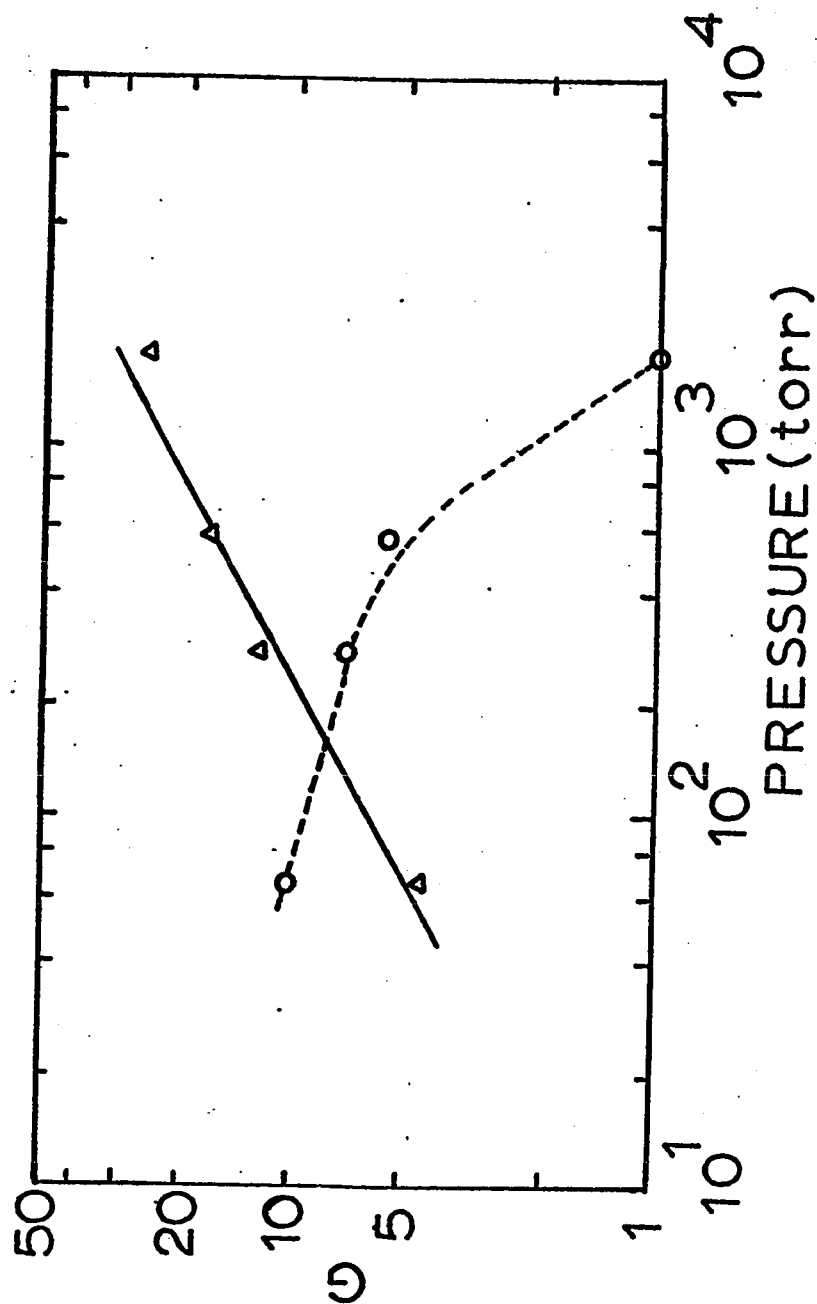


FIGURE IV-6

Product yields from ethanol radiolysis as a function of pressure. Temperature = 350°.

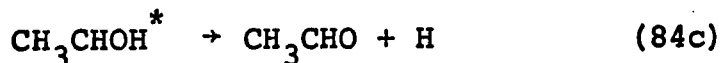
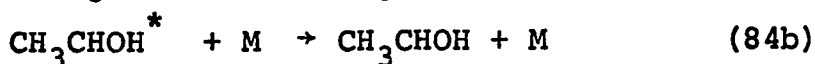
○ Diethyl ether  
 △ Methanol

$$\begin{aligned}\frac{d[X]}{dt} &= 10^{-2} D G(X) \\ &= G(X) \cdot B [C_2H_5OH]\end{aligned}$$

where  $B = 10^{-2} D / [C_2H_5OH]$  and

absorbed dose rate  $(\frac{eV}{ml \ sec})$  is  $\propto [C_2H_5OH]$

so a slope  $n$  of a plot of  $\log G(X)$  vs ethanol pressure corresponds to an order of  $(n+1)$  for the formation of product  $X$ . Therefore, the formation of hydrogen is about 0.8 order at the lower pressures and about 0.6 order at the higher pressures. The fact that the order is greater than 0.5 indicates that under the conditions of the present study, the decomposition of  $CH_3CHOH$  radicals is in the pressure dependent region. Reaction 84 in fact should be written as the combination of reactions 84a-c.



where  $M$  is ethanol.

By applying the steady state treatment to the concentration of  $CH_3CHOH^*$  radicals, it can be shown that:

$$[CH_3CHOH^*] = \frac{k_{84a} [CH_3CHOH] [M]}{k_{84c} + k_{84b} [M]} \quad (xxxiii)$$

Now, 
$$\frac{d[CH_3CHO]}{dt} = k_{84c} [CH_3CHOH^*] \quad (xxxiva)$$

Substituting for  $[CH_3CHOH^*]$  according to (xxxiii), we get:

$$\frac{d[CH_3CHO]}{dt} = k_{84c} \frac{k_{84a} [CH_3CHOH] [M]}{k_{84c} + k_{84b} [M]} \quad (xxxiv)$$

From the previous, oversimplified mechanism:

$$\frac{d[\text{CH}_3\text{CHO}]}{dt} = k_{84} [\text{CH}_3\text{CHOH}] \quad (\text{xxxv})$$

From the comparison of equations xxxiv and xxxv we get:

$$k_{84} = \frac{k_{84a} k_{84c} [M]}{k_{84c} + k_{84b} [M]} \quad (\text{xxxvi})$$

By substituting  $k_{84}$  from xxxvi into xxxii, we get:

$$\frac{d[\text{H}_2]}{dt} = \frac{k_{84a} k_{84c}}{k_{84c} + k_{84b} [\text{C}_2\text{H}_5\text{OH}]} \left( \frac{A}{k_{85}} \right)^{\frac{1}{2}} [\text{C}_2\text{H}_5\text{OH}]^{3/2} \quad (\text{xxxia})$$

This illustrates that at higher pressures, the formation of hydrogen is 0.5 order, and at lower pressure it is 1.5 order.

It should be pointed out that the radicals R in the chain termination step (reaction 85) are probably mainly  $\text{CH}_3\text{CHOH}$  radicals, as the formation of hydrogen and acetaldehyde is the major chain in the present system. This does not affect the conclusions reached.

The concentration of ethanol was kept constant in a study of the effect of temperature (Fig. III-7). One obtains the value of  $(E_{84} - \frac{1}{2}E_{85}) = 30 \text{ kcal mole}^{-1}$  from the plot of  $\log G(\text{H}_2)_{\text{chain}}$  against  $1/T(^{\circ}\text{K})$  in the region of  $350^{\circ}$  (Fig. IV-7). The yield of hydrogen is nearly constant over the temperature range  $80^{\circ}$  to  $200^{\circ}$  (Table III-6). So, about 8.5 units of hydrogen (average hydrogen



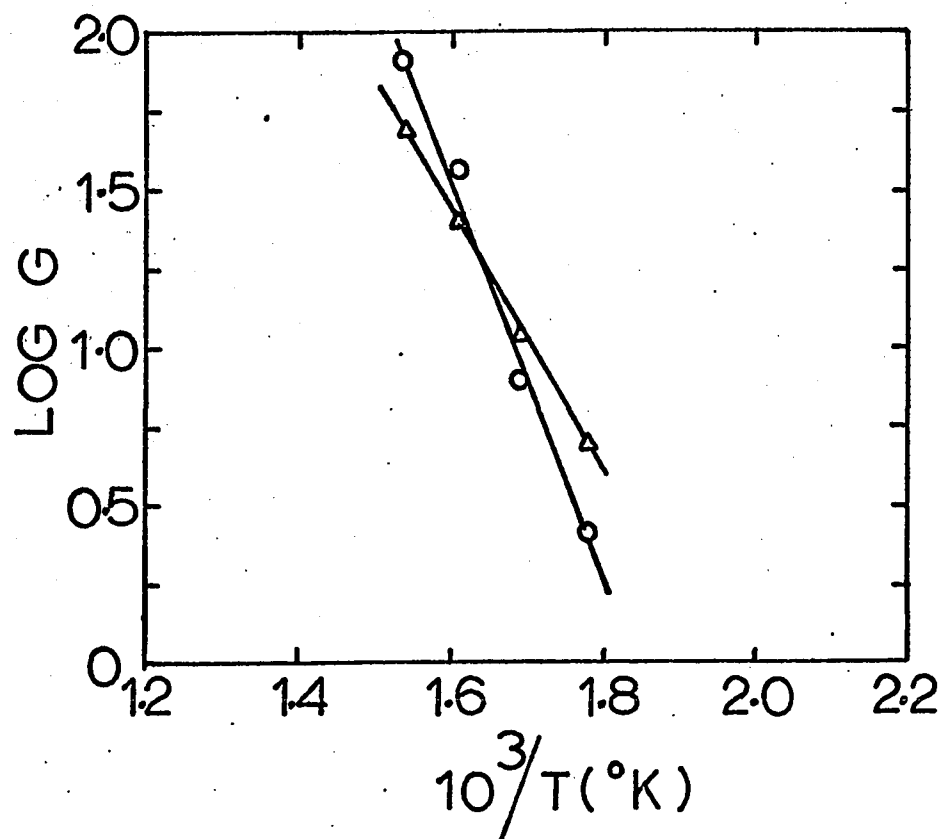
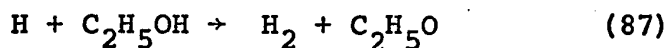
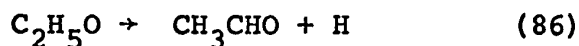


FIGURE IV-7

Arrhenius plot of (O) hydrogen, ( $\Delta$ ) methane  
 yields:  $G(\text{H}_2)_{\text{chain}} = G(\text{H}_2) - 8.5$ ;  $G(\text{CH}_4)_{\text{chain}} =$   
 $[G(\text{CH}_4)_T - G(\text{CO})] - 3.1$

yield over the temperature range 80° to 200°) are obtained by a non-chain mechanism. This yield was subtracted from the higher temperature (290° to 375°) hydrogen yields in the present treatment to obtain  $G(H_2)_{\text{chain}}$ . As the value of  $E_{85}$  is zero,  $E_{84} = 30 \text{ kcal mole}^{-1}$ .

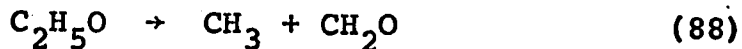
Reaction 84 is  $30 \text{ kcal mole}^{-1}$  endothermic. The thermochemical data needed to calculate the  $\Delta H$  values are presented in Table IV-9. The value of activation energy  $E_{84}$  ( $30 \text{ kcal mole}^{-1}$ ) estimated in the present work may be low, as previous observations on the decomposition of oxy radicals to form carbonyl compounds indicate that the activation energy is higher than the enthalpy change for such reactions (98,62,130). The low value of  $E_{84}$  may be explained in the following manner. Some of the acetaldehyde and hydrogen may be formed by reactions 86 and 87.



Therefore, the above estimate of the activation energy of reaction 84 may actually be some average between the activation energies of reactions 84 and 86. The activation energy for reaction 86 has been estimated to be ca.  $21 \text{ kcal mole}^{-1}$ ;  $\Delta H(86)$  is  $19 \text{ kcal mole}^{-1}$  (62).

Gray and Style (131) suggested that in the photolysis of

ethyl nitrate, 47% of ethoxy radicals formed decompose according to reaction 86 and 53% decompose according to reaction 88.



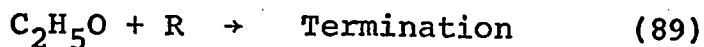
The activation energy for reaction 88 was also estimated to be 21 kcal mole<sup>-1</sup> (62).

Because of the complexity of the present system, no estimates can be made as to the relative importance of reactions 86 and 88. So, the conclusion of Gray and Style (131) that reaction 86 occurs to the extent of about 50 percent in the photolysis of ethyl nitrate in the vicinity of 100° is used in the present treatment. As the activation energies of reactions 86 and 88 are the same, at higher temperatures reaction 86 will still occur to the extent of about 50 percent. Therefore,

$$E(\text{observed}) = \frac{1}{2}(E_{84} + E_{86})$$

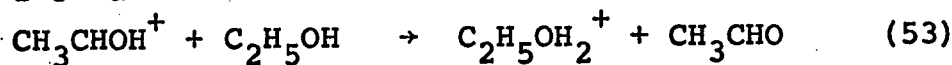
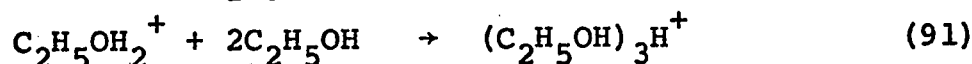
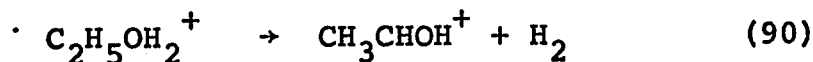
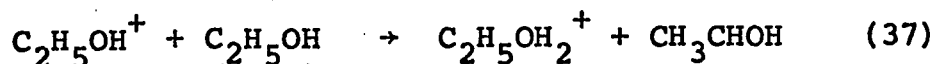
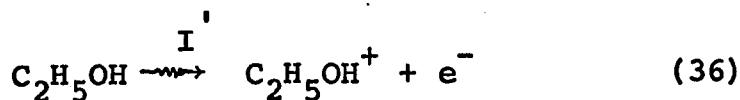
The value of  $E(\text{observed})$  is 30 kcal mole<sup>-1</sup> and  $E_{86}$  is 21 kcal mole<sup>-1</sup> (62). So,  $E_{84} = 39$  kcal mole<sup>-1</sup>.

The chain represented by reactions 86 and 87 may be terminated by reaction 89.



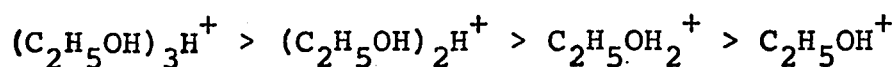
The inclusion of reactions (87)-(89) will not alter the kinetic conclusions reached earlier because the formation

of hydrogen and acetaldehyde by both the chain mechanisms with  $\text{CH}_3\dot{\text{C}}\text{HOH}$  and  $\text{C}_2\text{H}_5\dot{\text{O}}$  radicals involve the competition between the unimolecular decomposition of a radical (reactions 84 or 86) and a bimolecular termination reaction 85 or 89. In addition to the above mentioned free radical chain mechanism, the following ionic chain mechanism was also considered.



From a crude extrapolation of the results of Kebarle et al (115) on the studies of the clustering of water molecules about hydrogen ions in the gas phase, it was expected that under the conditions of the present study, the hydrogen ions will on the average be clustered by about three ethanol molecules. Therefore, the main neutralization reaction in the system should be 92. Reaction 91 occurs in two steps and is reversible, but the conclusions will not be altered by the present oversimplification.

A corollary to the fact that the chain is long and the assumption that it is terminated by reaction 92 is:



Therefore,

$$[e^-] \sim (C_2H_5OH)_3H^+ \quad (xxxviii)$$

By applying a steady state treatment to the concentration of  $[e^-]$ , we get;

$$\frac{d[e^-]}{dt} = 0 = I' - k_{92}\{(C_2H_5OH)_3H^+\}[e^-] \quad (xxxix)$$

Substituting for  $[e^-]$  from xxxviii into xxxix we get,

$$[(C_2H_5OH)_3H^+] = (I'/k_{92})^{1/2} \quad (xxxixa)$$

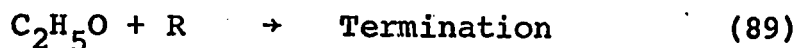
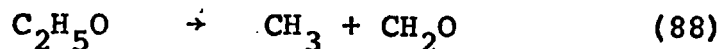
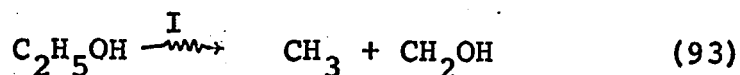
By applying the steady state treatment to the concentration of the various ions and using the value of  $[(C_2H_5OH)_3H^+]$  according to equation (xxxixa), it can be shown that:

$$\frac{d[H_2]}{dt} = \frac{k_{90}A'}{k_{91}[(C_2H_5OH)_3H^+]} \quad (x1)$$

This indicates that the formation of hydrogen should be -1.0 order. But in the present study the formation of hydrogen is +0.8 order at the lower pressures and +0.6 order at the higher pressures. Therefore, the ionic mechanism is discarded.

### c. Methane + formaldehyde

The formation of methane and formaldehyde can be explained by the following reactions;



By applying the steady state treatment to the concentration of  $CH_3$ ,  $CH_2OH$  and  $C_2H_5O$  radicals and by assuming that  $[R] = (I/k_{89})^{1/2}$ , it can be shown that:

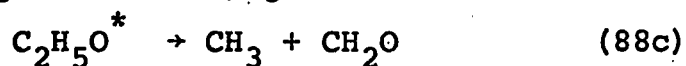
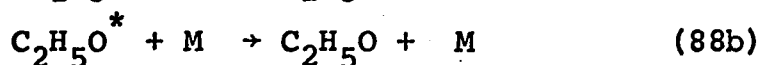
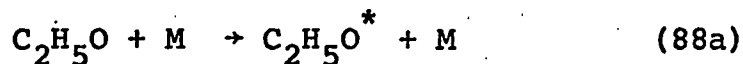
$$\frac{d[CH_2O]}{dt} = k_{88} \left( \frac{A}{k_{89}} \right)^{1/2} [C_2H_5OH]^{1/2} \quad (xli)$$

and for the long chains:

$$\frac{d[CH_4]}{dt} = k_{88} \left( \frac{A}{k_{89}} \right)^{1/2} [C_2H_5OH]^{1/2} \quad (xlii)$$

This mechanism indicates that the formation of formaldehyde and methane should be 0.5 order. As methane and carbon monoxide are also formed by the chain decomposition of acetaldehyde at these high temperatures, the actual methane yield from the above mechanism is taken as  $[G(CH_4)_{\text{total}} - G(CO)]$ . The slope of the plot of  $\log[G(CH_4)_{\text{total}} - G(CO)]$  against  $\log P_{C_2H_5OH}$  is 0.3 (Fig. IV-4B), which indicates that the formation of methane at  $350^\circ$  is  $1.0 + 0.3 = 1.3$  order. This increase in order from 0.5 to 1.3 is probably due to the pressure dependence of the decomposition of  $C_2H_5O$  radicals under

the conditions of the present study. Therefore, reaction 88 should be written as the combination of reactions 88a-c.



where M is ethanol.

By applying the steady state treatment to the concentration of  $\text{C}_2\text{H}_5\text{O}^*$  and solving in a manner similar to the one used for  $\text{CH}_3\text{CHOH}$  radicals before, we get:

$$k_{88} = \frac{k_{88a}k_{88c}[\text{M}]}{k_{88c} + k_{88b}[\text{M}]} \quad (\text{xliii})$$

By substituting  $k_{88}$  from xliii into xlii, we get:

$$\frac{d[\text{CH}_4]}{dt} = \frac{k_{88a}k_{88c}}{k_{88c} + k_{88b}[\text{C}_2\text{H}_5\text{OH}]} \left( \frac{A}{k_{89}} \right)^{\frac{1}{2}} [\text{C}_2\text{H}_5\text{OH}]^{\frac{3}{2}} \quad (\text{xliia})$$

This illustrates that methane formation should be 0.5 order at higher pressures and 1.5 order at lower pressures.

The concentration of ethanol was kept constant in the study of the temperature effect (Figs. III-8 and III-9). The yield of methane is nearly constant over the temperature range 110° to 200° (Table III-6) and, therefore, may be formed by a non-chain mechanism. In order

to obtain  $G(\text{CH}_4)_{\text{chain}}$ , the non-chain yield of methane ( $G(\text{CH}_4) \approx 3.1$ , average value over the temperature range  $110^\circ$  to  $200^\circ$ ) was subtracted from the yields of  $[G(\text{CH}_4)_T - G(\text{CO})]$  at higher temperatures. From the plot of  $\log G(\text{CH}_4)_{\text{chain}}$  vs  $1/T(^{\circ}\text{K})$  (Fig. IV-7), one obtains the value of  $(E_{88} - \frac{1}{2}E_{89}) = 19$ . The value of  $E_{89} = 0$ , so  $E_{88} = 19$  kcal mole<sup>-1</sup>.

It will be shown later that in the present experiments formaldehyde is converted into methanol, so the total yield of formaldehyde is taken as the yield of unconverted formaldehyde plus the methanol yield. No non-chain correction to the yields of (methanol + formaldehyde) could be applied, as the yields of these products formed by a non-chain mechanism over the temperature range  $60^\circ$  to  $200^\circ$  was not determined. Again, from a plot of  $\log G(\text{CH}_3\text{OH} + \text{CH}_2\text{O})$  against  $1/T(^{\circ}\text{K})$  (Fig. IV-8), one could obtain the value of  $(E_{88} - \frac{1}{2}E_{89}) = 19$ . As  $E_{89} = 0$ , so  $E_{88} = 19$  kcal mole<sup>-1</sup>. From the plot of  $\log (G(\text{CH}_4))$  vs  $1/T(^{\circ}\text{K})$  (Fig. IV-7), one obtains the value of  $E_{88} = 19$  kcal mole<sup>-1</sup> and also from the plot of  $\log G(\text{CH}_3\text{OH} + \text{CH}_2\text{O})$  vs  $1/T(^{\circ}\text{K})$  (Fig. IV-8), one obtains the value of  $E_{88} = 19$  kcal mole<sup>-1</sup>. Therefore, it is concluded that  $E_{88} = 19$  kcal mole<sup>-1</sup>. By way of comparison, an activation energy of 21 kcal mole<sup>-1</sup> for reaction 88 has been reported (62). Reaction 88 is 10 kcal mole<sup>-1</sup> endothermic (62).

#### d. Methanol + acetaldehyde

The following reactions explain the formation of



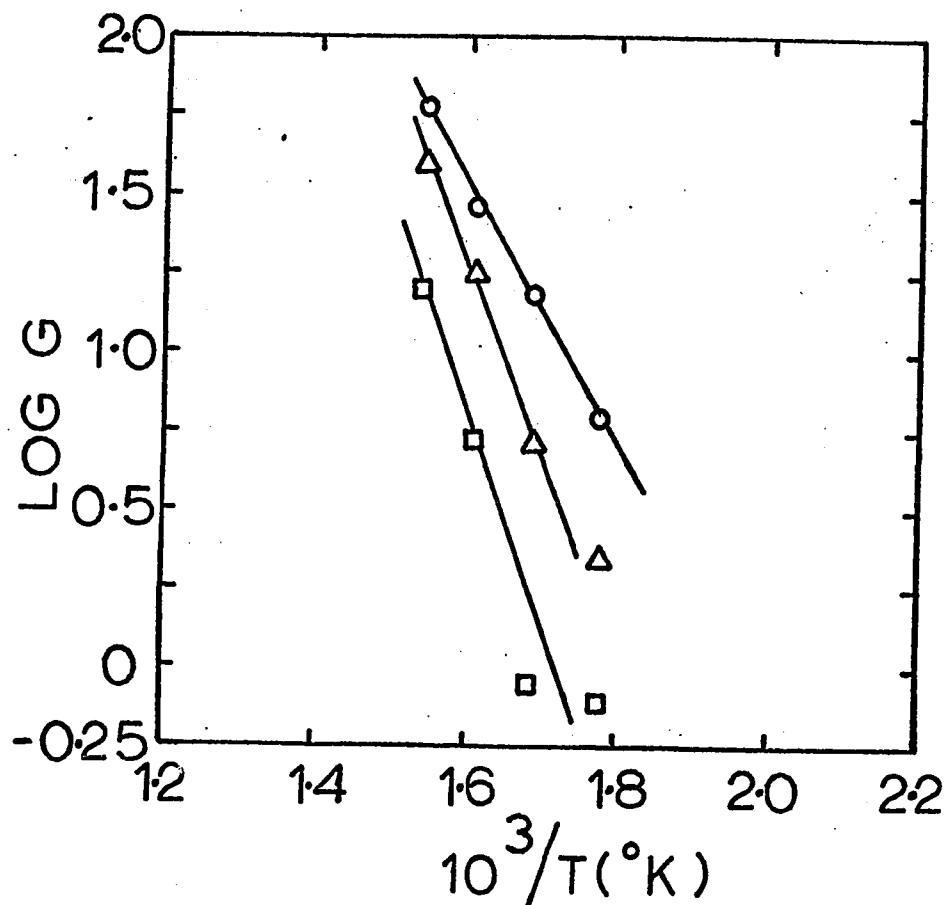
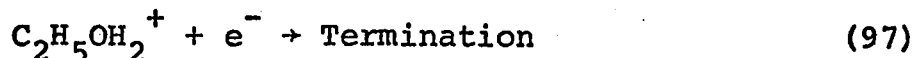
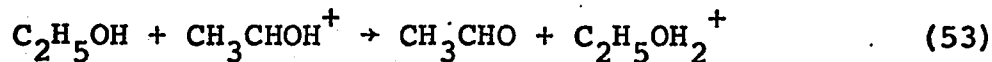
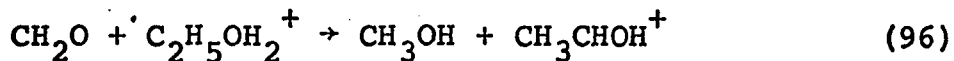


FIGURE IV-8

Arrhenius plot of (O) methanol + formaldehyde,  
 (Δ) ethylene and (□) diethyl ether.  $G(\text{C}_2\text{H}_4)_{\text{chain}} =$   
 $[G(\text{C}_2\text{H}_4) - 1.2]$ ;  $G(\text{ether})_{\text{chain}} = [G(\text{ether}) - 0.2]$

methanol and part of the acetaldehyde.



No evidence of the hydrogen molecule transfer reactions from  $\text{C}_2\text{H}_5\text{OH}_2^+$  to formaldehyde has been reported previously. But it is known that alkane and cycloalkane ions can donate  $\text{H}_2$  to unsaturated hydrocarbons (25).

Reaction 96 is about 9 kcal mole<sup>-1</sup> endothermic. The thermochemical data needed to calculate  $\Delta H(96)$  is presented in Table IV-9.

The occurrence of reaction 96 was confirmed in the following way. In the radiolysis of ethanol at 375° (ethanol density 0.66 g l<sup>-1</sup>) in the presence of 5 mole percent formaldehyde, the yields of acetaldehyde and methanol were found to be 640 and 608 respectively. The yields of acetaldehyde and methanol in the absence of formaldehyde were 119 and 45 respectively (Table III-6). Therefore, the increase in the yields of acetaldehyde and methanol in the presence of formaldehyde were 521 and 563 units respectively. The cause for the difference in the increase of the yields of acetaldehyde and methanol is probably the chain decomposition of acetaldehyde at these high temperatures. From the increase in the methanol yield, it was calculated that about 70

percent of the formaldehyde was converted into methanol.

The yields of methanol and formaldehyde in the radiolysis of ethanol vapor (0.66 g/l) at 375° are 45 and 14 G units respectively. If no conversion of formaldehyde into methanol had occurred by reaction 96, the formaldehyde yield would have been 45 + 14 = 59 G units. This indicates that about  $\frac{45}{59} \times 100 = 75\%$  of formaldehyde was converted into methanol by reaction 96. This is similar to the conclusion reached from the study of radiolysis of ethanol vapor in the presence of 5 mole percent formaldehyde.

The rate constant value for reaction 96 may be estimated in the following manner. By assuming a rate constant value of  $10^{14} \text{ l mole}^{-1} \text{ sec}^{-1}$  (2) for the electron-ion neutralization reaction, the steady state concentration of ions at a dose rate of  $4 \times 10^{19} \text{ eV/ghr}$  is calculated to be about  $2 \times 10^{-12} \text{ moles l}^{-1}$ .

The average concentration of unconverted formaldehyde during the experiment is  $4.6 \times 10^{-4} \text{ moles l}^{-1}$ . This concentration of formaldehyde is used in the present calculations.

$$\text{Now, } \frac{d[\text{CH}_3\text{OH}]}{dt} = k_{96} [\text{CH}_2\text{O}] [\text{C}_2\text{H}_5\text{OH}_2^+] \quad (\text{xliv})$$

$$\text{and } \frac{d[\text{CH}_3\text{OH}]}{dt} = 10^{-2} D G(\text{CH}_3\text{OH})_{\text{inc}} \quad (\text{xlv})$$

where  $G(\text{CH}_3\text{OH})_{\text{inc}}$  is the increase in methanol yield caused by the presence of 5 mole percent formaldehyde in the radiolysis of ethanol vapor at  $375^\circ$  and  $D$  is the dose rate in  $\text{ev ml}^{-1} \text{ sec}^{-1}$ .

$$\begin{aligned} \text{Therefore, } \frac{d[\text{CH}_3\text{OH}]}{dt} &= \frac{10^{-2} \times 6.8 \times 10^{12} \times 563}{6.02 \times 10^{20}} \\ &= 6.3 \times 10^{-8} \text{ moles l}^{-1} \text{ sec}^{-1} \text{ (x1va)} \end{aligned}$$

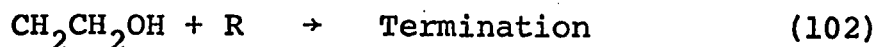
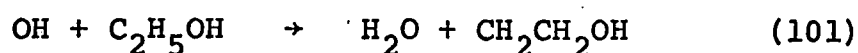
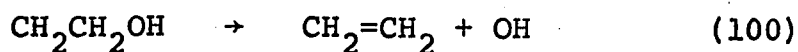
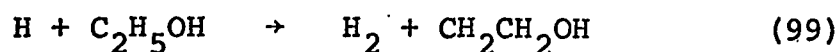
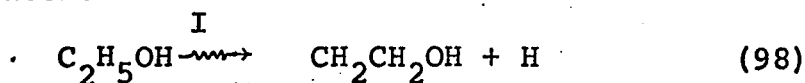
$$\text{So, } k_{96} \approx \frac{d[\text{CH}_3\text{OH}]/dt}{[\text{CH}_2\text{O}][\text{C}_2\text{H}_5\text{OH}_2^+]} \approx 7 \times 10^7 \text{ l mole}^{-1} \text{ sec}^{-1}$$

This value of  $k_{96} \approx 7 \times 10^7 \text{ l mole}^{-1} \text{ sec}^{-1}$  has been estimated on the assumption that the majority of ions present under the conditions of the present study are  $\text{C}_2\text{H}_5\text{OH}_2^+$ . But from a crude extrapolation of the results of Kebarle et al (115) on the studies of the clustering of water molecules about hydrogen ions in the gas phase, it is expected that in the present system, the hydrogen ions will on the average be clustered by about three ethanol molecules. Extrapolation of the water results (115) indicates that the concentration of  $\text{C}_2\text{H}_5\text{OH}_2^+$  would only be 1-10 percent of the total concentration of ions. Thus the rate constant  $k_{96}$  is about  $10^9 \text{ l mole}^{-1} \text{ sec}^{-1}$ .

#### e. Ethylene + water

The following reactions explain the formation of

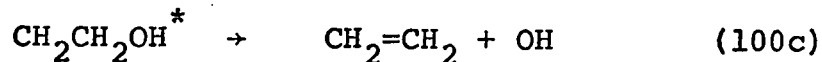
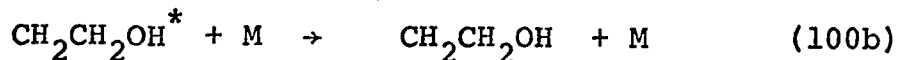
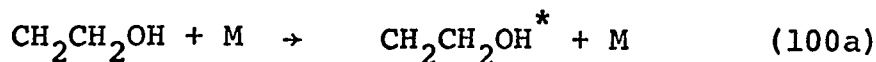
ethylene and water.



By applying the steady state treatment to the concentration of  $\text{CH}_2\text{CH}_2\text{OH}$ ,  $\text{H}$  and  $\text{OH}$  radicals and using the assumption that  $[\text{R}] = (\text{I}/k_{102})^{1/2}$ , it can be shown that

$$\frac{d[\text{C}_2\text{H}_4]}{dt} = k_{100} (\text{A}[\text{C}_2\text{H}_5\text{OH}]/k_{102})^{1/2} \quad (\text{xlv})$$

This mechanism indicates that the formation of ethylene should be 0.5 order. The slope of the line in the plot of  $\log G(\text{C}_2\text{H}_4)$  against  $\log P_{\text{C}_2\text{H}_5\text{OH}}$  is 0.0 (Fig. IV-5B). This indicates that the formation of ethylene is  $1.0 + 0.0 = 1.0$  order at  $350^\circ$ . The increase in order from 0.5 to 1.0 is probably due to the pressure dependence of the decomposition of the  $\text{CH}_2\text{CH}_2\text{OH}$  radicals. Therefore, reaction 100 should be written as the combination of reactions 100a-c.



where M is ethanol.

By applying steady state treatment to the concentration of  $\text{CH}_2\text{CH}_2\text{OH}^*$  and solving in a manner similar to the one used for  $\text{CH}_3\text{CHOH}$  radicals, it can be shown that:

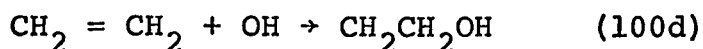
$$k_{100} = \frac{k_{100a}k_{100c} [\text{C}_2\text{H}_5\text{OH}]}{k_{100c} + k_{100b} [\text{C}_2\text{H}_5\text{OH}]} \quad (\text{xl vii})$$

By substituting  $k_{100}$  from xlvii into xlv, we get:

$$\frac{d[\text{C}_2\text{H}_4]}{dt} = \frac{k_{100a}k_{100c} [\text{C}_2\text{H}_5\text{OH}]^{\frac{3}{2}}}{k_{100c} + k_{100b} [\text{C}_2\text{H}_5\text{OH}]} \left( \frac{A}{k_{102}} \right)^{\frac{1}{2}} \quad (\text{xl via})$$

This illustrates that ethylene formation should be 0.5 order at higher pressures and 1.5 order at lower pressures.

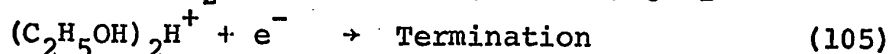
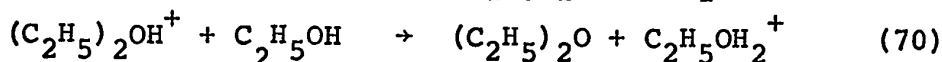
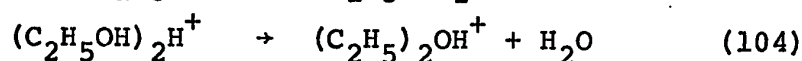
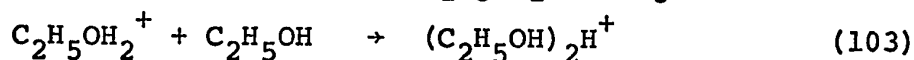
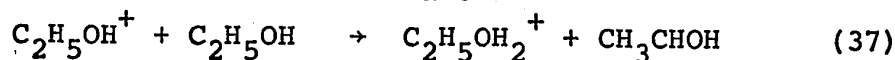
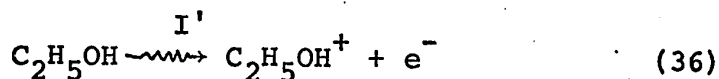
The concentration of ethanol was kept constant in the study of the effect of temperature (Fig. III-7). The yield of ethylene is nearly constant over the temperature range  $60^\circ$  to  $200^\circ$  (Table III-6) and, therefore, is formed by a non-chain mechanism. So,  $G(\text{C}_2\text{H}_4)$  chain was obtained by subtracting the non-chain yield of ethylene ( $G \approx 1.2$  average yield over the temperature range  $60^\circ$  to  $200^\circ$ ) from the yields at higher temperatures. From the plot of  $\log G(\text{C}_2\text{H}_4)_{\text{chain}}$  vs  $1/T(^{\circ}\text{K})$  (Fig. IV-8), one obtains the value of  $(E_{100} - \frac{1}{2}E_{102}) = 28$ . Since  $E_{102} = 0$ , we get  $E_{100} = 28 \text{ kcal mole}^{-1}$ . Reaction 100 is about 29  $\text{kcal mole}^{-1}$  endothermic. So this means the activation energy of the reverse reaction



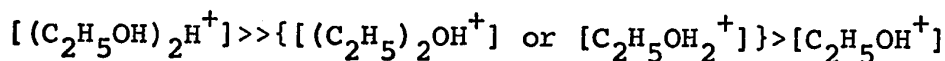
is zero.

f. Diethyl ether

The formation of diethyl ether at lower pressures can be explained as follows:



A corollary to the fact that the chain is long and the assumption that it is terminated by reaction 105 is



Therefore,

$$[e^-] \approx [(C_2H_5OH)_2H^+] \quad (\text{xlvi})$$

By applying steady state treatment to the concentration of  $e^-$ , we get:

$$\frac{d[e^-]}{dt} = 0 = I' - k_{105} [(C_2H_5OH)_2H^+][e^-] \quad (\text{xlix})$$

Substituting for  $[e^-]$  from xlviii into xlix and rearranging, we get:

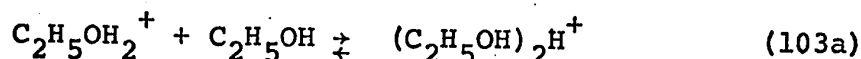
$$[(C_2H_5OH)_2H^+] = (I'/k_{105})^{1/2} \quad (1)$$

By applying the steady state treatment to the concentration of various ions and using the value of  $[(C_2H_5OH)_2H^+]$  according to equation 1, it can be shown that;

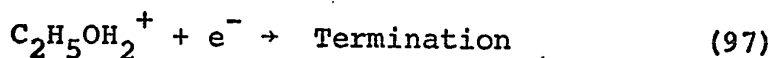
$$\frac{d[(C_2H_5)_2O]}{dt} = k_{104} \left( \frac{I'}{k_{105}} \right)^{1/2} [C_2H_5OH]^{1/2} \quad (\text{li})$$

This indicates that the ether formation should be 0.5 order.

As an analogy to the work of Kebarle et al (115) on the studies of the clustering of hydrogen ions by water molecules in the gas phase, reaction such as 103 should, in fact, be written as an equilibrium reaction.



If reaction 103 is considered as an equilibrium reaction, the relative concentrations of ions  $\text{C}_2\text{H}_5\text{OH}_2^+$  and  $(\text{C}_2\text{H}_5\text{OH})_2\text{H}^+$  will depend on the pressure. Two cases will be considered separately, depending on whether reaction 105 is the chain termination step or reaction 97 is the chain termination reaction.



#### i. Case I

Reaction 105 is considered as the main chain termination reaction. The other reactions are 36, 37, 103a, 104 and 70. Reaction 105 is considered as the main chain termination reaction, therefore;

$$[e^-] \sim [(\text{C}_2\text{H}_5\text{OH})_2\text{H}^+] \quad (\text{xlvi})$$

By applying the steady state treatment to the concentration of  $e^-$ , and solving the resulting equation and using the value for  $[e^-]$  according to equation xlviii, we get:

$$[(\text{C}_2\text{H}_5\text{OH})_2\text{H}^+] = (I'/k_{105})^{1/2} \quad (1)$$



Therefore, as before,

$$\frac{d[(C_2H_5)_2O]}{dt} = k_{104} \left( \frac{A'}{k_{105}} \right)^{\frac{1}{2}} [C_2H_5OH]^{\frac{1}{2}} \quad (1i)$$

This equation indicates that the formation of ether should be 0.5 order.

### ii. Case II

Reaction 97 is considered as the main chain termination step. The other reactions are 36, 37, 103a, 104 and 70. The consideration of reaction 97 as the main chain termination step requires :

$$[C_2H_5OH_2^+] \approx [e^-] \quad (1ii)$$

By applying the steady state treatment to the concentration of  $e^-$ , we get :

$$\frac{d[e^-]}{dt} = I' - k_{97}[C_2H_5OH_2^+][e^-] \quad (1iii)$$

Substituting the value of  $[e^-]$  in 1iii according to equation 1ii and rearranging, we get:

$$[C_2H_5OH_2^+] = (I'/k_{97})^{\frac{1}{2}} \quad (1iv)$$

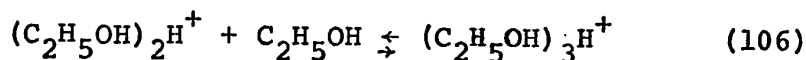
By applying the steady state treatment to the concentration of various ions and using the value of  $[C_2H_5OH_2^+]$  according to equation 1iv, it can be shown that:

$$\frac{d[(C_2H_5)_2O]}{dt} = \frac{k_{103a}k_{104}}{k_{-103a}+k_{104}} \left( \frac{A'}{k_{97}} \right)^{\frac{1}{2}} [C_2H_5OH]^{3/2} \quad (1v)$$

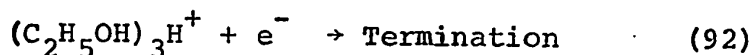
This equation indicates that the formation of ether should be 1.5 order.

In the plot of  $\log G(\text{ether})$  against  $\log P$  (Fig. IV-6), at lower pressures, the slope is -0.3 which indicates that the formation of ether is  $1.0 - 0.3 = 0.7$  order. This experimental value of 0.7 for the order of formation of ether at lower pressures indicates that reaction 105 is the main chain termination step.

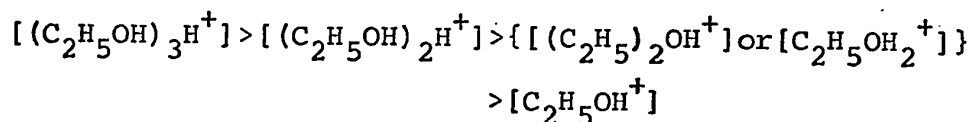
From a crude extrapolation of the results of the clustering of hydrogen ions by water molecules in the gas phase (115), it is expected that in the present system at the higher pressures, the hydrogen ions on the average will be clustered by about three ethanol molecules. Therefore, at higher pressures, reaction 106 should also be considered in addition to reactions 36, 37, 70, 103a and 104.



Reaction 92 is considered as the main chain termination step.



A natural consequence of the fact that the chain is long and the assumption that reaction 92 is the main chain termination reaction is;



Therefore,

$$[e^-] \approx [(C_2H_5OH)_3H^+] \quad (xxxviii)$$

By applying a steady state treatment to the concentration of  $e^-$ , we get:

$$\frac{d[e^-]}{dt} = 0 = I' - k_{92}[(C_2H_5OH)_3H^+][e^-] \quad (xxxix)$$

Substituting for  $[e^-]$  into xxxix from xxxviii and using  $I' = A' [C_2H_5OH]$ , we can show that:

$$[(C_2H_5OH)_3H^+] = (A' [C_2H_5OH]/k_{92})^{\frac{1}{2}} \quad (xxxixa)$$

By applying the steady state treatment to the concentration of various ions and using the value of

$[(C_2H_5OH)_3H^+]$  according to xxxixa, we can show that:

$$\frac{d[(C_2H_5)_2O]}{dt} = \frac{k_{104}}{k_{106}} A' + \frac{k_{104}k_{-106}}{k_{106}} \left( \frac{A'}{k_{92}} \right)^{\frac{1}{2}} [C_2H_5OH]^{-\frac{1}{2}} \quad (lvi)$$

This equation indicates that ether formation should be -0.5 order.

The slope of the plot of  $\log G(\text{ether})$  vs  $\log P$  (Fig. IV-6) at higher pressure is -1.5 which means that the formation of ether is  $-1.5 + 1.0 = -0.5$  order. This agreement between the two sets of values for the order of formation of ether indicates that reaction 92 is the main chain termination step.

The concentration of ethanol ( $0.66 \text{ g/l}^{-1}$ ) was kept constant in the study of the effect of temperature (Fig.

III-9). The value of  $G(\text{ether})_{\text{chain}}$  over the temperature range  $200^{\circ}$  to  $375^{\circ}$  was obtained by subtracting the yield of ether ( $G(\text{ether}) = 0.2$ ) at  $150^{\circ}$  from the yields at higher temperatures. From a plot of  $\log G(\text{ether})_{\text{chain}}$  vs  $1/T(^{\circ}\text{K})$  (Fig. IV-8), one obtains a value of  $30 \text{ kcal mole}^{-1}$  for the activation energy of formation of ether. The pressure of ethanol at  $350^{\circ}$  corresponding to a concentration of  $0.66 \text{ g/l}$  is  $568 \text{ torr}$ . The study of the effect of ethanol pressure on the yield of ether indicates (Fig. IV-6) that the pressure of  $568 \text{ torr}$  is in the transition zone between the low and high pressure regions.

The rate of ether formation is given by equation 1i in the low pressure region. If the pressure at which the temperature study was carried out were in this region, the slope in the plot of  $\log G(\text{ether})_{\text{chain}}$  vs  $1/T(^{\circ}\text{K})$  (Fig. IV-8) would yield the value for  $E_{104} - \frac{1}{2}E_{105}$ . But as  $E_{105}$  is zero, the value of  $E_{104}$  would be obtained.

The rate of ether formation is given by equation 1vi in the high pressure region. As indicated earlier, in the high pressure region  $(\text{C}_2\text{H}_5\text{OH})_3\text{H}^+$  is the main ion. For long chains equation 1vi reduces to:

$$\frac{d[(\text{C}_2\text{H}_5)_2\text{O}]}{dt} \approx \frac{k_{104}k_{-106}}{k_{106}} \left( \frac{A'}{k_{92}} \right)^{\frac{1}{2}} [\text{C}_2\text{H}_5\text{OH}]^{-\frac{1}{2}} \quad (1vii)$$

If the pressure at which the temperature study was carried out were in this region, the slope of the plot of  $\log$

$G(\text{ether})_{\text{chain}}$  vs  $1/T(^{\circ}\text{K})$  (Fig. IV-8) would yield the value of:

$$E_{104} + E_{-106} - E_{106} - \frac{1}{2}E_{92}$$

The value of  $E_{92}$  is zero and  $(E_{106} - E_{-106}) = \Delta H(106)$ . Therefore, the value of  $(E_{104} - \Delta H(106))$  would be obtained. No estimate for the value of  $\Delta H(106)$  has been reported, but the  $\Delta H$  value for the analogous reaction in water vapor is  $-22 \text{ kcal mole}^{-1}$  (115). Using this value for  $\Delta H(106)$ , the slope would yield the value of  $(E_{104} - 22) \text{ kcal mole}^{-1}$ .

The value of the activation energy obtained from the plot of  $\log G(\text{ether})_{\text{chain}}$  vs  $1/T(^{\circ}\text{K})$  (Fig. IV-8) is  $30 \text{ kcal mole}^{-1}$  and the pressure at which the temperature study was carried out is in the transition zone between the low and high pressure regions, therefore,  $30 > E_{104} > 8 \text{ kcal mole}^{-1}$ . Since  $\Delta H(104) = 19 \text{ kcal mole}^{-1}$ , it is concluded that  $30 > E_{104} > 19 \text{ kcal mole}^{-1}$ .

#### g. Ethane

The yield of ethane increases from 0.7 to 1.5 over the temperature range  $200^{\circ}$  to  $320^{\circ}$  and from 1.5 to 7.5 over the temperature range  $320^{\circ}$  to  $375^{\circ}$ . Therefore, a minor chain appears to occur over the temperature range  $320^{\circ}$  to  $375^{\circ}$ . The reactions appearing in the chain are not known.

5. Inhibition studies at 350°

The use of scavengers was prompted by the idea that the study of the variation in product yields by the scavenging of different reactive intermediates would provide a test for the chain mechanisms presented in the previous section.

Propylene was used because it is expected to affect the product yields by the scavenging of the free radical intermediates.

The proton affinities of ammonia and ethanol in kcal mole<sup>-1</sup> are 202 and 193  $\pm$  8 respectively (2). Therefore, ammonia may be expected to affect the product yields by behaving as a proton scavenger.

Sulphur hexafluoride has a large capture cross-section for thermal electrons (125). Therefore, it will influence the reactions involving positive ion-electron neutralization processes by changing them to positive ion-negative ion neutralization processes. This change may affect the yield of radicals produced by the neutralization reactions which will, in turn, affect the product yields.

The effects of propylene, ammonia and sulphur hexafluoride on product yields in the radiolysis of ethanol at 350° are summarized in Table IV-14. The effects of the scavengers on each of the chain mechanisms will be discussed separately.

TABLE IV-14

Summary of the results of the effects of scavengers on product yields in the radiolysis of ethanol at 350°

<u>Product</u>	<u>H<sub>2</sub></u>	<u>CH<sub>3</sub>CHO</u>	<u>CH<sub>4</sub></u>	<u>CH<sub>3</sub>OH</u>	<u>C<sub>2</sub>H<sub>4</sub></u>	<u>C<sub>2</sub>H<sub>5</sub>OC<sub>2</sub>H<sub>5</sub></u>
----- G <sub>O</sub> <sup>*</sup> -----						
	45.9	42.0	39.0	17.0	19.8	5.6
----- Δg <sub>max</sub> <sup>†</sup> -----						
<u>Scavenger</u>						
C <sub>3</sub> H <sub>6</sub>	35	no effect	19	11	4.5 <sup>††</sup>	no effect
SF <sub>6</sub>	29	uncertain	30	11	11.6	no effect
NH <sub>3</sub>	no effect	not determined	no effect	10	no effect	5.3

\* G<sub>O</sub> is the yield of the product in the absence of the scavenger.

† Δg<sub>max</sub> is the maximum decrease in the product yield caused by the addition of the scavenger.

†† This decrease in the ethylene yield is caused by the presence of 1.4 mole percent propylene and is presumably not the maximum decrease.

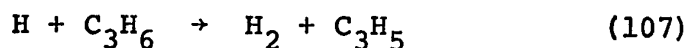
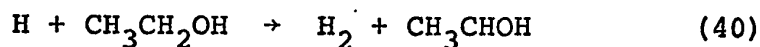
a. Hydrogen + acetaldehyde

The free radical chain mechanism presented in the previous section to explain the formation of hydrogen and acetaldehyde indicates that the yields of these products should decrease by the addition of propylene or sulphur hexafluoride and should remain unaffected by the addition of ammonia.

Propylene scavenger

It was observed that in the radiolysis of ethanol-propylene mixtures (ethanol density  $0.66 \text{ gl}^{-1}$ ), propylene decreased the yield of hydrogen from 45.9 to 11.0 whereas the yield of acetaldehyde remained unaffected (Table III-16 and Figures III-23A and III-24A).

The decrease in the yield of hydrogen is caused by the competition between reactions 40 and 47.



Takahasi and Cvetanovic (132) have reported a value of  $k_{107}/k_{47} = 0.04$  in their studies on their mercury photo-sensitized decomposition of n-butane in the presence of propylene at  $25^\circ$ . Therefore, it is expected that reaction 107 will not make any significant contribution under the conditions of the present work.



The simple competition between reactions 40 and 47 leads to the relationship:

$$\frac{1}{\Delta g(H_2)} = \frac{1}{\Delta g(H_2)_{\max}} \left[ 1 + \frac{k_{40}}{k_{47}} \frac{[C_2H_5OH]}{[C_3H_6]} \right] \quad (xv)$$

where  $\Delta g(H_2)$  is the reduction in hydrogen yield caused by the addition of propylene and  $\Delta g(H_2)_{\max}$  is the maximum decrease in hydrogen yield caused by propylene. The values of  $1/\Delta g(H_2)$  and  $[C_2H_5OH]/[C_3H_6]$  are presented in Table IV-15. From the intercept and slope of the line in the plot of  $1/\Delta g(H_2)$  against  $[C_2H_5OH]/[C_3H_6]$  (Fig. IV-9) we get  $\Delta g(H_2)_{\max} = 36$  and  $k_{40}/k_{47} = 0.105$ . The rate constant value  $k_{47} = 2.7 \times 10^9 \text{ l mole}^{-1} \text{ sec}^{-1}$  at  $350^\circ$  ( $623^\circ K$ ) is calculated from the reported values of  $\log A_{47} = 10.3$  ( $\text{l mole}^{-1} \text{ sec}^{-1}$ ) and  $E_{47} = 2.5 \text{ kcal mole}^{-1}$  (120). Using this value of  $k_{47}$ , a rate constant value  $k_{40} = 2.8 \times 10^7 \text{ l mole}^{-1} \text{ sec}^{-1}$  is obtained for  $350^\circ$ . The value of the rate constant  $k_{40}$  has not been reported before.

The yield of unscavengable hydrogen in the radiolysis of ethanol-propylene mixtures at  $350^\circ$  (ethanol density  $0.66 \text{ g l}^{-1}$ ) is 11.0 (plateau value in the plot of  $g(H_2)$  vs mole percent propylene, Fig. III-23A). The number of moles of hydrogen corresponding to  $G(H_2) = 11.0$  at the dose used is nearly equal to the number of moles of hydrogen obtained in the blank sample (Table III-22). The number of moles of hydrogen obtained in the pyrolysis

TABLE IV-15  
Data for kinetic plot from propylene additive in the radiolysis of  
ethanol vapor at 350°. Ethanol density 0.66 g/l

Mole % propylene	$g(H_2)$	$\Delta g(H_2)$	$\frac{1}{\Delta g(H_2)}$	no. of moles of $C_3H_6$	$\frac{[C_2H_5OH]}{[C_3H_6]}$
0.0	45.9	-----	-----	-----	-----
0.43	39.1	6.8	0.15	$3.1 \times 10^{-5}$	235.5
1.44	-----	-----	-----	$10.5 \times 10^{-5}$	69.5
1.82	23.4	22.5	0.044	$13.3 \times 10^{-5}$	54.9
8.68	14.0	31.9	0.031	$63.4 \times 10^{-5}$	11.5
16.41	9.7	36.2	0.028	$119.8 \times 10^{-5}$	6.1
24.68	14.9	31.0	0.032	$180.2 \times 10^{-5}$	4.1
40.7	11.8	34.1	0.029	$297.2 \times 10^{-5}$	2.5

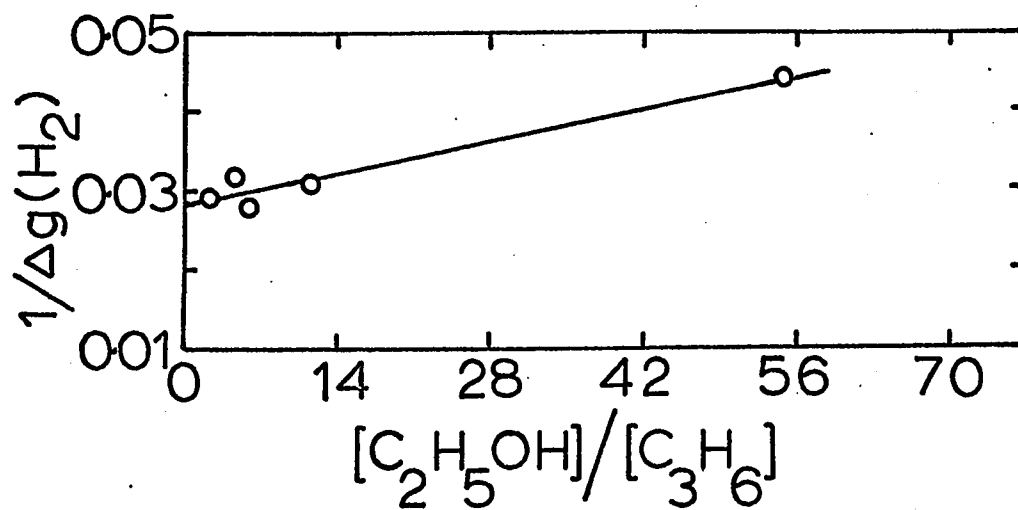
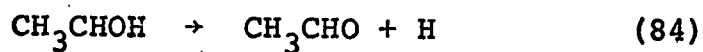
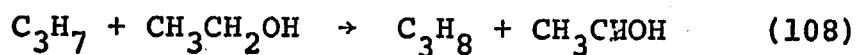


FIGURE IV-9

Kinetic plot for the hydrogen yield in the radiolysis of ethanol-propylene mixtures at 350°. Ethanol density = 0.66  $\text{gl}^{-1}$

of pure ethanol (ethanol density  $0.66 \text{ gl}^{-1}$ ) at  $350^\circ$  is  $6.5 \times 10^{-6}$  (Table III-21). This value remains unaffected in the presence of propylene within experimental error (Table III-22). This indicates that the formation of hydrogen in the blank sample is probably due to catalytic dehydrogenation of ethanol on the walls of the vessel.

The yield of acetaldehyde remained unaffected in the presence of propylene (Table IV-14). This is due to the chain propagation by  $\text{C}_3\text{H}_7$  radicals formed by reaction 47.

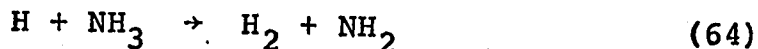


The evidence for the occurrence of reaction 108 comes from the observation that in the radiolysis of ethanol-propylene mixtures at  $350^\circ$ , the yield of propane increased from 0.1 to 9.1 (Table III-16) and the yield of hydrogen decreased from 46.0 to 33.0 (Fig. III-23A) as the propylene concentration was increased from 0 to 1.44 mole percent.

#### Ammonia scavenger

Ammonia did not affect the yield of hydrogen, in agreement with expectation from the proposed free radical

mechanism for hydrogen formation. The rate constant  $k_{64}$  at  $350^\circ$  is  $1 \times 10^6 \text{ l mole}^{-1} \text{ sec}^{-1}$ .

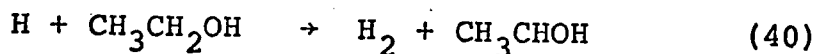
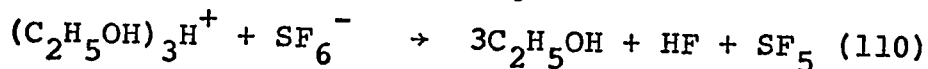
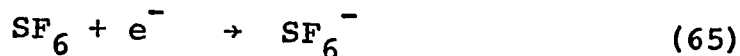
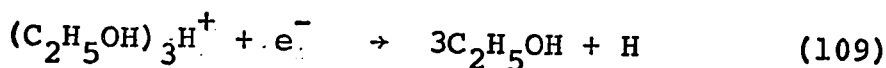


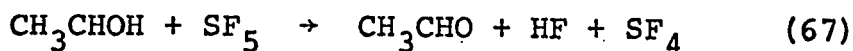
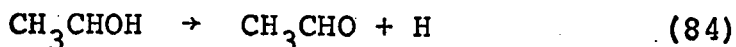
This was calculated from the value of  $k_{64} = 1 \times 10^4 \text{ l mole}^{-1} \text{ sec}^{-1}$  at  $150^\circ$  and  $E_{64} = 10-15 \text{ kcal mole}^{-1}$  (124). The value of rate constant  $k_{40}$  at  $350^\circ$ , as estimated in the present study is  $2.8 \times 10^7 \text{ l mole}^{-1} \text{ sec}^{-1}$ . The concentration of ethanol in the present study is  $1.43 \times 10^{-2} \text{ moles l}^{-1}$  and the maximum concentration of ammonia used in the present study is  $0.2 \times 10^{-2} \text{ moles l}^{-1}$ . Therefore, reaction 64 is not expected to make significant contribution under the conditions of the present work.

The yield of acetaldehyde could not be measured as it reacts with ammonia to give acetaldehyde ammonia (93).

#### Sulphur hexafluoride scavenger

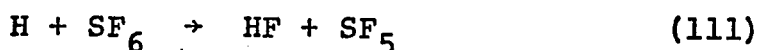
Sulphur hexafluoride decreases the yield of hydrogen from 45.9 to 16.8 (Fig. III-27). The decrease in hydrogen yield is probably due to the competition between reactions 65 and 109.





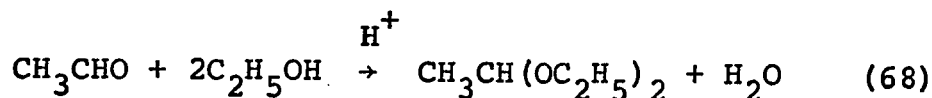
This competition between reactions 65 and 109 indicates that sulphur hexafluoride should decrease the yield of hydrogen.

The rate constant  $k_{111}$  is  $40 \text{ l mole}^{-1} \text{ sec}^{-1}$  at  $350^\circ$ .



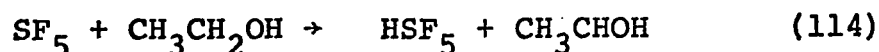
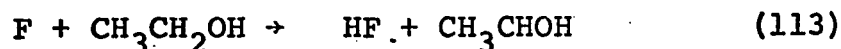
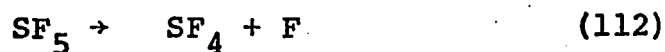
This was calculated from the reported values of  $\log A_{111} = 12.3$  ( $\text{l mole}^{-1} \text{ sec}^{-1}$ ) and  $E_{111} = 30 \pm 5 \text{ kcal mole}^{-1}$  (133). The rate constant value  $k_{40}$  is  $2.8 \times 10^7 \text{ l mole}^{-1} \text{ sec}^{-1}$  at  $350^\circ$  as estimated in the present study. This indicates that the contribution of reaction 111 is negligible under the conditions of the present work.

The product acetaldehyde was not measurable as such from the radiolysis of ethanol-sulphur hexafluoride mixtures. It was changed into acetal, probably by reaction 68. It is known that:



addition of alcohols to aldehydes occurs rapidly in the presence of acids (127) and acid is formed by reactions 67, 110 and 114. The effect of the presence of up to 1 mole percent sulphur hexafluoride on the yield of (acetaldehyde + acetal) is uncertain because of the large amount of scatter in the points in the plot of

g(acetaldehyde + acetal) against mole percent sulphur hexafluoride (Fig. III-27). If the (acetaldehyde + acetal) yield is actually constant, it may be due to the occurrence of reactions 112 and 113 and/or 114.

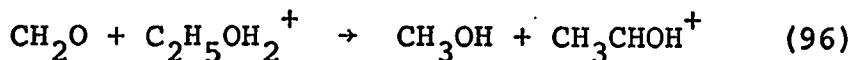


The increase of sulphur hexafluoride concentration over the range 1 to 20 mole percent increases the yield of (acetaldehyde + acetal) from about 43 to 84 G units (Fig. III-27). The cause for this increase is not known.

b. Methane + formaldehyde

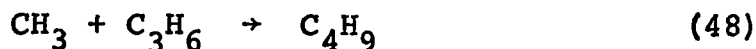
The mechanism presented in the previous section to explain the formation of methane and formaldehyde shows that the yield of these products should decrease in the presence of propylene and sulphur hexafluoride and should remain unaffected in the presence of ammonia.

The yield of formaldehyde in the ethanol-scavenger mixtures was not measured. It will be pointed out later that the evidence for the decrease in formaldehyde yield by the presence of propylene and sulphur hexafluoride comes from the measured decrease in the methanol yield. It was mentioned earlier that formaldehyde is converted into methanol by reaction 96.



#### Propylene scavenger

The decrease in the yield of methane may be due to the competition between reactions 95 and 48.



The unscavengable yield of methane in the present study is 20.0 (plateau value in the plot of  $g(\text{CH}_4)$  against mole percent propylene, Fig. III-24A). The number of moles corresponding to the plateau value of methane yield do not correspond to the number of moles obtained in the blank sample (Table III-22), but as indicated before the number of moles of unscavengable hydrogen is approximately equal to the number of moles obtained in the blank sample. This high value of the unscavengable methane yield probably indicates that propylene participates in methane formation.

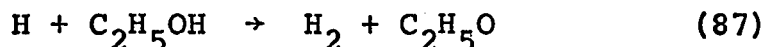
#### Sulphur hexafluoride scavenger

Sulphur hexafluoride decreases the yield of methane from 38.9 to 9.0. This may be explained in the following manner.

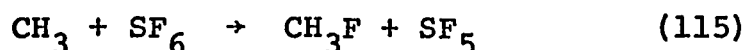
The competition between reactions 65 and 109 will affect the yield of hydrogen atoms which may, in turn, affect the yield of  $\text{C}_2\text{H}_5\text{O}$  radicals produced by reaction



87. These  $C_2H_5O$  radicals are the chain carriers in the mechanism of formation of methane and formaldehyde.

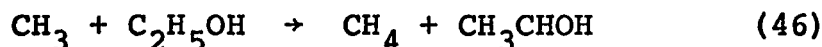


The rate constant  $k_{115}$  is  $2 \times 10^5 \text{ l mole}^{-1} \text{ sec}^{-1}$  at  $350^\circ$ . This was calculated from the reported values



of  $\log A_{115} = 10.3 \text{ (l mole}^{-1} \text{ sec}^{-1}\text{)}$  and  $E_{115} = 14 \text{ kcal mole}^{-1}$  (134).

$$\text{A value of } \frac{k_{46}}{k_{51}^{\frac{1}{2}}} = 9.3 \times 10^{-2} \text{ (l mole}^{-1} \text{ sec}^{-1}\text{)}^{\frac{1}{2}}$$

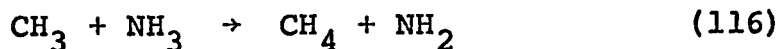


at  $182^\circ$  has been reported (122). The activation energy of reaction 46 is  $8.7 \text{ kcal mole}^{-1}$  (122). The rate constant  $k_{51}$  is  $2.2 \times 10^{10} \text{ l mole}^{-1} \text{ sec}^{-1}$  (72). From this data, the rate constant  $k_{46} = 2 \times 10^5 \text{ l mole}^{-1} \text{ sec}^{-1}$  at  $350^\circ$  is calculated. The concentration of ethanol used in the present study is  $1.43 \times 10^{-2} \text{ moles l}^{-1}$ . The concentration of sulphur hexafluoride used in the present study was varied from  $3 \times 10^{-7}$  to  $0.2 \times 10^{-2} \text{ moles l}^{-1}$ . The yield of methane decreased from 38.9 to 9.0 as the concentration of sulphur hexafluoride was varied from  $3 \times 10^{-7}$  to  $3 \times 10^{-5} \text{ moles l}^{-1}$ . The variation of

sulphur hexafluoride concentration over the range  $3 \times 10^{-5}$  to  $0.2 \times 10^{-2}$  moles  $l^{-1}$  did not affect the methane yield. Therefore, occurrence of reaction 115 is not expected to make significant contribution under the conditions of the present study.

Ammonia scavenger

As expected, ammonia does not affect the yield of methane (Fig. III-25B). The rate constant  $k_{116}$  is  $2.5 \times 10^4$   $l \text{ mole}^{-1} \text{ sec}^{-1}$  at  $350^\circ$ . This was calculated



from the reported values of  $\log A_{116}$  7.8  $l \text{ mole}^{-1} \text{ sec}^{-1}$  and  $E_{116} = 9.8 \text{ kcal mole}^{-1}$  (135). The value of the rate constant  $k_{46} = 2 \times 10^5$   $l \text{ mole}^{-1} \text{ sec}^{-1}$  at  $350^\circ$  was calculated earlier. The concentration of ethanol used in this study is  $1.43 \times 10^{-2}$  moles  $l^{-1}$  and the maximum concentration of ammonia used is  $0.2 \times 10^{-2}$  moles  $l^{-1}$ . Therefore, reaction 116 is not expected to make any significant contribution.

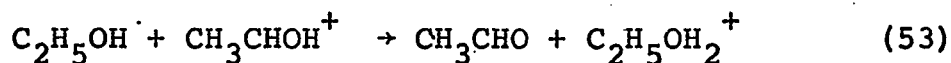
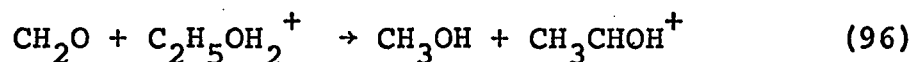
c. Methanol + acetaldehyde

The mechanism presented in the previous section to explain the formation of methanol and part of the acetaldehyde yield indicates that the yield of these products should decrease by the presence of propylene, ammonia and sulphur hexafluoride.

### Propylene scavenger

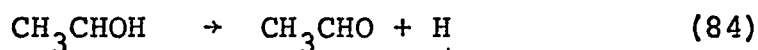
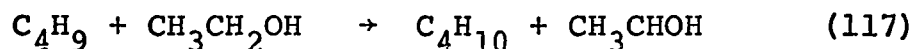
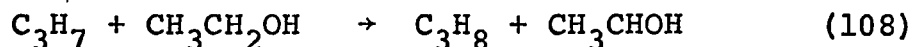
Propylene decreases the yield of methanol from 17.0 to 6.0 (Fig. III-23A).

The formation of methanol and part of the acetaldehyde yield was explained earlier by reactions 53 and 96. Propylene is not expected to interfere with the occurrence



of reactions 53 and 96. Therefore, the decrease in methanol yield by propylene is associated with the decrease in formaldehyde yield. Propylene inhibits the free radical chain that forms formaldehyde.

The occurrence of reactions 96 and 53 indicates that the decrease in formaldehyde yield should in turn decrease the yield of acetaldehyde formed by reaction 53. But it was pointed out earlier that the total acetaldehyde yield was unaffected by propylene. The constancy of the acetaldehyde yield may be due to a fortuitous balance between the decrease caused by the various inhibited reactions and an increase caused by reactions such as 108 and 117.

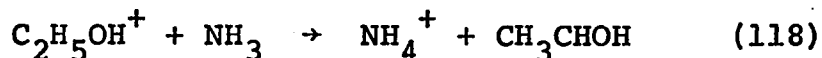
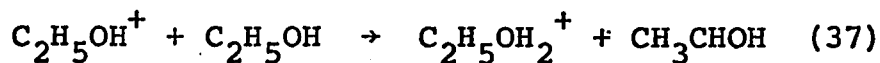


### Ammonia scavenger

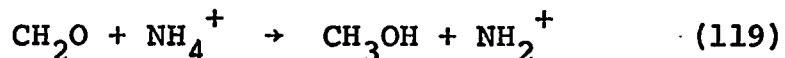
The maximum decrease in the yield of methanol caused by ammonia is 11 G units (Table IV-14). This can be due to two reasons.

(i) Formaldehyde is known to react with ammonia to give hexamethylene tetramine (93 ). The decrease in formaldehyde yield because of this will, in turn, cause the methanol yield to decrease.

(ii) The proton affinities (in kcal mole<sup>-1</sup>) of ammonia and ethanol are 202 and 193  $\pm$  8 respectively (2), Therefore, reaction 118 can compete with reaction 37.



The reaction 119 is 70 kcal mole<sup>-1</sup> endothermic,



therefore, it is not expected to occur.

The yield of acetaldehyde could not be measured as it reacts with ammonia to give acetaldehyde ammonia (93 ).

### Sulphur hexafluoride scavenger

Sulphur hexafluoride decreases the yield of methanol from 17.0 to 6.3.

Sulphur hexafluoride is not expected to affect the occurrence of reactions 53 and 96. Therefore, the decrease in the yield of methanol is associated with the de-

crease in formaldehyde yield. In the proposed mechanism for the formation of formaldehyde, sulphur hexafluoride was expected to decrease its yield. This was because the competition between reactions 65 and 109 would affect the yield of hydrogen atoms which would affect the yield of  $C_2H_5O$  free radical chain carriers. The yield of formaldehyde in the radiolysis of ethanol-scavenger mixtures was not measured. But the decrease in methanol yield caused by sulphur hexafluoride gives further support to the proposed mechanism for the formation of formaldehyde.

d. Ethylene + water

The proposed mechanism for formation of ethylene and water indicates that the yields of these products should decrease by the presence of propylene and sulphur hexafluoride, and that ammonia should have no effect.

Due to experimental difficulties, the yield of water was not determined in the radiolysis of ethanol-scavenger mixtures. Therefore, the effects of the various scavengers on this mechanism will be judged from their effect on the ethylene yield.

The decrease in ethylene yield caused by the presence of 1.4 mole percent propylene is 4.5 G units (Table IV-14). The ethylene yield in the presence of greater than 1.4 mole percent propylene could not be measured because of the interference of propylene. Therefore, the de-

crease of 4.5 G units in the ethylene yield may not be the maximum decrease that could result from the presence of propylene. This decrease in the ethylene yield is probably due to the fact that propylene scavenges the radicals which are the chain carriers in the mechanism for its formation.

The maximum decrease in the ethylene yield caused by sulphur hexafluoride is 11.6 G units (Table IV-14). The competition between reactions 65 and 109 will affect the yield of hydrogen atoms which will subsequently affect the yield of  $\text{CH}_2\text{CH}_2\text{OH}$  radicals which are the chain carriers for the chain formation of ethylene. Thus the effect of sulphur hexafluoride is due to the scavenging of the chain initiators rather than the chain propagators.

In accordance with expectations, the yield of ethylene is unaffected by ammonia (Table IV-14).

e. Diethyl ether

The mechanism of formation of diethyl ether indicates that its yield should remain unaffected by the presence of propylene and sulphur hexafluoride and should be decreased by the presence of ammonia.

As expected propylene and sulphur hexafluoride did not affect the yield of diethyl ether (Table IV-14).

The yield of diethyl ether was decreased from 5.6 to 0.3 G units by the addition of ammonia (Fig. III-26B). The proton affinities (in kcal mole<sup>-1</sup>) of ammonia and ethanol are 202 and 193 ± 8 respectively (2). Therefore, reaction 118 can compete with reaction 37. The occurrence of reaction 118 will cause the concentration of C<sub>2</sub>H<sub>5</sub>OH<sup>+</sup> ions to decrease which will in turn decrease the concentration of ions C<sub>2</sub>H<sub>5</sub>OH<sub>2</sub><sup>+</sup>, (C<sub>2</sub>H<sub>5</sub>OH)<sub>2</sub>H<sup>+</sup> and (C<sub>2</sub>H<sub>5</sub>)<sub>2</sub>OH<sup>+</sup>. Therefore, the yield of diethyl ether will decrease.

f. Ethane

The yield of ethane decreased from 3.5 to 2.6 G units as the concentration of propylene was increased from 0 to 1.4 mole percent (Table III-16).

Ammonia decreased the yield of ethane from 3.5 to 1.6 (Fig. III-25D).

As the reactions involved in the formation of ethane are not known, no explanation for the effect of propylene and ammonia can be presented. However, the inhibiting effect of ammonia is strong evidence that a positive ion reaction is involved in ethane formation.

R E F E R E N C E S

1. J. W. T. Spinks, R. J. Woods, 'An Introduction to Radiation Chemistry', Wiley, New York, (1964).
2. G. R. Freeman, Rad. Res. Rev., 1, 1, (1968).
3. S. C. Lind, 'Radiation Chemistry of Gases', Reinhold Publishing Corporation, New York, p.313 (1961).
4. L. W. Sieck and R. H. Johnsen, J. Phys. Chem., 69, 1699, (1965).
5. J. A. Hearne and R. W. Hummel, Rad. Res., 15, 254 (1961).
6. G. R. A. Johnson, J. Inorg. Nucl. Chem., 24, 461, (1962).
7. F. T. Jones and T. J. Sworski, J. Phys. Chem., 70, 1546, (1966).
8. R. A. Back, T. W. Woodward and K.A. McLauchlan, Can. J. Chem., 40, 1380, (1962).
9. P. Ausloos, Ann. Rev. Phys. Chem., 17, 205, (1966).
10. R. A. Lee, R. S. Davidow and D. A. Armstrong, Can. J. Chem., 42, 1906, (1964).
11. G. G. Meisels, J. Chem. Phys., 41, 51, (1964).
12. M. Leblanc and J.A. Herman, J. Chim. Phys., 63, 1055, (1966).
13. L. M. Hunter and R. H. Johnsen, J. Phys. Chem., 71 3228, (1967).



14. L. I. Bone, L. W. Sieck and J. H. Futrell, J. Chem. Phys., 44, 3367, (1966).
15. G. G. Meisels, J. Chem. Phys., 42, 3237 (1965).
16. R. Doepker and P. Ausloos, J. Chem. Phys., 43 3814, (1965).
17. R. Doepker and P. Ausloos, J. Chem. Phys., 44, 1951, (1966).
18. I. B. Sandoval and P. Ausloos, J. Chem. Phys., 38, 2454, (1963).
19. L. W. Sieck, F. P. Abramson and J. H. Futrell, J. Chem. Phys., 45, 2859, (1966).
20. M. S. B. Munson, J. Am. Chem. Soc., 87, 5313, (1965).
21. J. M. S. Henis, J. Am. Chem. Soc., 90, 844, (1968).
22. A. M. Hogg, R. M. Haynes and P. Kebarle, J. Am. Chem. Soc., 88, 28, (1966).
23. F. H. Field and F. W. Lampe, J. Am. Chem. Soc., 80, 5587, (1958).
24. P. Ausloos, S. G. Lias and A. A. Scala, Adv. Chem. Ser., 58, 264, (1966).
25. P. Ausloos and S. G. Lias, in 'Actions chimiques et Biologiques des Radiations', ed. M. Haissinski, onzième série, p.1, Masson, Paris (1967).
26. P. Ausloos and S. G. Lias, J. Chem. Phys., 38, 2207, (1963).
27. P. Ausloos, S. G. Lias, I. B. Sandoval, Disc. Faraday Soc., 36, 66, (1963).

28. M. S. B. Munson, J. L. Franklin and F. H. Field, J. Phys. Chem., 88, 3098, (1964).
29. G. A. W. Derwish, A. Galli and V. G. Giardini-Guidoni, J. Chem. Phys., 41, 2998, (1964).
30. F. P. Abramson and J. H. Futrell, J. Phys. Chem., 71 1233, (1967).
31. P. Ausloos and S. G. Lias, J. Chem. Phys., 43, 127, (1965).
32. P. Ausloos, A. A. Scala and S. G. Lias, J. Am. Chem. Soc., 89, 3677, (1967).
33. S. J. Rzađ and R. H. Schuler, J. Phys. Chem., 72, 228, (1968).
34. P. Kebarle, R. M. Haynes and S. Searles, Adv. Chem. Ser., 58, 210, (1966).
35. (a) H. Budziekiewicz, C. Djerassi and D. H. Williams, 'Interpretation of Mass spectra of organic compounds', p.29, Holden-Day Inc., San Francisco, (1964).  
(b) J. G. Burr, J. Am. Chem. Soc., 79, 751, (1957).
36. T. W. Woodward and R. A. Back, Can. J. Chem., 41, 1463, (1963).
37. S. G. Lias and P. Ausloos, J. Chem. Phys., 43, 2748, (1965).
38. G. R. A. Johnson and J. M. Warman, Trans. Far. Soc., 61, 1709, (1965).
39. W. J. Holtslander and G. R. Freeman, J. Phys. Chem., 71, 2562, (1967).

40. R. F. Hampson, J. R. McNesby, H. Akimoto and I. Tanaka, J. Chem. Phys., 40, 1099, (1964).
41. H. R. Carmichael, R. Gordon and P. Ausloos, J. Chem. Phys., 42 343, (1965).
42. J.R. McNesby, in 'Actions chimiques et Biologiques des Radiations', ed. M. Haissinski, Masson et cie, Paris, 9, 39, (1966).
43. G. G. Meisels and T. J. Sowerski, J. Phys. Chem., 69, 2867, (1965).
44. P. Ausloos and S. G. Lias, Rad. Res. Rev., 1, 75, (1968).
45. R. L. Platzman, Rad. Res., 17, 419, (1962).
46. R. Gordon, R. Doepker and P. Ausloos, J. Chem. Phys., 44, 3733, (1966).
47. N. T. Williams and H. Essex, J. Chem. Phys., 17, 995, (1949).
48. H. Essex, J. Phys. Chem., 58, 42, (1954).
49. R. R. Williams, J. Phys. Chem., 63, 776, (1959).
50. W. G. Burns and R. Parker, in 'Progress in Reaction Kinetics' ed. G. Porter, Pergamon Press, London, 3, 303, (1965).
51. T. Ohmae and H. Sakurai, Bull-chem. Soc. (Japan), 40, 1368, (1967).
52. R. H. Schuler and R. R. Kuntz, J. Phys. Chem., 67, 1004, (1963).

53. R. A. Holroyd and G. W. Klein, J. Phys. Chem., 69, 194, (1965).
54. C. Chachaty and E. Hayon; J. chim. Phys., 61, 115, (1964).
55. J. A. Leone and W. Koski, J. Am. Chem. Soc., 88, 224, (1966).
56. R. W. Fessenden and R. H. Schuler, J. Chem. Phys., 39 2147, (1963).
57. I. A. Taub and L. Dorfman, J. Am. Chem. Soc., 84, 4053, (1962).
58. D.R. Smith and J. C. Tole, Can. J. Chem., 45, 779, (1967).
59. W. A. Pryor, Free radicals, McGraw Hill, New York, (1966).
60. W. A. Waters (Ed.), Vistas in Free radical chemistry, Pergamon Press, London (1959).
61. G. H. Williams (Ed.), Advances in Free radical chemistry, vol. 1, Academic Press, London, (1965); and subsequent volumes.
62. P. Gray, R. Shaw and J. C. J. Thynne, in 'Progress in Reaction Kinetics', ed. G. Porter, Pergamon Press, 4, 63, (1967).
63. K. H. Jones, J. Phys. Chem., 71, 709, (1967).
64. C. M. Wodetzki, P. A. McCusker and D. B. Peterson, J. Phys. Chem., 69, 1045 (1965).

65. C. M. Wodetzki, P. A. McCusker and D. B. Peterson, *ibid.*, 69, 1056 (1965).
66. M. Trachtman, *ibid.*, 70, 3382, (1966).
67. Y. Toi, D. B. Peterson and M. Burton, *Rad. Res.*, 17, 399, (1962).
68. M. Nishikawa and N. Shinohara, *Rad. Res.*, 33, 194 (1968).
69. (a) R. D. Koob and L. Kevan, *Trans. Far. Soc.*, 64, 422, (1968).  
(b) R. D. Koob and L. Kevan, *Trans. Far. Soc.*, 64, 706, (1968).
70. K. Yang and P. Grant, *J. Phys. Chem.*, 65, 1861 (1961).
71. L. W. Sieck, N. K. Blocker and J. H. Futrell, *ibid.*, 69, 889, (1965).
72. K. J. Laidler, 'Chemical Kinetics', McGraw Hill Co., (1965).
73. V. N. Kondratev 'Chemical Kinetics of Gas Reactions', Pergamon Press (1964).
74. A. A. Frost and R. G. Pearson 'Kinetics and Mechanism' John Wiley, New York (1961).
75. J. G. Calvert and J. N. Pitts, 'Photochemistry', John Wiley, New York (1966).
76. A. H. Laufer and J. R. McNesby, *J. Phys. Chem.*, 70, 4094, (1966).
77. H. Okamoto, K. Fueki and Z. Kuri, *J. Phys. Chem.* 71, 3222, (1967).

78. J. H. Baxendale and G. P. Gilbert, *Discussions Faraday Soc.*, 36, 186 (1963).
79. M. K. M. Ng and G. R. Freeman, *J. Am. Chem. Soc.*, 87, 1639, (1965).
80. J. M. Ramaradhya and G. R. Freeman, *Can. J. Chem.*, 39, 1836, (1961).
81. J. M. Ramaradhya and G. R. Freeman, *ibid.*, 39, 1843, (1961).
82. J. J. J. Myron and G. R. Freeman, *ibid.*, 43, 1484, (1965).
83. H. Hotta, H. Kurihara and T. Abe, *Bull. Chem. Soc. Japan*, 40, 714, (1967).
84. J. W. Fletcher, Ph.D. Thesis, University of Alberta (1967).
85. G. R. Freeman, *Proc. Roy. Soc. (London)*, A245, 49, (1958).
86. K. J. Laidler and D. J. McKenney, *Proc. Roy. Soc. (London)* A278, 505, (1964).
87. J. A. Barnard and H. W. D. Hughes, *Trans. Far. Soc.*, 56, 55, (1960).
88. G. R. Freeman, *Proc. Roy. Soc. (London)*, A245, 75 (1958).
89. C. G. Moore, *J. Chem. Soc.*, 236 (1951).
90. R. S. Juvet and J. Chiu, *J. Am. Chem. Soc.*, 83, 1560 (1961).

91. M. C. Sauer and L. M. Dorfman, J. Phys. Chem., 66, 322 (1962).
92. J. Frederick Walker, "Formaldehyde", American Chemical Soc. Monograph Series, Reinhold Publication division, 3rd edition, p. 486.
93. J. D. Roberts and M. C. Caserio, "Basic Principles of Organic Chemistry", W. A. Benjamin, Inc., p. 442, (1965).
94. F. T. Jones and T. J. Sworski, Trans. Faraday Soc., 63, 2411 (1967).
95. M. K. M. Ng, Ph.D. Thesis, University of Alberta, (1964).
96. J. C. J. Thynne, Trans. Faraday Soc., 58, 676 (1962).
97. J. Long and G. Skirrow, Trans. Faraday Soc., 58, 1403 (1962).
98. L. F. Loucks and K. J. Laidler, Can. J. Chem., 45, 2767 (1967).
99. L. F. Loucks and K. J. Laidler, Can. J. Chem., 45, 2795 (1967).
100. R. L. East and L. Phillips, J. Chem. Soc. (A), 1939 (1967).
101. S. W. Benson, J. Chem. Edu., 42, 502 (1965).
102. G. Pilcher, H. A. Skinner, A. S. Pell and A. E. Pope, Trans. Faraday Soc., 59, 316 (1963).

103. F. H. Field and J. L. Franklin, "Electron Impact Phenomena," Academic Press Inc., New York, (1957).
104. A. G. Harrison, A. Ivko and D. Van Raalte, Can. J. Chem., 44, 1625 (1966).
105. F. T. Wall, "Chemical Thermodynamics", W. H. Freeman and Co., San Francisco, p. 54, (1965).
106. G. Pilcher, A. S. Pell and D. J. Coleman, Trans. Faraday Soc., 60, 499 (1964).
107. R. W. Kiser, "Introduction to mass spectrometry and its applications," Prentice-Hall Inc., Englewood Cliffs, N. J., (1965).
108. P. Gray and A. Williams, Chem. Rev., 59, 239 (1959).
109. M. S. B. Munson and F. H. Field, J. Am. Chem. Soc., 88, 2621 (1966).
110. M. S. B. Munson and F. H. Field, J. Am. Chem. Soc., 88, 4337 (1966).
111. M. S. B. Munson, Private communication.
112. derived from information in Table 10 of A. F. vol. 1, (ed. G. H. Williams), Academic Press, New York, (1965).
113. L. M. Terman, Russ. Chem. Rev., 34, 185 (1965).
114. M. K. M. Ng and G. R. Freeman, J. Am. Chem. Soc., 87, 1635 (1965).
115. P. Kebarle, S. K. Searles, A. Zolla, J. Scarborough and M. Arshadi, J. Am. Chem. Soc., 89, 6393 (1967).



116. P. Kebarle, R. M. Haynes and J. G. Collins, J. Am. Chem. Soc., 89, 5753 (1967).
117. "Handbook of Chemistry and Physics," 46th ed, Chemical Rubber Co., Cleveland, Ohio, 1965-66, pp F154 and F155.
118. V. L. Talrose and E. L. Frankevich, J. Am. Chem. Soc., 80, 2344 (1958).
119. L. Bouby, F. Fiquet-Fayard and H. Abgrall, Compt. Rend., 261, 4059 (1965).
120. A. F. Trotman-Dickenson in 'Advances in Free Radical Chemistry', ed. G. H. Williams 1, 1 (1965).
121. R. J. Cvetanovic and R. S. Irwin, J. Chem. Phys., 46, 1694 (1967).
122. A. F. Trotman-Dickenson, J. Chem. Phys., 19, 329 (1951).
123. K. R. Ryan, L. W. Sieck and J. H. Futrell, J. Chem. Phys., 41 111 (1964).
124. M. Schiavello and G. G. Volpi, J. Chem. Phys., 37, 1510 (1962).
125. A. N. Prasad and J. D. Craggs, 'Atomic and Molecular Processes', Academic Press, New York, Chap. 6, (1962).
126. P. Adler and H. K. Bothe, Z. Fur. Naturf. 20a, 1700 (1965).

127. D. J. Cram and G. S. Hammond, 'Organic Chemistry', McGraw-Hill Book Company, p. 295, (1964).
128. J. A. Kerr, Chem. Rev., 66, 465 (1966).
129. H. L. Roberts, Quart. Rev. Chem. Soc. (London), 15, 30 (1961).
130. K. M. Bansal and G. R. Freeman, J. Am. Chem. Soc., 88, 4326 (1966).
131. J. A. Gray and D. W. G. Style, Trans. Faraday Soc., 49, 52 (1953).
132. M. Takahasi and R. J. Cvetanovic, Can. J. Chem., 40, 1037 (1962).
133. C. P. Fenimore and G. W. Jones, Combust. Flame, 8, 231 (1964).
134. L. Batt and F. R. Cruickshank, J. Phys. Chem., 70, 723 (1966).
135. P. Gray and J. C. J. Thynne, Trans. Faraday Soc., 60, 1047 (1964).
136. G. R. Freeman and J. M. Fayadh, J. Chem. Phys., 43, 86 (1965).
137. A. Hummel, A. O. Allen and C. H. Watson, Jr., J. Chem. Phys., 44, 3431 (1966).
138. P. H. Tewari and G. R. Freeman, J. Chem. Phys., (in press).
139. S. Sato, R. Yugeta, K. Shinsaka and T. Terao, Bull. Chem. Soc. Japan, 39, 156 (1966).

140. M. G. Robinson and G. R. Freeman, J. Chem. Phys., 48, 983 (1968).
141. N. H. Sagert, Can. J. Chem., 46, 95 (1968).
142. F. Williams, J. Am. Chem. Soc., 86, 3954 (1964).
143. L.G. Walker, Ph.D. Thesis, University of Alberta, (1967).
144. V. L. Tal'rose, 'Actions Chimiques et Biologiques Des Radiations,' Masson et Cie, Paris, 11, 86 (1967).
145. V. I. Gusynin and V. L. Tal'rose, Dokl. Akad. Nauk SSSR, 170, 135 (1966).
146. H. A. Bethe and J. Ashkin, in "Experimental Nuclear Physics," ed. E. Segré, vol. 1, J. Wiley and Sons, New York, (1953).

A P P E N D I X

A. Effect of electric field strength on  $\gamma$ -radiolysis of cyclohexane liquid

1. Introduction

Under the influence of ionizing radiation, hydrocarbon liquids become conductors of electricity. From the magnitude of the induced conductance at low field strengths, one can estimate the yield of ions that escape geminate recombination. For example, the yield of free ions in each of the liquids cyclohexane, n-hexane and n-pentane has been found to be 0.1 (136, 137, 138).

One of the important questions of radiation chemistry is the chemical consequences of the reactions of ions. Two approaches have been taken to study the contribution of ion-molecule reactions to the overall distribution of products in the radiolysis of hydrocarbon liquids.

(i) The effect of various ion scavengers on product yields has been studied. For example, it has been shown that the decrease in hydrogen yield caused by nitrous oxide, in the radiolysis of nitrous oxide-hydrocarbon solutions, is due to the electron capture by nitrous oxide (139, 140).

Sagert (141) has studied the effect of perfluorocarbons on the radiolysis of cyclohexane liquid and found that the decrease in hydrogen yield from 5.6 to 2.6 G units is due to the capture of electrons by perfluorocarbons.

Williams (142) has found that the irradiation of cyclohexane -  $\text{ND}_3$  solutions gives an appreciable yield of HD, and interprets this in terms of the reactions of positive ions with the  $\text{ND}_3$ . The formation of HD in the radiolysis of cyclopentane -  $\text{ND}_3$  solutions has also been ascribed to the reactions of positive ions with  $\text{ND}_3$  (143).

(ii) The application of the electric fields across the hydrocarbon liquids under radiation may affect the product yields as some of the ions will be collected at the electrodes, thereby changing the homogeneous recombination of ions into a heterogeneous one. The amount of energy liberated from the neutralization of an ion on the surface of an electrode is usually less than if the neutralization had taken place by a homogeneous process. This difference is nearly equal to the electron work function of the electrode (144). Therefore, the amount of excess energy in the molecule will be lower by this amount. This may change the mode of decomposition of the molecules which, in turn, would affect the product yields.

A study of the effect of electric field on hydrogen yield during the radiolysis of liquid normal paraffins (dodecane, tetradecane and hexadecane) has been carried out by Gusynin and Tal'rose (145). They observed an increased rate of hydrogen evolution when an electric field of  $1.5 \times 10^4 \text{ v cm}^{-1}$  was applied during the irradiation with

1.6 MeV electrons (145). At about  $3 \times 10^{16}$  eV cc<sup>-1</sup> sec<sup>-1</sup>, the rate of hydrogen evolution in the presence of the electric field was more than double that in the absence of the field (145).

### Object of the present work

The present project was undertaken to study the consequences of ion neutralization at electrode surface.

## 2. Experimental

### a. Materials used

(i) For irradiation: Eastman Spectrograde cyclohexane was used for some experiments and for other experiments purified Phillips Research grade cyclohexane was used. The following method was used for purification.

300 ml of cyclohexane was shaken two times, each for one hour duration, with 75 ml of concentrated nitric acid and 75 ml of concentrated sulphuric acid. A yellowish color developed in the cyclohexane layer which disappeared by successive shaking of cyclohexane layer four times, each time for four hours using fresh concentrated sulphuric acid. The cyclohexane layer was separated and washed with double-distilled water, followed by a dilute solution of sodium carbonate and finally several times with double-distilled water. It was then dried over anhydrous magnesium sulphate. It was then fractionally distilled using a

standard Vigreux column packed with glass helices. Only the middle fraction was retained and stored under vacuum in a reservoir in the vacuum rack. This was used for making the samples. Ten ml. of the cyclohexane was vacuum distilled into a special cell (Fig. A-2). After thorough degassing, the cell was sealed off from the vacuum rack with a flame.

For polymer product analysis Eastman Spectrograde cyclohexane dried over lithium aluminium hydride was used.

(ii) Compounds used for identification and calibration standards.

<u>No</u>	<u>Compound</u>	<u>Supplier</u>
1.	Dicyclohexyl	Aldrich Chemical Co.
2.	Cyclohexene	Phillips Research grade. This was distilled before use.
3.	Hexene-1	Phillips Research grade. This was distilled before use.

(b) VPC Columns used for analysis

1. 2½ meter silica gel (medium activity) column
2. 2½ meter, 10% Ucon 75 H 1400 on Firebrick 30-60 mesh.
3. 2½ meter, 30% ββ'-oxydipropionitrile on Firebrick 30-60 mesh
4. 2½ meter, 20% Apiezon-L on Diatoport WAW 60-80 mesh
5. 2½ meter, activated charcoal column

c. High voltage source

A Spellman High Voltage Company Model PN-30 dc power supply gave voltages over the range 1 to 30 kV.

d. Electric circuit

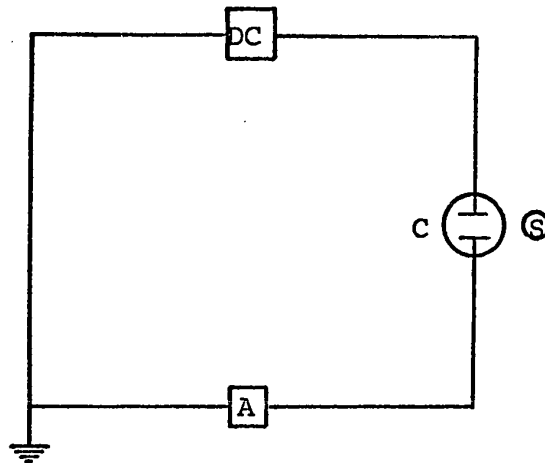
The electric circuit is schematically shown in Fig. A-1.

The cell C and gamma source S were located in an irradiation 'cave'. The voltage source DC and the micro-micro ammeter were in an adjoining room. The cell was connected to the voltage generator and the micromicro-ammeter through 26 ft long connecting cables.

e. Cell for irradiation of cyclohexane liquid

The cell used for irradiation of cyclohexane liquid under the influence of electric field is shown in Fig. A-2. The platinum electrodes are 25.7 mm diameter discs with rolled edges, to prevent sparking. The distance between the electrodes is  $5.6 \pm 0.1$  mm. The tungsten stems are spot welded to the backs of platinum electrodes. The electrical wire connections from the tungsten stem are very well insulated to prevent sparking. No metal portion of the lead wires or connections is left exposed to the air. Furthermore, in experiments where  $4.5 \times 10^4$  Vcm<sup>-1</sup> voltage is applied, a 14-in x 16-in rubber sheet was hung between the cathode and anode leads. Air is also circu-





- DC     Source of dc voltage
- C     Cell
- S     Gamma source
- A     Micromicro ammeter (E-H Research  
Laboratories Inc. Co. Model 240)

FIGURE A-1  
Electric Circuit

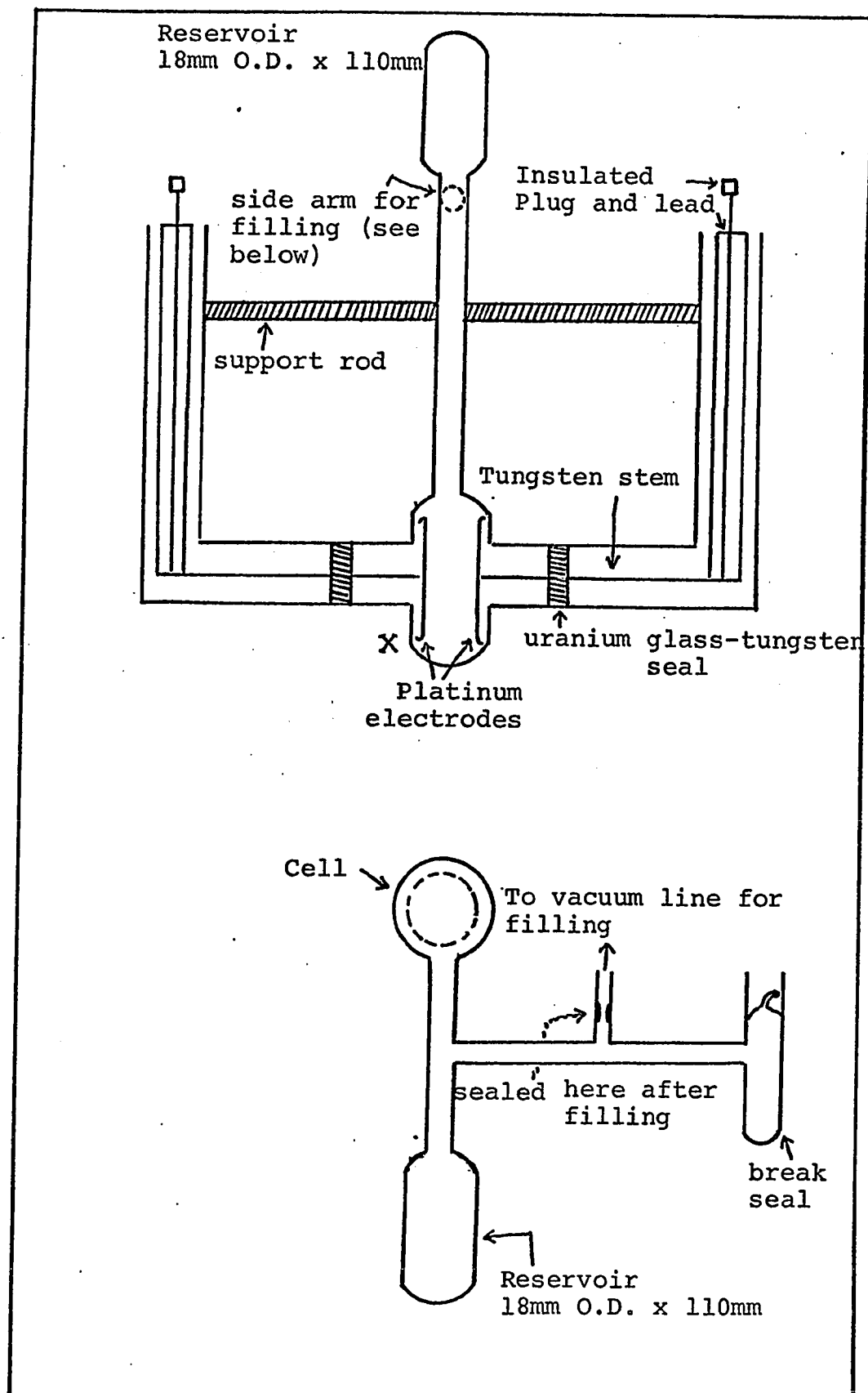


FIGURE A-2

Cell for irradiation of cyclohexane liquid

lated around X (Fig. A-2) so as to keep it at the room temperature.

The cell was cleaned with a 3:1 mixture of hot concentrated sulphuric and nitric acids. It was then thoroughly rinsed with doubly distilled water. The last two fillings of water remained in the cell 15 minutes each. After this procedure, the cell was evacuated. During evacuation, the cell was heated many times to drive off all the moisture. The cell was evacuated overnight before introducing the hydrocarbon. Ten ml. of cyclohexane was used each time. The active volume (volume of cyclohexane in between the electrodes) was 2.6 cc.

f. Cell for dosimetry.

A cell similar in design to the one used for electric field experiments but without any electrodes was used for dosimetry.

The dose rate was determined with the Fricke dosimeter, making the appropriate electron density corrections.

The dose rate used in all the experiments was about  $8 \times 10^{17}$  eV/ml hr.

g. Sample preparation and product analysis

The techniques employed for sample preparation and product analysis were similar to those described earlier in the experimental section of this thesis.

For polymer analysis, the following procedure was

adopted. The irradiated liquid was poured out of the cell into a small weighed beaker. It was then evaporated in a stream of nitrogen for about 15 minutes. The beaker was weighed again. The residue was dissolved in carbon tetrachloride and then analyzed for  $C_6$  compounds using  $\beta\beta'$ -oxydi-propionitrile column and for  $C_{12}$  compounds using Apiezon-L column.

### 3. Results and Discussion.

The yields of various products as a function of applied electric field strength over the range 0 to 44.6 kV/cm are presented in Table A-1 and Fig. A-3. The yields of products obtained by the irradiation of cyclohexane liquid in a cell without platinum electrodes are also presented in Table A-1.

The yields of cyclohexene and dicyclohexyl obtained in the radiolysis of cyclohexane in a cell with platinum electrodes are less by  $0.4 \pm 0.1$  and  $0.11 \pm 0.03$  G units whereas the yield of the polymer is greater by 0.3 G units as compared to the yields of cyclohexene, dicyclohexyl and polymer obtained in the radiolysis of cyclohexane in a cell without platinum electrodes. The yield of hydrogen is the same in both cases (Table A-1). Therefore, this indicates that the platinum electrodes do have a small effect on the yields of liquid products. The cause for this effect is not known.

TABLE A-1

Effect of electric field on product yields in the radiolysis of cyclohexane liquid.

Total dose =  $8.5 \times 10^{19}$  eV/cc

Voltage applied in kV/cm	Hydrogen	cyclohexene	hexene-1	G			cyclohexyl cyclohexene	polymer
-*	5.25	2.17	0.25	1.45	0.19			$2.0 \pm 0.1^\dagger$
0.0	$5.4 \pm 0.1$	$1.8 \pm 0.1$	----	$1.34 \pm 0.03$	----			$2.3 \pm 0.5^\dagger$
13.7	5.43	1.60	----	1.60	----			-----
26.8	5.37	1.81	----	1.39	----			-----
44.6	5.49	1.90	0.23	1.40	----			$2.5 \pm 0.1^\dagger$

\* Sample was irradiated in a cell without platinum electrodes.

$^\dagger$  The G value of polymer is in  $C_6$  units.

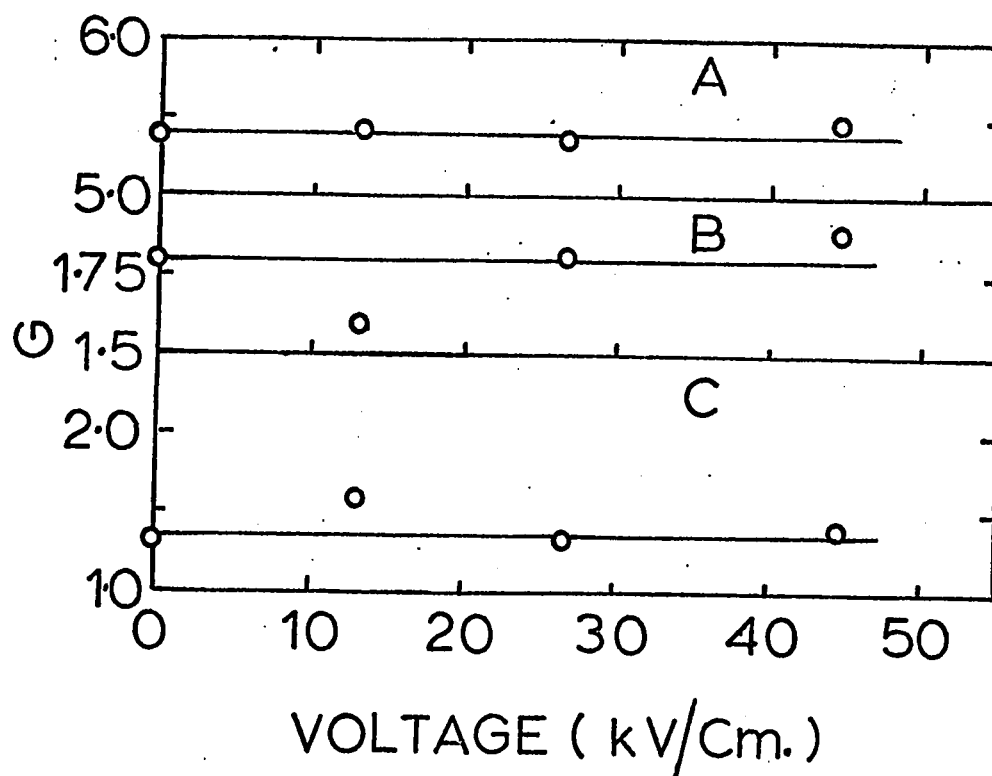


FIGURE A-3

Effect of electric field on product yields in the radiolysis of cyclohexane liquid

A	O	Hydrogen
B	O	Cyclohexene
C	O	Dicyclohexyl

The yields of hydrogen, cyclohexene, dicyclohexyl and polymer remain unchanged by the application of electric fields (Table A-1 and Fig. A-3). It must, however, be pointed out that the active volume (volume of cyclohexane in between the electrodes) is only 2.6 cc out of the total 10 cc of sample. Therefore, the total observed effect will be 1/4 th of the real effect. The value of  $G(H_2)$  in the absence of any applied field is  $5.4 \pm 0.1$  (Table A-1). The application of electric fields of upto  $4.5 \times 10^4 \text{ V cm}^{-1}$  had no effect on product yields (Table A-1) within an estimated error of  $\frac{0.1}{5.4} \times \frac{10}{2.6} \times 100 = 7$  percent. This is contrary to the earlier observation of Gusynin and Talrose (145) that the application of electric field has a large effect on the hydrogen yield in the radiolysis of dodecane, tetradecane and hexadecane. In a later publication, Talrose (144) concluded that the earlier observations of effect of electric field on the hydrogen yield is probably due to the occurrence of convective motion induced by the field and is, therefore, not the direct effect of electric field on the ionic reactions.

B. Calculation of stopping power ratios.

The rate of energy loss of a high energy electron per unit path length in a medium is given by Bethe's equation (146).

$$-\left(\frac{dT}{dx}\right)_{\text{coll}} = \frac{2\pi e^4 ZN}{m_o v^2} \left[ \ln \frac{m_o v^2 T}{2I^2 (1-\beta^2)} - \left( 2\sqrt{1-\beta^2} - 1 + \beta^2 \right) \ln 2 + (1-\beta^2) + \frac{1}{8}(1-\sqrt{1-\beta^2})^2 \right]$$

where  $dT$  = collisional loss of kinetic energy in ergs per increment of path length,  $dx$ , in cm

$N$  = number of molecules/cc = (molecules/mole) x (moles/cc) =  $6.02 \times 10^{23}$  x (moles/volume (V))

$Z$  = number of electrons/molecule

$e$  = electronic charge =  $4.80 \times 10^{-10}$  esu

$T$  = relativistic kinetic energy of the electron, assumed to be 0.6 MeV ( $9.6 \times 10^{-7}$  ergs) for  $\text{Co}^{60}$   $\gamma$ -radiation.

$v$  = velocity of the electron =  $c(1 - (1 + \frac{T}{m_o c^2})^{-2})^{\frac{1}{2}}$   
=  $2.7 \times 10^{10}$  cm/sec

$C$  = velocity of light =  $3.0 \times 10^{10}$  cm/sec

$m_o$  = rest mass of the electron =  $9.11 \times 10^{-28}$  g

$\beta$  =  $v/c$  = 0.89

$I$  = average excitation potential of the molecule

$$\ln I = \frac{N_1 Z_1 \ln I_1 + N_2 Z_2 \ln I_2 + \text{-----}}{N_1 Z_1 + N_2 Z_2 + \text{-----}}$$



where  $N_1$  = number of atoms of element 1 per molecule

$Z_1$  = number of electrons/atom of element 1

$I_1$  = average excitation potential of element 1

If the number of cc (V) is kept constant and the calculation is done for 1 mole of gas then

$$N = \frac{6.02 \times 10^{23}}{V}$$

Define  $\frac{dT'}{dx}$  = rate of energy loss per cm per mole,  
ergs/cm/mole, then

$$\frac{dT'}{dx} = YZ \left[ \ln \frac{A}{I_1^2} + B \right]$$

$$\text{where } Y = \frac{2\pi e^4}{m_o v^2} \times \frac{6.02 \times 10^{23}}{V}$$

$$A = \frac{m_o v^2 T}{2(1-\beta^2)} = 1.55 \times 10^{-12} \left( \frac{\text{gcm}^2}{\text{sec}^2} \right)^2$$

$$B = -(2\sqrt{1-\beta^2} - 1 + \beta^2) \ln 2 + (1-\beta^2) + \frac{1}{8} (1-\sqrt{1-\beta^2})^2$$

$$= -0.24$$

The relative stopping power per mole for compounds 1 and 2 will be given by

$$\rho_2' = \frac{(dT/dx)_1'}{(dT/dx)_2'} = \frac{Z_1}{Z_2} \left[ \frac{\ln A/I_1^2 + B}{\ln A/I_2^2 + B} \right]$$

The values of  $Z_1$ ,  $I$ ,  $(dT/dx)'$  for various compounds used during the course of this work are presented in Table A-2.

TABLE A-2

Values of  $Z$ ,  $I$ ,  $(dT/dx)$  for various compounds

Material	$Z$	$I$ ev	$I$ ergs	$A/I^2$	$\ln A/I^2 + B$	$(dT/dx)$
$C_2H_4$	16	51.3	$82.2 \times 10^{-12}$	$2.29 \times 10^8$	19.01	$Y(3.04 \times 10^2)$
$C_3H_6$	24	51.3	$82.2 \times 10^{-12}$	$2.29 \times 10^8$	19.01	$Y(4.56 \times 10^2)$
$NH_3$	10	52.5	$84.1 \times 10^{-12}$	$2.19 \times 10^8$	18.97	$Y(1.90 \times 10^2)$
$SF_6$	70	117	$187.4 \times 10^{-12}$	$4.42 \times 10^7$	17.38	$Y(1.22 \times 10^3)$
$(C_2H_5)_2O$	42	54.9	$87.95 \times 10^{-12}$	$2.0 \times 10^8$	18.87	$Y(7.93 \times 10^2)$
$C_2H_5OH$	26	57.5	$92.12 \times 10^{-12}$	$1.82 \times 10^8$	18.78	$Y(4.88 \times 10^2)$
$C_6H_{12}$	48	51.3	$82.18 \times 10^{-12}$	$2.29 \times 10^8$	19.01	$Y(9.13 \times 10^2)$